MOVEMENT AND MIGRATION OF FLATHEAD MULLET *MUGIL CEPHALUS* IN A WARM TEMPERATE SOUTH AFRICAN ESTUARY

A thesis submitted in fulfilment of the requirements for the degree of

DOCTOR OF PHILOSOPHY

of

RHODES UNIVERSITY

By

DINAH LORRAINE MUKHARI

ORCID ID

https://orcid.org/0000-0001-7558-4360

July 2025

ABSTRACT

The global decline of estuary-associated fish species is largely attributed to anthropogenic impacts, including overexploitation, habitat modification and altered flow, and thermal regimes driven by climate change. The flathead mullet *Mugil cephalus* is an estuary-associated cosmopolitan species of high fisheries value, and plays a crucial role in aquatic estuarine food webs. Despite this, little is known about their movement patterns in estuaries, particularly on the African continent, and how these movements may be affected by a changing climate, which in turn will impact fisheries and the presence of predators who feed on them. As such, we used acoustic telemetry, thermal tolerance laboratory experiments and otolith microchemistry to gain a better understanding of movements and habitat connectivity of *M. cephalus* linked to changes in temperature. Acoustic telemetry was used to monitor the fine-scale habitat use of *M. cephalus* for a period of one year between March 2023 and April 2024 in the warm temperate permanently open Kowie Estuary, South Africa. Results revealed extensive estuary use, with significant individual variation in movement patterns, ranging from high residency to the estuary exhibited by half of population to high levels of connectivity between the estuary and adjacent marine environment by the other half. Movement patterns also changed seasonally, with fish exhibiting high levels of activity and utilising the entire length of the estuary during austral summer, and being absent in the upper reaches of the estuary during austral winter. Linear Mixed-effects Models (LMM) showed that river flow and both sea and river water temperature significantly affected the daily average position of fish in the estuary. Periods of increased freshwater flow and decreased river temperatures led to downstream movements by most individuals from the upper reaches to the lower-middle reaches; however, despite the downstream movement, fish did not move into the mouth region and marina, which could be attributed to the cooler sea water, particularly during summer. Thermal tolerance experiments aligned with the movements observed in the wild. Despite the revealed broad upper and lower critical thermal limits (CT_{min} = 3.2 °C; CT_{max} = 37.7 °C), thermal stress (identified by breakpoints in ventilation rates) was experienced at temperatures above and below critical limits (13.5 and 29.3 °C). Water temperatures in the upper reaches of the Kowie Estuary during austral winter dropped below the lower critical limit, suggesting that thermal constraints play a significant role in shaping habitat use and seasonal distribution of *M. cephalus* in warm temperate estuaries. Using Random Forest machine learning, otolith microchemistry results (Sr:Ca, Ba:Ca, Mg:Ca, Rb:Ca and Mn;Ca) showed that the spatial and temporal movement patterns and seasonal drivers of this species into and out of the Kowie Estuary are consistent throughout their lifetime, from larval estuarine recruitment to moving to the marine environments during winter season. Furthermore, the combined acoustic telemetry and otolith microchemistry results revealed substantial individual variation in movement behaviour and responses to environmental conditions, thus supporting a condition-dependent framework for partial migration, whereby inter-individual differences in thermal tolerance, such as greater tolerance to warmer or cooler waters may directly influence the likelihood of an individual becoming migratory or resident. Framed within the movement ecology paradigm, these findings underscore the role of internal state (e.g., physiological thresholds) interacting with external drivers (e.g., temperature, flow) in shaping movement decisions and connectivity patterns of estuary-associated species such as *M. cephalus*. Both intra-and inter-seascape connectivity of the Kowie Estuary and the adjacent marine environment is crucial for the persistence of *M. cephalus* especially under the growing human and climate pressures which are expected to intensify and alter estuarine ecosystems. The results of this study underscores the importance of a multimethod approach, combining fine scale and lifetime habitat connectivity data with environmental drivers to understand the mechanisms underlying fish movement across dynamic estuarine and marine environments.

DECLARATION

I, Dinah Lorraine Mukhari hereby declare that this thesis, submitted to the Department of Ichthyology and Fisheries Science, Rhodes University, is my original work and has not been previously submitted in any form to another university. I have not included ideas, phrases or illustrations from other people's work without acknowledging their authorship.

ETHICS STATEMENT

Ethical clearance for this study was obtained from the Rhodes University Animal Research Ethics Committee (Approval number: 2022-5511-6832) and the South African Institute for Aquatic Biodiversity Animal Ethics Committee (Approval number: 25/4/1/7/5_2019-03).

TABLE OF CONTENTS

ABSTRACT .... *I*

DECLARATION .... *III*

ETHICS STATEMENT .... *IV*

LIST OF FIGURES .... *VII*

LIST OF TABLES .... *XII*

LIST OF APPENDICES .... *XIV*

PREFACE .... *XV*

ACKNOWLEDGEMENTS .... *XVI*

CHAPTER 1 .... *1*

GENERAL INTRODUCTION *1*

CHAPTER 2 .... *7*

STUDY SPECIES AND STUDY SITE *7*

2.1. Study species **7**

2.2. Study site **9**
2.2.1. The South African coastline 9
2.2.2. Kowie Estuary 10

CHAPTER 3 .... *21*

HABITAT CONNECTIVITY, ESTUARINE USE AND THE EFFECT OF SELECTED ENVIRONMENTAL FACTORS ON SPACE USE *21*

3.1. Introduction **21**

3.2. Methods and materials **24**
3.2.1. Acoustic receiver array 24
3.2.2. Fish collection and tagging 25
3.2.3. Data acquisition 27
3.2.4. Data analysis 28

3.3. Results **35**
3.3.1. Habitat connectivity 38
3.3.2. Spatial and temporal use of the Kowie Estuary 42
3.3.3. Effects of environmental variables (time of day, temperature and flow) .. 52

3.4. Discussion **56**

CHAPTER 4 .... *62*

ASSESSING THE THERMAL TOLERANCE OF A COSMOPOLITAN SPECIES, MUGIL CEPHALUS *62*

4.1. Introduction 62

4.2. Methods and materials 66
4.2.1. Thermal environment.. 66
4.2.2. Fish collection and husbandry 66
4.2.3. Experimental approach.. 67
4.2.4. Statistical analyses 70

4.3. Results 71

4.4. Discussion 76

CHAPTER 5.. 83

USING OTOLITH MICROCHEMISTRY TO DETERMINE THE LIFETIME HABITAT USE AND CONNECTIVITY OF FLATHEAD MULLET MUGIL CEPHALUS IN A WARM TEMPERATE SOUTH AFRICAN ESTUARY... 83

5.1. Introduction 83

5.2. Methods and materials 86
5.2.1. Otolith collection 86
5.2.2. Sea chemical signature acquisition 87
5.2.3. Otolith preparation and laser ablation.. 88
5.2.4. Signal treatment 89
5.2.5. Sea chemical signature acquisition 91
5.2.6. Habitat discrimination 92
5.2.7. Lifetime habitat use 93

5.3. Results 94
5.3.1. Sea chemical signature acquisition 94
5.3.2. Habitat discrimination 95
5.3.3. Lifetime habitat use 102

5.4. Discussion 105

CHAPTER 6...112

GENERAL DISCUSSION 112

REFERENCES 127

APPENDICES.. 149

LIST OF FIGURES

CHAPTER 2

Figure 2.1. (A) An illustration of an adult flathead mullet *Mugil cephalus* (Material provided courtesy of the South African Institute for Aquatic Biodiversity, SAIAB), and (B) an image of a juvenile *M. cephalus* collected from Kowie Estuary, South Africa on the 14th January 1995 by JA Cambray; specimen available at the SAIAB National Collection Facility (Ref: 119820)... 8

Figure 2.2. The global distribution of flathead mullet *Mugil cephalus*, shown in red. Data downloaded and plotted from Global Biodiversity Information Facility (human observation data). 9

Figure 2.3. Map of the South African coastline showing the four biogeographic regions (van Niekerk et al. 2020) separated by dashed lines, and the location of the study site, Kowie Estuary, at the coastal town of Port Alfred shown by the yellow box. 10

Figure 2.4. Map of South Africa showing the study site, the Kowie Estuary, divided into three reaches based on sedimentation patterns and salinity (following Heinecken and Grindley 1982). 11

Figure 2.5. The aerial view showing the (A) artificially modified Kowie mouth and the (B) Port Alfred marina residential area including the surrounding land-use... 12

Figure 2. 6. The causeway at Kowie River on the 7 October 2022 (A) at 10h28 during spring high tide, and (B) at 15h11 during the outgoing tide........................... 13

Figure 2.7. The Kowie Weir and fish ladder during (A and B) low flow on the 7th July 2022 and (C and D) high flow on the 2 August 2023. 13

Figure 2.8. (A) Average daily air temperature and (B) total daily rainfall at Port Alfred (data obtained from the South African Weather Service), and (C) average daily river flow of the Kowie River (data obtained from the Department of Water and Sanitation) from January 2023 to June 2024. 16

Figure 2.9. Wind speed and direction recorded at Port Alfred by the South African Weather Service between January 2023 and June 2024. The lighter the colour, the stronger the wind speed.. 17

Figure 2.10. Daily average water temperatures recorded in the Kowie Estuary mouth (Mouth) and at three inshore coastal stations (PA001, PA002, PA003) at Port Alfred from July 2012 to June 2024. 18

Figure 2.11. The *in situ* river, estuary and sea temperature recorded during the study period from July 2023 to June 2024 in and adjacent to the Kowie Estuary, South Africa. The bold line shows the daily average and the shaded lines indicate the daily minimum and maximum temperature recorded in each environment (river, estuary and sea). 19

Figure 2.12. The *in situ* average daily salinity recorded at different stations at various reaches (blue – lower, yellow – middle, green – upper) within the Kowie Estuary, South Africa from July 2023 to June 2024. 20

CHAPTER 3

Figure 3.1. Map of the Kowie Estuary and neighbouring estuaries showing the position of acoustic receivers deployed during the study period. The Kowie Estuary is divided into three reaches based on sedimentation patterns and salinity (following Heinecken and Grindley 1982). Green dots represent temperature loggers deployed between July 2023 and June 2024. 24

Figure 3.2. (A) The standard mooring design used by the Acoustic Tracking Array Platform for receivers deployed in estuaries (after Cowley et al. 2017), (B) a standard cement block mooring with receiver (painted red) inserted ready for deployment, and (C) a photograph of the mooring underwater. The smaller black receiver is an AquaMeasure (Innovasea, Canada) logger which recorded *in situ* salinity and temperature. 25

Figure 3.3. Scatterplots showing the Spearman correlation between temperatures recorded in the Kowie River, Kowie Estuary and sea between July 2023 and June 2024. 34

Figure 3.4. (A) Photo of a *Mugil cephalus* immediately after acoustic transmitter surgical insertion prior to release, and (B-D) photos of the same individual that was recaptured seven days post-surgical procedure, showing advanced signs of healing. 37

Figure 3.5. Abacus plot showing presence of acoustically tagged *Mugil cephalus* in the Kowie Estuary (grey bars), at sea (blue bars), and neighbouring estuaries (Bushmans, purple bars; Great Fish, green bars) and coastal environments (Kleinemonde, yellow bars) during the monitoring period (01 March 2023 to 30 April 2024). 40

Figure 3.6. The schematic diagram showing the Port Alfred coastline with arrows representing trips to sea (blue) and other estuaries (black) undertaken by *Mugil cephalus* acoustically tagged and monitored in the Kowie Estuary between 01 March 2023 and 30 April 2024. 41

Figure 3.7. The residency indices of *Mugil cephalus* acoustically tagged and monitored in the Kowie Estuary (Kowie), sea (Sea) and neighbouring estuaries (Other) between 01 March 2023 and 30 April 2024. Crosses (x) indicate the mean proportions of time spent within each reach of the Kowie Estuary; the boxes show the interquartile range (IQR), and the lines represent the median for each habitat. 42

Figure 3.8. The proportion of time spent in each reach of the Kowie Estuary by tagged *Mugil cephalus* between 01 March 2023 and 30 April 2024. Crosses (x) indicate the mean proportions of time spent within each reach of the Kowie Estuary; the

boxes show the interquartile range (IQR), the whiskers extend to 1.5 x IQR, and the lines represent the median for each reach. 43

Figure 3.9. The average proportion of time spent by all *Mugil cephalus* at each acoustic receiver station deployed in the Kowie Estuary, South Africa throughout the monitoring period (01 March 2023 to 30 April 2024). The red stars represent fish capture location and the black cross represents Station 13, which malfunctioned during this study and for which there were no detection data. 44

Figure 3.10. (A) The box and whisker plot showing the overall proportions of time spent at each acoustic receiver station deployed in the Kowie Estuary, South Africa by all *Mugil cephalus* throughout the monitoring period (01 March 2023 to 30 April 2024). The crosses represent the mean proportion of time spent at each acoustic receiver station. The boxes show the interquartile range (IQR), the whiskers extend to 1.5 x IQR, and the lines represent the median for each reach. (B) Bubble plot showing the proportions of time spent by each individual *Mugil cephalus* at different acoustic receivers stations deployed in the Kowie Estuary between 01 March 2023 and 30 April 2024. (indigo = lower reaches, turquoise = middle reaches and yellow = upper reaches). 45

Figure 3.11. The overall monthly proportion of time spent by all *Mugil cephalus* at different reaches within the Kowie Estuary during the monitoring period (01 March 2023 to 30 April 2024). 46

Figure 3.12. Proportions of time spent in the lower, middle and upper reaches of the Kowie Estuary area per season by six tagged *Mugil cephalus* that were monitored for more than 300 days between 01 March 2023 and April 2024. Circles indicate individual fish, crosses (x) indicate the mean proportions of time spent within each reach of the Kowie Estuary; the boxes show the interquartile range (IQR), the whiskers extend to 1.5 x IQR, and the lines represent the median for each reach. 47

Figure 3.13. Daily detection plots of *Mugil cephalus* movements throughout the Kowie Estuary during the monitoring period (01 March 2023 to 30 April 2024), with different stations coloured according to estuarine reach (indigo = lower reaches, turquoise = middle reaches and yellow = upper reaches). 49

Figure 3.14. The monthly proportion of time spent by acoustically tagged *Mugil cephalus* at various acoustic receiver stations in the Kowie Estuary during the monitoring period (01 March 2023 and 30 April 2024). 50

Figure 3.15. The relationship between fish length and proportion of time spent by acoustically tagged *Mugil cephalus* at different reaches within the Kowie Estuary during the monitoring period (01 March 2023 to 30 April 2024)........ 51

Figure 3.16. The overall average hourly position from the mouth (Station 1) to uppermost receiver (Station 21) of individual *Mugil cephalus* in the Kowie Estuary during the monitoring period between 01 March 2023 and April 2024. Grey bars represent night hours (18:00 to 05:00) and clear represent day hours (06:00 to 17:00). 53

Figure 3.17. Average daily fish positions (as indicated by acoustic receiver stations from the mouth [1] to the river-estuary interface [21]) of the 12 tagged *Mugil cephalus* (black dots) included in the modelling analyses plotted from 01 March 2023 to 30 April 2024. with multiple variables river temperature (blue)and sea temperature (purple) on the secondary y-axis, both river flow (yellow) and square root of total rainfall (green) were scaled to the y-axis. Fish that had movement data for only March 2023 were removed. 55

CHAPTER 4

Figure 4.1. Map of the Kowie Estuary in South Africa, showing the two sites for fish collection (yellow squares) and the position of the temperature and salinity loggers (green circles). 66

Figure 4.2. (A) The experimental tank set up for thermal tolerance trials, (B, C) Visual Implant Elastomer (VIE) tagging procedure on *Mugil cephalus*, applied to facilitate individual identification during the opercular beat (OB) quantification and (D) three tagged fish in a trial tank pictured during the experiment. 69

Figure 4.3. The visual representation of thermal breadth ($CT_{max} – CT_{min}$) of individual *Mugil cephalus* during critical thermal limit trials. The dashed lines represent the average CT_{min} and CT_{max} of 3.2°C and 37.7°C respectively. Stars represent fish that did not complete CT_{min} trials. 74

Figure 4. 4. Opercular beat rate (beats per minute) of *Mugil cephalus* during the CT_{max} and CT_{min} trials at every 2 °C water temperature change, the dashed lines indicate the minimum and maximum ventilation breaking points (BP) of 13.5 and 29.3 °C, respectively. 75

Figure 4.5. The *in situ* water temperature recorded at various sites in the Kowie Estuary between July 2023 and July 2024, with average CT_{min}, CT_{max} and upper and lower breakpoints (BP) overlaid (From Station 2: closest to the mouth to Station 21: riverine-estuarine interface). 76

CHAPTER 5

Figure 5.1. Images (Olympus SZX16 microscope, 2.5 magnification under transmitted light) of otolith transverse sections for three contrasted specimens of *Mugil cephalus* captured in the Kowie Estuary (A. YoY, B. age 2 juvenile and C. age 4 sub-adult) and corresponding Sr:Ca concentrations measured along the transect analysed on their ventral side. Circle = core, dotted line = LA-ICPMS transect line, green arrows = end of the larval life, black arrows = winter annulus deposition when present. 91

Figure 5.2. Comparison of sea chemical signatures of Sr:Ca (left) and Ba:Ca (right) in *Mugil cephalus* from controlled laboratory experiments (n = 14) versus the marine signatures incorporated during the larval life of all fish (n = 24)......... 95

Figure 5.3. The number of elements included in the random forest and prediction accuracy of the spatial discrimination of the three habitats used by *Mugil*

cephalus in the Kowie Estuary, South Africa and the Mean Decrease in Gini index of these optimal classifiers. 96

Figure 5.4. Box plots showing the data distributions of multiple otolith chemical elements describing habitats for *Mugil cephalus* collected in the Kowie Estuary, South Africa. Circles indicate the mean of the distribution and letters denote significant differences and the error bars denote the 25 and 75% quartiles. . 99

Figure 5.5. Results of the Principle Component Analysis (Axis 1 to 3) on the otolith multi-elemental signatures (Sr, Ba, Mn, Mg and Rb) of *Mugil cephalus* of the three habitats investigated (sea, estuary lower and middle reaches) around the Kowie Estuary, South Africa. 101

Figure 5.6. Sr:Ca (black) and Ba:Ca (grey) profiles of 24 *Mugil cephalus* all sampled in the Kowie Estuary, South Africa. The grey vertical panel = larval life and growth annulus, dark grey horizontal bands and the grey dotted line = threshold values indicative of a sea chemical signature for Sr:Ca and Ba:Ca, respectively. Fish are categorized by life stage: Y = young-of-year, J = juvenile, and SA = sub-adult. Otolith annuli for individuals J1, J6, and SA5 were unclear and thus excluded from analysis; larval signatures were not detected in SA1 and SA2. Length at 50% maturity is 440 mm FL (Wallace 1975). 104

CHAPTER 6

Figure 6. 1. A graphical representation of the general life cycle of *Mugil cephalus* across multiple habitats (adapted from Whitfield et al. 2012), highlighting the predominant movement patterns assessed during this study (from number 3 to 5). The numbers represent the order of events during the life cycle. 117

Figure 6. 2. Schematic representation of the (A) fish movement and habitat use in the Kowie Estuary under current conditions, and the effect of temperature change such as (B) decreased river water temperature in winter, and (C) decreased sea water temperature as a result of upwelling events combined with an increase in river water temperature in summer, both of which predicted to increase in frequency and intensity as a result of climate change (figure adapted from Grant et al. 2017). 121

LIST OF TABLES

CHAPTER 3

Table 3.1. Summary of tagging data for 21 *Mugil cephalus* captured in the Kowie Estuary (December 2022–May 2023), including fish code, fork length (mm FL), total length (mm TL), standard length (mm SL), Weight (g), tag date, tag type, surgery and recovery duration (minutes: seconds) and capture location. Fish are ordered by fish length (smallest to largest), and are grouped in life stages (sub-adult and adult). 28

Table 3.2. Seasonal temperature (mean ± standard deviation °C) and range (minimum to maximum) recorded at sea, the Kowie River and Kowie Estuary between July 2023 and June 2024. Season is broken up by month and includes summer (Dec to Feb), autumn (Mar to May), winter (Jun to Aug) and spring (Sept to Nov) (SAWS 2025). 32

Table 3.3. Summary analysis data for 17 *Mugil cephalus* that were detected in the Kowie Estuary, South Africa between 1 March 2023 and 30 April 2024. Asterisk (*) represent individuals for which more than 300 days of data were collected (used for further analysis). 36

Table 3.4. The overall information on sea trips undertaken by *Mugil cephalus* from the Kowie Estuary, including the departure date, time and season, habitats visited, frequency and length of sea trips and return date (where applicable) during the monitoring period (01 March 2023 to 30 April 2024). * represent departures of tagged fish that did not return to the Kowie Estuary...................................... 39

Table 3.5. The results of the Linear Mixed-effect Model output modelling the effect of temperature (river and sea, °C), river flow ($m^3. s^{-1}$) and rainfall (mm) on the daily average fish position of *Mugil cephalus* tagged and monitored in the Kowie Estuary between 01 March 2023 and 30 April 2024. Bold values indicate a significant result. 54

CHAPTER 4

Table 4.1. The length (mm fork length), critical thermal maximum (CT_{max}), critical thermal minimum (CT_{min}) and thermal breadth (CT_{max} – CT_{min}) of individual *Mugil cephalus* during critical thermal limit trials. NA represents fish that did not complete CT_{min} trials.. 73

CHAPTER 5

Table 5.1. Fish ID, length (mm), age estimates, life history stage, total otolith size (radius µm) and size (radius µm) at the end of larval life of all individual *Mugil cephalus* specimens collected from the Kowie Estuary, South Africa. In the fish code column, Y denotes young-of-year fish, J denotes juveniles, and SA denotes sub-adults and adults. 87

Table 5.2. The training dataset (75%) and test dataset (25%) were used for discrimination of two estuary habitats (lower and middle reaches) and the sea

habitat. For each fish specimen, the length, whether it was part of the validation experiment, number of spots on the otolith used and wrongly assigned by the Random Forest optimal classifier. On the fish ID, Y denotes young-of-year fish, J denotes juveniles, and SA denotes sub-adults. 98

LIST OF APPENDICES

Appendix 1. Top five outputs and ranking of the linear mixed effects models (LMM) to assess the influence of various environmental variables on average daily position of *Mugil cephalus* tagged in the Kowie Estuary, South Africa. The selected best-fit model (lowest AIC) is presented in boldface. 149

Appendix 2. Detailed monthly movements of acoustically tagged *Mugil cephalus* in the Kowie Estuary, South Africa between March 2023 and April 2024. 149

Appendix 3. The rate of temperature change in the experimental tanks during the *Mugil cephalus* CT_{max} and CT_{min} trials. 156

PREFACE

This thesis comprises three data chapters, some of which have been presented at various conferences. One has been accepted for publication, while another is ready for submission to peer-reviewed journals. Further included is the general introduction (Chapter 1), a description of the study site and study species (Chapter 2) and the general discussion (Chapter 6).

- Mukhari DL, Childs A-R, Ziko BA, Murray TS (2025) Assessing the thermal tolerance of a cosmopolitan species, *Mugil cephalus. African Journal of Maine Science*. (*Accepted with* minor revision)
- Mukhari DL, Darnaude AM, Labonne M, Childs A-R, Ziko BA, Murray TS (*ready for submission to Estuarine, Coastal and Shelf Science Journal*). Using otolith microchemistry to determine the lifetime habitat use and connectivity of flathead mullet *Mugil cephalus* in a warm temperate South African estuary.

ACKNOWLEDGEMENTS

First and foremost, I would like to express my deepest gratitude to my supervisors, Dr Taryn Murray and Prof Amber Childs. Working with you has been one of the greatest privileges of this PhD. Thank you for your unwavering support, insightful guidance, and patience throughout this journey. You are not only brilliant scientists, but also women I deeply admire, your leadership, integrity and generosity have made a lasting impact on me, both professionally and personally. I could not have asked for better supervisors.

Many thanks to the following organisations for the financial support: National Research Foundation (NRF) postgraduate scholarship (Grant no. MND210623614868), the South African Institute for Aquatic Biodiversity for the interim bursary, Thuthuka Instrument Funding (Grant no. 121941) for covering fieldwork and conference expenses, NRF Equipment-elated training and travel grant (Grant number: ERT230824145462) for funding the training on otolith microchemistry at the Marine Biodiversity Exploitation and Conservation (MARBEC) research institute at University of Montpellier, France, the Water Research Commission (WRC) for funding registration at the South African Society of Aquatic Scientists (SASAqS) conference, Rhodes University Council Research Grant for providing financial support for the laboratory running and fish husbandry expenses, Rhodes University Travel and Subsistence fund (Grant no. TSS06/2024 & TSS62/2024) for travel grants to attend the 7th I-MarCo and the 6th Southern African Marine Linefish Symposium (SAMLS), and the Acoustic Tracking Array Platform (ATAP) for funding project operational expenses throughout this project.

I am very grateful to the South African Weather Service (SAWS) for providing access to environmental datasets upon request, and to the Eastern Cape Parks and Tourism Agency (ECPTA) for granting permits to work within the protected Waters Meeting Nature Reserve.

I would like to thank Dr Josephine Pegg and Prof Paul Cowley for mentorship and inputs during the early stages of this project. Many thanks to Dr Audrey Darnaude and Dr Maylis Labonne the training on otolith microchemistry at MARBEC, University of Montpellier, France. The experience of living in France for a month was not only intellectually enriching but personally transformative and looking forward to future

collaborative research. Additional thanks to Dr O. Bruguier for his help with LA-ICPMS analyses.

Fieldwork would not have been possible without the incredible support of the following people: Dr Matthew Parkinson, Dr Anthony Bernard, Monty du Toit, Dr Alex Winkler, Dr Matthew Farthing, Prof Warren Potts, Vuyolwethu Mxo, Nonhle Mlotshwa and Samkele Ngcefa. The Aquatic Ecophysiology Research Lab team: Zunaid Suleman, Ndzali Songongo, Christian Hampel, William Selapa and the late Joshua Frachet. From the Aquatic Genomics Research Lab: Dr Gwyneth Matcher, Jody Oliver and Sibusiso Yokwana. From the SAIAB National Fish Collection: Nkosinathi Mazingula and Sphamanda Mceleli.

I would also like to thank the many departments at the South African Institute for Aquatic Biodiversity (SAIAB) and the Department of Ichthyology and Fisheries Sciences for their ongoing kindness and support throughout this degree. A special shout-out to sis Lulama Makana for your positive energy and the much-needed laughs, to Prof. Albert Chakona for your encouraging words and motivation throughout this journey, and to Wesley Philips for the IT support, assisting during countless technical crises (especially the many times my laptop decided to quit on me). To the library family, Maditaba Meltaf and Siya Mnguni, thank you for always bringing a sense of fun to the library and for going above and beyond to help me find the resources I needed, including ordering books you did not have. Your support made the long study sessions more enjoyable.

On a personal note, I would like to thank my lab mate and friend, Bantony Ziko, thank you for your academic collaboration, random chats and our much-needed tennis sessions that kept me sane along the way. To my best friend, Dr Siyasanga Mnciva, thank you for always being there, for encouraging me through the highs and lows, and for always offering a fresh perspective. To my partner and biggest cheerleader, Albert Libambo thank you for your endless love, support and encouragement throughout, we continue to celebrate every milestone, big or small. You somehow always believe in me, it makes all the difference.

To my family, too big to name individually, thank you for the countless sacrifices to ensure that I could have access to high-quality education. I am deeply grateful for the values you have instilled in me: curiosity, hard work, tenacity and patience which

continue to guide me both academically and personally. Your unwavering support and constant prayers carried me through this journey. A special mention to Mike, Selma and Thato: you gave me the final push I needed to cross this finish line.

I dedicate this doctoral degree to my late father David Mukhari and my late grandmother Caroline Teffo!

What a privilege it is to be weary, not from burden, but from the pursuit of something you are truly passionate about.

CHAPTER 1

GENERAL INTRODUCTION

Frameworks of landscape processes in relation to animal movements between resource patches have been developed (Pulliam 1988; Dunning et al. 1992; Taylor et al. 1993). These frameworks describe how animal movements do not occur randomly but as a response to spatial, temporal and connectivity of resources in a heterogeneous environment in which they occur (Dunning et al. 1992; Cushman et al. 2010). Animals move across various patches in their environment to maximise resources and meet their biological needs, such as food, habitat and reproduction (Pulliam 1988; Dunning et al. 1992). When studying animal movements in an environment, it is important to understand landscape connectivity, the degree to which the landscape permits or restricts movement of individuals between resource patches (Taylor et al. 1993; Green 1994). In this context, connectivity is broadly defined as the extent to which different subpopulations are linked through genetic or demographic exchange, serving as a key driver of population resilience (Palumbi 2003; Cowen et al. 2007; Gillanders et al. 2011a), and can be assessed from a physical (e.g., intra- and inter-seascape connectivity) and biological (e.g., functional and migratory connectivity) perspective depending on the spatial scale and habitat type (Welch et al. 2025). Knowledge of connectivity across habitats provides insights into the complex interactions between fish and their environment – information critical for their sustainability (Darnaude et al. 2022).

Species connectivity incorporates both the spatio-temporal continuity of habitats and the physiological mechanisms that underpin individual movement (Patterson et al. 2008). Coastal ecosystems, particularly estuaries, function as crucial ecological interfaces that link terrestrial, freshwater and marine environments (Ray 2005; Whitfield et al. 2023). These systems support species across multiple life history stages by providing access to resource-rich nursery habitats (Beck et al. 2001; Able 2005; Whitfield 2020). However, estuaries are increasingly threatened by anthropogenic pressures, including overexploitation, habitat modification and altered flow exacerbated by a changing climate (Bice et al. 2018; Cooke et al. 2022; van Niekerk et al. 2022). Compounding these pressures, climate-driven shifts in hydrological and thermal regimes as seen by extreme weather events (e.g. floods, droughts) can disrupt connectivity between important habitats, and affect critical environmental cues of estuary-associated species, thus affecting population dynamics and fish assemblages (Gehrke and Harris 2001; Elliot and Quintino 2007; Whitfield et al. 2023). Given these escalating threats, it is important to understand how estuarine systems play a role in mediating ecological connectivity between riverine and marine environments for estuary-associated species, particularly as fish movement through these transitional habitats is influenced by various biological, physiological and environmental factors operating across multiple spatial and temporal scales (Beitinger et al. 2000; Cooke et al. 2022). Therefore, identifying and understanding the factors that drive movement is a critical first step toward elucidating both the short-term and lifetime movement patterns, as well as habitat selection, of many fish species.

Advancing our understanding of fish movement ecology requires multidisciplinary research approaches that integrate physiology, behaviour, hydrology and landscape ecology (Verhelst et al. 2023). Although there is growing interest from ecologists and fisheries managers in quantifying the drivers of fish movement (Cooke et al. 2022), studying these dynamics in natural environments remains challenging due to significant logistical and methodological constraints (Gillanders et al. 2011a; Verhelst et al. 2023). Several methods exist to date, including mark-release-recapture, external and internal tagging with satellite-transmitting, radio and acoustic telemetry tags, and natural markers such as otolith elemental signatures. These methods can be limited at spatial and temporal scales and, at times, high tag loss (telemetry), and lack of accuracy and spatial resolution (natural markers) (Kramer and Chapman 1999; Crossin et al. 2017; Cooke et al. 2022). However, they can be used in combination to make up for the limitations.

Measuring connectivity, particularly for estuary-associated species with plastic life histories that involve multiple, spatially distinct habitats during various life cycle stages, is also challenging (Whitfield 1990; Sheaves 2009). Despite this, some studies have quantified the degree of connectivity in estuary-associated species using methods such as telemetry, microchemistry and a combination of both (Ray 2005; Tournois et al. 2017; Baker et al. 2019; Russell et al. 2022), identifying environmental drivers, i.e. temperature, photoperiod, tidal cycles and habitat availability as major influences of fish movements between connected resource patches (Childs 2013; Murray et al. 2018). In addition to understanding fish movement, it is important to determine the physiological (through controlled experiments) and environmental drivers of movement at the individual and population level (Cooke et al. 2008). Understanding these multifaceted aspects of connectivity for estuary-associated species will provide a better understanding into the evolutionary mechanisms that underpins species persistence and resilience especially in the face of increasing climate variability. An example is the contingent behaviour observed in clupeid fishes along the United States of America east coast, where individuals of the same species adopted different migratory routes and diverse habitat use strategies depending on environmental conditions (Ray 2005). Such contingent behaviour can enhance the overall species stability, productivity and resilience against environmental change (Kerr et al. 2010; Vinagre et al. 2011). There are multiple fish species that exhibit similar behavioural plasticity, through partial migration, the existence of contingents within a population is made possible by the connectivity between and within these habitats (Clark 1968; Secor 1999; Kerr et al. 2009; Childs et al. 2015; Murray et al. 2018; Russell et al. 2022). Although contingents within a population may not be genetically distinct, this strategy evolved as an adaptation mechanism to heterogenous environment experienced by most coastal fishes (Secor 1999; Kerr et al 2010). Partial migration in fish has therefore been widely accepted as a conditional strategy instead of a genetically fixed threshold, with the extent of migratory behaviour and divergence in habitat use, in a population largely influenced by individual physiology, particularly energy allocations during early life stages (Clark 1968; Secor 1999; Kerr et al. 2009). To further explore mechanisms that drive contingencies within a population, there is a need for integrative multimethod approaches that links fish individual movement, physiological capacities and environmental variability at various life stages.

Acoustic telemetry, a method which was developed approximately 60 years ago (Hockersmith and Beeman 2012), involves the surgical implantation or external attachment of an acoustic transmitter into the body cavity of a fish or onto a fish (Heupel and Webber 2012). The transmitter emits a sonic pulse that is then detected by deployed acoustic receivers should the fish be within the detection range of the acoustic receiver (Hockersmith and Beeman 2012). Acoustic telemetry can provide high-resolution, fine-scale data especially when receivers are placed close together, revealing seasonal and life-stage-related variation in habitat use crucial for understanding population dynamics (Crossin et al. 2014; Hussey et al. 2015; Cooke et al. 2016; Matley et al. 2022).

In contrast to tagging animals, natural markers can be used to provide insights into the lifetime movement patterns of fish (Campana et al. 2000). Calcified structures such as otoliths have accurately facilitated the investigation of both age and growth of many fishes, as well as habitat use and migration, including that of important commercial species (Biolé et al. 2019; Soeth et al. 2019; Nazir et al. 2021). Otoliths grow daily with the individual fish and store trace elements during the biomineralization processes (Campana 1999). This elemental deposition is influenced by physiological attributes such as metabolism, growth, feeding habits and environmental factors, including food availability, ambient temperature and seasonal cycles (Buckel et al. 2004; Avigliano et al. 2020). Therefore, deposited elements represent a permanent record of the environmental conditions experienced by the fish at a particular time, and can thus be used to reconstruct individual life history, including lifetime connectivity and habitat use (Campana 1999; Sturrock et al. 2012; Bae and Kim 2020).

Ongoing research shows that the migratory strategies of estuary-associated fishes across salinity gradients is more flexible and complex than previously recognized (Clark 1968; Kerr et al. 2010; Whitfield et al. 2023). Multimethod approaches, particularly the integration of otolith microchemistry and acoustic telemetry, is thus essential for understanding these across spatial and temporal scales (Crook et al. 2016). For example, a study on rainbow trout *Oncorhynchus mykiss* in Canada showed that although acoustic telemetry revealed limited marine excursions of this species over short periods of time, otolith microchemistry identified broader patterns and contingency within the population by identifying freshwater residents in addition to estuarine residency (Roloson et al. 2020). Similarly, in a study on the movement of pinkeye mullet *Trachystoma petardi*, otolith microchemistry revealed the differences between life stages, while acoustic telemetry explained ambiguous chemical elemental signatures that resulted from rapid movements across salinity gradients, some of which were not clearly recorded on the otolith signatures (Miles et al. 2018). Furthermore, these studies showed the importance of also incorporating validation experiments, as inter-species variation in elemental incorporation on otolith is common (Hicks et al. 2010).

However, a holistic understanding of movement ecology requires a consideration of the physiological capacities of individuals to explain what enables or constrains such movement. Recent perspectives in ecological physiology emphasize the need to integrate animal's biomechanics, energetics and physiology, which provide mechanistic insights into how abiotic constraints, such as temperature, may affect individual movement, occupancy and habitat connectivity within thermally dynamic environments (Di Santo 2022). These differences in individual behaviour in similar ecosystems corroborate earlier studies that highlighted that fish movement in an environment is not random but is a response to overall environmental cues and individual physiological thresholds (Dunning et al. 1992).

Mugilidae is an important family of fishes, and dominates coastal systems globally, being both socio-economically and ecologically important (Whitfield 2016; James et al. 2016). *Mugil cephalus* (Linnaeus 1758), commonly known as flathead mullet, has a cosmopolitan distribution, occurring in the tropical, subtropical and temperate zones between the latitudes 42° N and 42° S (Whitfield et al. 2012). As detritivores and primary consumers, *M. cephalus* occupy an important position in the food web, facilitating energy transfer from basal resources to higher trophic levels, including piscivorous fishes, marine mammals and avian predators (Whitfield 2021). *Mugil cephalus* is therefore considered an important component of aquatic food webs, and regarded as a keystone species in certain estuarine systems (e.g. St Lucia Estuary in South Africa) (Whitfield 2021). Due to its global distribution and socioeconomic importance (Crosetti 2016), the life history and movement ecology of *M. cephalus*, including migration patterns is well studied; however, regional variation in movements has been highlighted in Asia (i.e., Taiwan, Korea; Chang et al. 2004b; Hsu et al. 2009; Chang and Iizuka 2012; Wang 2014), Mediterranean Sea (i.e., Fortunato et al. 2017), Australia (Fowler et al. 2016) and New Zealand (Górski et al. 2015). Despite its economic and ecological importance, very little research has been conducted on *M. cephalus* in Africa.

This thesis therefore aimed to address these knowledge gaps by linking spatial and temporal movement behaviours of *M. cephalus* in a warm temperate estuary in South Africa with physiological thresholds and environmental variability. By adopting a multimethod approach – integrating acoustic telemetry which will provide insights on the spatio-temporal movement patterns of *M. cephalus* in relation to environmental variability (Chapter 3), thermal tolerance of the species quantified through laboratory experiments using the Critical Thermal Method (Chapter 4), and otolith microchemistry with the use of otolith elemental signatures to reconstruct the lifetime movement patterns and habitat use (Chapter 5) – this study provides the opportunity to empirically quantify habitat connectivity of *M. cephalus* across multiple spatial and temporal scales in a South African estuary. Such an approach is essential not only for species-specific management, but also for broader ecosystem-based conservation planning for this, and other ecologically and socio-economically important estuary-associated fish species (Hays et al. 2019).

CHAPTER 2
STUDY SPECIES AND STUDY SITE

2.1. Study species

Mugil cephalus (Figure 2.1A, B) is a widely distributed estuary-associated species found throughout the globe in tropical, subtropical and temperate zones ranging in latitudes from 42° N and 42° S (Whitfield et al. 2012) (Figure 2.2). It is a euryhaline species that occurs in many aquatic systems ranging from freshwater rivers to hypersaline systems (Wallace 1975; Young and Potter 2002; Whitfield et al. 2012). *Mugil cephalus* is found in both clear and highly turbid waters over a wide range of dissolved oxygen concentration levels (Thomson 1966; Hoese 1985). Taxonomic studies have shown that this species may be part of a cryptic species complex (Shen et al. 2011), and may comprise more than 14 sub-groups which occur across different parts of the world (Whitfield et al. 2012).

There is high variability in biological traits of *M. cephalus* such as length-at-age, growth rate and length-at-50% maturity (L_{M50}) across their distributional range due to differences in local climate and food availability (Bok 1983; Whitfield et al. 2012), and evolutionary processes, such as size selective mortality (Conover 1990). Generally, *M. cephalus* growth rate is rapid during the first year, with fish reaching a length of 140–180 mm standard length (SL) in tropical and subtropical waters and 130–160 mm SL in temperate regions (Whitfield et al. 2012). *Mugil cephalus* can grow up to a maximum length of 680 to 720 mm total length (TL) (Wallace 1975). Although females have been shown to grow faster than males (Bok 1983), males attain sexual maturity earlier than females within the 3-year size classes, and the associated length also varies by regions (Whitfield et al. 2012). For example, in North Carolina, USA, where the climate is subtropical, *M. cephalus* mature at a smaller length (L_{M50}; 283 mm fork length [FL] for males and 324 mm FL for females) (Bichy 2004), compared to the North coast of Senegal population in a hot arid climate (L_{M50}; 390 mm FL for males and 420 mm FL for females) (Ndour et al. 2013). In South Africa, L_{M50} for *M. cephalus* occurs at a larger size of 420 mm FL for males and 440 mm FL for females in the tropical St Lucia Estuary (Wallace 1975). Furthermore, sexual maturity of *M. cephalus* in the St Lucia Estuary has been recorded to only begin at 300 mm FL (male) and 320 mm FL (female) (Whitfield and Blaber 1978). This was similar to the results of first maturity in the warm temperate Kowie Estuary, South Africa, whereby males matured at 308 mm FL and females at 344 mm FL (Bok 1983).

Spawning occurs at sea throughout its distribution range (Wallace 1975; Whitfield et al. 2012). The larvae of *M. cephalus* are planktivorous (Cardona 2016), and after approximately one month at sea, they recruit into estuaries which serve as nursery habitats (Whitfield 2016). After recruitment into estuaries (at 10–20 mm SL) they undergo a change in diet, from small benthic invertebrates to detritus and microalgae (Blaber and Whitfield 1977; Cardona 2016).

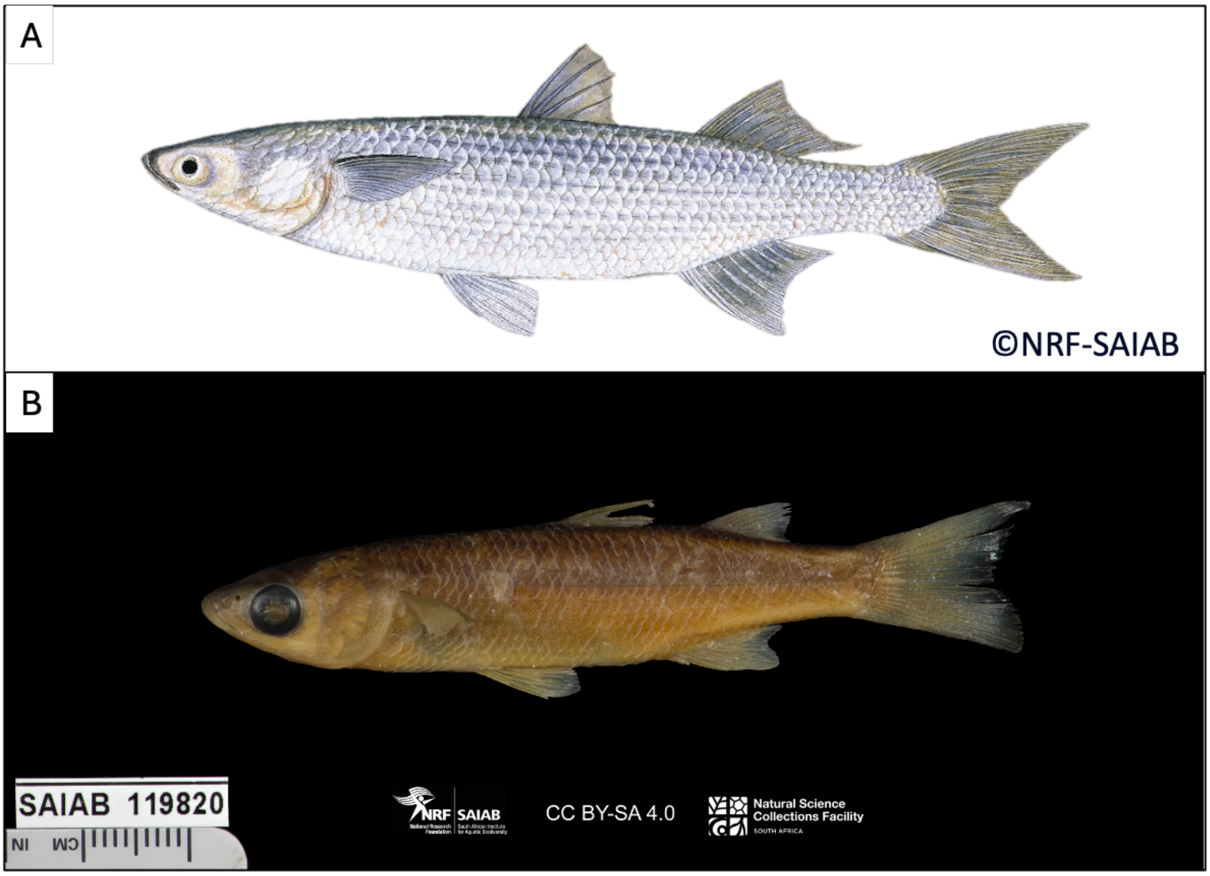

Figure 2.1. (A) An illustration of an adult flathead mullet *Mugil cephalus* (Material provided courtesy of the South African Institute for Aquatic Biodiversity, SAIAB), and (B) an image of a juvenile *M. cephalus* collected from Kowie Estuary, South Africa on the 14th January 1995 by JA Cambray; specimen available at the SAIAB National Collection Facility (Ref: 119820).

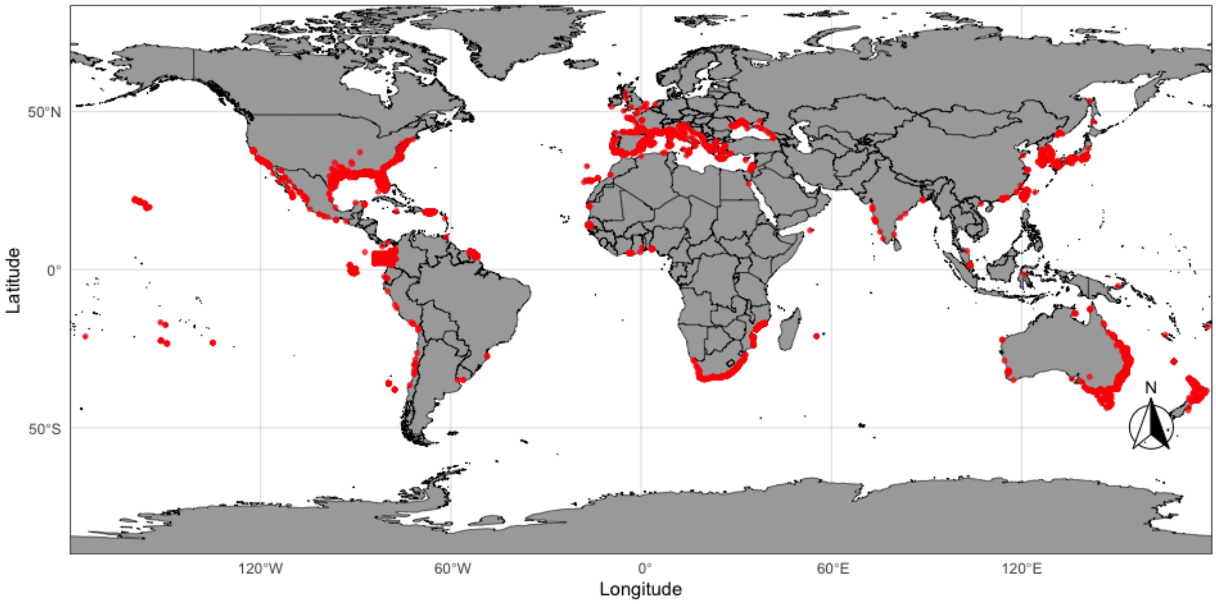

Figure 2.2. The global distribution of flathead mullet *Mugil cephalus*, shown in red. Data downloaded and plotted from Global Biodiversity Information Facility (human observation data).

2.2. Study site

2.2.1. The South African coastline

South Africa, situated at the southern tip of the African continent, is bordered by two major oceanic systems: the warm Indian Ocean to the east and the cold Atlantic Ocean to the west (Branch and Griffiths 1988). These coastal systems are influenced by the warm Agulhas Current on the east coast and the cold Benguela Current on the west coast, which shape resource availability and species distributions along the coastline. As a result, four primary biogeographic regions are recognized along the South African coast and inshore environment, including the cool temperate, warm temperate, subtropical and tropical biogeographic regions (van Niekerk et al. 2020). The warm temperate biogeographic region, which stretches from approximately Cape Point in the Western Cape Province, to Port St Johns in the Eastern Cape Province (Figure 2.3), represents a transition zone between the cool temperate biogeographic region, which exhibits lower species richness, but high endemicity, and the subtropical biogeographic region, which supports high species richness and low endemicity, respectively (James and Harrison 2010). Approximately 290 estuaries occur along the

3000-km South African coastline (Whitfield 2000; van Niekerk et al. 2020). The study site, the Kowie Estuary at the coastal town of Port Alfred, is a permanently open estuary, and falls in the warm temperate biogeographic region (Figure 2.3). This stretch of coastline is influenced by a wind-driven upwelling cell that occasionally brings cold (below 14 °C) nutrient-rich waters to the surface in austral summer (Heinecken and Grindley 1982; Lutjeharms et al. 2000; James and Harrison 2010; Goschen et al. 2012).

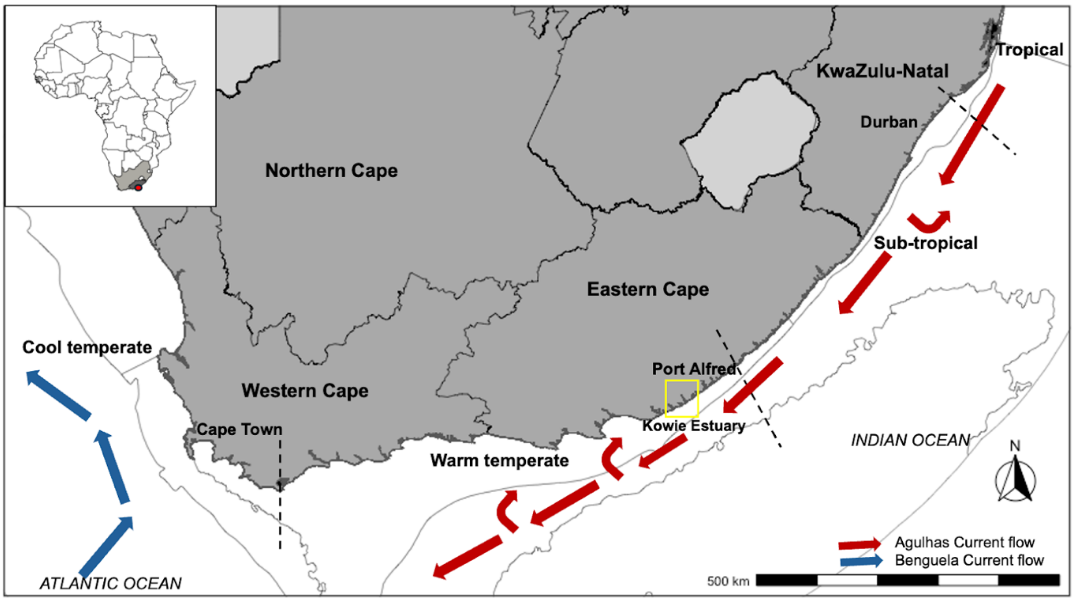

Figure 2.3. Map of the South African coastline showing the four biogeographic regions (van Niekerk et al. 2020) separated by dashed lines, and the location of the study site, Kowie Estuary, at the coastal town of Port Alfred shown by the yellow box.

2.2.2. Kowie Estuary

This study took place in the Kowie Estuary (Figure 2.4), a permanently open system flowing into the Indian Ocean at 33.603056° S, 26.902778° E, is approximately 21 km in length, with a maximum width of 100 m and depths reaching up to 8 m (Heinecken and Grindley 1982; James and Harrison 2010). It connects to the Kowie River, a perennial system characterized by deep pools (~6 m) and shallow, stony rapids (Day 1981). The Kowie Estuary can be divided into three reaches based on sedimentation patterns and salinity (Figure 2.4) (Heinecken and Grindley 1982). The upper reaches are narrow and shallow (2-–6 m deep), meandering through a valley with dense, wooded banks and a narrow intertidal zone (<10 m), with aquatic macrophytes such as widgeon weeds *Ruppia* species and common reed *Phragmites australis* present. The middle reaches widen to 100 m, with depths of 3–8 m around bends, and is characterised by sandy bottoms, intertidal mud banks and salt marshes (James and Harrison 2010). The banks of the estuary are dominated by Cape eelgrass *Zostera capensis*, Cape cordgrass *Spartina maritima* and perennial glasswort *Sarcocornia perennis* (Whitfield et al. 1994). Flow rates vary across reaches due to tides and currents, ranging from 12–20 $cm.s^{-1}$ in the upper reaches, 12 $cm.s^{-1}$ in the middle reaches and 25 $cm.s^{-1}$ in the lower reaches (Day 1981).

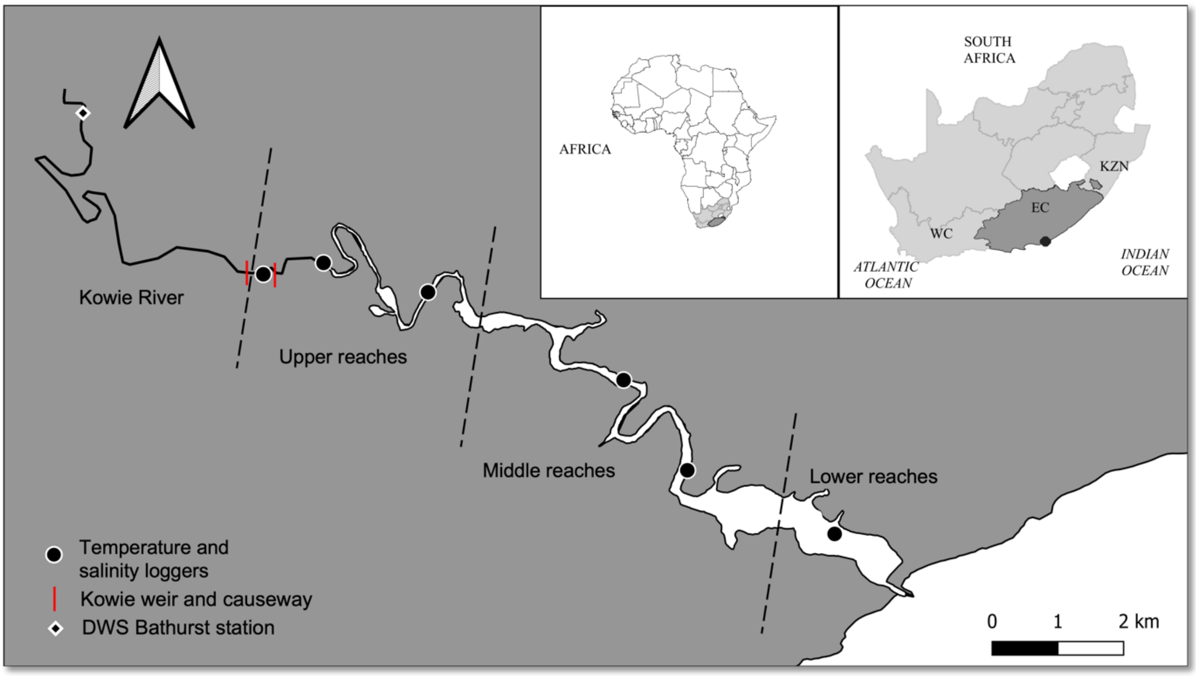

Figure 2.4. Map of South Africa showing the study site, the Kowie Estuary, divided into three reaches based on sedimentation patterns and salinity (following Heinecken and Grindley 1982).

The lower reaches and the mouth have developed banks that include jetties and residential areas (Whitfield et al. 1994; Schumann et al. 2001). Since the 19th century (1839-1841), the estuary mouth has been blocked and redirected through a man made channel to sea (Figure 2.5A) made of stone-lined embankments which were designed to support navigation for commercial shipping (Kruger and Strydom 2011; Royal Alfred Marina 2025). A century later, this was followed by the construction of the Royal Alfred Marina (Figure 2.5B) a private residential area with connected canals systems within the estuary (Whitfield et al. 1994).

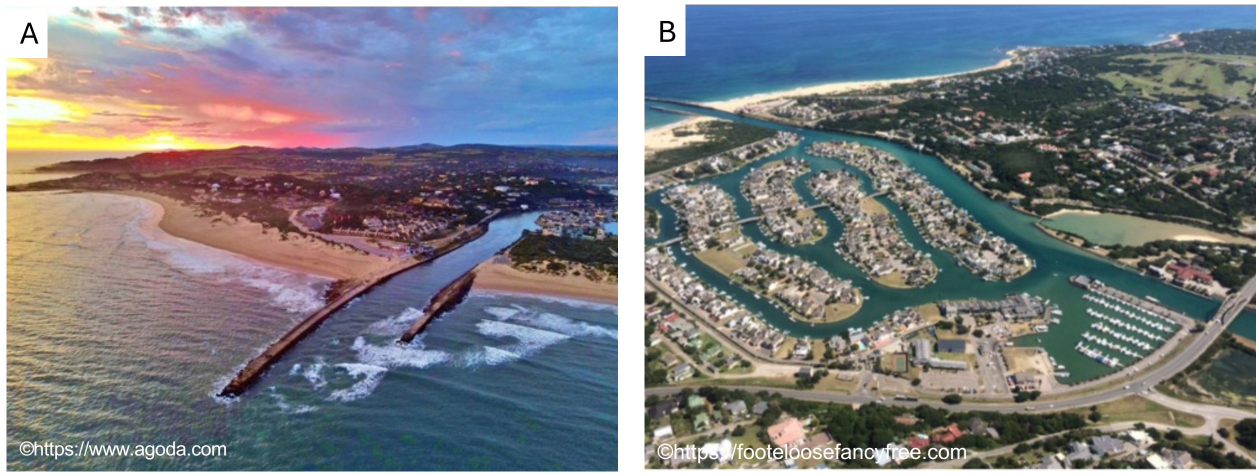

©https://www.agoda.com

©https://footeloosefancyfree.com

Figure 2.5. The aerial view showing the (A) artificially modified Kowie mouth and the (B) Port Alfred marina residential area including the surrounding land-use.

The river-estuary interface is just above the ebb and flow (approximately 21 km from the mouth) and is followed by the Kowie River (Figure 2.4) which extends approximately 70 km inland, with two main tributaries, the Bloukrans and Lushington rivers. The Kowie River drains a catchment area of 576 km² (Heinecken and Grindley 1982; James and Harrison 2010). Multiple dams and irrigation furrows along its length influence freshwater inflows, and water is also extracted to supply Port Alfred and surrounding areas. A dam, located 27 km from the estuary mouth, regulates flow. The catchment is predominantly agricultural, contributing nutrient-rich runoff and some sewage input (Heinecken and Grindley 1982). Several anthropogenic structures, including a causeway, have been constructed along the river, though most do not obstruct flow as the water level changes during the day (Figure 2.6A, B). The Kowie Weir situated at the tidal limit in the river may act as a barrier to fish movement during low-flow periods (Heinecken and Grindley 1982) (Figure 2.6A, B); however, a fish ladder has been built to facilitate movement between the estuary and river during periods of high flow (Figure 2.7C, D) (also see Figure 2.4).

Figure 2. 6. The causeway at Kowie River on the 7 October 2022 (A) at 10h28 during spring high tide, and (B) at 15h11 during the outgoing tide.

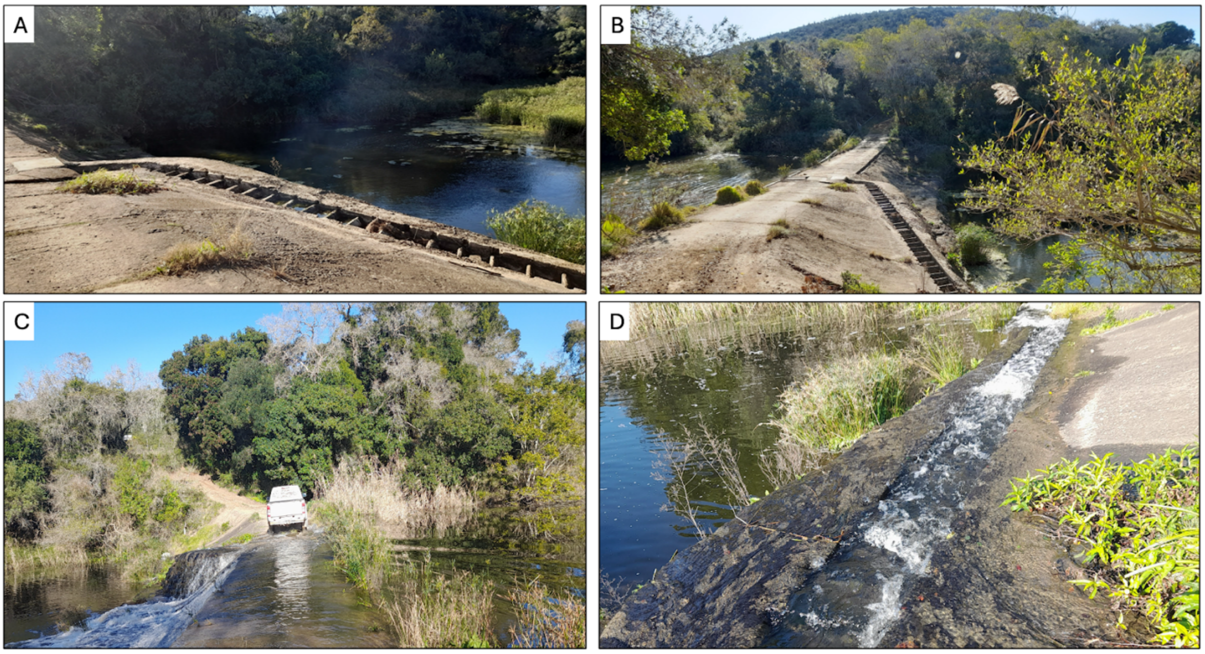

Figure 2.7. The Kowie Weir and fish ladder during (A and B) low flow on the 7th July 2022 and (C and D) high flow on the 2 August 2023.

The Kowie Estuary supports a diverse fish assemblage (Whitfield 1994), with 46 recorded species, of which members of the Mugilidae and Sparidae families dominate

(James and Harrison 2010). The presence of mature, immature and newly recruited individuals highlights the estuary's importance as a nursery habitat for estuary-associated species. This nursery function is critical for sustaining resident fish populations and maintaining connectivity between marine and freshwater environments.

Seasons in this study were classified according to the South African Weather Services as follows: summer – December to February, autumn – March to May, winter – June to August, and spring – September to November (SAWS 2025). The climate of Port Alfred is temperate, with this region lying in a transition zone where rainfall seasonality is less pronounced, but can follow a spring-autumn bimodal pattern (James and Harrison 2010). The area receives an average annual rainfall of 650 mm (Heinecken and Grindley 1982). The Kowie River has a mean annual runoff of 40.6 x 10^{-6}.m^3, with peak flows typically occurring in March and August (Heinecken and Grindley 1982).

The environmental data used in this study were obtained from four primary sources. First, the South African Weather Service (http://www.weathersa.co.za) provided data on air temperature (°C), rainfall (mm), wind speed ($m.s^{-1}$) and wind direction recorded at the Port Alfred airport station (ID: 00375741; -33.5590° S, 26.8800° E). Second, river flow data were sourced from the Department of Water and Sanitation (https://www.dws.gov.za) recorded at the Bathurst station (ID: P4H001, -33.50677° S, 26.74440° E) (See Figure 2.4). Third, the long-term temperature data spanning over a decade, were obtained from the Acoustic Tracking Array Platform (ATAP), which, in addition to a nationwide network of acoustic receivers (Murray et al. 2022), maintains three inshore coastal monitoring acoustic receiver stations with temperature loggers located off the east coast of Port Alfred –three offshore stations: PA001 (33.58778° S, 26.99384° E; 31 m depth), PA002 (33.59359° S, 26.99729° E; 34.4 m depth), and PA003 (33.59972° S, 26.99986° E; 39.9 m depth), and one 0.6 km upstream of the estuary mouth (Mouth). These moorings have been recording water temperature since 2012 using either temperature loggers (HOBO Pro V2 U22-001, 2012 to October 2016) or the temperature sensors in acoustic receivers themselves (model VR2AR, Innovasea, Halifax, Canada; October 2016 to 2024) every hour, for 12 years; 2012 to 2024. Lastly, during this study, *in situ* temperature and salinity were recorded at multiple stations along the Kowie Estuary, including the lower, middle and upper reaches (Figure 2.4).

Between January 2023 and June 2024, the daily average air temperatures in Port Alfred ranged from 9.4 to 26.8 °C, with a mean daily temperature of 17.9 ± 4.1 °C, and a range of 2.7 °C (minimum) and 37.9 °C (maximum) (Figure 2.8A). Total rainfall for this period was 548 mm, with the highest daily rainfall recorded on 01 June 2024 (76.4 mm, winter), followed by late September 2023 (51.4 mm, spring). Daily rainfall averaged 1.8 ± 5.9 mm, ranging from 0 to 76.4 mm. The daily average river flow rate during the study period was 0.58 ± 1.4 $m^3.s^{-1}$, with values ranging from 0.007 $m^3.s^{-1}$ in February (summer) to 14.3 $m^3.s^{-1}$ in mid-October (spring), following a high-rainfall event (Figure 2.8B). A second peak in river flow was 2.7 $m^3.s^{-1}$ in June 2024 (winter), coinciding with the highest recorded rainfall during the study period (Figure 2.8C).

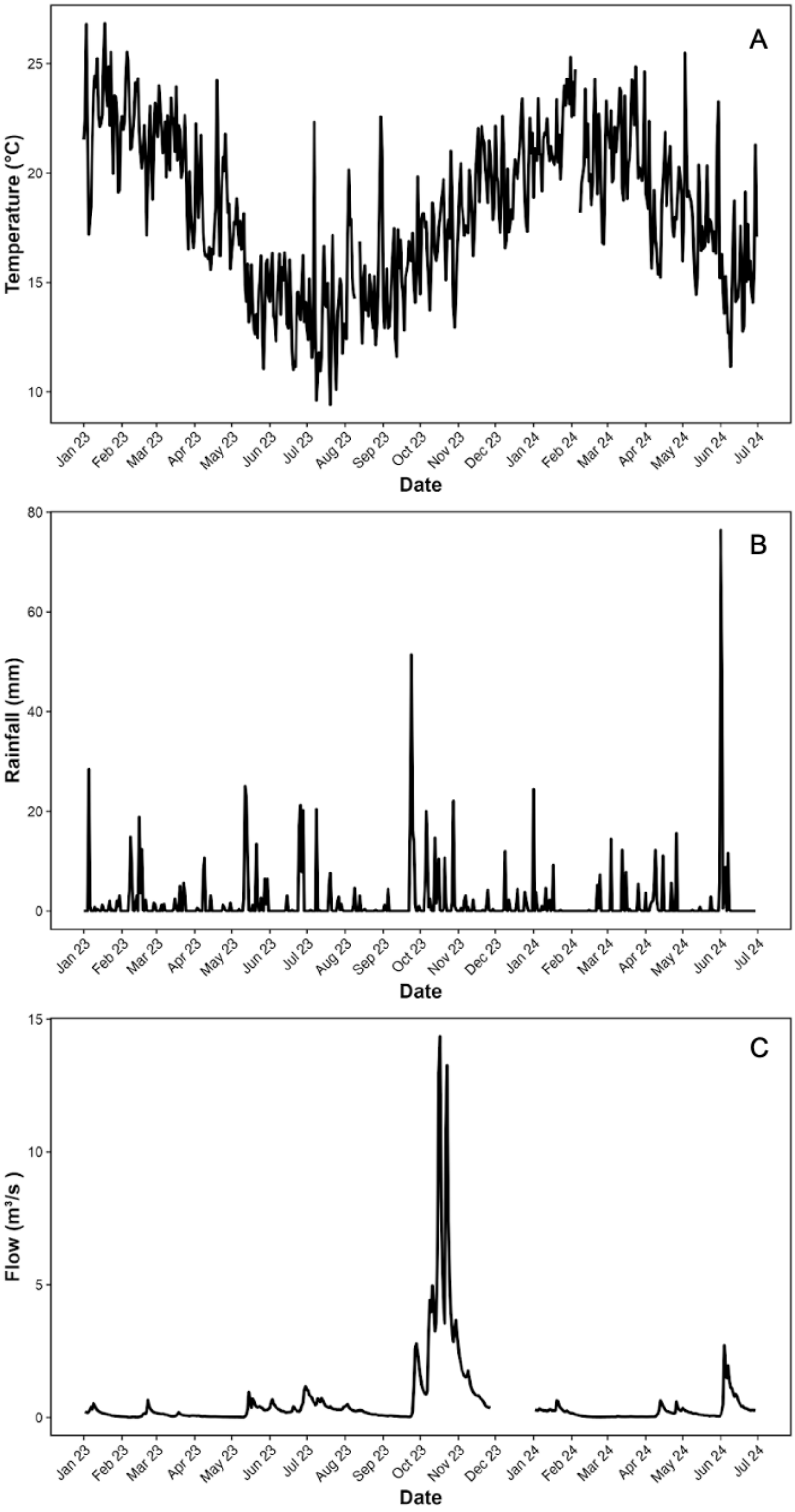

Figure 2.8. (A) Average daily air temperature and (B) total daily rainfall at Port Alfred (data obtained from the South African Weather Service), and (C) average daily river flow of the Kowie River (data obtained from the Department of Water and Sanitation) from January 2023 to June 2024.

During the study period, easterly winds dominated in summer, shifting to much stronger westerly winds in winter (Figure 2.9). The daily wind speed ranged from 2.4 to 5.5 m.s^{-1} with an average of 4.0 ± 2.2 m.s^{-1}. Stronger winds were, on average, recorded in winter and spring compared to summer and autumn.

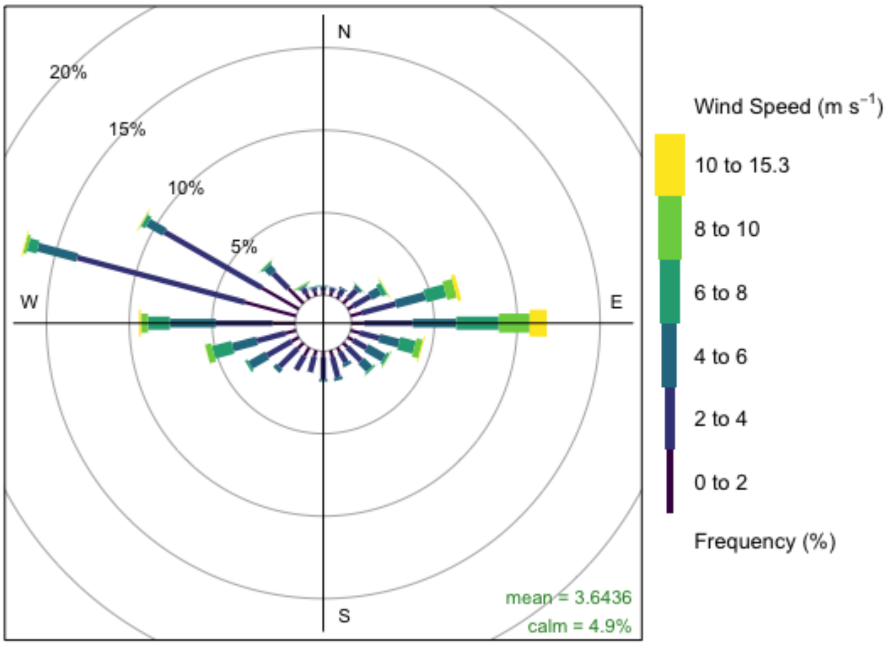

Figure 2.9. Wind speed and direction recorded at Port Alfred by the South African Weather Service between January 2023 and June 2024. The lighter the colour, the stronger the wind speed.

The Port Alfred coastline is influenced by the south-flowing warm Agulhas Current (Schumann et al. 2001; Lutjeharms et al. 2000), with inshore water temperatures in the past decades varying seasonally between 14 and 20 °C (Grant et al. 2017).

On average annual temperature at the mouth was higher than the three inshore coastal stations (PA001–PA003), with an average annual temperature of 17.7 ± 1.7 °C (min: 17.1 °C in 2021 and max: 18.2 °C in 2013 and 2023), compared to 14.2 – 14.7 °C at the three marine inshore stations. The three inshore stations had similar temperatures, with PA001 averaging annual temperature of 14.7 ± 1.6 °C (min: 13.8 °C in 2014, max: 15.5 °C in 2019 and 2020), PA002 averaged 14.2 ± 1.4 °C (min: 12.9 °C in 2022, max: 15.8 °C in 2020) and lastly, the furthest inshore coastal station, PA003, had an average temperature of 14.2 ± 1.4 °C (min: 13.6 °C in 2018, max: 14.7 °C in 2023) (Figure 2.10).

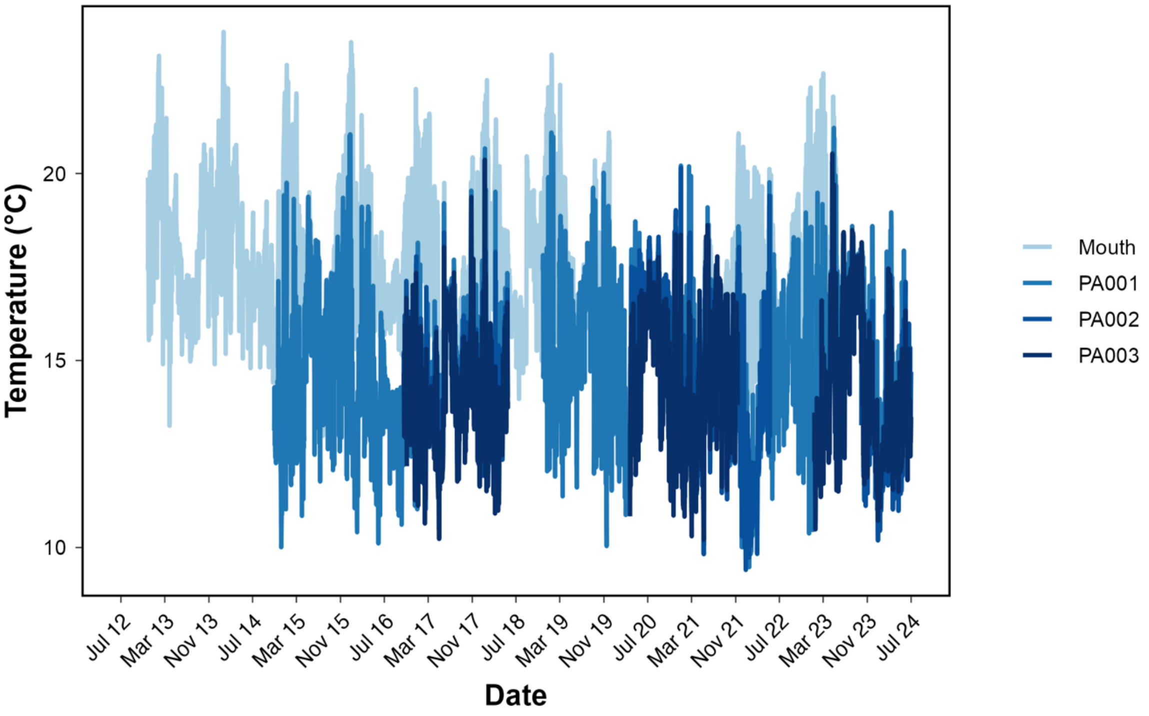

Figure 2.10. Daily average water temperatures recorded in the Kowie Estuary mouth (Mouth) and at three inshore coastal stations (PA001, PA002, PA003) at Port Alfred from July 2012 to June 2024.

To complement these historical records, temperature and salinity loggers (AquaMeasure, Innovasea, Canada) were deployed every 5 km along the length of the Kowie Estuary as part of this study (Figure 2.4), recording fine-scale temperature and salinity data every 30 minutes from July 2023 to June 2024. The water temperature recorded during this study period was averaged to represent the three environments: the river temperature was the average of two uppermost loggers (located approximately 20 and 21 from the mouth), the estuary temperature was the average of the four loggers deployed in the lower-middle reaches of the estuary (located approximately 2, 6, 10 and 15 km from the mouth), and finally, the sea temperature was an average of three inshore loggers.

The average river temperature during the study period was 27.7 ± 4.35 °C, reaching a minimum of 11.08 °C on the 21 July 2023 (winter) and maximum of 31.08 °C on the 5 February 2024 (summer) (Figure 2.11). The average estuary temperature was 20.1 ± 3.52 °C, reaching a minimum of 11.9 °C on the 9 July 2024 (winter) and maximum of 29.7 °C on the 12 March 2024 (summer) (Figure 2.10). The average sea temperature was 16.0 ± 1.99 °C, with a minimum of 9.8 °C recorded on the 30 December 2023 (summer) and a maximum of 19.7 °C on the 13 March 2024 (during autumn) (Figure 2.11).

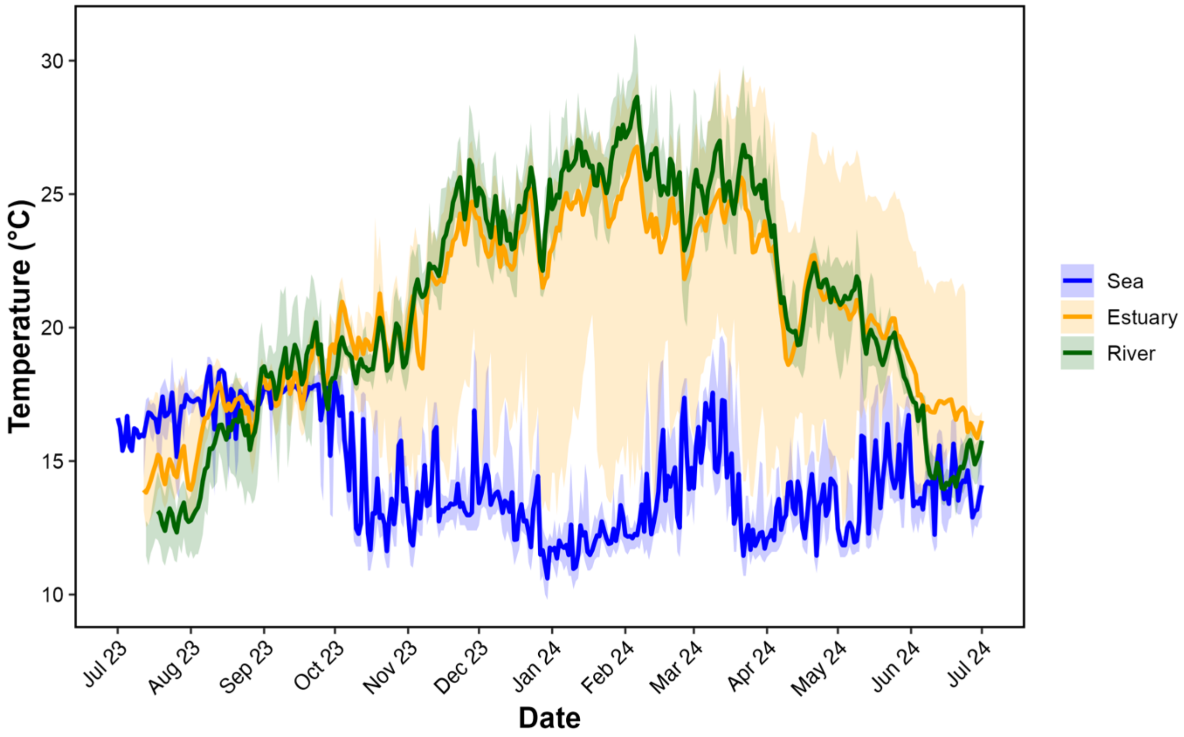

Figure 2.11. The *in situ* river, estuary and sea temperature recorded during the study period from July 2023 to June 2024 in and adjacent to the Kowie Estuary, South Africa. The bold line shows the daily average and the shaded lines indicate the daily minimum and maximum temperature recorded in each environment (river, estuary and sea).

Salinity at the surface and bottom of the Kowie Estuary generally follows a decreasing gradient from 32.9 to 24.7 and decreases in the upstream direction (James and Harrison 2010). Due to tidal influence, riverine water is typically brackish, with salinity around 2, but during prolonged river floods, vertical stratification can cause surface salinity to drop to nearly 0 (Heinecken and Grindley 1982). Salinity at the estuary mouth typically ranges between 22 and 35 as a result of the tides, droughts and flood events (James and Harrison 2010). The salinity logger deployed in the lower reaches (2 km from the mouth) during this study (July 2023 to June 2024) (Figure 2.4) became buried in sand in January 2024, limiting data availability beyond that point. Prior to this (June 2023 to January 2024), salinity in the lower reaches ranged from 15.8 to 35.1, with an average of 31.2 ± 3.2. In the middle reaches (6 km from the mouth), salinity ranged from 12.4 to 25.2, with an average of 19.2 ± 2.9, while in the upper reaches (20 km from the mouth), salinity varied between 0.8 and 11.9, averaging 6.5 ± 3.7 (Figure 2.12). Salinity fluctuations corresponded with changes in river flow, particularly after rainfall events (see Figure 2.7B). For example, an increase in river flow in October 2023 resulted in a marked decrease in salinity in both the upper and lower reaches, while the middle reaches appeared less affected (Figure 2.8C and Figure 2.12).

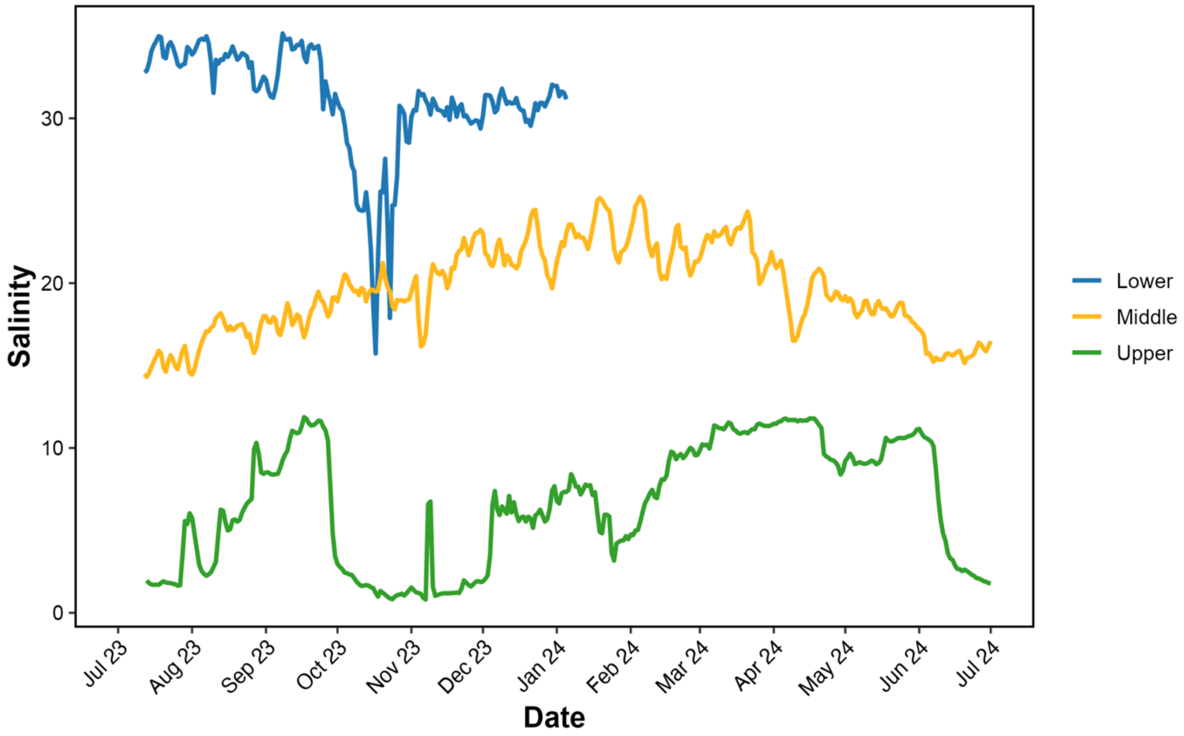

Figure 2.12. The *in situ* average daily salinity recorded at different stations at various reaches (blue – lower, yellow – middle, green – upper) within the Kowie Estuary, South Africa from July 2023 to June 2024.

CHAPTER 3

HABITAT CONNECTIVITY, ESTUARINE USE AND THE EFFECT OF SELECTED ENVIRONMENTAL FACTORS ON SPACE USE

3.1. Introduction

In aquatic ecosystems, landscape connectivity i.e. movements among resources patches which are either facilitated or impeded by the landscape, plays an important role not only in ecological functioning, but also species distributions and persistence (Taylor et al. 1993; Green 1994). Landscape connectivity has two main forms – structural and functional connectivity. While structural connectivity describes the physical features and arrangement of the landscape, such as the longitudinal link of the river, estuary and sea in an aquatic context, functional connectivity describes the individual movement patterns through connected patches or spatially distinct habitats as defined by species-specific traits and environmental conditions (adapted from Taylor et al. 1993). Functional connectivity in the marine environment has been increasingly studied in the last decade, focusing on the functional link between spatially distinct habitats at sea, and at the terrestrial and marine interface (Darnaude et al. 2022); for example, the spatial and temporal exchange of energy, genes, individuals and populations.

Because individual spatial and temporal movements between connected habitats vary in response to a changing environment (Secor et al. 1995; Cooke et al. 2022), a thorough understanding of this relationship for a species can provide crucial insights on ecosystem functioning (Olds et al. 2012; Carr et al. 2017) and species-specific ecology (Able 2005; Donaldson et al. 2014). Both these insights are crucial for the development of efficient management and conservation plans, including mitigating synergistic effects of human activities and climate change (Cooke et al. 2022; Welch et al. 2025). As such, the extent of habitat connectivity has been shown to be an important factor to consider for the success of conservation initiatives (Olds et al. 2012; 2016). Most marine species exhibit variability in their dependence on coastal habitats such as estuaries across life stages, or in response to changing environmental conditions (Whitfield 1994; Cooke et al. 2022), and their ability to successfully complete their life cycle is influenced by both the structure and functionality of their connected habitats (Grober-Dunsmore et al. 2009).

Mugil cephalus occurs in various coastal environments (Whitfield et al. 2012). It has been described as a facultative estuarine user (Whitfield 2020; Whitfield et al. 2023), capable of flexible habitat use, including using estuaries as nurseries or transitional zones between freshwater and marine environments (Whitfield 2020), but in some cases, completing its entire life cycle solely within the marine environment (Chang et al. 2004a; Górski et al. 2015; Fortunato et al. 2017). Furthermore, this species exhibits diverse levels of estuarine dependency such that a single population may consist of sub-populations with diverse strategies for spawning and habitat use in different regions across its distribution range (Whitfield et al. 2012), and this can be attributed to variations in environmental conditions and habitat connectivity.

One of the most effective tools used to study the movement behaviour and drivers of habitat use of aquatic species in their natural environment is acoustic telemetry (described in Chapter 1). Given the interconnectedness of habitats (particularly across the river-estuarine-marine ecotone as is the case for *M. cephalus*), Welch et al. (2025) highlighted the fundamental role of acoustic telemetry in assessing fish connectivity across seascapes, and provided a conceptual framework in which researchers can use to understand this link for improved conservation and management of fishes. In this framework, habitat connectivity is described at two spatial scales: inter-seascape connectivity, which is movements of animals between different large-scale seascape habitats (such as movement between the estuary and sea and/or other estuaries), and intra-seascape connectivity, which is the movement of animals within a seascape (small-scale connected habitat such as estuary reaches and including estuary-river interface and estuary-sea interface) (Welch et al. 2025). Through tracking individual fish and monitoring environmental variables simultaneously, acoustic telemetry also provides an opportunity to determine both individual and population level responses to environmental change (Crossin et al. 2017). Using telemetry, several studies have modelled fish movement and found that water temperature, photoperiod, flow and geophysical cycles play a significant role in shaping daily fish movement and habitat selection (e.g., Currey et al. 2015; Grant et al. 2017). Water temperature, in particular, is a fundamental regulator of physiological processes, influencing metabolic rates, stress responses and behavioural thermoregulation (Brett 1971; Beitinger et al. 2000).

Previous studies have shown that similar to *M. cephalus,* some species can experience physiological stress under rapid temperature fluctuations, making movement a crucial strategy for avoiding unfavourable conditions (Heupel and Simpfendorfer 2008). With the current projections of climate change in the global south, temperate species, for example, are expected to extend their distribution northward in winter (James et al. 2013; 2016), and most estuary-associated species are predicted to face thermal bottlenecks (Grant et al. 2017). Estuaries, situated at the interface of riverine and marine systems, are highly vulnerable to climatic shifts from both terrestrial and oceanic sources, and the projected changes, such as rising temperatures, altered rainfall patterns, rise in sea level, frequency and intensity of climate extremes are anticipated to lead to changes in salinity gradients which will impair key ecological processes, including the use of estuaries as suitable nursery habitats for estuary-associated species (Gillanders et al. 2011b; James et al. 2016; van Nierkerk et al. 2022). Understanding the movement and habitat use of estuary-associated species such as *M. cephalus* is important, particularly in the context of changing climate in order to assess their vulnerability to shifting environmental conditions and inform adaptive management strategies for estuarine ecosystems.

Currently, there is limited information about the movement behaviour and habitat use of *M. cephalus* in South Africa. However, given their high levels of exploitation, with large daily bag limits (at least 50 fish per person per day) and no size limits (Whitfield and Lamberth 2012), and the anticipation that temperate species' (such as *M. cephalus*) distributions may change with changes in the climate (James et al. 2013), understanding movement and habitat connectivity of this species is crucial. Therefore, this chapter aimed to examine the movement patterns and habitat connectivity of *M. cephalus* in a temperate coastal system, the Kowie Estuary, using acoustic telemetry. The specific objectives were to:

1. Evaluate the habitat connectivity between the Kowie Estuary, the adjacent marine environment and neighbouring estuaries,
2. Assess the spatial and temporal use of the Kowie Estuary, and
3. Assess the effects of temperature on movement patterns within the estuary.

3.2. Methods and materials

3.2.1. Acoustic receiver array

An array of stationary acoustic receivers (VR2W-69 kHz, Innovasea, Halifax, Canada) were deployed approximately 1 km apart in the main channel of the Kowie Estuary, from the mouth to the upper reaches (see Chapter 2 for full study site description) (Figure 3.1). An additional three receivers were deployed in the Royal Alfred Marina near the mouth and three in the Kowie River (Figure 3.1). To quantify movements of tagged fish into other estuaries (i.e., habitat connectivity), acoustic receivers forming part of the greater Acoustic Tracking Array Platform (ATAP), an expanded network of acoustic receivers along the South African coastline (Cowley et al. 2017; Murray et al. 2022) managed by the South African Institute for Aquatic Biodiversity, were deployed in the neighbouring Bushmans Estuary (~25 km west), Kariega Estuary (~23 km west), Kleinemonde coastline (~16 km east) and Great Fish Estuary (~28 km east) (Figure 3.1).

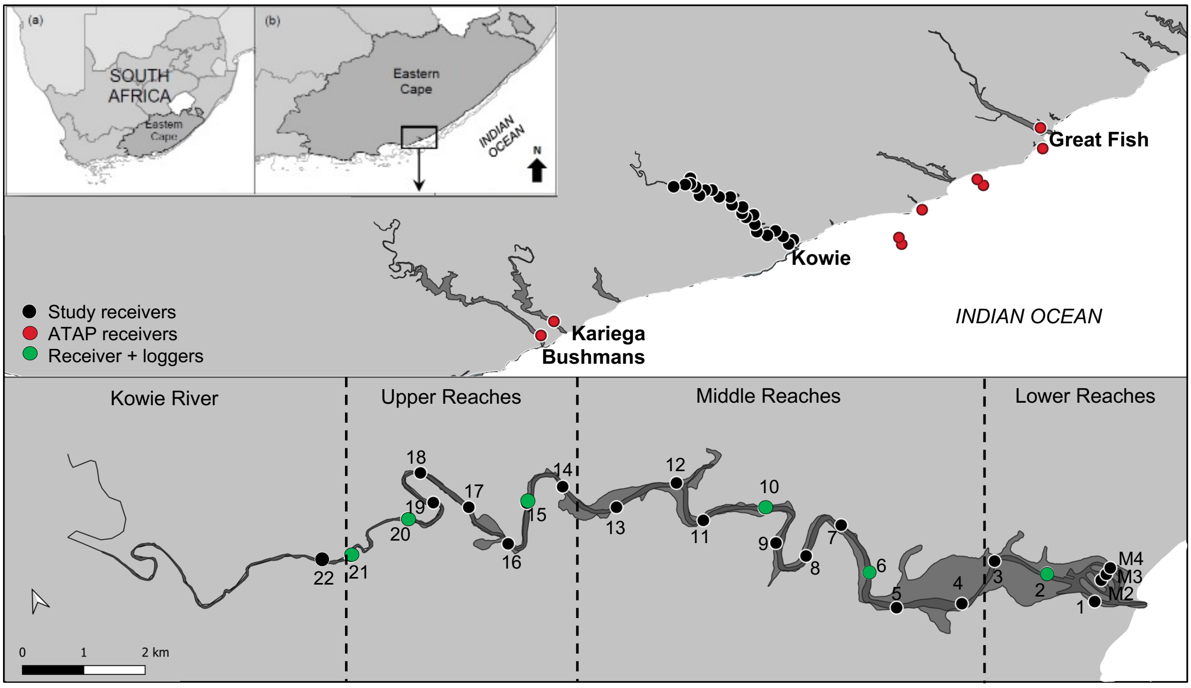

Figure 3.1. Map of the Kowie Estuary and neighbouring estuaries showing the position of acoustic receivers deployed during the study period. The Kowie Estuary is divided into three reaches based on sedimentation patterns and salinity (following Heinecken and Grindley 1982). Green dots represent temperature loggers deployed between July 2023 and June 2024.

Prior to deployment, all receivers were coated with anti-fouling paint (International® Micron Extra 2, Biolux® Technology) and placed in a PVC pipe which was embedded on a concrete mooring block to prevent displacement as a result of strong tides (Figure 3.2).

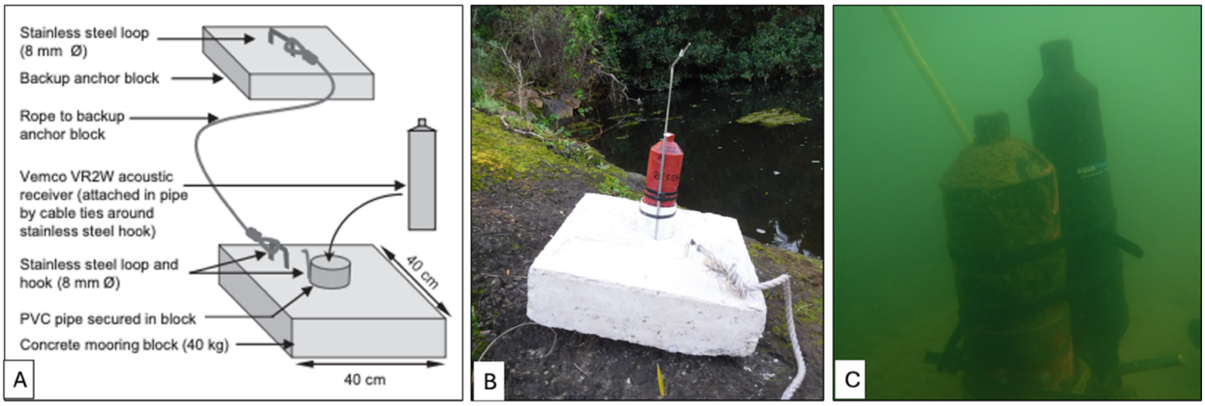

Figure 3.2. (A) The standard mooring design used by the Acoustic Tracking Array Platform for receivers deployed in estuaries (after Cowley et al. 2017), (B) a standard cement block mooring with receiver (painted red) inserted ready for deployment, and (C) a photograph of the mooring underwater. The smaller black receiver is an AquaMeasure (Innovasea, Canada) logger which recorded *in situ* salinity and temperature.

3.2.2. Fish collection and tagging

A total of 21 *M. cephalus*, consisting of juveniles to adults, were caught in the Kowie Estuary using cast nets from a boat between 7 December 2022 and 23 May 2023 (Table 3.1). Upon capture, the fish were placed in a 40-L black rectangular tub containing fresh estuarine water from the capture location and 2-phenoxyethanol (concentration of approximately 0.5 ml.l^{-1}) which was used to anaesthetise the fish. After losing equilibrium, fish were placed ventral-side up in a V-shape sling for transmitter insertion with a continuous supply of fresh estuarine water slowly poured over the gills throughout the surgery. A wet cloth covered the eyes to reduce stress and fish were handled minimally and with wet hands to reduce loss of mucous from the surface layer of the fish. A small opening (1.5–2 cm) was made on the ventral musculature behind the pelvic fin through which an acoustic transmitter was inserted into the body cavity and closed with two independent sutures (silk sutures, Clinisilk black braided silk suturesn3/0). Two types of acoustic transmitters were used: 69 kHz coded V9-2L (Innovasea, Halifax, Canada) (n = 18), which have a diameter of 9 mm, a length of 29 mm, weighing 4.7 g in air and 2.9 g in water battery life, estimated battery life of 476 days and a nominal delay 60 seconds (emitting a signal every 30 to 90 seconds), and 69 kHz coded V13-1L (Innovasea, Halifax, Canada) (n = 3), which have a diameter of 13 mm, a length of 36 mm, weighing 11 g in air and 6 g in water, estimated battery life of 1460 days and a nominal delay of 120 seconds (emitting a signal every 80 to 160 seconds). Each transmitter had a unique ID code. The standard length (SL) of each fish was calculated based on the measured relationship between SL and TL: SL = 0.737(TL) + 6.5613 (James, NRF-SAIAB, unpublished) and used to calculate the fish mass based on the length-weight relationship of *M. cephalus* in South African estuaries; $Wt(g) = 0.0233 \times SL\ (cm)^{0.979}$ (Harrison 2001). Based on the fish weight, efforts were made to follow Winter (1996)'s recommendations that the in-water weight of the acoustic transmitters should not exceed the recommended limit of 2% of the individual fish's mass. Post-surgery, a wound gel powder (antibacterial powder), which turns into a paste on contact with water, was placed on the closed wound to deter infection. The fish was then placed in a 40-L black rectangular tub of fresh estuarine water (different to the tub used for the anaesthesia bath) and allowed to fully recover (recognised through regular opercula beat and swimming in an upright position) before being released back at the capture site. Each fish was handled for an average of 8 min ± 2.4 min (mean ± SD), including anaesthetisation, measurements and surgery (incision, transmitter insertion and suturing), followed by recovery before being released (Table 3.1). Efforts were made to distribute capture locations throughout the estuary to reduce bias in movement behaviour; however, almost all fish were captured between 3 to 6 km from the mouth with an exception of one fish captured 14 km from the mouth (Figure 3.1).

3.2.3. Data acquisition

Each time a tagged fish was within the range of an acoustic receiver, its transmitter ID, date and time of detection were automatically logged. Based on previous studies in the Kowie Estuary, the detection range in this system is between 200 and 550 m (Grant et al. 2017) and given that the system is 100 m at its widest, is it therefore unlikely that a fish would pass a receiver without being detected. Receivers were retrieved every six to eight months, and data were downloaded from the receivers using Innovasea's VUE software and exported as .csv files for further data processing. All raw acoustic detection data were filtered prior to analyses to improve data quality and biological interpretation (Heupel et al. 2006; Kessel et al. 2014). Firstly, data from the initial 24-hour period post-release were excluded from all individual datasets. This is a standard procedure commonly applied to mitigate the effects of post-capture stress and tagging-induced behavioural alterations which can include reduced activity, erratic movement, or temporary displacement unrelated to natural behaviour (Hartill et al. 2003). To identify and remove false or biologically implausible detections, the *Explore* function from the *actel* package (Flávio and Baktoft 2021) using RStudio (R Core Team 2024) in R (Version 4.4.1) was used to visualise and inspect detection sequences across stations thus identifying anomalies. Transmitter loss was inferred when an individual showed prolonged detection at a single receiver location (i.e. no detection elsewhere) for more than 90 consecutive days followed by no subsequent detections for the remainder of the study. This stationary detection pattern is a strong indicator of transmitter loss or fish mortality. However, detections recorded prior to the stationary period were retained for analysis. The analysis period was constrained from 1 March 2023 to 30 April 2024 since more than 50% of individuals had been tagged by March 2023.

Table 3.1. Summary of tagging data for 21 *Mugil cephalus* captured in the Kowie Estuary (December 2022–May 2023), including fish code, fork length (mm FL), total length (mm TL), standard length (mm SL), Weight (g), tag date, tag type, surgery and recovery duration (minutes: seconds) and capture location. Fish are ordered by fish length (smallest to largest), and are grouped in life stages (sub-adult and adult).

Life stage	Fish code	FL (mm)	TL (mm)	SL (mm)	Weight (g)	Tag date	Tag type	Surgery time (min:sec)	Recovery time (min:sec)	Capture location (Station number)
Sub-adults	FH1	183	201	66.6	81.4	02/02/2023	V9-2L	08:31	00:48	3
	FH2	186	205	70.1	86.2	02/02/2023	V9-2L	07:52	00:57	3
	FH3	224	254	123.9	159.3	16/05/2023	V9-2L	07:13	05:58	3
	FH4	243	268	143.6	185.9	14/03/2023	V9-2L	08:51	02:19	6
	FH5	245	264	137.7	178.0	07/12/2022	V9-2L	06:31	00:31	14
	FH6	257	286	171.8	224.2	02/05/2023	V9-2L	07:57	02:35	5
	FH7	260	290	178.6	233.4	09/03/2023	V9-2L	09:04	01:46	4
	FH8	260	289	176.9	231.1	09/03/2023	V9-2L	10:26	03:19	4
	FH9	305	336	270.1	357.6	23/05/2023	V9-2L	07:01	00:48	5
	FH10	319	352	308.2	409.3	14/03/2023	V9-2L	06:03	02:22	6
	FH11	353	398	437.8	585.1	02/02/2023	V13-1L	08:35	02:23	6
	FH12	388	428	539.6	723.2	02/02/2023	V13-1L	07:49	02:26	6
	FH13	392	445	603.7	810.3	02/02/2023	V13-1L	10:57	02:31	6
	FH14	399	452	631.6	848.1	14/03/2023	V9-2L	08:21	06:24	4
	FH15	415	445	603.7	810.3	23/05/2023	V9-2L	08:56	00:55	4
	FH16	416	472	715.9	962.5	10/03/2023	V9-2L	09:55	05:43	5
	FH17	416	473	720.3	968.5	16/05/2023	V9-2L	06:31	05:15	4
Adults	FH18	439	492	807.5	1086.7	16/05/2023	V9-2L	06:52	05:18	4
	FH19	459	519	943.1	1270.7	10/03/2023	V9-2L	07:11	02:40	6
	FH20	462	525	975.1	1314.2	14/03/2023	V9-2L	07:17	03:42	5
	FH21	507	574	1264.7	1707.1	23/05/2023	V9-2L	06:01	03:10	4

3.2.4. Data analysis

All analyses and data visualisations were conducted in R version 4.1 (R Core Team 2024) and Microsoft Excel (Office 365). All data were tested for statistical model assumptions and when assumptions were not met, the equivalent non-parametric analyses were used.

Habitat connectivity

The number of days *M. cephalus* spent at sea after exiting the estuary were identified by filtering the individual detection data to show detections at the lower most receivers which included the estuarine mouth receiver (Station 1) and the three marina receivers (M2 to M4, Figure 3.1). The individuals that were last detected at one of these, followed by either a 24-hour or longer period of absence were assumed to have left the estuary, undertaking a sea trip (following Murray et al. 2018). The number of days spent at sea was estimated as the duration between the last detection within the estuary and the subsequent return.

For individuals that did not return to the Kowie Estuary after taking sea trips (n = 7, 41%) or were not recorded anywhere else along the coastline or other estuaries, the total time from their last estuarine detection to the end of the monitoring period (30 April 2024) was assigned as time at sea. Considering that several estuaries occur near the Kowie Estuary, including the permanently open Bushmans, Kariega and Great Fish, and the temporarily open/closed Kasouga, and West and East Kleinemonde, however, all the temporary open/closed systems were closed during this study period and all the permanently open estuaries had an acoustic receivers deployed approximately 1 km upstream of these estuary mouths.

This assumption is supported by observed patterns of *M. cephalus* including an individual (FH15), that departed from the Kowie Estuary on 10 April 2024 and not detected in neighbouring estuaries or any other ATAP coastal receivers until it returned to the Kowie Estuary on 15 September 2024 (5 months later, after the monitoring for this study was concluded). This long absence, followed by reappearance in the tagging estuary, indicates that some individuals may undertake extended sea trips without detections elsewhere in the ATAP coastal array. Trips to the neighbouring estuaries were confirmed by two or more detections on a particular receiver within the visited estuary. To define degrees of habitat connectivity, two terms were used: short-term movements, which referred to return trips to sea (left the Kowie Estuary and returned), and multiple habitat connectivity, which referred to trips to the neighbouring estuaries.

A residency index (RI) was calculated to assess overall residency to the Kowie Estuary and adjacent marine and estuarine environments. To calculate the RI, the total number of days a fish was detected (Dd) in each habitat (Kowie Estuary, sea or other estuaries) was divided by the number of days between first and last detection (Di) (Kraft et al. 2023). This method was fit for this study because it is specific to each individual and accounts for variation in overall detection duration among individuals, and allows for comparisons of spatial use irrespective of differences in the length of monitoring periods. To compare the RI across the three environments (Kowie Estuary, sea and other estuaries), since data did not meet assumptions of a parametric tests (Shapiro-Wilk test before and after transformation) the non-parametric Kruskal-Wallis rank-sum test was used followed by the post-hoc pairwise comparisons with Dunn’s test with Bonferroni-adjusted p-values using the *FSA* package (Ogle et al. 2025). Further, an abacus plot was used to visualise daily detections between different large-scale habitats representing habitat connectivity (Kowie Estuary, sea and neighbouring estuaries).

Spatial and temporal use of the estuary

All fish had time allocated to each station on which they were detected in the Kowie Estuary. To calculate the total time spent by individuals at each station, and subsequent reaches of the estuary (lower, middle and upper), the *glatos* package (Holbrook et al. 2024) was used to create detection events. Detection events were defined as temporally distinct sequences of subsequent detections of a fish at a given station. A one-hour threshold was selected to ensure that short absences resulting from potential missed detections (such as physical barriers, fluctuations in detection range, environmental interference and behaviourally driven movements like predator avoidance [Heupel et al. 2006; Kessel et al. 2014]) did not fragment continuous detection events.

Spatial use within the Kowie Estuary was quantified individually as the proportion of time (days or hours) spent within each reach (lower, middle, upper, Figure 3.1) and station divided by the total time each fish was detected. Because all the proportion data did not meet the assumptions for parametric tests, the data were transformed using square root-arcsine transformation to stabilise the variance and improve the normality of the data. Normality was tested using Shapiro-Wilk test and homogeneity of variance was tested with Levene’s test using the *car* package (Fox and Weisberg 2019). After assumptions of a parametric test were met, a one-way ANOVA was used to compare the proportions of time spent at different reaches followed by post hoc comparison using Tukey's Honestly Significant Difference (HSD).

To assess temporal use of the Kowie Estuary during the monitoring period, an abacus plot of daily detections at different habitats representing inter-seascape connectivity (Kowie Estuary, sea and neighbouring estuaries) was plotted, as well as daily detections at small-scale habitats (lower, middle and upper estuary reaches), representing intra-seascape connectivity. On the temporal scale, the monthly proportions of time each fish spent in different reaches and at stations were calculated. Furthermore, the daily fish position in the Kowie Estuary was calculated as the average daily positions of each fish using numerical station numbers since each station number (1 to 21) corresponded to distance in kilometres (km) from the mouth. Furthermore, for fish with longer monitoring periods (>300 days), the seasonal proportions (ranging from 0 to 1) of time spent in different estuary reaches were calculated and arcsine-square-root-transformed to approximate normality and compared using Linear Mixed-effects Model (LMM), fitted with restricted maximum likelihood (REML) in the *lme4* package (Bates et al. 2015). This was done to minimize underrepresentation in later periods of the study due to declining sample size. Seasons in this study were classified according to the South African Weather Services as follows: summer – December to February, autumn – March to May, winter – June to August, and spring – September to November (SAWS 2025) as described in Chapter 2. The proportion of time in each reach at a given season was the response variable and the fixed effects were the estuary reach, season and the interaction between the two, with fish code included as the random intercept accounting for repeated measures. Residual plots were used to validate the model diagnostics and post-hoc pairwise comparisons of means were conducted using the *emmeans* package (Lenth 2025).

Environmental variables (temperature, flow and time of day)

To compare the daytime and nighttime position of fish in the estuary, the average hourly position of each fish was calculated based on the where an individual spent majority of its time within a given hour, grouped into day and night and compared using a paired Student T-Test. To explore seasonal variation in water temperature across the three habitats, the daily averaged river, estuary and sea temperatures (described in Chapter 2), were further grouped into seasons and compared (Table 3.2). Since the data did not meet the assumptions of independence and homoscedasticity required for parametric tests (such as, two-way ANOVA) as a result of temporal autocorrelation and an unbalanced sample sizes, the data were fitted with a LMM model. The habitat consisted of three levels: river, estuary and sea; while season consisted of four levels and their interactions were treated as fixed effects, and month was included as a random intercept to account for variation and repeated seasonal sampling.

The results showed that there were significant difference in daily temperature across habitats ($F_{2,5124}$ = 1713.7, $p < 0.05$) and season ($F_{3,18.4}$ = 350.6, $p < 0.05$). On average, both river and estuary habitats were significantly warmer than the marine habitat throughout the year, with mean temperature differences of 6.5 °C and 6.1 °C, respectively. However, the interaction between habitat and season showed seasonal divergence; for example, river and estuary habitats experienced higher summer temperatures (+2.0 to +3.0 °C) relative to the sea and steep declines during winter (-6.3 to -7.8 °C) relative to the sea. The average estuary (24 ± 1.19 °C) and river summer temperatures (25 ± 1.39 °C) were significantly higher than the sea summer temperatures (15.9 ± 2.57 °C) ($p < 0.05$) (Table 3.2).

Table 3.2. Seasonal temperature (mean ± standard deviation °C) and range (minimum to maximum) recorded at sea, the Kowie River and Kowie Estuary between July 2023 and June 2024. Season is broken up by month and includes summer (Dec to Feb), autumn (Mar to May), winter (Jun to Aug) and spring (Sept to Nov) (SAWS 2025).

	Sea (°C)	**Min-Max**	**Estuary** (°C)	**Min-Max**	**River** (°C)	**Min-Max**
Summer	15.9 ± 2.57	8.8 - 21.9	24 ± 1.19	13.0 - 29.6	25.4 ± 1.39	20.0 - 31.0
Autumn	15.8 ± 2.08	9.4 - 22.3	21.8 ± 1.99	12.5 - 29.7	22.3 ± 2.67	17.2 - 29.8
Winter	16.1 ± 1.16	10.0 - 20.2	15.8 ± 1.41	11.9-23.1	14.8 ± 1.46	11.1 - 20.2
Spring	16.2 ± 1.88	9.1 - 20.6	20 ± 1.97	13.2 - 27.0	20.2 ± 2.40	14.2 - 28.4

During this study, selected environmental variables were modelled to determine their effect on the average daily position of fish. These variables included temperature (river, estuary and sea), flow (rainfall and river flow) and time of day. For the purpose of this analysis, stations M2 to M4 were assigned the value 1 and since Station 13 malfunctioned and could not be used, from Station 14 onward, each was assigned the next subsequent number.

Prior to modelling, correlations between river, estuary and sea temperatures were calculated using a Spearman Correlation test, after the Shapiro-Wilk test showed that none of the habitat temperature data were normally distributed ($p < 0.05$). The river and estuary water temperatures were strongly correlated ($r = 0.97$) and both negatively correlated with sea temperature ($r = -0.3$) (Figure 3.3). Since estuary and river temperatures were strongly correlated, likely due to their geographic proximity, including both in the model would have introduced redundancy and multicollinearity, and thus obscure the relative contribution of each variable. River temperature was retained because it exhibited greater seasonal changes and more extreme temperature fluctuations, making it particularly relevant for detecting its influence on the average daily position of tagged *M. cephalus*.

To determine the influence of time of day on fish position, the daytime (06:00 to 18:00) and nighttime (18:00 to 06:00) hourly fish positions of each fish were compared using a Wilcoxon signed rank exact test.

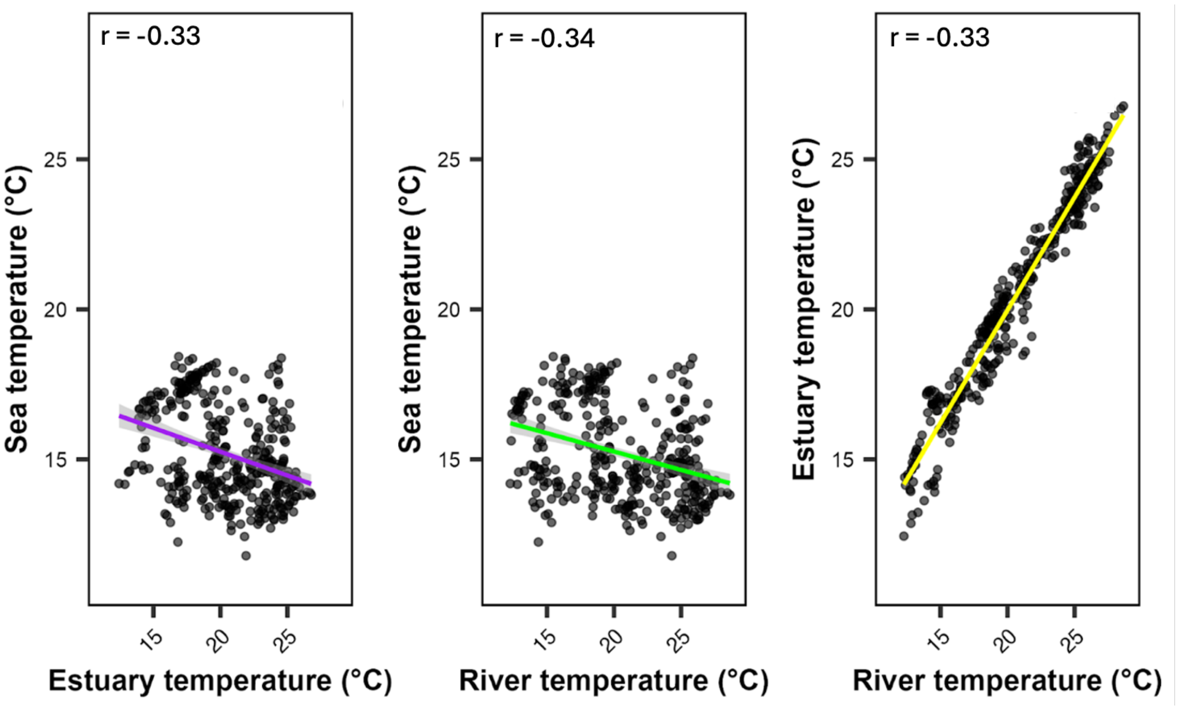

Figure 3.3. Scatterplots showing the Spearman correlation between temperatures recorded in the Kowie River, Kowie Estuary and sea between July 2023 and June 2024.

To determine whether selected environmental variables influenced the daily average position of tagged fish in the Kowie Estuary, LMM was fitted. The response variable was the average daily position of each individual, and the fixed effects were river and sea temperature, river flow and rainfall (square rooted). A random effects structure of individual fish code was included as a random intercept. The residual diagnostics were performed using the *DHARMa* package (Hartig 2024) to assess model fit and identify zero-inflation, or influential observations. To select the best model, the Akaike's Information Criterion (AIC) of multiple combinations of fixed effects calculated through the *MuMIn* package (Bartoń 2025) were compared, and the top ranked model was selected based on the lowest AIC value (Burnham and Anderson 2002) (see Appendix 1 for more model outputs).

3.3. Results

A total of 21 *M. cephalus* were acoustically tagged for this study, with a mean fork length (FL) of 339.4 ± 98.5 mm FL (range: 183 – 507 mm FL), comprising 17 sub-adults (183 – 416 mm FL) and four adults (439 – 507 mm FL) (L_{M50} = 440 mm FL, Wallace 1975, length at first maturity = 344 mm FL, Bok 1983). No data were collected on the three smallest fish tagged (F1, 183mm FL; F2, 186 mm FL; F3, 224 mm FL) most likely due to excessive tag burden, ranging from approximately 2.9 to 5.8% of their body weight, resulting in mortality within the first 24 hours post tagging.

Further, one individual (FH12, 388 mm FL) emigrated to sea shortly after release, and one (FH5, 245 mm FL) was likely subjected to fishing mortality within one week of tagging as it was last detected at Station 15 (Table 3.1). Due to a lack of, or few detections, a total of four fish were excluded from all analyses. Since fish tagging took place in multiple batches over a four-month period, fish were not monitored for the same length of time (Table 3.3; Figure 3.4). The first fish was tagged on 6 December 2022 and monitored for only 20 days, suggesting either fishing or natural mortality. Five fish were tagged in February 2023, eight in March 2023, and lastly seven fish in May 2023 (Table 3.3). The monitoring period was from 1 March 2023 to 30 April 2024, since the majority of fish were already tagged by the end of March 2023, spanning 427 days. The 17 analysed individuals were detected for periods ranging from 28 to 424 days (218 ± 135 days) (Figure 3.4).

The number of detection days per individual ranged from 11 to 479 days (199 ± 165 days), reflecting substantial variability in residency and activity patterns. Five fish were detected for more than one month, six individuals had detection periods exceeding six months, and six individuals were detected for more than 10 months. The number of detectable tagged fish in the estuary declined over time. Three individuals (FH8, FH9, and FH13; 260 – 292 mm FL) were inferred predated upon since their movement became stationary after several months of active movement; these transmitters were likely excreted into the estuary where they continued to emit signals at single stations until the end of the monitoring period. Fishing mortality was confirmed for one fish (FH4, 243 mm FL), which was recaptured and sold at a fish market in Durban, South Africa, more than 700 km from the tagging site (contacted via a contact number of a reward sticker on the transmitter). An additional six individuals (35%) were assigned fishing mortality, as their transmitters ceased transmitting entirely and were never detected again in the Kowie Estuary or the surrounding receiver array.

Table 3.3. Summary analysis data for 17 *Mugil cephalus* that were detected in the Kowie Estuary, South Africa between 1 March 2023 and 30 April 2024. Asterisk (*) represent individuals for which more than 300 days of data were collected (used for further analysis).

Life stage	Fish code	Fork length (mm)	First detection	Last detection	Total detections	Valid detected days	Number of stations detected on	Last station detected on
Sub-adults	FH3*	224	2023/05/16 18:37	2024/08/02 09:48	55467	442	19	5
	FH4	243	2023/03/14 20:31	2023/11/29 13:51	38001	258	21	21
	FH6	257	2023/05/02 19:52	2023/10/30 09:59	47916	179	20	3
	FH7	260	2023/03/09 18:40	2023/09/20 09:32	61589	166	17	Sea
	FH8	260	2023/03/09 19:21	2024/04/27 00:00	13006	45	19	17
	FH9	305	2023/05/23 18:16	2023/12/30 00:00	74914	219	17	10
	FH10*	319	2023/03/14 18:53	2024/04/09 12:25	79151	387	20	Sea
	FH11*	353	2023/02/02 23:00	2023/12/18 03:41	77994	316	20	Sea
	FH13*	392	2023/02/02 23:29	2023/12/28 00:00	53980	327	17	5
	FH14	399	2023/03/14 22:00	2023/10/13 10:13	11052	193	17	Sea
	FH15*	415	2023/05/23 22:28	2024/04/10 08:29	75012	320	20	Sea
	FH16*	416	2023/03/09 23:14	2024/04/07 09:01	59833	393	18	Sea
	FH17	416	2023/05/16 21:11	2023/07/12 00:00	5416	55	20	4
Adults	FH18	439	2023/05/16 20:30	2023/08/21 03:41	6425	73	18	Sea
	FH19	459	2023/03/09 23:40	2023/04/06 22:22	4417	26	9	5
	FH20	462	2023/03/14 20:56	2023/05/11 12:17	10735	56	19	Sea
	FH21	507	2023/05/23 20:09	2023/12/26 13:57	26729	215	18	4

During the study, two receivers (stations 13 and 22) malfunctioned and another two had limited data (i.e., Station 19: data available from 1 March and 20 October 2023 and Station 16: data available from 15 October 2023 to 30 April 2024). However, the close spacing of stations (approximately 1 km apart) ensured a robust detection coverage and effective tracking of *M. cephalus* within the Kowie Estuary. Furthermore, no fish was assumed to have expelled the transmitter because post-tagging recovery appeared to be rapid (Figure 3.4). This was evident for one individual that was recaptured by the research team one week after tagging, and showed signs of advanced wound healing and normal behaviour, suggesting low, short-term tagging stress and high, post-tagging survival (Figure 3.4).

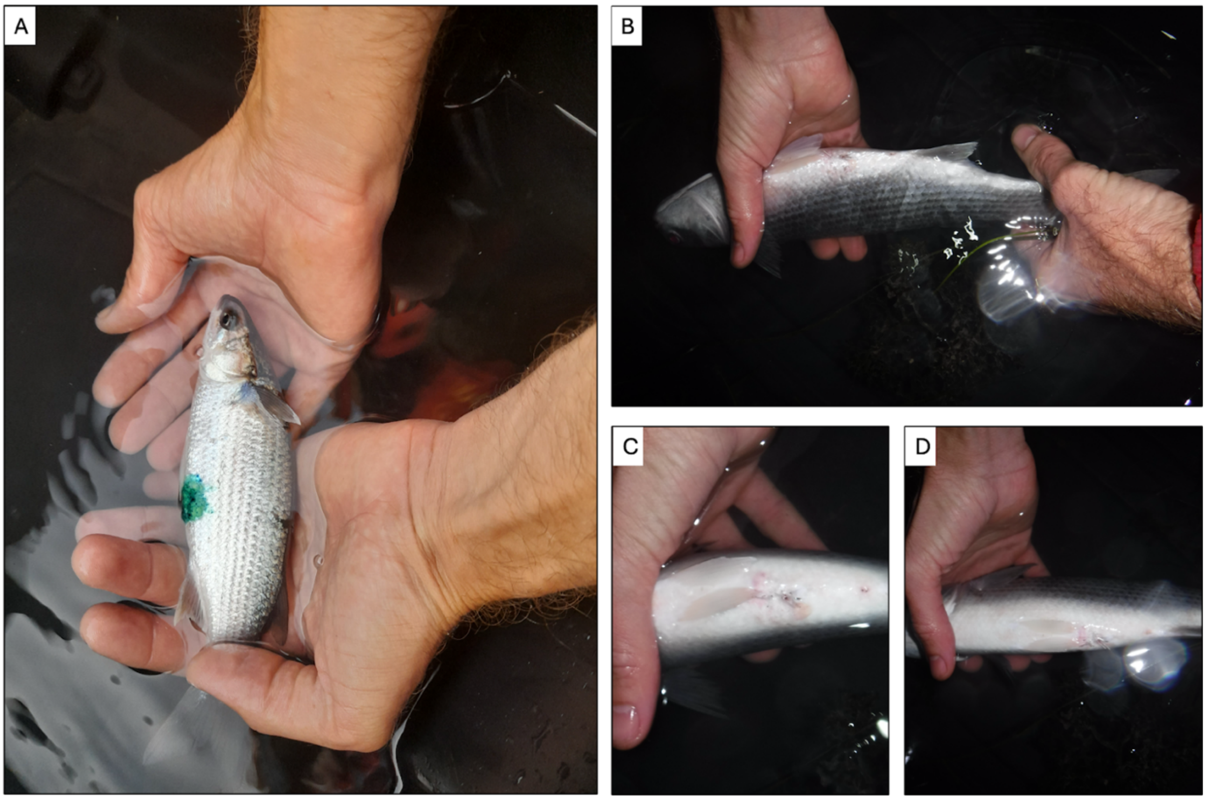

Figure 3.4. (A) Photo of a *Mugil cephalus* immediately after acoustic transmitter surgical insertion prior to release, and (B-D) photos of the same individual that was recaptured seven days post-surgical procedure, showing advanced signs of healing.

3.3.1. Habitat connectivity

During the monitoring period, 58% (n = 10) of tagged individuals of various sizes undertook at least one sea trip, together accumulating 15 sea trips. The number of sea trips undertaken by individuals ranged from 1 to 3 trips, and 50% (n = 5) of the fish returned to the Kowie Estuary at one point (return sea trip), of which 60% (n = 3) departed again. Of the seven fish (41%) that emigrated to sea during the monitoring period, one individual (FH15, 415 mm FL) returned to the Kowie Estuary five months after the end of the monitoring period. Sea trips (including movements to other estuaries) had a duration of between one and 30 days, and approximately half these trips were undertaken during the day (53%), with the other half at night (47%). Departures from the estuaries were not synchronised, with only two fish (FH14 and FH21) moving into the sea less than two hours apart on 13 October 2023 (Table 3.4; Figure 3.5). Fifty five percent (n = 6) of all sea trips occurred in autumn, 27% (n = 3) occurred in spring and 19% (n = 2) in winter (Table 3.4). The longest return sea trip was undertaken by FH21 (507 mm FL) in October 2023 and lasted 30 days (Figure 3.5).

Table 3.4. The overall information on sea trips undertaken by *Mugil cephalus* from the Kowie Estuary, including the departure date, time and season, habitats visited, frequency and length of sea trips and return date (where applicable) during the monitoring period (01 March 2023 to 30 April 2024). * represent departures of tagged fish that did not return to the Kowie Estuary.

Fish code	Date and time of departure	Season of departure	Habitat visited	Date and time of return	Duration of sea trip (days)	Total number of sea trips
FH7	11/03/2023 22:20 21/08/2023 03:48 17/09/2023 05:00	Autumn Winter Spring	Sea KLM Sea	16/03/2023 06:45 15/09/2023 11:46 -	5 15 *	3
FH8	13/03/2023 16:18 16/03/2023 02:49	Autumn Autumn	Sea Sea	14/03/2023 18:50 17/03/2023 09:55	1 1	2
FH10	09/04/2024 11:25	Autumn	Sea	-	*	1
FH11	01/12/2023 18:38 17/12/2023 23:52	Summer Summer	Bushmans Great Fish	11/12/2023 13:23 -	10 *	2
FH14	13/10/2023 09:13	Spring	Sea	-	*	1
FH15	09/04/2023 18:32	Autumn	Great Fish	-	*	1
FH16	06/12/2023 12:05 07/04/2024 08:01	Summer Autumn	Bushmans Sea	22/12/2023 06:53 -	16 *	2
FH18	30/07/2023 10:23	Winter	Sea	-	*	1
FH20	11/05/2023 11:17	Autumn	Sea	-	*	1
FH21	13/10/2023 07:39	Spring	Sea	12/11/2023 16:37	30	1

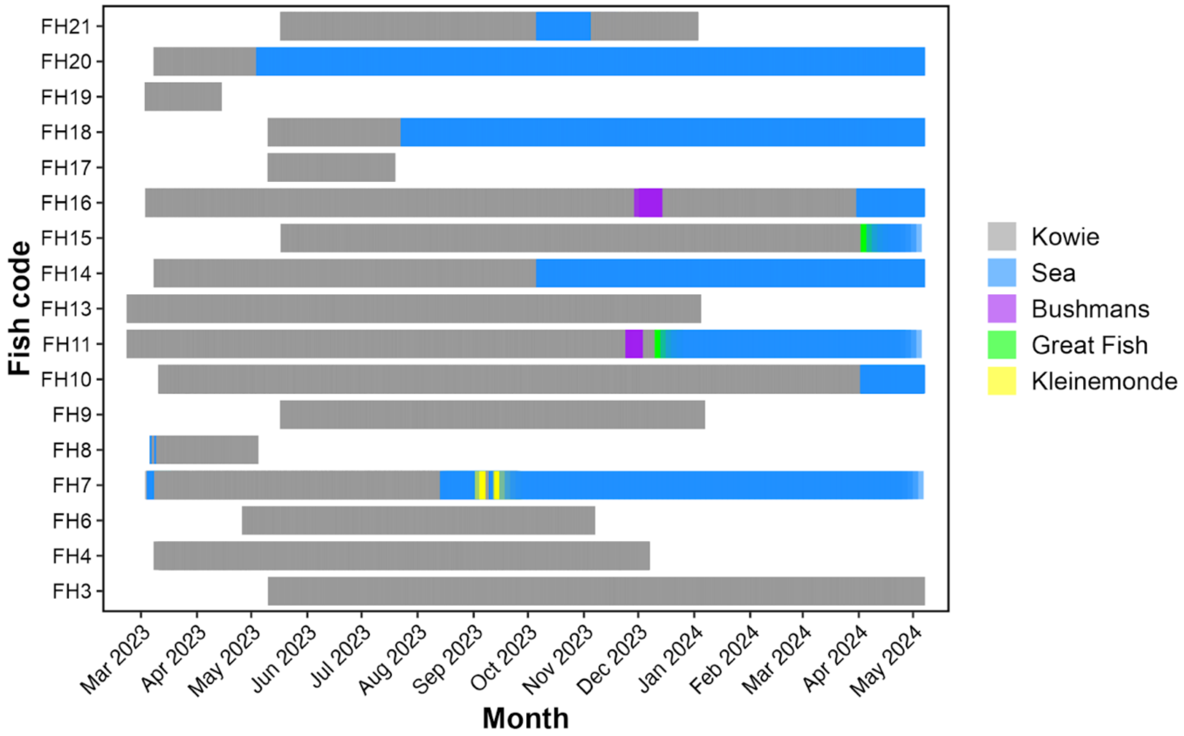

Figure 3.5. Abacus plot showing presence of acoustically tagged *Mugil cephalus* in the Kowie Estuary (grey bars), at sea (blue bars), and neighbouring estuaries (Bushmans, purple bars; Great Fish, green bars) and coastal environments (Kleinemonde, yellow bars) during the monitoring period (01 March 2023 to 30 April 2024).

Three (17.6%) *M. cephalus* (FH11, FH15, FH16; 353–416 mm FL) were recorded moving into neighbouring estuaries (Bushmans, approximately 25 km west; Great Fish, 28 km east; Figure 3.5; Figure 3.6), with three of four visits taking place in summer (only one in autumn). The longest trip to a neighbouring estuary was undertaken by FH16 (416 mm FL) into the Bushmans Estuary in December 2023, spanning 16 days before returning to the Kowie Estuary. In the same month, FH11 (353 mm FL) briefly entered the Bushmans Estuary for two days before returning to the Kowie Estuary. Shortly thereafter, this same fish visited the Great Fish Estuary (approximately 28 km east of the Kowie Estuary) for 10 days, after which it was no longer detected. Fish FH15 (416 mm FL) was detected in the Great Fish Estuary in April 2024 for two days and no longer detected (Figure 3.6).

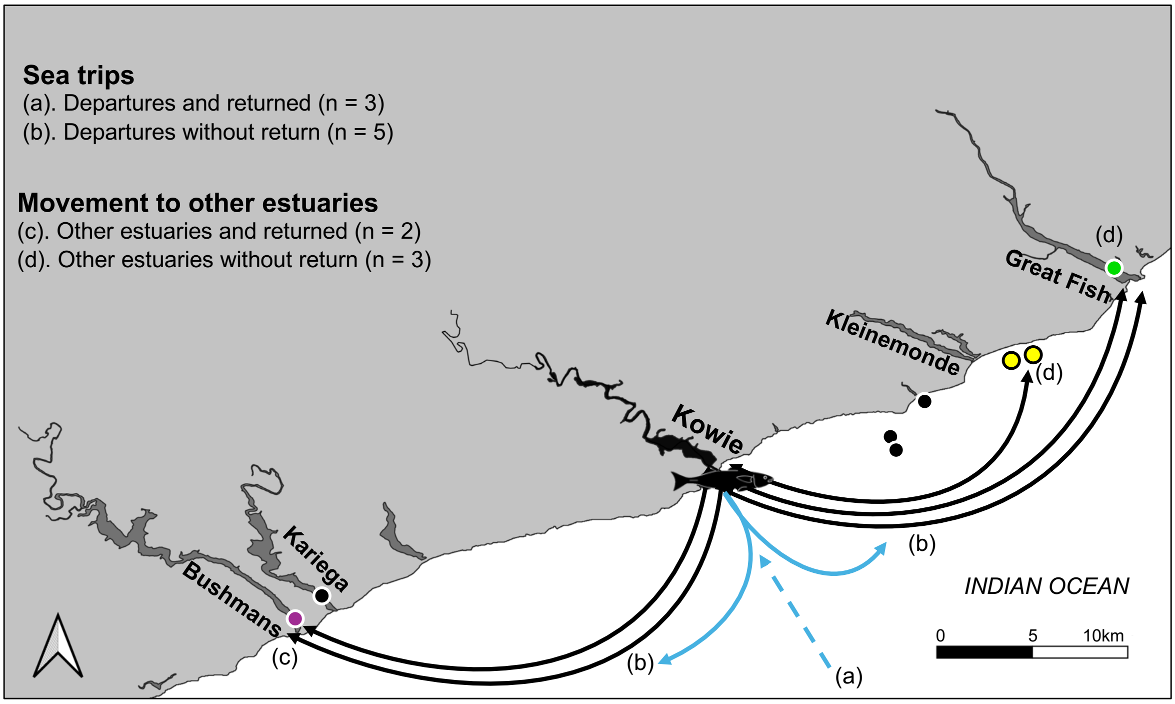

Figure 3.6. The schematic diagram showing the Port Alfred coastline with arrows representing trips to sea (blue) and other estuaries (black) undertaken by *Mugil cephalus* acoustically tagged and monitored in the Kowie Estuary between 01 March 2023 and 30 April 2024.

In terms of residency, on average, fish were highly resident to the Kowie Estuary (RI = 83.5% ± 28%, range: 13.8 – 100%), followed by sea (RI = 17% ± 28%, range: 0 – 86.4%), and neighbouring estuaries (RI = 0.3% ± 0.8%, range: 0 – 3%) and these differences were statistically significantly ($\chi^2 = 38.5$, $p < 0.05$) (Figure 3.7). The RI at the Kowie Estuary was significantly higher than at sea ($Z = 4.19$, $p < 0.05$), and the neighbouring estuaries ($Z = 6.06$, $p < 0.05$). However, the was no significant difference in the RI at sea and the neighbouring estuaries ($Z = -1.89$, $p > 0.05$) (Figure 3.7).

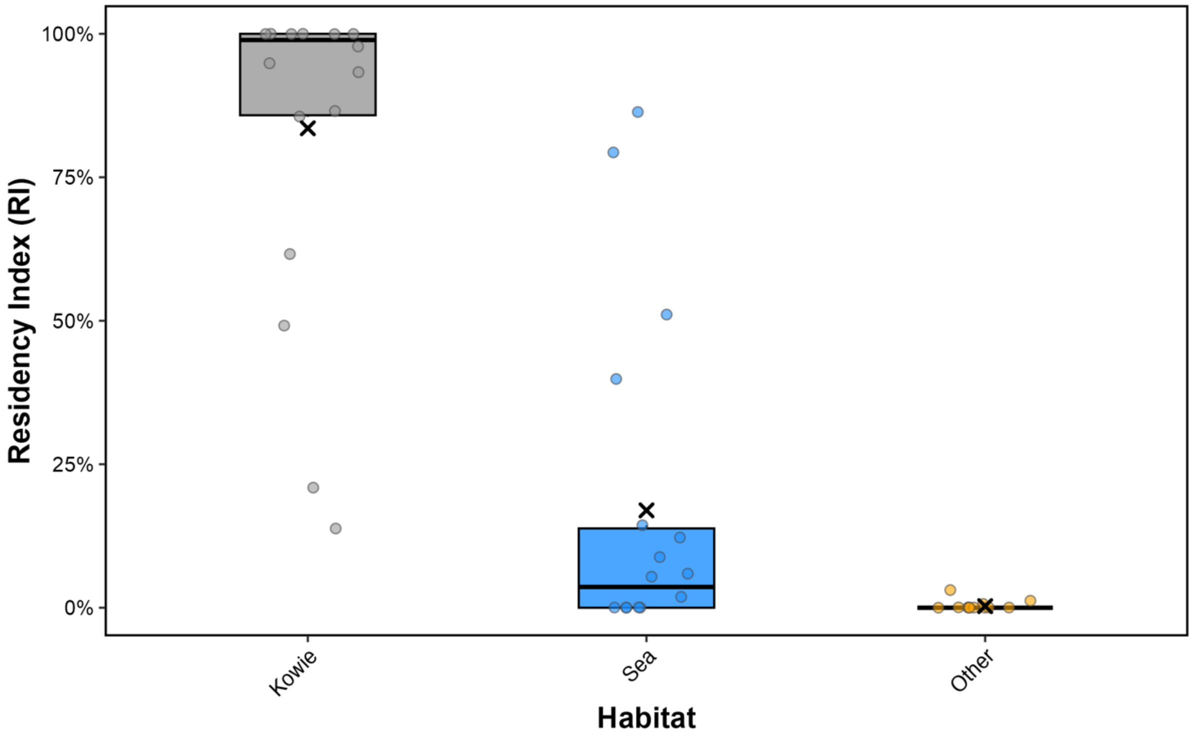

Figure 3.7. The residency indices of *Mugil cephalus* acoustically tagged and monitored in the Kowie Estuary (Kowie), sea (Sea) and neighbouring estuaries (Other) between 01 March 2023 and 30 April 2024. Crosses (x) indicate the mean proportions of time spent within each reach of the Kowie Estuary; the boxes show the interquartile range (IQR), and the lines represent the median for each habitat.

3.3.2. Spatial and temporal use of the Kowie Estuary

Tagged *M. cephalus* were recorded using the entire length of the Kowie Estuary; however, there was a significant difference in the proportion of time spent in the different reaches (F= 47.32, $p < 0.05$) (Figure 3.8). The highest proportion of time was spent in the middle reaches (76 ± 26%; range: 16 to 100%), and then the lower reaches (13 ± 21%; range: 0.3 to 71%) and upper reaches (12 ± 12%; range: 0 to 40%) (Figure 3.8). Time spent in the middle reaches was significantly higher than both the lower (mean difference = 0.82, 95% CI = 0.58 – 1.05, $p < 0.05$), and upper reaches (mean difference = -0.79, 95% CI = -1.03 – -.56, $p < 0.05$), but there was no significant difference in the overall proportion of time spent between the lower and the upper reaches (mean difference = 0.02, 95% CI = -0.21 – 0.26, $p > 0.05$).

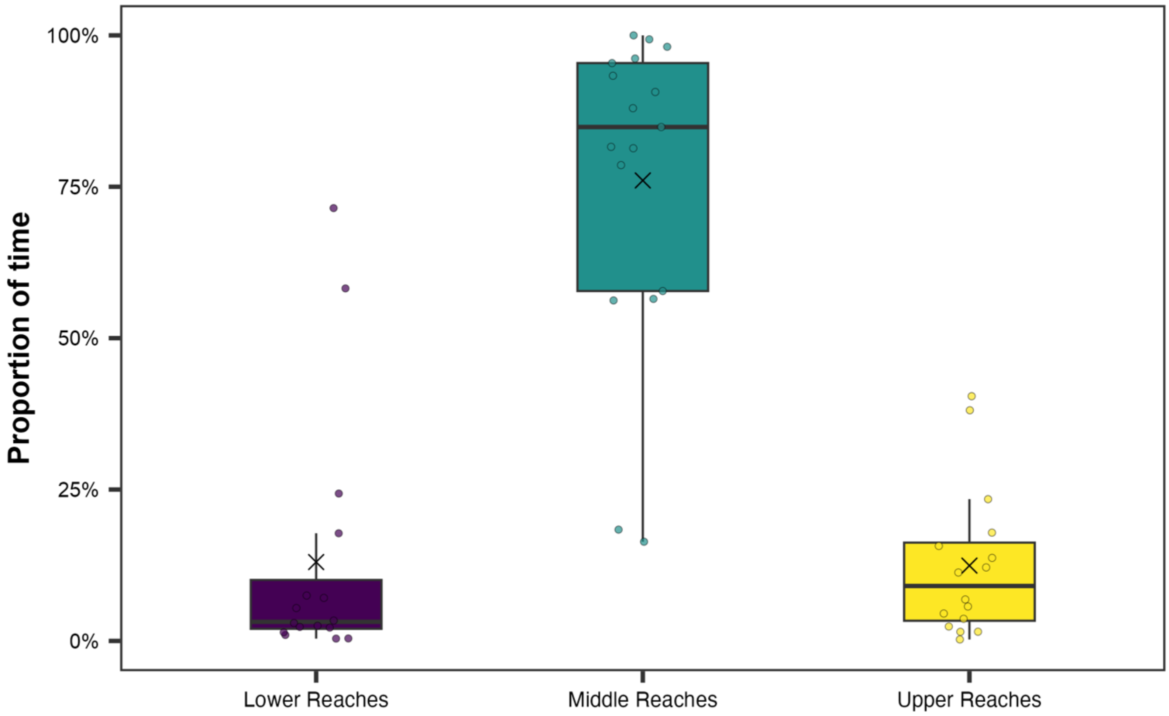

Figure 3.8. The proportion of time spent in each reach of the Kowie Estuary by tagged *Mugil cephalus* between 01 March 2023 and 30 April 2024. Crosses (x) indicate the mean proportions of time spent within each reach of the Kowie Estuary; the boxes show the interquartile range (IQR), the whiskers extend to 1.5 x IQR, and the lines represent the median for each reach.

Within the different reaches of the estuary, key areas were identified as high use ('hotspot') areas, while others were identified as highly frequented areas (i.e. many fish visited certain stations but did not spend much time in the vicinity of that area) (Figure 3.9, Figure 3.10). The most intensively used station, Station 4, located in the lower end of the middle reaches of the estuary, was visited by 94% (n = 16) of fish, spending 0.3 to 92% of their time in this area (32% ± 35%) (Figure 3.10). Notably, 29% of fish (n = 5, FH11, FH13, FH15, FH17 and FH21) spent over 60% of their time in the proximity of Station 4 throughout the monitoring period. The second highly used station was Station 3 in the lower reaches with 18% of tagged fish (n = 3, FH3, FH14, FH18) spending 50% of their time in its proximity. Although the average proportion of time spent by all fish in Station 3 was only 13 ± 9% (range: 1 to 70%), this area was frequently visited by almost all fish (88%, n = 15). The estuarine mouth (Station 1) and marina stations (stations M2–M4) were the least used stations throughout this study, only visited by 35% of fish (n = 6, FH3, FH4, FH7, FH8, FH18), for a short period of time (less than 1%) (Figure 3.10). Finally, the upper reaches, conversely, were frequented by 94% of the fish (n = 16), although for a limited time (2 ± 2%, range: 0.1 to 35%) was spent in this area. The uppermost station at the estuarine-riverine interface (Station 21) was visited by 35% of fish (n = 6) for brief periods (<1%), with the highest proportion (3%) recorded for FH3 (224 mm FL), the smallest monitored fish (Figure 3.10b).

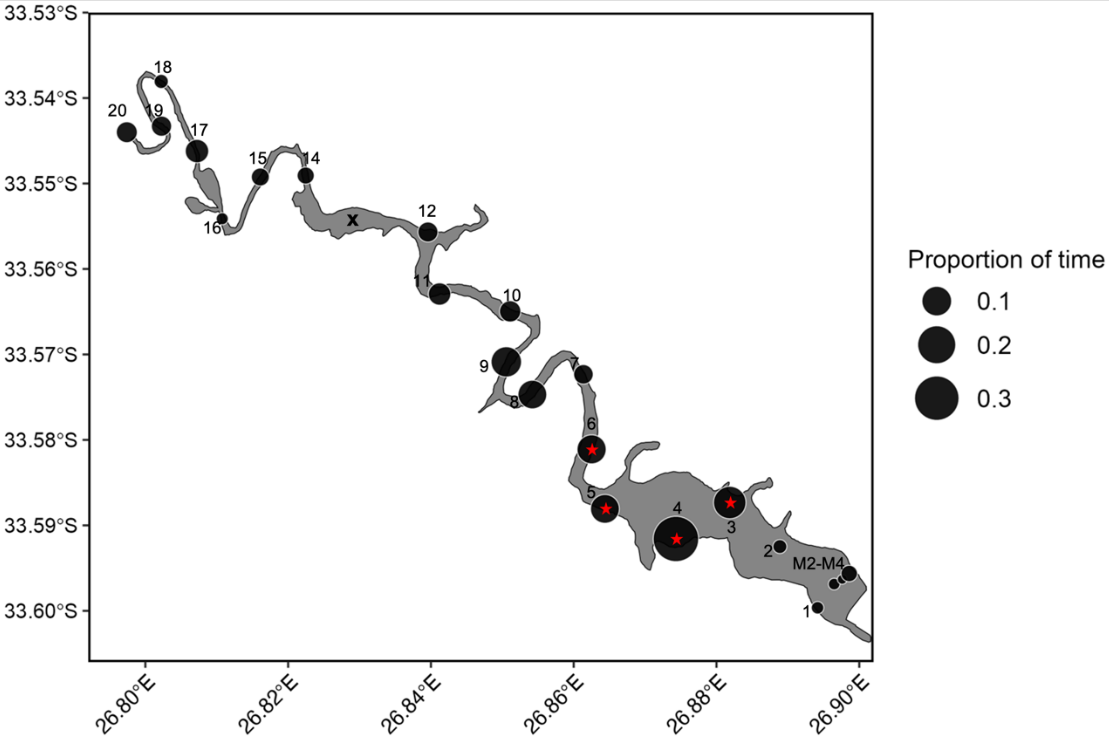

Figure 3.9. The average proportion of time spent by all *Mugil cephalus* at each acoustic receiver station deployed in the Kowie Estuary, South Africa throughout the monitoring period (01 March 2023 to 30 April 2024). The red stars represent fish capture location and the black cross represents Station 13, which malfunctioned during this study and for which there were no detection data.

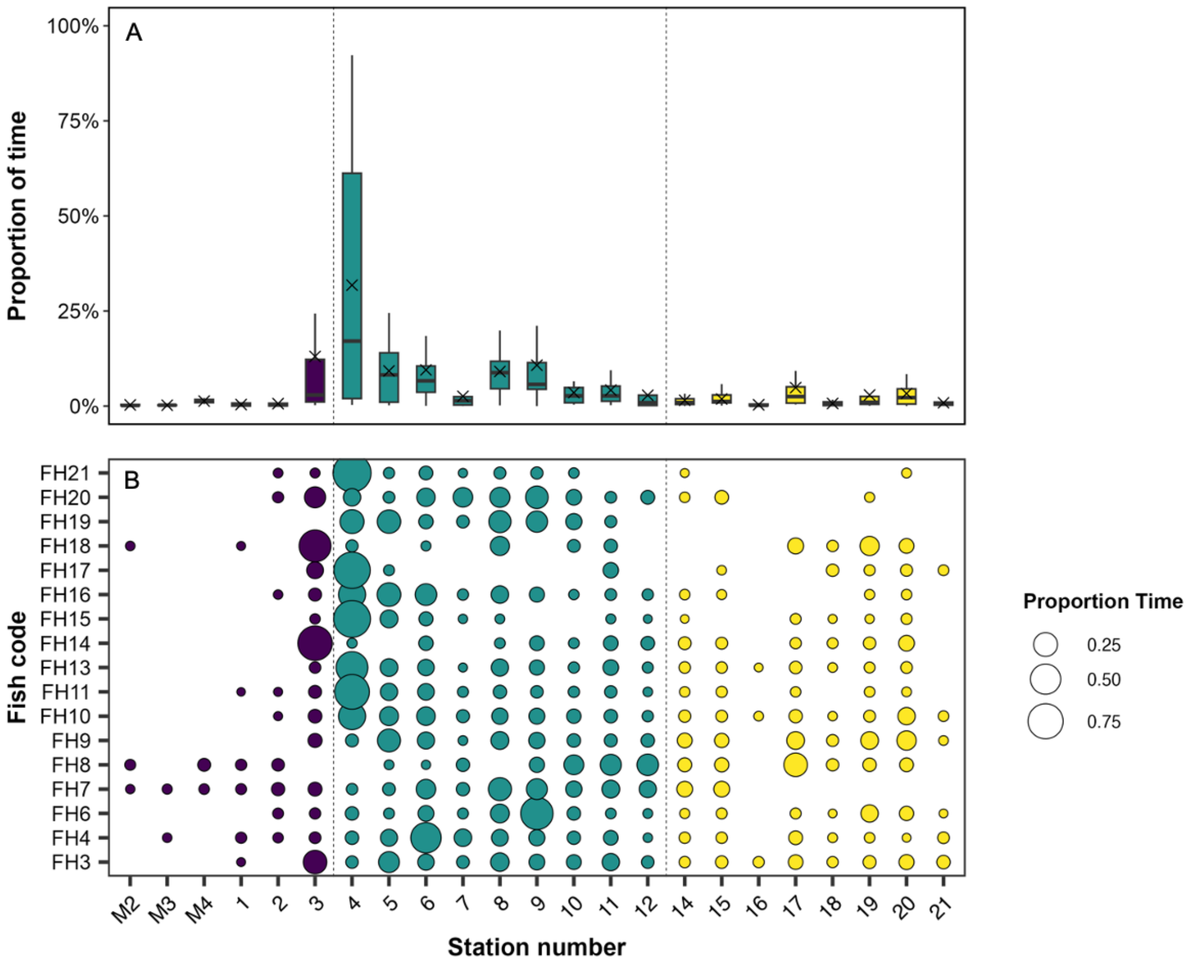

Figure 3.10. (A) The box and whisker plot showing the overall proportions of time spent at each acoustic receiver station deployed in the Kowie Estuary, South Africa by all *Mugil cephalus* throughout the monitoring period (01 March 2023 to 30 April 2024). The crosses represent the mean proportion of time spent at each acoustic receiver station. The boxes show the interquartile range (IQR), the whiskers extend to 1.5 x IQR, and the lines represent the median for each reach. (B) Bubble plot showing the proportions of time spent by each individual *Mugil cephalus* at different acoustic receivers stations deployed in the Kowie Estuary between 01 March 2023 and 30 April 2024. (indigo = lower reaches, turquoise = middle reaches and yellow = upper reaches).

Overall, there was high variability in space use of the estuary over time. Although the middle reaches were extensively used throughout the year, the use of the lower reaches increased in winter (May to October) with the simultaneous decrease in use of the upper reaches (Figure 3.11). The opposite pattern followed in summer, when the use of the lower reaches decreased drastically to almost zero from November to February, which also corresponded with an increase in the use of upper reaches (Figure 3.11).

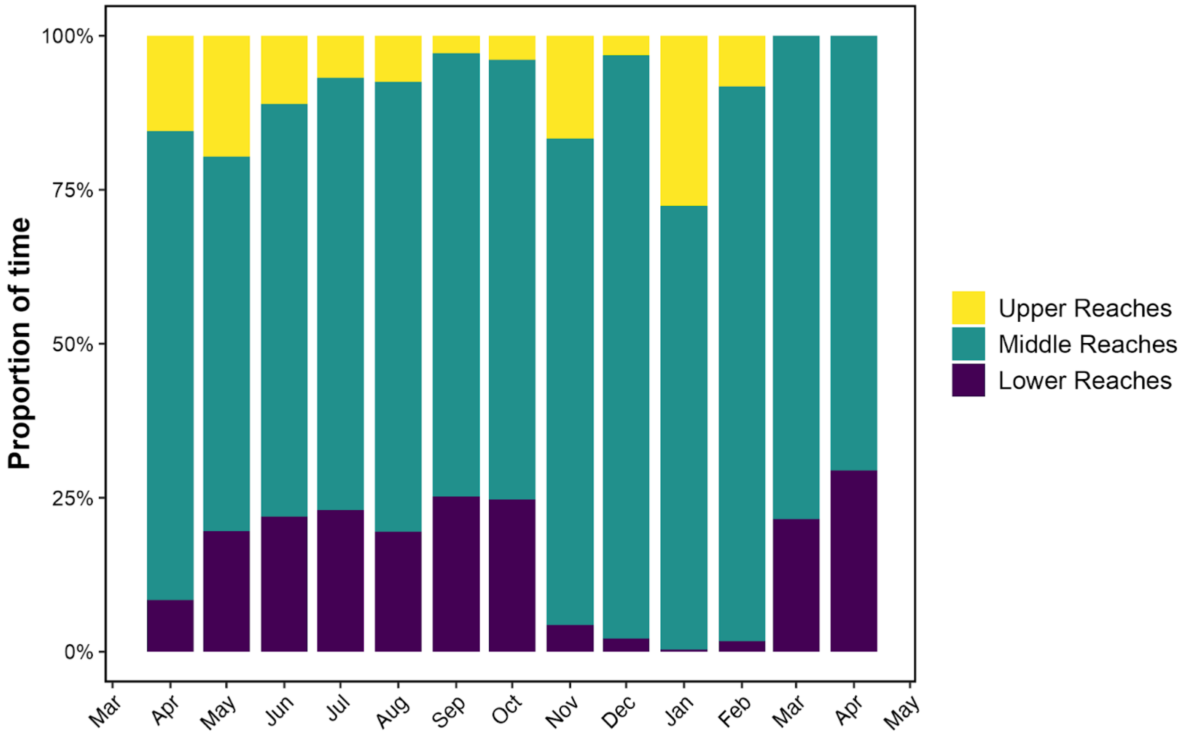

Figure 3.11. The overall monthly proportion of time spent by all *Mugil cephalus* at different reaches within the Kowie Estuary during the monitoring period (01 March 2023 to 30 April 2024).

To further explore seasonal variation in movement patterns of tagged *M. cephalus* in the Kowie Estuary, a sub-sample of six fish (35%) consisting of fish monitored across all seasons for a period of almost one year (>300 days) was analysed. This excluded fish with shorter monitoring periods (due to predation, fishing mortality, tag related mortality and emigration) for which data across all seasons were unavailable. The results of the LMM further supported the significantly high use of the middle reaches throughout the year, particularly during the winter season (β = 8.18, $p < 0.05$). Although outliers were clearly visible during different seasons, indicative of individual variation, almost all tagged fish spent 99% (± 1%) of their time in the middle reaches during winter. The use of the upper reaches was highest in summer (26 ± 23%) followed by spring (15 ± 14%); however, there was no significant difference in the proportion of time *M. cephalus* spent in the lower and upper reaches across seasons (β = –0.30, $p > 0.05$) (Figure 3.12).

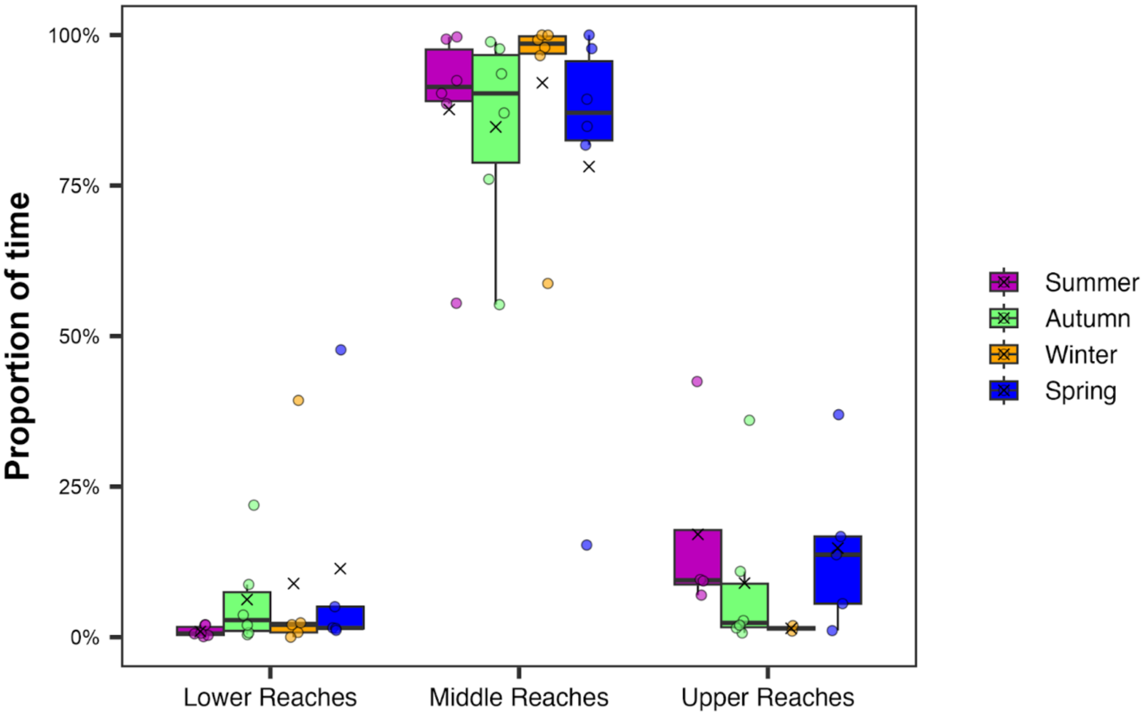

Figure 3.12. Proportions of time spent in the lower, middle and upper reaches of the Kowie Estuary area per season by six tagged *Mugil cephalus* that were monitored for more than 300 days between 01 March 2023 and April 2024. Circles indicate individual fish, crosses (x) indicate the mean proportions of time spent within each reach of the Kowie Estuary; the boxes show the interquartile range (IQR), the whiskers extend to 1.5 x IQR, and the lines represent the median for each reach.

There was high individual variability in daily movement patterns and space use in different habitats within the Kowie Estuary (Figure 3.10B, Figure 3.13, Appendix 2 for more detailed movement patterns). All fish showed heightened activity across various stations (up to 21 km upstream) during certain months (March to May), and this was followed by reduced movement, confined to 1–5 km during the second half of the year (June to October). However, FH7 and FH9 were the exceptions with high activity throughout the monitoring period between the higher-middle reaches to upper reaches (Figure 3.13). Site fidelity to Station 4 was shown by most fish (Figure 3.10B) as they would return to this area even after moving distances up to 21 km up the estuary, as well as those that undertook return sea trips (e.g., FH11, FH16 and FH21) (Figure 3.13).

In addition to Station 4, other stations in the middle reaches were also identified as high use areas. For example, FH4 and FH7 spent more than 50% of their time in the proximity of Station 6 and Station 9, respectively (Figure 3.10B, Figure 3.14). Some individuals spent a proportion of their time at the upper most station (FH3, FH4, FH6, FH10 and FH18), indicating limited but notable use of the upper reaches of the estuary compared to the lower reaches, which were infrequently visited for short periods of time (Figure 3.10B, Figure 3.14).

Figure 3.13. Daily detection plots of *Mugil cephalus* movements throughout the Kowie Estuary during the monitoring period (01 March 2023 to 30 April 2024), with different stations coloured according to estuarine reach (indigo = lower reaches, turquoise = middle reaches and yellow = upper reaches).

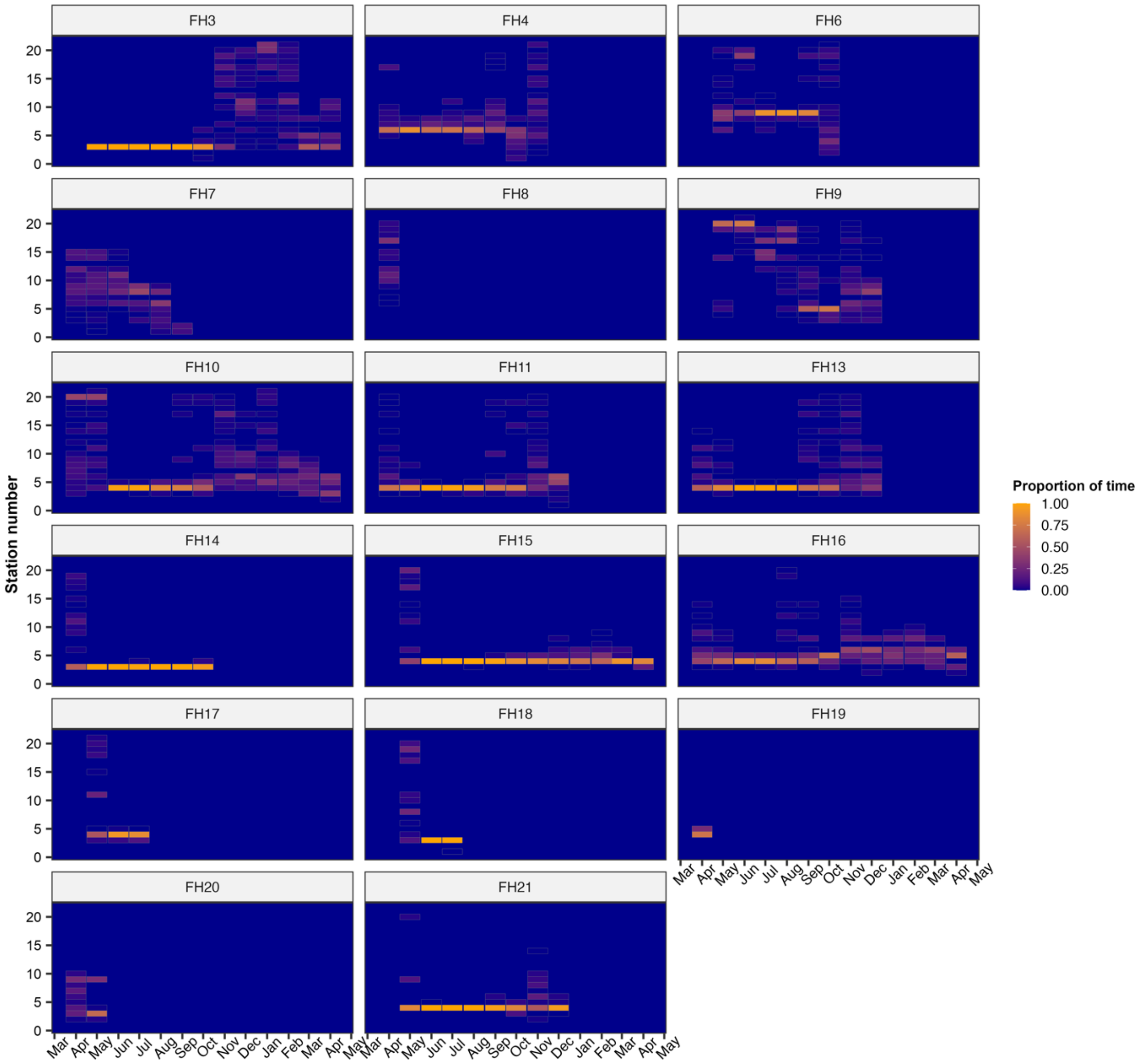

Figure 3.14. The monthly proportion of time spent by acoustically tagged *Mugil cephalus* at various acoustic receiver stations in the Kowie Estuary during the monitoring period (01 March 2023 and 30 April 2024).

There was no correlation between fish length and the proportion of time tagged *M. cephalus* spent at the lower reaches (r = -0.03), indicating that all fish irrespective of size, spent less time in the lower reaches (Figure 3.15). A weak positive correlation between fish length and time spent in the middle reaches (r = 0.33) indicated that larger fish may be spending more time in the middle reaches; however, notably, two fish (400 – 450 mm FL) showed the opposite pattern. Lastly, there was a moderate negative correlation between fish length and time spent in the upper reaches (r = -0.56), indicating that smaller fish spent more time in the upper reaches compared to larger fish (Figure 3.15).

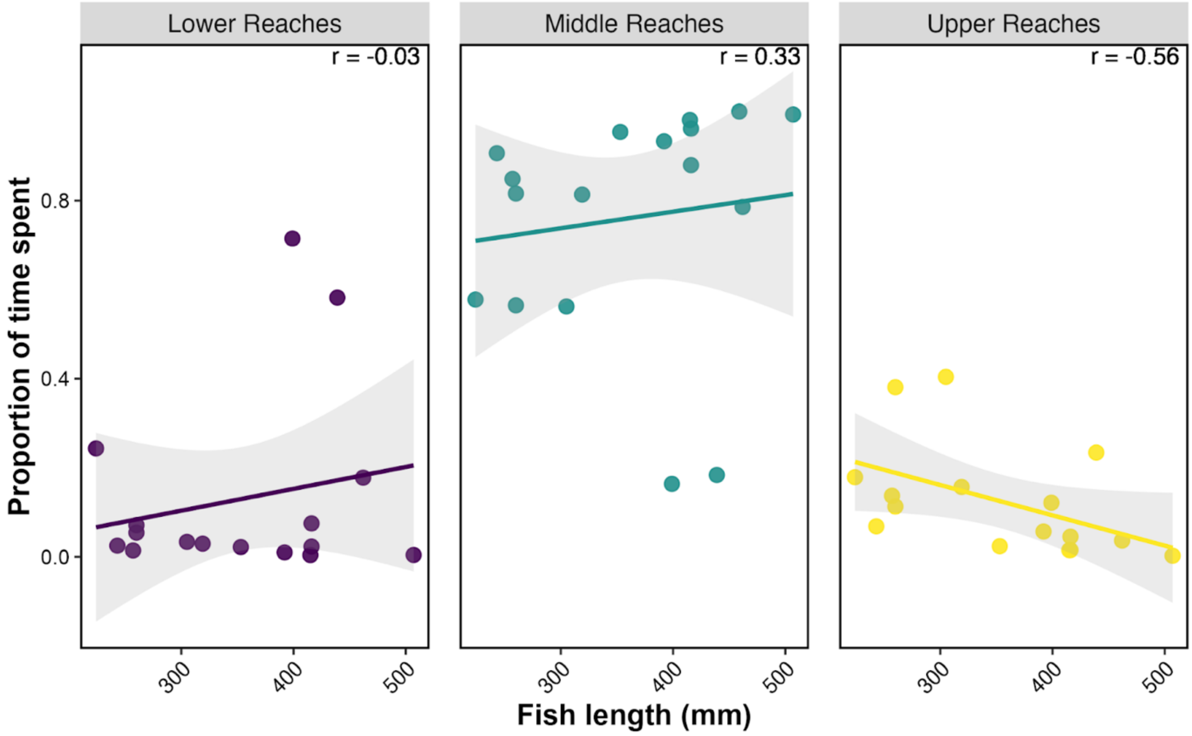

Figure 3.15. The relationship between fish length and proportion of time spent by acoustically tagged *Mugil cephalus* at different reaches within the Kowie Estuary during the monitoring period (01 March 2023 to 30 April 2024).

3.3.3. Effects of environmental variables (time of day, temperature and flow)

The average hourly position of fish during the day was 7.5 ± 3.8 (range: 4.1 to 16.3) and during the night was 7.0 ± 2.0 (range: 4.3 to 12.4), with no significant difference in fish position between day and night ($t = 31$, $p > 0.05$) (Figure 3.16). There was, however, individual variation in fish movement patterns between the day and night, with some fish (e.g., FH5, FH8, FH7 and FH9) having a higher average fish position (i.e. fish located further downstream at night compared to the day, while others (e.g., FH12, FH19) exhibited the opposite patterns (Figure 3.16).

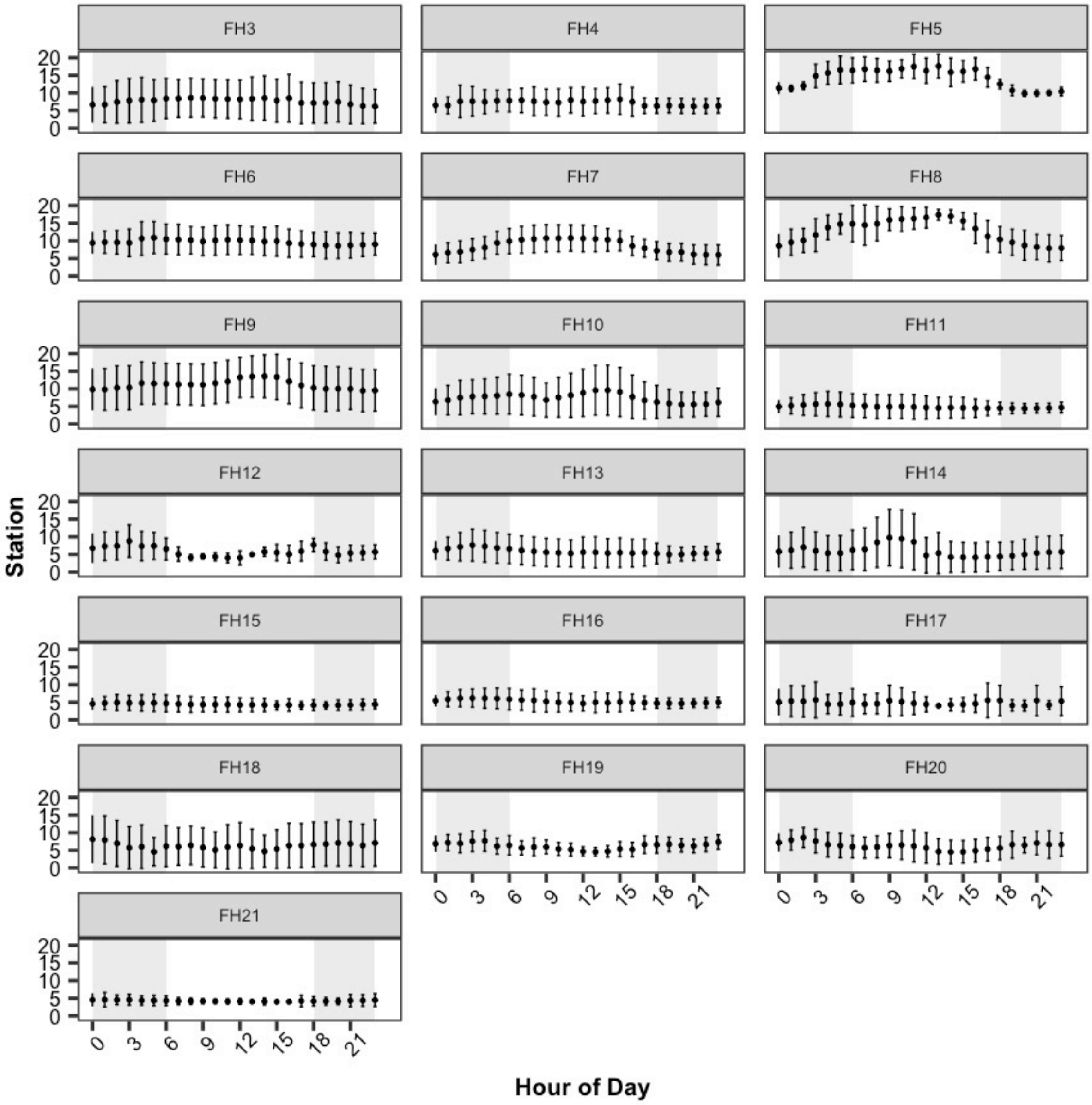

Figure 3.16. The overall average hourly position from the mouth (Station 1) to uppermost receiver (Station 21) of individual *Mugil cephalus* in the Kowie Estuary during the monitoring period between 01 March 2023 and April 2024. Grey bars represent night hours (18:00 to 05:00) and clear represent day hours (06:00 to 17:00).

The results of the LMM analyses revealed relationships between selected environmental variables and average daily fish position (Table 3.5, Figure 3.17). The selected model (station ~ flow + river + sea + sqrt(rainfall) + (1 | fish_code) showed an relatively good balance between model fit and complexity, with an AIC of 9787 and BIC of 9725 (for other models, see Appendix 1). The residual standard deviation of

3.25 and the variance among individual fish was 4.11 (SD = 2.03), indicating meaningful variation in spatial behaviour among individuals. River flow showed a strong negative association with average daily fish position (intercept = -0.36 ± 0.15, $p < 0.001$), indicating that higher flows were associated with fish being located further downstream. Similarly, sea temperature also had a strong negative association with average daily fish position (estimate = -0.33 ± 0.07, $p < 0.001$), with fish located further upstream during colder sea temperatures. In contrast, river temperature positively influenced average daily fish position (estimate = 0.17 ± 0.02, $p < 0.001$), with warmer river temperatures corresponding to upstream occupation. Rainfall, however, did not have a significant influence on average daily fish position (estimate = -0.02, $p > 0.05$).

Table 3.5. The results of the Linear Mixed-effect Model output modelling the effect of temperature (river and sea, °C), river flow ($m^3 . s^{-1}$) and rainfall (mm) on the daily average fish position of *Mugil cephalus* tagged and monitored in the Kowie Estuary between 01 March 2023 and 30 April 2024. Bold values indicate a significant result.

Fixed effects	Intercept	SE	df	t value	p value
Intercept	8.39	1.45	445.95	5.77	**< 0.001**
Sea temperature	-0.33	0.06	1848.32	-5.20	**< 0.001**
River temperature	0.17	0.02	1855.52	7.15	**< 0.001**
River flow	-0.36	0.04	1848.12	-9.13	**< 0.001**
Rainfall (sqrt)	-0.02	0.01	1844.24	-1.49	> 0.05

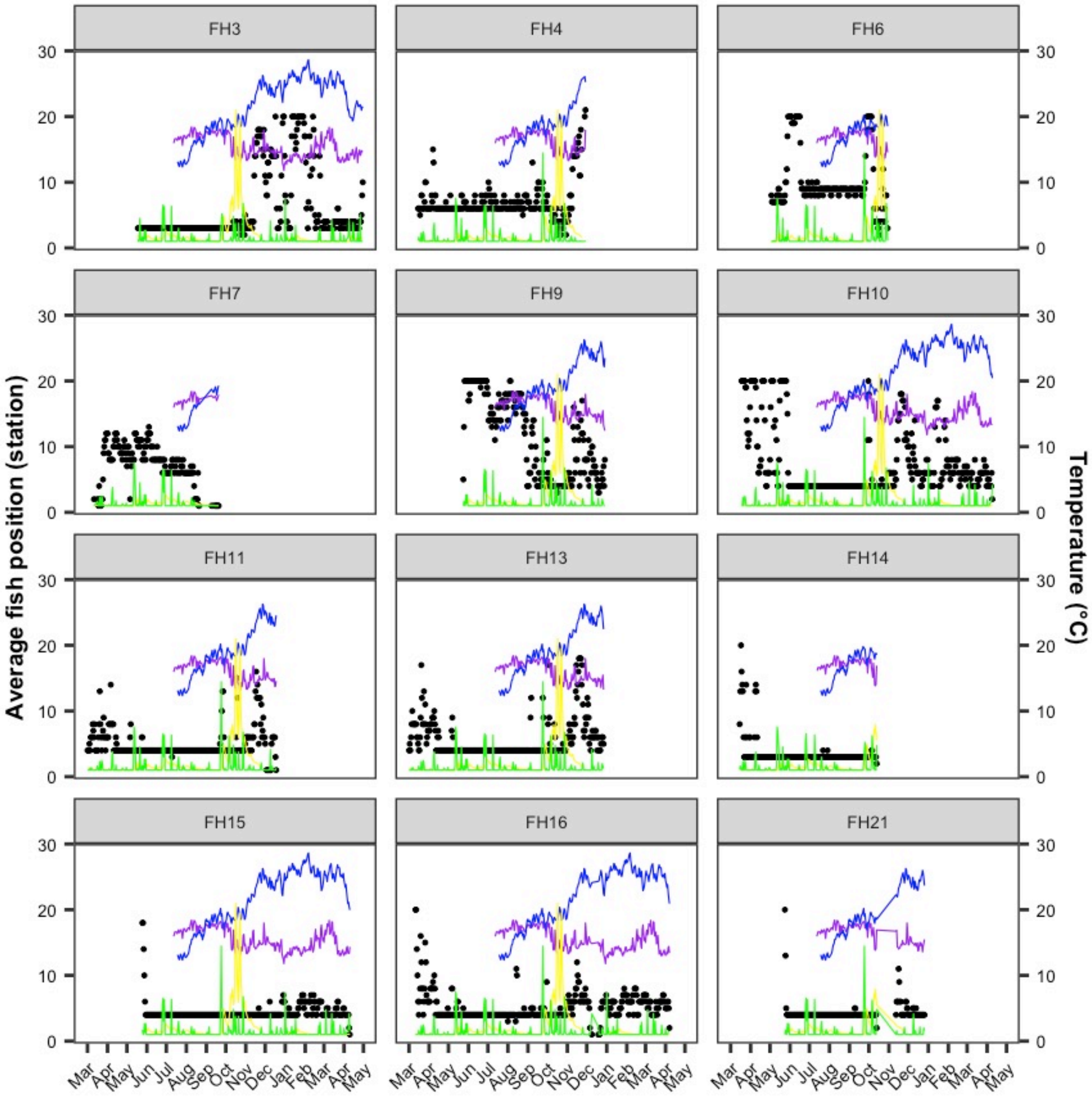

Figure 3.17. Average daily fish positions (as indicated by acoustic receiver stations from the mouth [1] to the river-estuary interface [21]) of the 12 tagged *Mugil cephalus* (black dots) included in the modelling analyses plotted from 01 March 2023 to 30 April 2024. with multiple variables river temperature (blue)and sea temperature (purple) on the secondary y-axis, both river flow (yellow) and square root of total rainfall (green) were scaled to the y-axis. Fish that had movement data for only March 2023 were removed.

3.4. Discussion

Fish can alter their behaviour in response to dynamic environmental conditions and such behavioural plasticity emerges from the interaction of evolutionary adaptation and individual experience (Mery and Burns 2010). The global distribution of *M. cephalus* has been attributed to its ecological generalist strategy and high behavioural flexibility, which enables it to thrive in diverse habitats across the marine-freshwater continuum (Whitfield et al. 2012). In the present study, acoustic telemetry over a 14-month period revealed the critical importance of both inter- and intra-seascape connectivity between the sea, estuary and river habitats for *M. cephalus* in a warm temperate South African estuary. The Kowie Estuary was identified as a key habitat, with tagged individuals spending up to 80% of their time within the system and repeatedly using identified hotspots in the middle reaches. Despite this strong estuarine residency, over half of the tagged fish undertook sea trips to the marine environments and neighbouring estuaries, while some fish used the estuary-river interface to varying degrees. The movement patterns of *M. cephalus* during this study were significantly influenced by environmental drivers, particularly sea and river temperatures and river flow; however, individuals responded differently to these changes. These patterns suggest a high degree of movement plasticity at an individual level, and the existence of different movement strategies within the population, which may have implications conservation plans and the overall species resilience to environmental change.

Estuaries offer significant survival and growth advantages to estuary-associated species, particularly during early life stages, due to their high-quality food resources, diverse habitats and reduced predation pressure (Beck et al. 2001; Sheaves 2009; Potter et al. 2015; Able et al. 2022). Members of the Mugilidae family, including *M. cephalus*, often dominate coastal habitats such as estuaries, and this is attributed not only to flexible physiology but also their position at the base of the food web (Whitfield 2016), and these systems offer vegetated habitats such as submerged macrophyte beds for foraging and shelter. During this study, almost half of the tagged *M. cephalus* individuals of various sizes remained resident within the Kowie Estuary throughout the monitoring period, indicating estuarine fidelity and highlighting the ecological importance of this estuary for some individuals throughout parts or all of their life cycle. Although, individuals made extensive use of the estuary, including the uppermost habitats at the estuary-river interface, habitat hotspots were identified such as Station 4, where some individuals spent up to 92% of their time. This area, located 3 to 4 km from the mouth is characterised by moderate salinities (15–35), shallow depths (2–4 m), and dense macrophyte beds, providing structurally complex, resource-rich habitat that supports diverse fish assemblages (Whitfield 1994; Kruger 2010; James and Harrison 2010). Other studies have also identified this area as an important nursery ground for estuarine species such as leervis *Lichia amia* juveniles (Murray 2016) and various Mugilidae species, including southern mullet *Chelon richardsonii* and freshwater mullet *Pseudomyxus capensis* (Kruger and Strydom 2011). The role of macrophyte beds in driving fish distribution and increasing diversity is well established (Sheppard et al. 2011; Whitfield 2017). Research has shown that the Kowie Estuary supports high fish species diversity compared to adjacent systems, largely due to extensive reed beds (e.g., *P. australis*) and submerged vegetation that enhance habitat complexity and offer refuge from predation (Whitfield 1994; James and Harrison 2010; Whitfield 2017). Experimental studies in the Mediterranean, have also shown that littoral fish, such as Mediterranean rainbow wrasse *Coris julis*, ocellated wrasse *Symphodus ocellatus* and common two-banded seabream *Diplodus vulgaris* actively select more structurally complex macrophyte configurations that provide greater refuge (Hinz et al. 2023). In contrast, the infrequent use of the Kowie Estuary mouth region and marina habitats by tagged *M. cephalus* in this study is likely a result of habitat unsuitability, primarily driven by intense anthropogenic disturbance in this area (Whitfield 2000) and infrastructure development, including the canalisation of the main estuary channel (Schumann et al. 2001; Kruger and Strydom 2010). Globally, urbanisation and coastal development have led to the degradation of both estuarine and coastal habitats (Wen et al. 2010), particularly affecting mobile species that rely on structural complexity for refuge and foraging (Sheaves 2009; Able et al. 2022). The construction of concrete structures (such as the Kowie Marina, along with the canalisation of the main channel), can significantly change the natural geomorphology of the estuary mouth resulting in homogenisation of the surrounding habitats and reduced ecological functionality (Clark and Edwards 1999). In the case of the Kowie Estuary, the physical characteristics of the mouth region, marked by high hydrodynamic energy, shifting sandbanks and substantial sediment loading, can further reduce habitat suitability for species such as *M. cephalus* (Whitfield 1997).

Despite the high residency of *M. cephalus* to the Kowie Estuary observed in this study, 58% of tagged individuals left the Kowie Estuary and moved into the sea and neighbouring estuaries (with various salinity gradients) at least once during this study. These trips, which ranged from 1 to 30 days, align with the well-documented behavioural plasticity and euryhaline nature of the species (Whitfield et al. 2012). Almost half of the trips occurred in autumn but were not synchronised, suggesting an individual exploratory or adaptive response to seasonal environmental change such as temperature and salinity, among other factors. This pattern, whereby a fraction leaving estuarine and coastal habitats and migrating offshore in autumn to escape winter conditions and returning in spring during warmer periods is a common behaviour within the Mugilidae family (Whitfield 2016; Edwards et al. 2025).

This movement variability is best explained by the framework of partial migration, in which both resident and migratory individuals coexist within a population (Jonsson and Jonsson 1993; Dingle and Drake 2007; Kerr et al. 2009; Chapman et al. 2012; Gillanders et al. 2015). The partial migration concept provides a mechanistic understanding of behavioural complexity, intrapopulation structure and alternative migratory behaviour (Childs et al. 2015). In *M. cephalus*, such partial migration may reflect ecological trade-offs between the energetic costs of movement and the benefits of accessing alternate foraging habitats. This strategy has been observed in *M. cephalus* across several geographic contexts. For example, in eastern Australia, 40% of adult *M. cephalus* migrated to sea for spawning, while others remained within estuarine habitats (Fowler et al. 2016). Higher levels of estuary residency have been described in early juvenile to adult *M. cephalus* in Taiwan (Chang et al. 2004b) and New Zealand (Górski et al. 2015). There are benefits to the residency strategy, including investing more energy into growth and reproduction, and can produce lower risk to fishing pressure (Chapman et al. 2011; 2015; Fowler et al. 2016). The persistence of both strategies suggests an evolutionary response to heterogeneous environments and adaptation to selection pressures such as fishing mortality and predation risk (Skov et al. 2013; Fowler et al. 2016). For example, Childs et al. (2015) suggested that the behavioural strategy of partial migration observed in the estuary-associated *Argyrosomus japonicus* in a warm-temperate estuary in South Africa, where some acoustically-tagged individuals remained resident in the estuary while others exhibited estuarine-marine connectivity, could confer population resilience given the increased vulnerability of the estuarine residents to fishing exploitation.

Partial migration could also confer resilience to a changing environment (Karr et al. 2010). In this context, partial migration patterns have been documented in other species from temperate estuaries; for example, co-occurring species in central-southern New Jersey, USA such as smooth dogfish *Mustelus canis*, black drum *Pogonias cromis* and hickory shad *Alosa mediocris* showed residency to an estuary in summer, but left the estuary in autumn and winter when temperatures started to decline (Able at al. 2014). Similarly, southern flounder *Paralichthys lethostigma* population from an estuarine complex in the Gulf of Mexico consists of both a migratory contingent and resident individuals, with the migratory individuals leaving the Galveston Bay Complex Estuary during late autumn (Steffen et al. 2023). Similar patterns have also been described for many other estuary-associated species where fluctuations in environmental factors such as temperature can alter fish position to access suitable habitats (Childs et al. 2008; Peterson et al. 2017; Grant et al. 2017; Murray et al. 2018). Childs (2013) attributed the observed partial migration strategy in *A. japonicus*, where individuals from the estuarine and marine contingents exhibited habitat connectivity during summer months (i.e. fish departed the estuary due to increased riverine temperatures and entered the estuary due to cold upwelled sea temperatures) to conditional strategy. Since conditional strategy is the interaction between individual physiological conditions and the environment (Kerr et al. 2009), this interplay could result in some individuals being more tolerant (residents) to environmental change than others (movers). The persistence of partial migration in animals therefore reflects not only behavioural plasticity, but also the role of intra- and inter- seascape connectivity in facilitating such movements, and in conferring resilience to environmental change.

Temperature has been identified as the abiotic master factor affecting fish survival, growth and distribution (Brett 1971; Pörtner and Knust 2007), to mitigate thermal stress, fish alter their physiology and behaviour such as by moving to thermally suitable habitats. Modelling the effects of selected environmental factors on the movement of *M. cephalus* during this study confirmed that indeed the daily movement patterns of individual fish were driven by environmental factors, particularly river and sea temperature and river flow. In winter, the majority of tagged fish moved downstream to the middle estuary as colder riverine water dominated the upper reaches, while in summer fish shifted upstream, likely to avoid cold upwelled coastal water entering from the mouth. In addition to temperature, river flow also influenced the daily position of fish in the estuary, for example, during increased river flow in October many individuals shifted downstream from the upper reaches to middle reaches. This active avoidance of freshwater intrusion and associated reduction in salinity can be expected from euryhaline species due to energetic costs associated with osmoregulation (Kültz 2015). These movement patterns identified in this study may thus reflect a condition-dependent migration strategy, in which individual movement decisions arise from the interaction between environmental variability and internal physiological states which prompt adaptive behavioural response (Dingle and Drake 2007; Vélez-Espino et al. 2013). For Mugilidae, similar patterns have been observed in the Patos Lagoon, Brazil, where freshwater flooding events dramatically altered estuarine abundance due to changes in salinity (Garcia et al. 2003). In Taiwan, long-term declines (over the last two decades) in *M. cephalus* catches have been attributed to shifting sea surface temperatures as a result of climate change which has led to poor recruitment (Lan et al. 2014, 2017).

Given the strong relationship between coastal water temperatures and the spatial distribution of mugilid species across South African estuaries (Whitfield 2005), it is likely that, as observed in Taiwan, the future dynamics of *M. cephalus* will be shaped by both seasonal and interannual fluctuations in temperature (James et al. 2016). The behavioural flexibility and partial migration strategies observed in this study highlight the ecological value of maintaining habitat connectivity across the marine–freshwater continuum, as climate-driven changes, such as temperature changes and flow alterations are expected to become more frequent and extreme (van Nierkerk et al. 2022). Ensuring access to thermally suitable habitats across these interconnected systems will be critical for the persistence of estuary-associated species under future climate scenarios (Vivier et al. 2010). However, to anticipate and manage such responses effectively, we must first understand the physiological thresholds of these species to thermal stress. Such information will also provide insights into determining whether conditional strategy may indeed be the mechanism driving observed partial migration patterns and responses to temperature in estuary-associated species. The following chapter will address this gap by experimentally quantifying the thermal tolerance limits of *M. cephalus*, providing a mechanistic basis for interpreting their observed movement patterns and predicting their vulnerability to climate change.

CHAPTER 4

ASSESSING THE THERMAL TOLERANCE OF A COSMOPOLITAN SPECIES, *MUGIL CEPHALUS*

Manuscript accepted in the African Journal of Marine Science:
https://doi.org/10.2989/1814232X.2025.2545924

4.1. Introduction

Temperature has been identified as the primary abiotic factor affecting all biochemical, life history and physiological activities of fish (Brett 1971; Beitinger et al. 2000). Unanticipated rapid fluctuations in water temperature, whether warming or cooling, can lead to fish altering their distribution by latitude or depth as they seek thermal refuges (Eme and Bennett 2009; James et al. 2013), particularly species with shorter lifespans (Bennett and Lenski 1993; Rijnsdorp et al. 2009; Alfonso et al. 2020). Species' spatial and temporal distributions are governed by their thermal niches – the temperature range a fish can tolerate to effectively survive, grow and reproduce (Bennett and Lenski 1993; Gvoždik 2018) – which are determined by their physiological requirements (Eme and Bennett 2009). Most fish sustain a good level of physiological performance i.e. swimming, foraging, reproduction and predator avoidance, in an optimal thermal regime until a thermal threshold is reached (Fry et al. 1942).

As a result of climate change, global average ocean temperatures are predicted to increase between 2.0 and 4.0 °C by the end of the century (Meyer and Pachauri 2014), and extreme thermal events such as marine heatwaves will become more frequent and severe (Hoegh-Guldberg and Bruno 2010; Vasseur et al. 2014). Coastal habitats, such as estuaries, are highly dynamic systems characterised by the continuous input of sediment from terrestrial, riverine and marine sources (Elliot and McLusky 2002). These environments are likely to be influenced by various interacting climatic and hydrological impacts of climate change, including flow dynamics, which affect both marine and freshwater ecosystems (James et al. 2013). Therefore, ecological patterns such as estuarine fish assemblages and distributions are likely to be influenced by the changing variability in the environment (e.g., salinity, dissolved oxygen and temperature) (Gillanders et al. 2011b). A considerable amount of research has been conducted on modelling species-environment relationships (Austin 2007), and in most cases, base level data on impacts of individual factors such as temperature is required to use as input for such models.

Temperature tolerance of fish has been quantified through laboratory trials using methods that gradually alter temperatures until biological stress is observed (e.g. Fry et al. 1942; Currie et al. 1998; Eme and Bennett 2009). The critical thermal methodology (CTM), developed in 1944 (Cowles and Bogert 1944), is a commonly used method to obtain a proxy for upper and lower thermal tolerance in fishes. During laboratory trials, fish undergo a constant temperature change until reaching a predefined endpoint and loss of equilibrium (LOE) is observed (Fry et al. 1942). The LOE can include muscle spasms and changes in orientation and the continued exposure will ultimately lead to death (Cowles and Bogert 1944). The upper temperature tolerance, critical thermal maximum (CT_{max}) and lower temperature tolerance, critical thermal minimum (CT_{min}), are the thermal endpoints at which the LOE is reached (Cox 1974), and are used to define a species' thermal niche.

The thermal niche of fish can vary both within species (intraspecific variation) and between species (interspecific variation) (Currie et al. 1998; Szekeres et al. 2016). Changes in temperature affect ectotherms by limiting their thermal performance through changes in oxygen supply and metabolic demand (Pörtner 2010). Fish usually respond to this change by moving to suitable thermal habitats; however, when these refuges are not available, individuals may alter behaviour (i.e., changes in breathing rate) as a response mechanism to coping with thermal stress (Biro et al. 2010; Bates and Morley 2020). For example, high temperatures can induce restlessness or heightened activity in fish, enabling them to seek cooler microhabitats and escape thermal stress (Somero 2010). In contrast, cold temperatures tend to cause lethargy, suppressing escape responses and reducing the ability to avoid unfavourable conditions (Doudoroff 1942; Allison et al. 2021). Within populations, individuals also display variability in thermal breadth, influenced by genetic diversity, life stage and environmental history. For example, juvenile fish may have narrower thermal niches compared to adults due to developmental constraints (Sylvester 1975). Additionally, thermal niche plays a critical role in determining the distribution, behaviour and ecological interactions of fish (Eme and Bennett 2009). Species with broader thermal niches or greater phenotypic plasticity are better positioned to adapt to changing climates, while those with narrow thermal ranges may face range shifts, population declines, or extinction (Dowd et al. 2015). As such, a broader understanding of how environmental stressors may shape the persistence of species is essential for predicting and managing the impacts of climate change on fish populations and their habitats.

In southern Africa, global warming is predicted to have severe impacts on the temperature regimes along the south-eastern coastline due to the expected increase in frequency of wind-driven upwelling events (Duncan et al. 2019; Allison et al. 2021). In warm-temperate estuarine environments, riverine temperatures are also predicted to increase (James et al. 2013, van Niekerk et al. 2022) which will influence fish species occupying these habitats. Since temperature is the main driver of fish metabolic processes and other biochemical processes, it is therefore important to understand how a species that occupies dynamic coastal environments, including estuaries, will respond to a changing thermal environment (Szekeres et al. 2016). Species in the middle latitudes (20° to 40°) are especially faced with a risk of performance decline as a result of climate variability brought on by increased extremes and duration of heat stress (Vasseur et al. 2014).

The flathead mullet *Mugil cephalus* (Linnaeus 1758) is a widely distributed eurythermal species found between latitudes 42° N and 42° S, where it primarily inhabits estuarine environments, migrating into the nearshore marine environment to spawn (Whitfield et al. 2012). Its ecological importance within estuarine ecosystems is significant, contributing to nutrient cycling and food webs (Soyinka 2008). With the current projections of climate change, the distribution patterns of estuary-associated species such as *M. cephalus* are likely to be affected, recent studies show that temperate species are extending their distribution northward in winter while tropical estuarine species are moving southward in summer (James et al. 2013). Furthermore, acoustic telemetry results (Chapter 3) revealed seasonal downstream movements and an absence of tagged *M. cephalus* from the upper reaches of the Kowie Estuary during winter, coinciding with the lowest recorded river temperatures. These observations raise questions regarding the thermal constraints of this species in warm temperate systems, particularly whether such movements are a behavioural response to avoid physiologically stressful temperatures. Despite their wide geographical distribution, surprisingly few studies have quantified the thermal tolerance range of *M. cephalus* under controlled laboratory conditions. To address this knowledge gap, the present study experimentally assessed both the lower and upper thermal tolerance thresholds of juvenile and adult *M. cephalus*, using standardized CTM methodology. This approach provides a mechanistic basis for interpreting spatial and seasonal distribution patterns observed in the field, and allows for the evaluation of how close natural thermal regimes approach the physiological limits of the species. As such, the aim of this study was to quantify the upper and lower thermal thresholds of *M. cephalus* in a laboratory setting and compare these thresholds with the *in situ* temperature at the capture location. The specific objectives of the study were to:

1. Expose the fish to simulated heating and upwelling event to determine the upper (CT_{max}) and lower temperature limits (CT_{min}),
2. Calculate individuals' thermal breadth (CT_{max} - CT_{min}), and
3. Measure the ventilation rate through opercula beat rates and identify breakpoints in ventilation, which serve as a proxy for physiological thermal stress.

4.2. Methods and materials

4.2.1. Thermal environment

The fish used in this study were collected from the Kowie Estuary, Port Alfred on the southeast coast of South Africa (Figure 4.1). See Chapter 2 for a more detailed description of the study site.

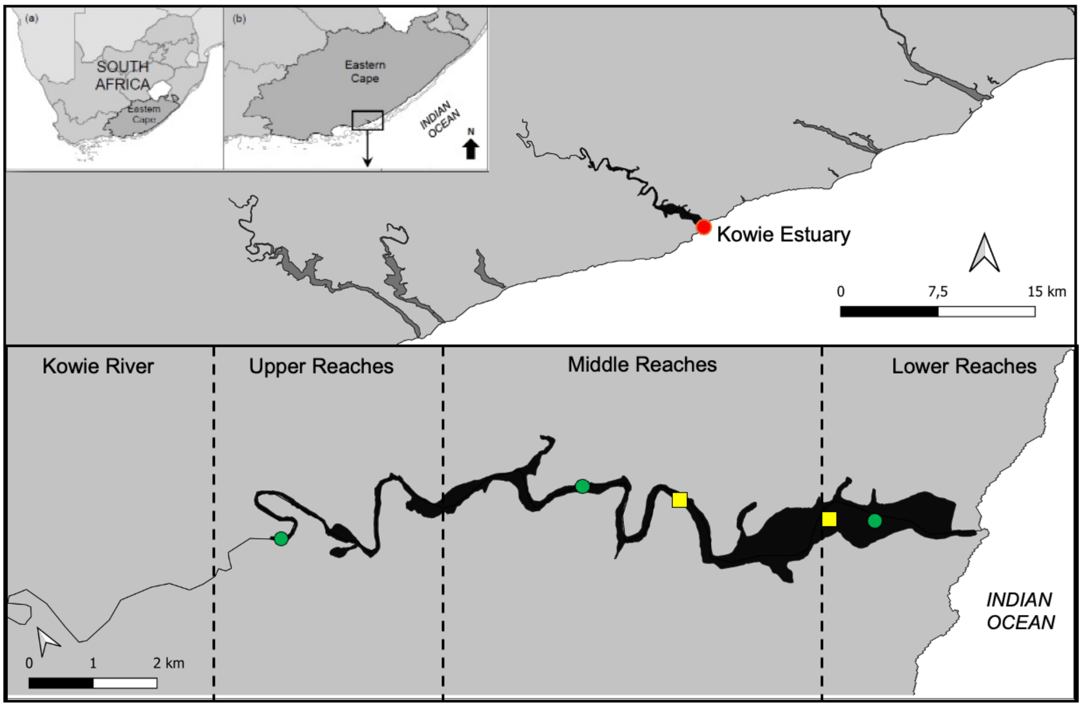

Figure 4.1. Map of the Kowie Estuary in South Africa, showing the two sites for fish collection (yellow squares) and the position of the temperature and salinity loggers (green circles).

4.2.2. Fish collection and husbandry

Mugil cephalus were collected using nylon cast nets at night on two occasions (30 January and 8 February 2024) in austral summer from the Kowie Estuary (Figure 4.1). Landed fish were temporarily kept in 50-L aerated tubs for identification and transferred to 250-L ventilated holding tanks with fresh estuary water collected directly from the site of capture for transportation to the South African Institute for Aquatic Biodiversity's Aquatic Ecophysiology Research Platform (AERP) marine laboratory at the Department of Ichthyology and Fisheries Science, Rhodes University (approximately 57 km away from the capture site).

Upon arrival, the fish were transferred into two large black circular tanks (5000-L) containing filtered and sterilized seawater with a temperature of 18 ± 0.3 °C and a salinity of 35.3 ± 1.3 with constant flow and aeration for a minimum acclimation period of 16 days. The dissolved oxygen (DO) and pH in the two holding tanks were 100% saturation and 8.3, respectively. A water temperature of 18 °C, maintained by a heat exchanger (AQUA HEAT, SF040P G/EVAP), was selected because it matched the *in situ* temperature at which the fish were collected. Fish were fed every day with Aqua-Plus Koi pellets until sated and the unconsumed food was siphoned out of the holding tanks. Water quality parameters such as DO ($mg.l^{-1}$), pH and temperature (°C) were measured daily using a Hach multi-probe meter (HQ11D, South Africa). Total ammonia (NH_4 $mg.l^{-1}$), nitrates (NO_3 $mg.l^{-1}$) and nitrites (mg NO_2 $mg.l^{-1}$) were measured daily for two weeks using chemical test kits manufactured by Lab Marine (Pro JBL Aquatest, USA Sera GmbH, Heinsberg) following standard operating procedures provided by the manufacturer. Thereafter, these parameters were measured every two days. Salinity was measured daily using a hand refractometer (ATAGO, Japan). Backwash and water changes were done for both holding tanks every two days, where 10–20% water was replaced with fresh sea water to prevent the build-up of ammonia, nitrates and nitrites. The fish were kept at a light: dark cycle of 12 h: 12 h.

4.2.3. Experimental approach

During this study, the dynamic method was used (following van der Walt et al. 2021) whereby fish were subjected to a simulated heating and cooling/upwelling event. In order to understand variability in thermal breadth within the sampled population, a repeated measures approach was taken whereby fish were exposed to both a simulated heating and cooling event (as per Allison et al. 2021). For individual identification, fish were tagged under a clove oil anaesthetic (dosage: 40 $mg.l^{-1}$, Neiffer et al. 2009) with Passive Inductive Transponder (PIT) tags in the dorsal abdominal area. Through the repeated measures approach, all fish were subjected to CT_{max} trials first, followed by a recovery period of two weeks, before being subjected to CT_{min} trials. This approach was informed by previous studies; e.g., Allison et al. (2021) found no significant difference in CTmin and CTmax end points of fransmadam *Boopsoidea* *inornata* first subjected to CTmin repeated measure thermal tolerance trials and then CTmax trials, and vice versa.

The experimental laboratory consisted of five 600-L tanks (Figure 4.1). To assess ventilation of each fish, each tank was fitted with two submerged GoPro (HERO 8) cameras on opposite sides of the tank. Ventilation rate of each fish was assessed by counting opercular beats (OB) during the trials as a proxy of thermal stress. To visibly identify individuals in the GoPro frames, fish were tagged (in addition to the PIT tags) with Visible Implant Elastomer (VIE) tags on the operculae and pectoral fins using three colours (blue, yellow, orange) (Figure 4.1). The tanks were connected to a temperature monitor, heat exchanger (AQUA HEAT, SF0040P STP) and a sump and water temperature was set to 18 °C to match the acclimation temperature at the start of each trial. Water quality parameters mentioned above were measured prior to the start of trials and aerator stones were connected to continuously supply oxygen during the course of the experiments.

Figure 4.2. (A) The experimental tank set up for thermal tolerance trials, (B, C) Visual Implant Elastomer (VIE) tagging procedure on *Mugil cephalus*, applied to facilitate individual identification during the opercular beat (OB) quantification and (D) three tagged fish in a trial tank pictured during the experiment.

Prior to the start of the laboratory trials, fish were starved for 24 h as per standard procedures to reduce postprandial effects before the experiments (Allison et al. 2021). During trials, each tank housed three fish (with different VIE tag colours-for individual distinction), randomly assigned to tanks in the order they were netted from the holding tank. The OB of fish in each tank were observed simultaneously using two GoPro cameras. For CT_{max} trials, the heating from the heat exchanger was supplemented by using heating rods (EHEIM GmbH & Co, Germany) plugged into the sump tank for the duration of the trial. During CT_{min} trials, a chiller (Hailer, HS-90A) and ice (sea water frozen in 20-L buckets two weeks prior to the trials) were used to supplement the heat exchanger to increase the rate of temperature change. During this study, the rate of temperature change during CT_{max} trials was 2.4 °C.h^{-1} and during CT_{min} trials was 1.2 °C.h^{-1} (See appendix 3 for hourly rate of change). Despite the difference in rates of change between CTmax and CTmin, both rates of temperature change were of ecological relevance as evidenced from the in situ estuarine and sea temperatures measured in the estuary of fish capture and adjacent coastal zone (range of temperature change: 1.03 to 2.73 °C.h-1). In addition, Vinagre et al. (2015) showed no effect of rate of warming on thermal end points of fish. To prevent handling stress, fish length (mm fork length, FL) was recorded at the end of the trials using a measuring tape mounted in a 20-L plastic tub.

The loss of equilibrium (LOE) and endpoints were identified by the failure of fish to swim in a dorso-ventral position and subsequently turning upside down or jumping out of the experimental tank. Upon reaching the endpoint, CT_{max} and CT_{min} were recorded and the fish were quickly removed from the experimental tanks and placed in the 50-L recovery bath with water temperature a few degrees higher/lower than the CT_{min}/CT_{max} with continuous aeration. Following recovery, individuals were identified using a PIT tag reader (VIRBAC, BackHome V800), measured (mm FL) and returned to the holding tanks. The videos from the GoPro cameras were analysed using VLC at a slowed speed to count the OB of individual fish identified by VIE tags.

4.2.4. Statistical analyses

All analyses were conducted using RStudio (R Core Team 2024) in R (Version 4.4.1). All data were tested for normality using a Shapiro-Wilk test and appropriate non-parametric tests were used on data that did not meet normality assumptions. *In situ* water temperature data were averaged to provide daily and seasonal minimum and maximum water temperatures. The seasonal temperature followed the South African Weather Service's guidelines of summer (December to February), autumn (March to May), winter (June to August) and spring (September to November).

The CT_{max} and CT_{min} were calculated as arithmetic mean of the collective thermal points at which the endpoint was reached by individuals (Lowe and Vance 1955). Thermal breadth of individuals was calculated as $CT_{max} – CT_{min}$. Simple Pearson, correlation tests with Bonferroni adjustments, were used to evaluate correlation between fish size and thermal tolerance as measured by the endpoints, CT_{max} and

CT_{min} and thermal breadth. A one-way ANOVA was conducted to test whether tank had a significant effect on the thermal endpoint (CT_{max} and CT_{min}).

To quantify the ventilation rate, videos of 10 minutes recorded at increments of 2 °C were watched during which the first two minutes were discarded to account for changes in behaviour as a result of lowering the camera into the tank. Using VLC multi media player, the videos were zoomed in and played as a slow speed to count the opercular beats per second for at least 30 seconds, this was repeated three times at along the length of the video and the average was recorded. A polynomial regression was used to determine the relationship between opercular beats and temperature during both the CT_{min} and CT_{max} trials. Furthermore, the breakpoints were calculated separately for the CT_{min} and CT_{max} by using a general linear model (GLM) and determining a point of deviation from linearity which indicated thermal stress, from the *segmented* package (Muggeo 2008) (following Allison et al. 2021). Prior to this, the data were assessed for normality and the outlier (Fish 1, the only sub-adult in the sample, Table 4.1) identified through model diagnostic plots, was removed, and the normality assumptions were met. As the only sub-adult in the sample, excluding this fish was further justified due to ontogenetic differences that could confound the analysis. Lastly, the in situ daily average temperature data were plotted using the *ggplot* package (Wickham 2016), and the average CT_{max} and CT_{min}, and the pooled upper and lower break points (BP) from the laboratory trials were superimposed.

4.3. Results

Fifteen *M. cephalus* ranging in length from 109 to 300 mm FL (170.1 ± 58.1 mm FL) were captured from the Kowie Estuary in January and February 2024 (Figure 4.1). The sample size consisted of seven young-of-year (YOY) individuals, seven juveniles of one year and one subadult of two years (length-at-maturity determined after Wallace 1975). The CT_{max} and CT_{min} trials were run for a period of 10 and 11 h, respectively, 14 days apart. In both trials when fish were nearing their thermal end points, fish were observed swimming on the water surface, changing streamline position, and during CT_{max} trials the fish would gulp for air at the water surface and some even jumped (n = 2), after which a LOE was observed. The rate of water temperature change was similar among tanks (Supplementary Table 4.1) and was, on average, 0.04 $°C.min^{-1}$

and 0.02 °C.min^{-1} for CT_{max} and CT_{min}, respectively. Fish assignment to tanks did not have a significant effect on both thermal end points, CTmax (F = 1.16, $p > 0.05$) and CTmin (F = 0.71, $p > 0.05$).

CT_{max} ranged from 37.2 °C to 38.7 °C with an average of 37.7 °C ± 0.4 °C (Table 4.1). There was no significant correlation between fish size and CTmax (Pearson, r = 0.2, $p > 0.05$). Four individuals were recorded jumping out of the experimental tanks during CT_{max} trials after which they were immediately put in a recovery bath and the temperature at which they jumped was recorded as CT_{max}. During CT_{min} trials, two fish (FH13 and FH15, Figure 4.2) did not complete the experiments due to them passing through the water pipes (smallest individuals). CT_{min} ranged from 2.6 °C to 3.8 °C with an average of 3.2 °C ± 0.5 °C. There was no significant correlation between CTmin and fish size (Pearson, r = 0.15, $p > 0.05$). Despite observed variability in the CTmax and CTmin estimates (Table 1), there was also no significant correlation between individual CTmax and CTmin (Pearson, r = 0.2, $p > 0.05$).

Table 4.1. The length (mm fork length), critical thermal maximum (CT_{max}), critical thermal minimum (CT_{min}) and thermal breadth (CT_{max} – CT_{min}) of individual *Mugil cephalus* during critical thermal limit trials. NA represents fish that did not complete CT_{min} trials.

Fish code	Length (mm FL)	CT_{max} (°C)	CT_{min} (°CC)	Thermal breadth (°C)
FH1	300	37.3	3.5	33.8
FH2	219	37.5	2.7	34.8
FH3	216	37.5	3.5	34.0
Fh4	210	37.2	2.7	34.5
FH5	206	37.4	3.8	33.6
FH6	199	38.0	2.6	35.4
FH7	199	38.7	3.5	34.3
FH8	198	37.8	3.8	34.0
FH9	125	37.3	2.7	34.6
FH10	123	37.5	2.8	34.7
FH11	118	38.0	3.5	34.5
FH12	117	37.9	2.7	35.2
FH13	111	38.0	NA	NA
FH14	110	37.5	3.5	34.0
FH15	109	38.3	NA	NA

The thermal breadth of fish (calculated as CT_{max} – CT_{min}) ranged from 33.6 °C to 35.4 °C with an average of 34.4 °C ± 0.5 °C (Figure 4.2). Thermal breadth appeared to decrease as fish size increased, although this relationship was not significant (Pearson, $r = -0.4$, $p > 0.05$). Eighty percent of the YOY had above average thermal breadths, while 42% of the one-year-old juveniles had above average thermal breadth. However, there was no significant difference in thermal breadth between the YOY and the one year old juveniles (Wilcox Test: $p > 0.05$). The repeated measures method used in this study allowed for quantification of individual variation in thermal tolerance; for example, some fish (e.g. FH2, FH6, FH10 and FH12) exhibited a broader thermal breadth, reaching an above average CT_{max} and below average CT_{min}. However, some fish had a narrow thermal breadth either reaching below average CT_{max} and above average CT_{min} (FH1, FH3, Fh5, FH11 and FH14), above average CT_{max} and above average CT_{min} (warm tolerant; FH7 and FH8) or below average CT_{min} and below average CT_{max} (cold tolerant; FH4, FH9).

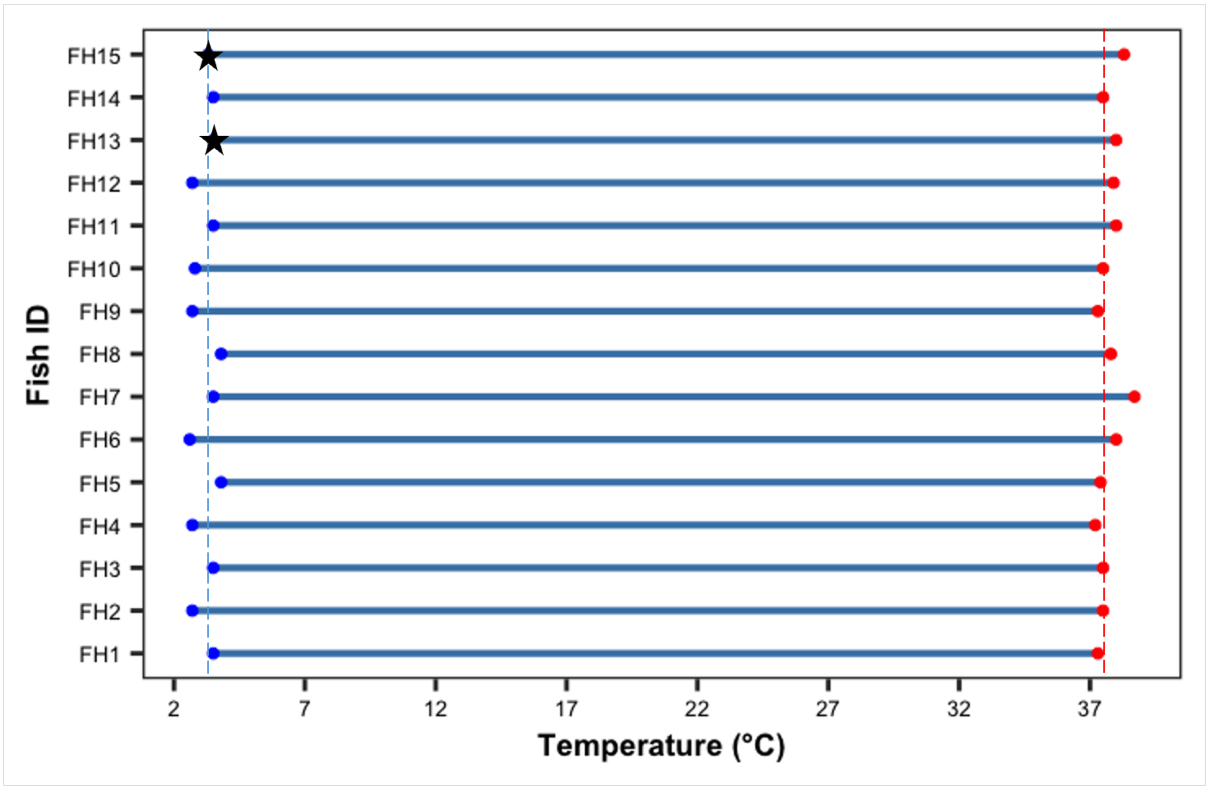

Figure 4.3. The visual representation of thermal breadth ($CT_{max} – CT_{min}$) of individual *Mugil cephalus* during critical thermal limit trials. The dashed lines represent the average CT_{min} and CT_{max} of 3.2°C and 37.7°C respectively. Stars represent fish that did not complete CT_{min} trials.

The OB rates ranged from 36 beats.min^{-1} at 8 °C by the only subadult *M. cephalus*, to 258 beats.min^{-1} at 36 °C by two juveniles (Figure 4.4). During the trials, the OB of individuals increased with an increase in temperature. The results of the model indicated an upper and lower breaking point of 29.3 °C and 13.5 °C, respectively. Additionally, there was a noticeable drop in OB at 36 °C and a noticeable increase in OB at 6 °C, , however, OB at temperatures below 6 °C could not be measured due to limited resolution of the video analysis setup. No mortalities occurred during or after both trials. Although not quantified, the swimming speed as recorded by the cameras increased and decreased with an increase and decrease in temperature, respectively.

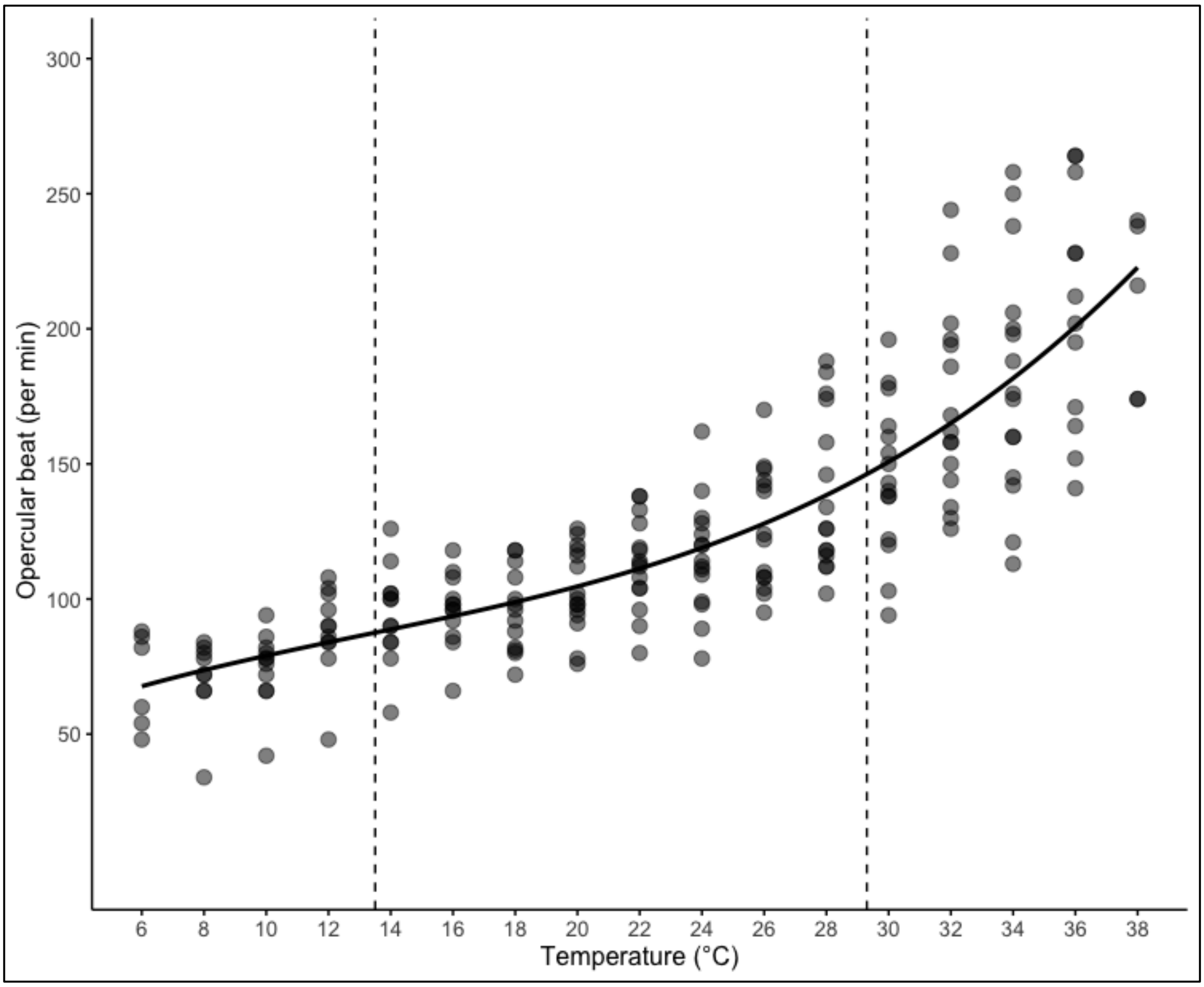

Figure 4. 4. Opercular beat rate (beats per minute) of *Mugil cephalus* during the CT_{max} and CT_{min} trials at every 2 °C water temperature change, the dashed lines indicate the minimum and maximum ventilation breaking points (BP) of 13.5 and 29.3 °C, respectively.

The average CT_{max} was considerably higher than the average upper BP of ventilation rate, which indicates thermal stress is experienced on average 7.9 °C before reaching critical upper thermal limits (Figure 4.3). While the average CT_{max} is higher than the *in situ* average temperature in summer (25.3 °C at Station 21) at the riverine-estuarine interface of the Kowie Estuary (Figure 4.5), the highest daily average temperature recorded in the Kowie Estuary during this study was 31 °C on 05 February 2024.

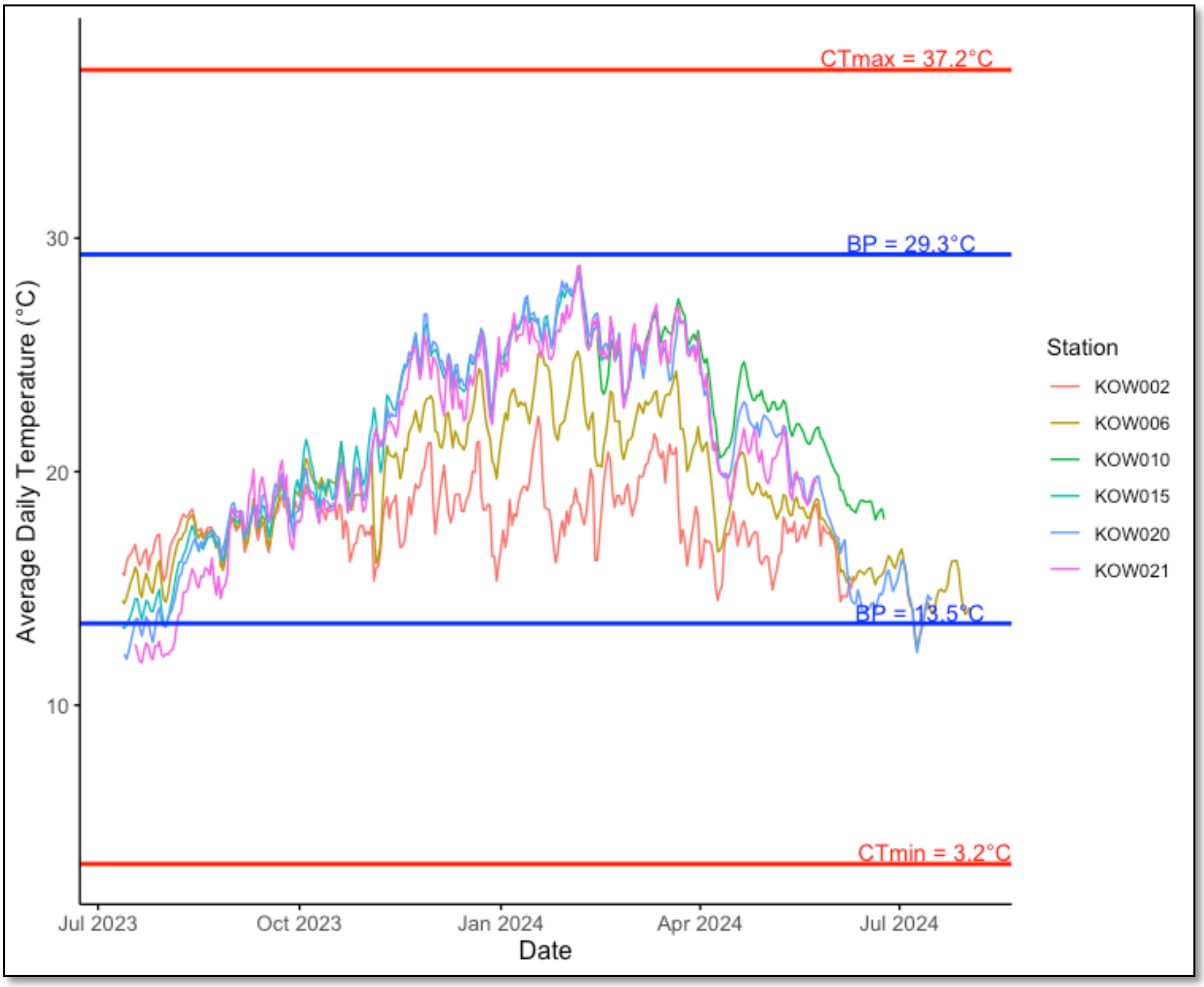

Figure 4.5. The *in situ* water temperature recorded at various sites in the Kowie Estuary between July 2023 and July 2024, with average CT_{min}, CT_{max} and upper and lower breakpoints (BP) overlaid (From Station 2: closest to the mouth to Station 21: riverine-estuarine interface).

4.4. Discussion

This study presents insights into the thermal tolerance of *M. cephalus*, with results revealing a wide thermal breadth of 34.4 °C, with a lower thermal limit of 3.2 °C and an upper thermal limit of 37.7 °C. Intra-specific variation in thermal breadth suggested smaller fish had a larger temperature tolerance range, which could reflect ecological and developmental adaptation strategies (Walsh et al. 1991). However, there was no relationship between fish size and upper and lower thermal limits in this study, most likely because all fish were juveniles, with only one sub-adult assessed during thermal tolerance trials. Despite the broad thermal tolerance of this species, the ventilation breakpoints of 29.3 °C and 13.5 °C during the upper and lower thermal limit trials, respectively, were close to the summer maximum and winter minimum temperatures in their *in situ* environment, which might have implications for future climate change predictions. A thermal niche is ideally narrower than thermal tolerance, because thermal niche is related to a species' temperature preference which is the best conditions for aerobic performance and reproduction (Gvoždik 2018). Therefore, although species such as *M. cephalus* in this study have a broad thermal tolerance range, their thermal stress is induced at temperatures below the upper thermal limits and above the lower thermal limits.

Fish sustain physiological processes such as metabolism, foraging and growth, within an optimal thermal range (Dowd et al. 2015). Exposure to temperatures outside these can result in altered physiological functions such as increased metabolic rates, oxygen demand and subsequent death (Pörtner and Knust 2007). Prior to reaching the limit, these temperatures can induce thermal stress response mechanisms, manifesting in altered locomotion to escape unfavourable conditions and muscle spasms, ultimately leading to a loss of equilibrium (Cowles and Bogert 1944; Bates and Morley 2020). For example, through changes in behaviour, individuals can escape from a slowly changing thermal environment or cease feeding; however, this can be time limited and energetically costly and if environmental change is rapid and extended, the thermal endpoint would be reached (Currie et al. 1998; Bates and Morley 2020). Thermal limits can be relatively easy to identify; however, determining the threshold at which thermal stress begins (departure from the thermal optimum when performance starts to decline) can be methodologically challenging. Given that oxygen consumption and therefore ventilation rate is strongly correlated with metabolic rate in fishes (Millidine et al. 2008; Prakoso et al. 2019), visually recording opercular beats as a proxy for ventilation rate provides a non-invasive method to identify the temperature at which individuals experience thermal stress prior to reaching their critical thermal endpoints. The CTM methodology (LOE and OB) used in this study thus allowed for the assessment of thermal limits (e.g., temperature during which LOE occurs) and thermal stress (temperature during which performance decline) information which is important for assessing how species would respond to climate change, via physiological plasticity (e.g., thermal optima -temperatures that maximise performance) and both short term acclimation and long term adaptation capabilities (Desforges et al. 2023).

High temperatures increase the average rate of biochemical reactions through enzymes to enable more activities (Houlihan and Innes 1984), thus requiring an increased oxygen supply (Pörtner and Knust 2007; Prakoso et al. 2019). The high upper thermal endpoint (37.7 °C) and behavioural response of *M. cephalus* during CT_{max} trials were consistent with previous studies (Sylvester 1975). Initially, individuals exhibited no response to increasing temperatures and remained stationary at the bottom of the tank. As temperatures rose, swimming activity and ventilation rate increased, with fish moving toward the water surface. This was followed by a rise in the frequency of muscle spasms, progressing to uncoordinated movements and, at critical temperatures, fish either attempted to jump out of the tank or lost equilibrium by turning upside down. During this study there was a difference of 1.4 °C in the highest and lowest CT_{max} during this study with the highest thermal limit of 38.7 °C. The high temperature tolerance in *M. cephalus* juveniles is common, for example, in a Hawaiian study, the juveniles (70–125 mm standard length, SL) acclimated between 20 and 29 °C achieved an average CT_{max} of 38.5 to 41.3 °C, respectively (Sylvester 1975). Furthermore, this pattern is also seen in other Mugilidae species such as *C. dumerili* juveniles (154–206 mm FL) from a South African warm temperate estuary acclimated at 18 °C and reached CT_{max} of 35.1 to 37.9 °C (Ziko et al. In review). However, prior to reaching the thermal limit (LOE) at an average CT_{max} of 37.7 °C, M. cephalus showed increased thermal stress at 29 °C, as indicated by the average breakpoint in ventilation rate. Indeed, increased ventilation can be a compensatory mechanism to enhance oxygen uptake (Das et al. 2004; Prakoso et al. 2019), and a proxy for metabolic rate (Millidine et al. 2008). These responses were expected, as elevated temperatures reduce oxygen solubility, impairing oxygen uptake, an essential process for aerobic metabolism (Pörtner and Knust 2007). Consequently, increased ventilation is a compensatory mechanism to enhance oxygen uptake (Das et al. 2004) and has been shown in *M. cephalus* experiments in brackish water (at 15, 20 and 25 °C at a salinity of 15) in South Korea, whereby the highest oxygen consumption was found at the highest temperature of 25 °C (Prakoso et al. 2019). Similarly, *M. cephalus* showed an increase in oxygen consumption when temperature was increased from 13 to 33 °C in both freshwater (salinity of 1) and seawater (salinity of 35) in a South African study, which was attributed to the concept of metabolic temperature compensation (Marais 1978).

Fish exposure to cold stress can result in significant physiological disturbances, including tissue degeneration, ion imbalance, lactate accumulation and the disruption of essential metabolic processes such as impaired feeding, reduced swimming capacity and an inability to escape predators (Donaldson et al. 2008; Allison et al. 2021). During CT_{min} trials, both movement and ventilation rates declined with decreasing temperatures. Although CT_{min} was 3.2 °C thermal stress was identified at 13°C, which was considerably higher than the lower critical limit. The extent of opercular bone movement (ventilation rate) of all individuals was reduced at low temperatures (below 6 °C), making opercular beat counts difficult to quantify. A study on the stress response of *M. cephalus* acclimated in freshwater at low temperatures in Korea has shown that low temperatures affects behavioural activity and increases the stress response through an increase in cortisol and glucose levels in the blood at 12 °C (Prakoso et al. 2015). The ventilation rate of the only subadult in this study (300 mm FL, acclimation: 18 °C), during the lower thermal limit was 48 beats.min^{-1} trial at 12 °C and during upper thermal limit trial was 95 beat.min^{-1} at 26 °C, both of which were lower than all fish in the study. This could be linked to previous exposure to thermal extremes (Walsh et al. 1991; Bates and Morley 2020); however, future studies will need a large sample size of adults to explore this. For comparison purposes, a similar study on *M. cephalus* (average: 280 mm total length [TL]) in South Korea identified a ventilation rate of 74–97 beat.min^{-1} at 12 °C of the fish that were acclimated at 25 °C with 95–114 beat.min^{-1}, concluding that lowering the water temperature activated a stress response which was seen in the behaviour of the species (Prakoso et al. 2015). Understanding the behavioural responses to thermal stress can provide valuable insights into potential thermal refugia that could support fish populations under changing environmental conditions.

During this study, there was individual variation in the overall thermal response to increasing and decreasing temperatures and thermal extremes although not linked to fish size, for example only a few individuals exhibited high tolerance to both cold and warm temperatures extremes (CT_{max} and CT_{min}). The majority of the population consisted of individuals that had narrow thermal breadth including a few that were only cold tolerant or warm tolerant. Physiological variation is necessary for species survival and reproduction and this can be a result of temporal variation in individual’s body temperature, spatial variation and inter-individual variation in biochemical and physiological capacities due to life stage (Dowd et al. 2015).

Aquatic organisms in systems that experience intermittent droughts or permanent closure of estuaries, can become confined to isolated pools for extended periods, exposing them to rapidly rising temperatures nearing their upper thermal thresholds (Vander Vorste et al. 2020). For example, *M. cephalus* faced extreme thermal stress during the prolonged closure of the St Lucia mouth in the eastern coast of South Africa leading to loss of estuarine-marine connectivity and experiencing extreme salinities of >60 in the summer months and later died when salinity increased to 70 and 80 (Whitfield 2021). In Piedra Blanca Creek (Ventura County, CA, USA), where water temperatures reached 28 °C, rainbow trout *Oncorhynchus mykiss* died, highlighting the lethal impact of such temperatures on certain species (Desforges et al. 2023). Regression analyses indicated that the rate of temperature increase in the studied pools (0.039 and 0.048 $°C.min^{-1}$), although slower than the standard recommended rate (0.3 $°C. min^{-1}$), however, according to Desforges et al. (2023) this was still insufficient to elicit an acclimation response in the species. Over time, the exposure to a changing thermal environment can therefore expose a population’s phenotypic and genetic variation which will then influence the heritability and evolvability of adaptation of the species (Bates and Morley 2020) but only if change is not rapid.

Previous CTM studies have demonstrated the importance of acclimation temperature and the rate of temperature change on thermal endpoints (Sylvester 1975; Menasveta 1981; Desforges et al. 2023). Ecologically, the acclimation temperature and duration allows an individual sufficient scope for activity (Fry et al. 1947). Acclimation is defined as a change in biochemical pathways that allows for a new stable physiological state in an altered environment (Bates and Morley 2020). Furthermore, since the CTM methodology provides insights that can help predict future species response to changing environment, it is also important to use an ecologically relevant rate of temperature change during trials which can vary with in the natural environment unless during extreme events (e.g. thermal discharge, upwelling) (Desforges et al. 2023). This study used the ramping rate of 0.05 $°C.min^{-1}$ (2.5 $°C.h^{-1}$) for CT_{max} and 0.02 $°C.min^{-1}$ (-1.2 $°C.h^{-1}$) for CT_{min}, which was ecologically relevant for the species in their natural environment (range of temperature change at Port Alfred nearshore marine environment: 1.03 to 2.73 $°C.h^{-1}$ (ATAP, unpublished, see Figure 2.10 in Chapter 2). For standardization a thermal ramping standard rate of 0.3 $°C.min^{-1}$ (18 $°C.h^{-1}$) is recommended to prevent the animal body from releasing an acclimation response (Desforges et al. 2023). However, such standardisation in trials still does not account for species' differences in morphology, size and physiology (Jutfelt 2020). To quantify individual stress levels during thermal tolerance experiments, future studies could measure the concentrations of hormones such as cortisol and adrenaline prior to and after the trials using parallel experimental set-ups to avoid posing additional stress to test fish (Darwood et al. 2017). Furthermore, thermal tolerance experiments could be determined at multiple acclimation temperatures and salinity across a species' range to account for latitudinal variation in the thermal distribution range of cosmopolitan species (Dalvi et al. 2009; Bates and Morley 2020) such as *M. cephalus.* The combined effects of temperature and salinity experiments showed that *M. cephalus* embryos developed at 20 to 30 °C and a salinity range of 15–36, however, only temperature had an impact on hatching time (Walsh et al. 1991). *Mugil cephalus* juveniles consume on average 18 mg.h-1 more oxygen in freshwater compared to seawater (Marais 1978), and Prosser (1973) concluded that metabolism is increased at reduced salinity for euryhaline species. Unlike *C. dumerili* which showed high stress levels as temperature increased in the freshwater compared to the sea water, *M. cephalus* response to thermal stress through oxygen uptake was not different between the freshwater and marine groups indicating the euryhaline nature of the *M. cephalus* species complex (Marais 1978), a key feature to its global success (Whitfield et al. 2012).

Despite these methodological constraints, this chapter provides valuable insights into the thermal tolerance of *M. cephalus* in an understudied region for this species and these findings offer a critical first step in assessing the species physiological responses to temperature fluctuations. The observed high breakpoint in ventilation rate at 13 °C during the lower thermal limit experiment raises concern in the context of this study, given that the thermal dynamic nature of the South African coastline, particularly, the Port Alfred coast which is situated within an active upwelling cell which frequently brings in cold seawater into the estuary in summer, with temperatures occasionally falling below 9 °C (James and Harrison 2010; Goschen et al. 2012). This suggests that thermal stress may affect the seasonal use of estuarine habitats for most individuals as seen in Chapter 3. Given the predicted global temperature change and the expected increase frequency and intensity of extreme thermal events, these baseline data are essential to explore if such patterns are consistent throughout *M. cephalus* life cycle stages. The next chapter will explore the lifetime movement patterns and habitat use of the species using otolith microchemistry.

CHAPTER 5

USING OTOLITH MICROCHEMISTRY TO DETERMINE THE LIFETIME HABITAT USE AND CONNECTIVITY OF FLATHEAD MULLET *MUGIL CEPHALUS* IN A WARM TEMPERATE SOUTH AFRICAN ESTUARY

5.1. Introduction

Coastal ecosystems, such as estuaries, are transition zones that provide a continuity of the aquatic medium between the riverine and marine environments (Whitfield and Elliott 2011; Day et al. 2012). Estuarine conditions are distinct from those found in the riverine and marine environments mainly because of changes in salinity that generally increase horizontally and sometimes vertically from zero at the head of the estuary to euhaline ranges at the estuary mouth (Whitfield 2021). Estuaries' unique properties, such as opposing current systems, which facilitate the mixing of freshwater from mineralised catchments with seawater, result in dynamic nutrient exchanges and high temporal variability in environmental parameters such as temperature and salinity (Whitfield and Elliott 2011). The estuarine water chemistry is shaped by geochemical and hydrological processes which includes estuary geomorphology, catchment runoff and tidal regime, all of which affect the distribution and bioavailability of trace elements within these systems (Boyden et al. 1979; Wilson 2002; Whitfield and Elliott 2011). These processes generate distinct chemical signatures across space and time, some of which can be archived in the biomineralized tissues of fish species (Campana 1999), and later used as a tool to reconstruct individual lifetime habitat use and connectivity.

Mugilidae species, such as *Mugil cephalus*, dominate fish assemblages in coastal systems such as estuaries worldwide (Blaber 2000; Whitfield et al. 2012), and are well adapted to fluctuating estuarine conditions, capitalising on them to increase their survival and fitness (Whitfield 2021). The main benefit is access to additional nursery area ecosystems providing extra food, habitat and refuge for juvenile fish (Beck et al. 2001; Able 2005; Sheaves et al. 2015). This makes estuaries an important habitat link for *M. cephalus* larval and adult life cycle stages, both located in the marine environment where spawning occurs (Whitfield et al. 2012). It is therefore important to understand how individuals move between these interconnected habitats.

One of the most powerful tools for reconstructing such movement across life stages is the analysis of otoliths. Otoliths (ear bones) are paired hard structures found in the inner ear of all teleost fish, which they rely on for balance and hearing (Elsdon et al. 2008). These structures continuously accrete layers of calcium carbonate that incorporate environmental chemical markers, creating a permanent record of habitat history (Campana 1999; Elsdon and Gillanders 2003, Sturrock et al. 2012). Since otoliths are metabolically inert, their elemental composition remains unchanged after deposit, allowing for precise environmental reconstructions throughout individual lifetime (Campana and Neilson 1985; Bath et al. 2000), following the assumption that the environmental changes experienced by an individual at any given time are reflected in the structure and composition of its otoliths (Elsdon and Gillanders 2006; Elsdon et al. 2008). Otolith elemental signatures in strontium (Sr) and barium (Ba) in particular, provide a reliable proxy for ambient salinity gradients due to their known relationship with salinity, allowing to infer habitat transitions in estuarine fishes (Campana 1999; Bath et al. 2000; Elsdon et al. 2008). However, the relationship between otolith chemistry and salinity can be species- and location-specific. Therefore, it is important to validate this relationship prior to habitat inferences (Martin and Wuenschel 2006; Chang and Iizuka 2012; Nelson and Powers 2019).

Since its development over 30 years ago, otolith microchemistry has become an important tool in fisheries science, and is now widely used to study different aspects of fish biology and ecology, including fish migration (Sturrock et al. 2012; Clarke et al. 2015), stock discrimination (Campana 2005; Elsdon et al. 2008; Nazir et al. 2021) and habitat connectivity (Tournois et al. 2017; Prichard et al. 2018; Russell et al. 2022; Gonzalez et al. 2023; Pease et al. 2023). Furthermore, it has been successfully used to reconstruct lifetime habitat use in various important species across geographic regions, including studies on *M. cephalus* in Taiwan (Chang et al. 2004a; Wang et al. 2010; Chang and Iizuka 2014), Australia (Fowler et al. 2016) and the Mediterranean Sea (Fortunato et al. 2017). However, applications of the technique in Africa remain limited, with most studies restricted to stock discrimination of only a few commercial species (Diouf et al. 2006; Labonne et al. 2009; Holbach et al. 2012; Panfili et al. 2012; Hampton et al. 2018). To our knowledge, this study is the first to apply otolith microchemistry to examine lifetime habitat use and estuarine-marine connectivity of *M. cephalus*, or any other mugilid species on the African continent.

Filling in this knowledge gap is particularly important given that *M. cephalus* dominates estuarine fish communities in South Africa and requires access to marine habitats for spawning (Wallace and van der Elst 1975; Whitfield et al. 2012). While global data on *M. cephalus* movement exist, they remain fragmented, especially in southern Africa, where estuarine use and marine connectivity are often inferred from indirect spatio-temporal occurrence data (Harrison and Whitfield 2006). Past studies have highlighted the biological importance of access to the marine environment to spawn for *M. cephalus*, as well as the negative consequences of disrupted estuarine-marine connectivity. For example, the closure of the St. Lucia Estuary in South Africa during the 1970s caused prolonged drought, and led to reproductive failure and gonad resorption in *M. cephalus* due to restricted access to marine spawning grounds (Wallace 1975; Whitfield 2021). Thus, understanding habitat use patterns across the sea-estuary-river continuum is critical for conservation and management of this species (Whitfield 2020). To this aim, this study investigated the value of otolith microchemistry for reconstructing the lifetime habitat use and estuarine-marine connectivity of *M. cephalus* from a warm-temperate estuary in South Africa. The objectives of this study were to:

1. Validate the stability of the sea chemical signature in *M. cephalus* otoliths across ontogeny by comparing Sr and Ba otolith records during fish larval life at sea and controlled laboratory experiments in seawater at the juvenile and adult stage,
2. Use multi-elemental otolith signatures to discriminate habitats within the estuary (lower and middle reaches) and the sea environment, and
3. Compare the lifetime movement and habitat use patterns of *M. cephalus* derived from multi-elemental otolith signatures with those inferred from Sr and Ba profiles

5.2. Methods and materials

5.2.1. Otolith collection

This chapter used the otoliths of individual *M. cephalus* previously assessed in the thermal tolerance study (Chapter 4), with additional specimen collected from fish that were not part of trials (see Figure 4.1 and Chapter 2 for full description of the study site and environmental parameters).

A total of 24 pairs of otoliths collected from *M. cephalus* specimen of various sizes (221.4 ± 124 mm for length [FL], range: 84 to 555 mm FL) captured during the austral summer (January–February 2024) at two discrete locations within the Kowie Estuary, were used for otolith microchemistry analysis. This included nine young-of-year (YOY), nine juveniles (1 to 2+ years), and six sub-adults/adults (3 to 6+ years) (L_{M50} = 440 mm FL, Wallace 1975), captured in the middle (n = 14) and lower reaches (n = 10) of the Kowie Estuary (Table 5.1). The individual age assignment and length-class groupings followed Thomson (1966) and Bok (1984), respectively. Otolith size exhibited substantial variation among individuals, with otolith radii (measured from the core to the edge on the ventral side) ranging from 607 to 2235 µm, with a mean of 1275.6 ± 471.5 µm (Table 5.1). Otolith size was strongly correlated with fish size, as indicated by the significant positive relationship between otolith radius and FL ($r = 0.93$, $p < 0.005$), demonstrating the expected proportionality between somatic growth and otolith accretion.

Table 5.1. Fish ID, length (mm), age estimates, life history stage, total otolith size (radius µm) and size (radius µm) at the end of larval life of all individual *Mugil cephalus* specimens collected from the Kowie Estuary, South Africa. In the fish code column, Y denotes young-of-year fish, J denotes juveniles, and SA denotes sub-adults and adults.

Fish code	Fork length (mm)	Age	Trial	Otolith radius (µm)	End of larval life (µm)	Capture location
Y1	84	0+	Non−trial	756.8	184	lower
Y2	90	0+	Non−trial	959.2	140.8	middle
Y3	95	0+	Non−trial	809.6	228	lower
Y4	110	0+	Trial	607.2	228	lower
Y5	110	0+	Trial	924	272.8	lower
Y6	117	0+	Trial	853.6	184	lower
Y7	123	0+	Trial	1038.4	228	middle
Y8	125	0+	Trial	721.6	316.8	lower
Y9	129	0+	Trial	1038.4	228	middle
J1	180	1+	Non−trial	1170.4	140.8	lower
J2	198	1+	Trial	1003.2	140.8	middle
J3	199	1+	Trial	1020.8	228	middle
J4	199	1+	Trial	1381.6	184	lower
J5	206	1+	Trial	1267.2	228	lower
J6	210	1+	Trial	1082.4	140.8	middle
J7	216	1+	Trial	1276	228	lower
J8	219	1+	Trial	1337.6	228	middle
J9	300	2+	Trial	1697.4	228	middle
SA1	324	3+	Non−trial	1513.6	228	middle
SA2	339	3+	Non−trial	1944.8	184	middle
SA3	370	4+	Non−trial	1962.4	184	lower
SA4	381	4+	Non−trial	1927.2	184	lower
SA5	435	4+	Non−trial	2085.6	96.8	lower
SA6	555	6+	Non−trial	2235.2	140.8	lower

5.2.2. Sea chemical signature acquisition

After their capture, all fish were immediately transported alive to the NRF-SAIAB Aquatic Ecophysiology Research Platform (AERP) marine laboratory at the Department of Ichthyology and Fisheries Science, Rhodes University in Makhanda (approximately 57 km from the estuary). Of the 24 captured fish, 14 individuals (Table 1) were kept alive in a controlled laboratory setting (temperature: 18 ± 0.3 °C, salinity: 35.3 ± 1.3, dissolved oxygen: 100% and pH: 8.3) for a period of two months to validate the sea chemical signature in the otoliths of juveniles and adult specimens of *M. cephalus*. During the whole experiment, these fish were fed every day with Aqua-Plus Koi pellets and kept at a light-dark cycle of 12 h:12 h. At the end of two months, all fish were euthanised using an overdose of clove oil (dosage: 40 mg.l^{-1}, Neiffer and Stamper 2009), measured fork length (FL mm) and kept in the freezer until dissection.

5.2.3. Otolith preparation and laser ablation

For all fish, the two sagittae (i.e., the biggest pair of otoliths in *M. cephalus*) were extracted using clean (90% ethanol) plastic tweezers, cleaned with distilled water to remove biological material, dried in dust-free conditions and stored in acid-washed Eppendorf tubes. All subsequent sample preparations and analyses were conducted at the University of Montpellier (France) within the otolith microchemistry laboratory of the MARBEC research unit. For all fish, one of the two otoliths (the left one where possible) was measured and photographed under transmitted light using a camera microscope (Leica MZ2700 Germany) and software. The otoliths were then individually embedded in epoxy resin (Araldite 2020, Escil), and left to set at 35 °C in an oven for 24 hours. Each otolith was sectioned transversely using a low-speed precision saw (Bluehler®, Leinfelden−Echterdingen, Germany, Isomet 1000) to produce thin sections (width < 1000 µm) including the core. These sections were then polished on both the anterior and posterior sides until the core was exposed on one side using a decreasing gradient of dry abrasive paper from 600, 800, 1200, 2400 and 4000 grit. The resulting otolith sections (final width: 200−300 µm) were photographed using a camera (software: ProgRes C5) linked to a microscope (Olympus BX41), then sonicated for five minutes with distilled water to decontaminate their surface, and dried under a Class 100 laminar flow hood. All sections were taped on a microscope slide in a clean room prior to their chemical analysis.

Otolith core-to-edge elemental transects of 11 elements – lithium (^{7}Li), magnesium (^{25}Mg), calcium (^{43}Ca), manganese (^{55}Mn), nickel (^{60}Ni), copper (^{65}Cu), zinc (^{66}Zn) rubidium (^{85}Rb), strontium (^{86}Sr), cadmium (^{112}Cd), barium (^{138}Ba) and lead (^{208}Pb) – were analysed by Laser Ablation Inductively Coupled Plasma Mass Spectrometry (LA-ICPMS using a Thermo Fisher Element2 XR system coupled to a 193-nm excimer laser) at the AETE-OSU OREME Laboratory of University of Montpellier (France). A pre-ablation (pulse rate 4 Hz, energy 3 J.cm^{-2}, speed 20 µm s^{-1}, beam diameter 85 µm) was used to clean the otolith surface along the transect prior to measurements (pulse rate 7 Hz, energy 4 J.c^{-2}, speed 15 µm.s^{-1}, beam diameter

50 µm). The signal to noise ratios were maximized for the isotopic mass range from Mg to Ba, while the oxide production rate was tuned to ≤0.5% UO2 (254UO2/238U). For external calibration and to allow for machine drift correction, a glass reference material (NIST 612—National Institute of Standard and Technology, Gaithersburg, USA) was analysed (two replicates) at the beginning and at the end of each session, and after every five samples during analyses. An additional reference material (MACS 3, United States Geological Survey, Lakewood, CO, USA) was also analysed at the beginning and the end of each session for assessing the machine's accuracy and quality control. For each otolith, sample analysis consisted in a 30 seconds blank measurement with the laser turned off, followed by ablation which varied according to the size of the otolith and 30 seconds of final washout. Calcium (^{43}Ca) was used as the internal otolith standard and all elemental results were given as ratios to Ca, assuming 38.3% weight in all otoliths (Yoshinaga et al. 2000). All raw data were processed using the *elementR* package for R (Sirot et al. 2017), allowing simultaneous calculations of concentration (ppm) and machine limits of detection (LOD) for all chemical elements and correction for potential machine drift (Jackson and Sylvester 2008; Lin et al. 2016). Relative standard deviations (RSD in %) based on replicate measurements of the MACS 3 standard reflect the level of precision achieved for each of these seven elements, which ranged from 2 to 8%.

5.2.4. Signal treatment

To ensure data robustness, only elements detected in at least 60% of the measured otoliths spots from at least one of the three defined habitats (sea, lower estuary, middle estuary) were retained for further analysis (Mg, Mn, Rb, Sr, and Ba). For each of the retained elements, concentrations below the limit of detection (LOD) in a given otolith were replaced by the minimum observed value on the same transect to mitigate non-detect bias. The measures on each transect were then resampled to produce, for each fish, sequential non-overlapping lifetime sequential signatures, ranging from 15 to 52 laser spots (of 50 µm spot diameter) from the otolith core to the otolith edge.

For each fish, the limits between successive life stages (larval, juvenile and adult - when relevant) along each otolith transect were inferred based on both otolith microstructure analysis and Sr (validated for *M. cephalus* by Chang et al. 2004b) and

Ba concentrations (used in other species, Elsdon and Gillanders 2005). The pelagic larval phase of *M. cephalus*, which occurs in the marine environment (Whitfield et al. 2012), was defined as the otolith region extending from the core to the transition zone, approximately 200 µm from the core (adapted from Pease et al. 2023). The transition zone (also referred to as the estuarine check) represented the period of estuarine recruitment (Chang et al. 2004b), and was identified visually through a shift in the otolith growth axis (visible as a change in the density of micro-increment deposition; see Figure 5.1) and chemically by a decrease in Sr concentration, consistent with a shift from high salinity environment (marine) to low salinity environment (estuary) (Hsu et al. 2009). Since otolith growth rate is proportional to fish somatic growth (Campana and Neilson 1985), changes in environmental conditions (salinity, temperature, diet) can influence both growth rate and otolith composition (Wilson and McCormick 1997; Elsdon et al. 2008), and the transition zone can reflect this ontogenetic and ecological shift. Beyond the transition zone, the otolith transect consists of the growth rings (annuli) indicative of juvenile to adult development in individuals older than YoY (see Figure 5.1). The outermost portion of the transect, referred to as the otolith edge, represented the most recent period of growth prior to capture and was interpreted as reflecting the fish's environmental exposure at the time of collection. Two key assumptions were made regarding the interpretation of the otolith edge elemental signatures: (i) fish captured from the same location within the estuary, regardless of age class (juveniles or adults), exhibited similar otolith edge elemental profiles; and (ii) fish kept in identical, controlled laboratory conditions displayed consistent edge elemental signatures.

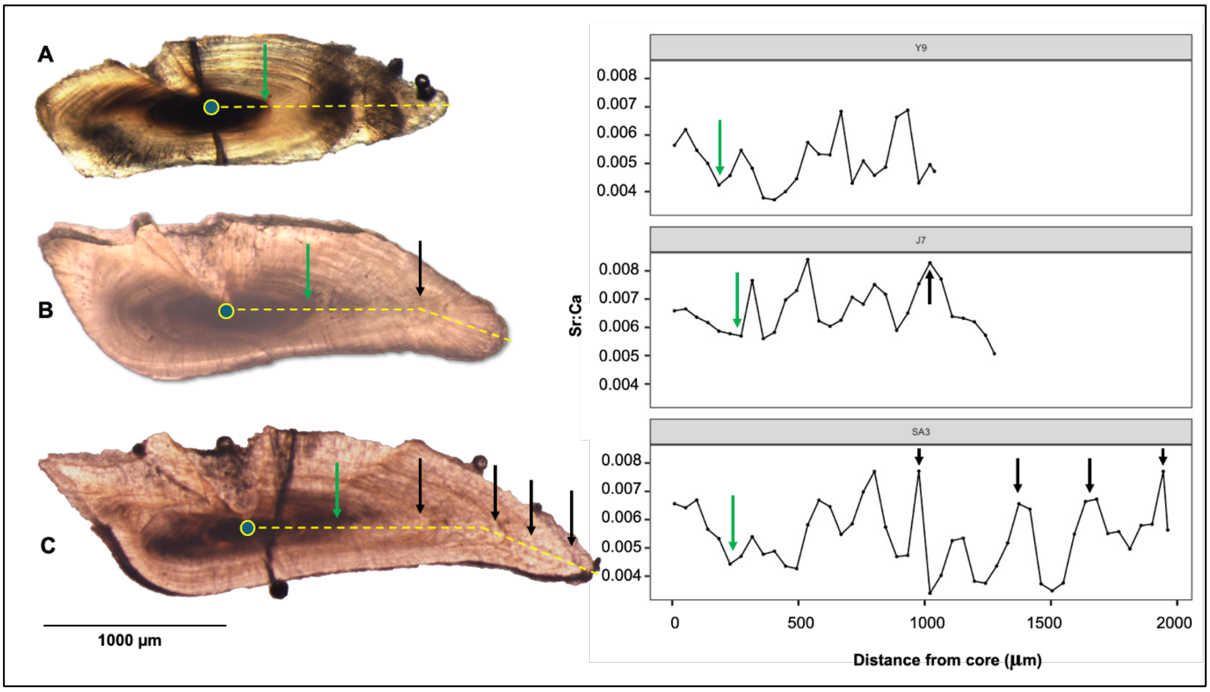

Figure 5.1. Images (Olympus SZX16 microscope, 2.5 magnification under transmitted light) of otolith transverse sections for three contrasted specimens of *Mugil cephalus* captured in the Kowie Estuary (A. YoY, B. age 2 juvenile and C. age 4 sub-adult) and corresponding Sr:Ca concentrations measured along the transect analysed on their ventral side. Circle = core, dotted line = LA-ICPMS transect line, green arrows = end of the larval life, black arrows = winter annulus deposition when present.

5.2.5. Sea chemical signature acquisition

To validate the stability of sea chemical signatures in the otolith across life stages, elemental signatures from the larval stage of *M. cephalus* were compared to those deposited during the final controlled laboratory experiment where all fish were kept at a constant salinity representative of marine environment. For this, the last spot on the transect of each laboratory-kept fish was assumed to reflect a sea chemical signature. The resulting 14 individual signatures (for juvenile and subadult fish of 110–300 mm FL) in Sr and in Ba were compared with those recorded by all fish during their larval life at sea (70 signatures per element) using the non-parametric Wilcoxon rank-sum test (after the Shapiro-Wilk Test indicated that the data did not meet the assumptions of normality).

5.2.6. Habitat discrimination

The *M. cephalus* otolith multi-elemental signatures for life at sea and in the lower and middle reaches of the Kowie Estuary were analysed for their potential to retrospectively identify lifetime habitat use of this species within the study area. For this, the subset of otolith signatures used (Random Forest [RF] classifier) consisted of i) all larval signatures for all fish (reflecting life during the pelagic life at sea), and ii) the multi-elemental signature of the otolith edge of all fish representing fish capture location (representing life in either the middle or lower reaches of the Kowie Estuary), identified as the last spot on the transect for all fish but for the 14 fish exposed to constant laboratory conditions post capture, the second-last spot was used instead. To identify the best element combination for discriminating among the three habitats (sea, lower and middle reaches), a cross-validation procedure based on the use of the RF algorithm (Breiman 2001) was applied. The RF machine learning method, widely used in otolith microchemistry studies, offers highest discrimination accuracy, particularly for chemically distinct habitats and when data violate the assumption of multi-normality (Mercier et al. 2012; Tournois et al. 2017; Gonzalez et al. 2023). The cross-validation analysis was conducted in two phases. A training dataset was first constructed by randomly selecting 75% of the otolith multi-elemental signatures in the global RF classifier (Table 5.2). Secondly, the remaining multi-elemental signatures in the RF classifier (25%), referred to as the test dataset, were used to predict fish habitat origin (Table 5.2). Comparisons of predicted and actual origin for these fish allowed us to validate the model through assessing its prediction accuracy. For each RF model, 5000 classification trees and 1000 iterations were used. All possible combinations of retained chemical elements (RF classifiers) were evaluated using a Bayesian bootstrapping approach to identify the optimal RF classifier (i.e. that leading to the maximum accuracy in the discrimination between all three habitats). For each elemental combination, the minimum and maximum accuracy and the mean accuracy and its standard deviation were calculated and used to compare between RF models.

Several additional metrics were computed to evaluate and explain classification performance for all RF classifiers. These included a confusion matrix, the mean decrease in the Gini Index, out-of-bag (OOB) error rate (Breiman 2001), and the True Skill Statistic (TSS, Allouche et al. 2006). Collectively, these metrics assessed the model reliability, potential class imbalances, and relative importance of each element in the classification process. For example, the TSS is a threshold-independent measure that incorporates both omission and commission errors. It is important in multi-class ecological classification, where class overlap and imbalanced sample sizes can obscure overall accuracy. Higher TSS values indicate stronger discriminatory performance, while lower values may signal overlap in class characteristics or insufficient predictor resolution.

A Principal Component Analysis (PCA) was performed on the elemental concentrations identified in the optimal RF classifier. By reducing the dimensionality of the dataset while retaining the maximum possible variance, this multivariate statistical technique allowed to further investigate the potential of the identified elements to discriminate the three habitat types (sea, lower and middle reaches), and identify similarities, differences and potential outliers within the individual fish data from otolith transects.

Furthermore, statistical analyses were conducted to evaluate patterns in elemental concentrations identified as important by the optimal RF classifier. To assess relationships among elements across the three habitat types, pairwise correlations were conducted using Spearman's rank correlation coefficient using the *Hmisc* package (Harrell 2024). To compare elemental signatures among habitats, a non-parametric Kruskal-Wallis test was used, with Dunn's post hoc tests for pairwise comparisons.

5.2.7. Lifetime habitat use

To reconstruct the lifetime habitat use of the 24 *M. cephalus* individuals, two complementary methods were applied to assign habitat types to each spot along the otolith transect, from the transition zone (end of larval life stage) to the otolith edge. The primary method used multi-elemental signatures identified by the RF optimal classifier to predict habitat use among three habitats (sea, lower and middle reaches). The second method used a simplified approach based on Sr and Ba thresholds derived from validation experiments of sea chemical signatures. Therefore, only two broad environments could be identified: the marine environment which includes the sea, estuary mouth, and lower reaches (since high tidal movement brings in seawater and salinity of 35), and brackish estuarine which includes the middle and upper reaches of the estuary. Therefore, this method comparison allowed for assessment of whether the two commonly used elements in otolith microchemistry, Sr and Ba are sufficient to infer habitat use in *M. cephalus*, and if incorporating additional elementals could yield more accurate results.

5.3. Results

5.3.1. Sea chemical signature acquisition

The 24 specimens investigated displayed a high variability in the duration of their larval life, as illustrated by the wide range in the distances measured between the core and the transition zone (170.9 ± 72.3 μm), ranging from 53 to 404 μm. Despite this variation, the extent of the larval life signatures on the otolith of individual fish ranged between 2 and 10 spots. Comparison of the concentrations acquired in the natural environment at sea during the larval phase (mean Sr concentration of the transect between the core and the transition zone $6.11 \pm 0.6 \times 10^{-3}$, with 25th and 75th percentiles of 5.67×10^{-3} and 6.46×10^{-3}, respectively) and the concentration acquired during the experiment in a controlled marine environment ($5.94 \pm 0.9 \times 10^{-3}$, with 25th and 75th percentiles of 5.19×10^{-3} and 6.65×10^{-3}, respectively) showed no significant difference ($W = -0.64$, $p > 0.05$) (Figure 5.2). However, there was a higher variability in Sr in the laboratory ranging from 4.72×10^{-3} to 7.36×10^{-3} compared to the sea, which ranged from 5.21×10^{-3} to 7.78×10^{-3}.

Similarly, for Ba, the concentration acquired at sea during larval life ($0.012 \times 10^{-3} \pm 0.01$, with 25th and 75th percentiles at 0.01×10^{-3} and 0.02×10^{-3}, respectively) was not significantly different from Ba under the controlled laboratory conditions ($0.014 \times 10^{-3} \pm 0.01$, with 25th and 75th percentiles of 0.01×10^{-3} and 0.02×10^{-3}, respectively) ($W = 0.86$, $p > 0.05$) (Figure 5.2). There was, however higher variation in Ba in samples at sea (range: 0.003×10^{-3} to 0.04×10^{-3}) compared to samples from the laboratory, which ranged from 0.009×10^{-3} to 0.02×10^{-3} (Figure 5.2).

Since no significant differences in otolith signatures (Sr and Ba concentrations) were detected between the laboratory and larval life (sea) chemical signature, the threshold for identifying the sea chemical signature in *M. cephalus* was defined as the 25th and

75th percentiles of Sr and Ba concentrations observed in this study to account for the observed variation in Sr and Ba sea chemical signature incorporation.

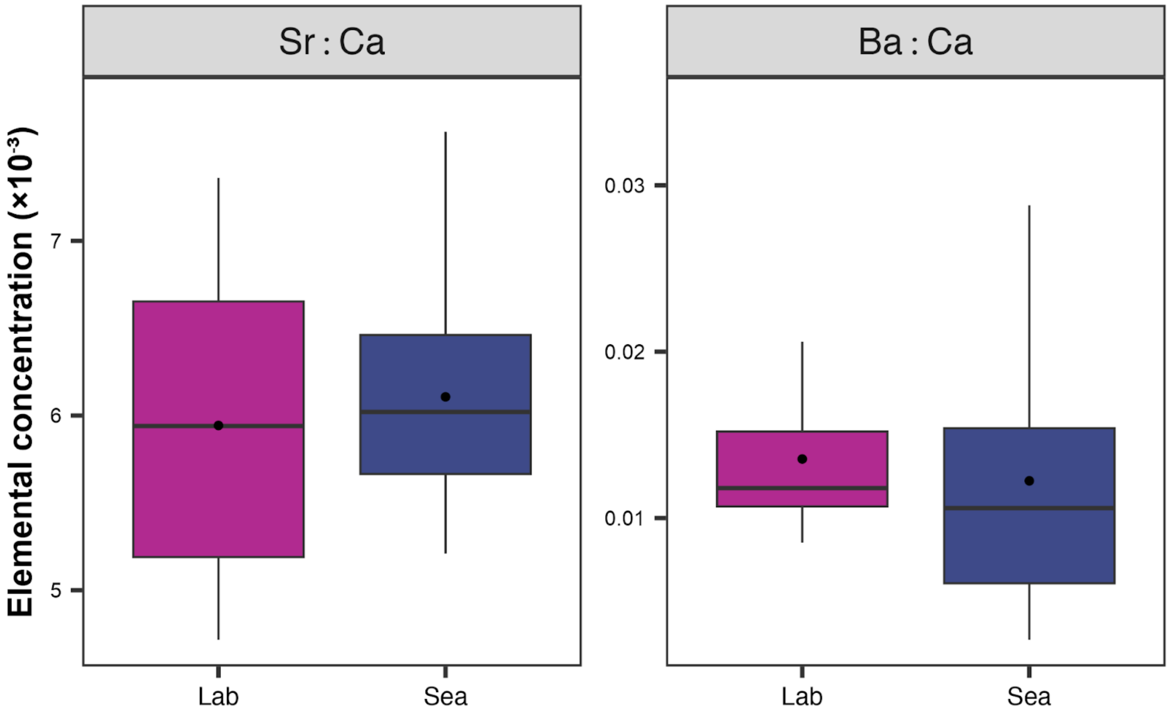

Figure 5.2. Comparison of sea chemical signatures of Sr:Ca (left) and Ba:Ca (right) in *Mugil cephalus* from controlled laboratory experiments (n = 14) versus the marine signatures incorporated during the larval life of all fish (n = 24).

5.3.2. Habitat discrimination

Of the 11 chemical elements that were measured during this study, seven (Sr, Ba, Mg, Rb, Mn, Zn and Cu) were above the defined LOD. A total of 143 otolith spots from 24 fish of known origin, representing the otolith record for *M. cephalus* in the three habitat types, were used in the analysis. Of these, 75% were assigned to the training dataset and 25% to the test dataset for model validation (Table 5.2). The optimal discrimination accuracy for the three habitats (sea, lower and middle reaches) was obtained with five out of the seven chemical elements analysed in the RF classifier: Sr, Ba, Mg, Rb and Mn (Figure 5.3), and the other two (Zn and Cu) bringing in noise instead of signal in the habitats discrimination. The optimal discrimination accuracy of 88.6% with high levels of re-assignment rate (83.9%) was reached with this combination. The estuary middle reaches habitat achieved the highest TSS (80.5%), followed by the sea (48.8%), and the estuary lower reaches habitat had the lowest TSS (24%). Habitat misclassification was the highest for lower reaches with 16 out of 22 spots from this habitat misclassified as sea, resulting in an error of 72.7%; however, the sea habitat had the lowest miss-classification error (4%) followed by the middle reaches (19%).

When comparing these five elements identified by the optimal classifier, none can fully discriminate against the three habitats. However, Sr contributed the most (more than double compared to others) to habitat discrimination such that losses to mean Gini Index were 22.38, 10.75, 9.45, 7.97, 3.85 after the removal of Sr, Ba, Mg, Mn and Rb, respectively (Figure 5.3). Although Sr was the dominant variable and likely sufficient for major habitat classification, Ba acted as a secondary signal, contributing additional precision in distinguishing transitional boundaries. Given the strong discriminatory power of Sr and the complementary role of Ba, their ability to independently distinguish between simplified habitat categories, i.e. marine (lower reaches and sea) and brackish (middle reaches), are explored further below.

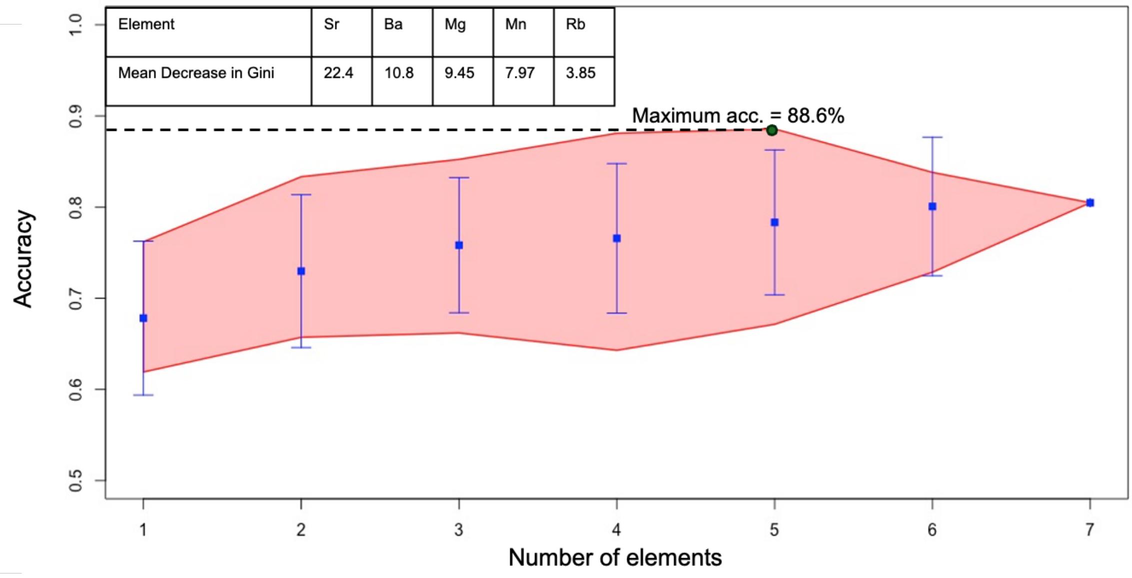

Figure 5.3. The number of elements included in the random forest and prediction accuracy of the spatial discrimination of the three habitats used by *Mugil cephalus* in the Kowie Estuary, South Africa and the Mean Decrease in Gini index of these optimal classifiers.

Misclassification of habitats only occurred in fish that were part of the validation experiments (64%) and sub-adults (50%). These were three YoY (Y4, Y5, Y8) and six juveniles (J3 to J8) (Table 5.2). One juvenile (J7) from the lower reaches had the highest misclassified spots with a total of three spots (on the otolith edge) assigned to sea instead of lower reaches (Table 5.2). Furthermore, three sub-adults (SA1 to 3) that were not part of the experiment were also misclassified as sea instead of one middle and two lower reaches habitats (Table 5.2).

Table 5.2. The training dataset (75%) and test dataset (25%) were used for discrimination of two estuary habitats (lower and middle reaches) and the sea habitat. For each fish specimen, the length, whether it was part of the validation experiment, number of spots on the otolith used and wrongly assigned by the Random Forest optimal classifier. On the fish ID, Y denotes young-of-year fish, J denotes juveniles, and SA denotes sub-adults.

Training dataset					Test dataset				
Fish ID	**Fork Length (mm)**	**Trial**	**No. of spots**	**No. of spots wrongly assigned**	**Fish ID**	**Fork Length (mm)**	**Trial**	**No. of spots**	**No. of spots wrongly assigned**
Y1	84	No	7	0	-	-	-	-	-
Y2	90	No	6	0	Y2	90	No	1	0
Y3	95	No	3	0	Y3	95	Yes	2	0
Y4	110	Yes	3	0	Y4	110	Yes	1	1
Y5	110	Yes	4	0	Y5	110	Yes	2	1
Y6	117	Yes	6	0	Y6	117	Yes	1	0
Y7	123	Yes	6	0	Y7	123	Yes	2	0
Y8	125	Yes	5	1	Y8	125	Yes	2	0
Y9	129	Yes	3	0	Y9	129	Yes	1	0
-	-	-	-	-	J1	180	No	5	0
J2	198	Yes	2	0	J2	198	Yes	1	0
J3	199	Yes	9	1	J3	199	Yes	2	0
J4	199	Yes	6	2					
J5	206	Yes	3	1	J5	206	Yes	1	0
J6	210	Yes	4	1	J6	210	Yes	1	0
J7	216	Yes	10	3	J7	216	Yes	2	1
J8	219	Yes	5	0	J8	219	Yes	4	1
J9	300	Yes	5	0	J9	300	Yes	1	0
SA1	324	No	1	1	-	-	-	-	-
-	-	-	-	-	SA2	339	No	2	2
SA3	370	No	4	1	SA3	370	No	2	0
SA4	381	No	3	0	SA4	381	No	3	0
SA5	435	No	6	0	SA5	435	No	1	0
SA6	555	No	5	0	-	-	-	-	-

The high reassignment error between the sea and lower reaches was shown when statistically comparing the individual elemental signatures among the three habitats, particularly Sr, since it showed the highest discriminatory power (Figure 5.4). There was no significant difference in Sr between the sea ($6.19 \pm 0.75 \times 10^{-3}$) and the lower reaches ($6.36 \pm 0.71 \times 10^{-3}$) ($\chi^2 = 2.35$, $p > 0.05$), while the middle reaches ($4.85 \pm 0.39 \times 10^{-3}$) differed significantly to the lower reaches ($\chi^2 = -5.92$, $p < 0.005$) and sea ($\chi^2 = -6.52$, $p < 0.005$). Furthermore, Ba, the secondary discriminator especially between sea and the estuary habitats, was significantly lower at sea (0.012 ± 0.01 × 10^{-3}) compared to the lower reaches (0.018 ± 0.01 × 10^{-3}) ($\chi^2 = 3.69$, $p < 0.05$) and middle reaches (0.018 ± 0.01 × 10^{-3}) ($\chi^2 = 2.32$, $p < 0.05$), and no significant difference in Ba occurred between the lower and middle reaches ($\chi^2 = -0.72$, $p > 0.05$). Mg was only significantly different between sea (0.06 ± 0.03 × 10^{-3}) and the middle reaches (0.08 ± 0.03 × 10^{-3}) ($\chi^2 = 2.58$, $p < 0.05$), while the lower reaches (0.06 ± 0.02 × 10^{-3}) was not significantly different to both the sea and middle reaches ($\chi^2 = 2.58$, $p > 0.05$). There were no significant differences in Mn between sea (0.008 ± 0.00 × 10^{-3}), lower (0.007 ± 0.00 × 10^{-3}) and middle reaches (0.008 ± 0.00 × 10^{-3}) ($p > 0.05$); similarly Rb in the sea (0.0002 ± 0.000007 × 10^{-3}), lower (0.0001 ± 0.000008 × 10^{-3}) and middle reaches (0.0002 ± 0.000005 × 10^{-3}) were not significantly different ($p > 0.05$) (Figure 5.4).

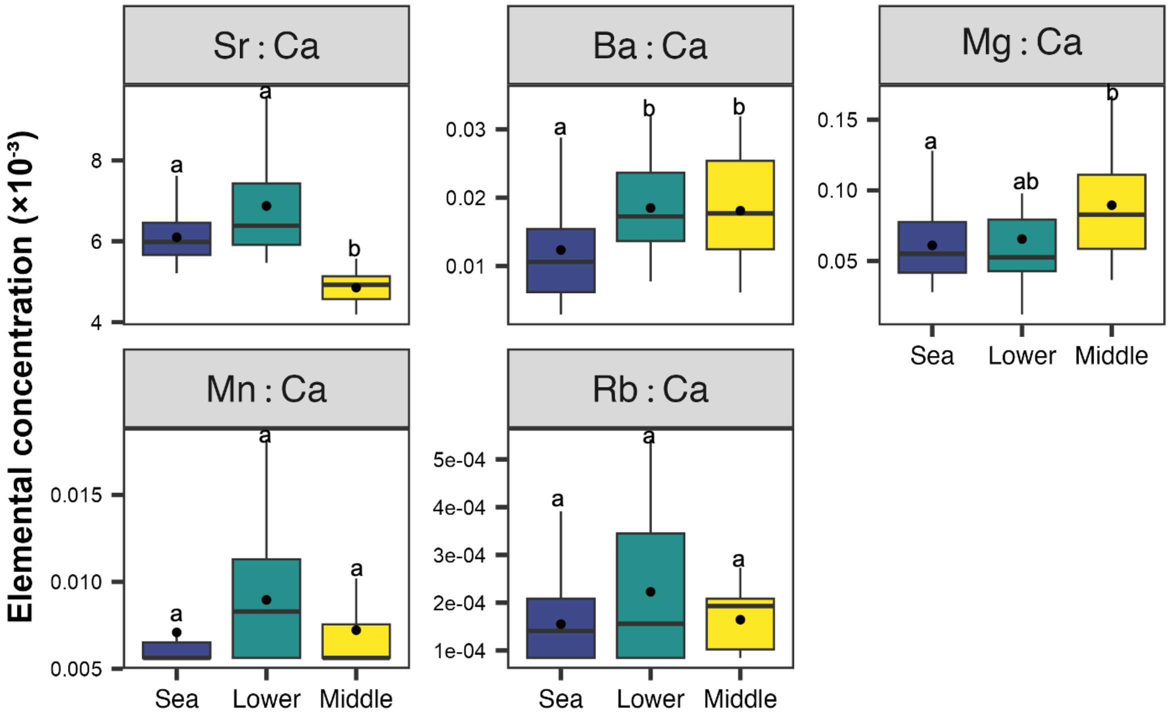

Figure 5.4. Box plots showing the data distributions of multiple otolith chemical elements describing habitats for *Mugil cephalus* collected in the Kowie Estuary, South Africa. Circles indicate the mean of the distribution and letters denote significant differences and the error bars denote the 25 and 75% quartiles.

The PCA analysis further illustrated this high degree of overlap among the three habitat types, as identified by precision matrices and RF optimal classifier, whereby individuals from the estuary lower reaches exhibited a wide spread in PCA space, with a large distribution encompassing much of the variation observed in the other two habitats (Figure 5.5). The substantial overlap indicates limited elemental differentiation, suggesting that fish may have experienced broadly similar environmental conditions (Figure 5.5). In contrast, the middle and sea habitats displayed more compact and narrowly clustered signatures, despite the overlap between them (Figure 5.5).The first principal axis (PC1) accounted for 26.6% of the variance, and was predominantly influenced by Rb (38%), Ba (36%) and Mn (22%). PC2 explained a further 24.3% of the variation, with strong contributions from Mg (54%) and Sr (35%), and PC3 accounted for an additional 19.5% of the variances, mainly driven by Mn (36%) and Sr (24%). Unlike the Mean Decrease in Gini Index that indicated Sr as the important habitat discriminator and Rb as the lowest contributing element, PCA identified Rb and Ba as the main drivers of habitat separation (Figure 5.5). There was a broad dispersion of points from the lower reaches, which likely reflects substantial within-habitat variability and overlapping elemental profiles with other zones. This overlap may explain the high misclassification rate observed in the RF model, which reassigned less than 25% of individuals correctly to the lower estuary. Overall, the RF optimal classier and PCA results showed there were inter-habitat similarities among the three habitats, but more closely between sea and estuary lower reaches habitats (possible frequent movement between the two habitats), thus leading to low model performance especially in identifying lower reaches.

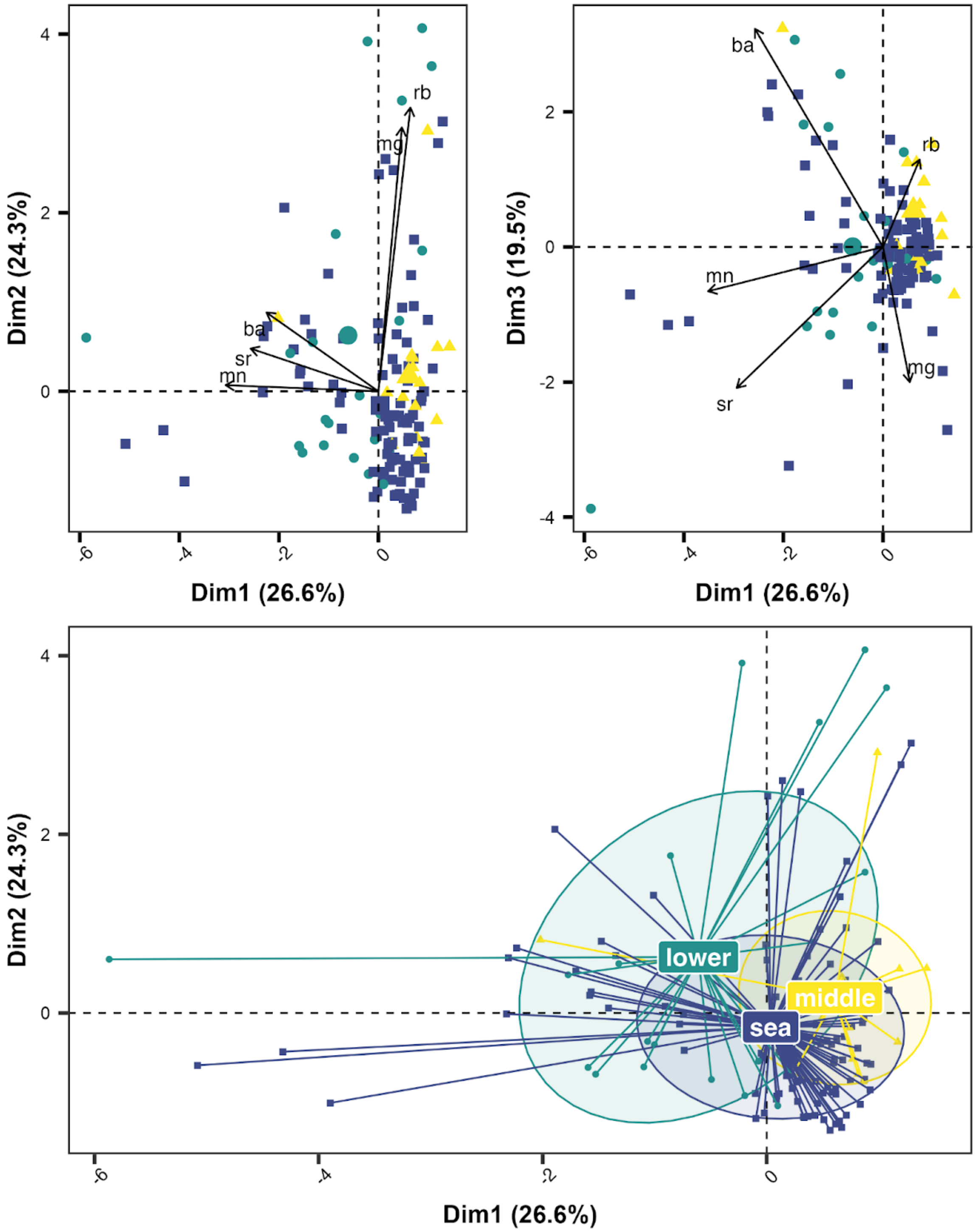

Figure 5.5. Results of the Principle Component Analysis (Axis 1 to 3) on the otolith multi-elemental signatures (Sr, Ba, Mn, Mg and Rb) of *Mugil cephalus* of the three habitats investigated (sea, estuary lower and middle reaches) around the Kowie Estuary, South Africa.

5.3.3. Lifetime habitat use

Reconstruction of lifetime habitats of life for 24 *M. cephalus* of 0 to 6 years old using the optimal RF classifier revealed common habitat use strategies among them, but also highlighted potential interindividual differences in lifetime movement patterns. Two fish (SA1 and SA2) were excluded from the larval life habitat discrimination because during processing, the core was unidentified; however, their lifetime habitat use was still analysed from the period of recruitment to capture. Despite the potential partial bias resulting from a small sample size and otolith multi-elemental signatures overlapping in habitat chemical signatures, 100% of the larval life spots were assigned to sea. There was variability in larval life period and growth rate as shown by differences in size during estuary recruitment (Figure 5.6). Habitat assignment using multi-elemental signatures showed that all but one (J7) fish used multiple habitats in their lifetime. Following the larval life in the marine environment, the model assigned recruitment into the middle reaches for most fish except for seven individuals (Y1, Y3, J3, J7, J9, SA5, SA6), who remained at sea at the end of the larval life (Figure 5.6). The YoY in this group showed high connectivity in habitat use, with 67% spending a more time in all three habitats compared to the rest. In the first year of life most fish used the middle reaches more compared to the period after. There was variation in the success of habitat re-assigned by the model: the capture location of YoY was successful for 89% fish, 50% subadults and juveniles were the least correctly assigned with 33%. Although there was less assignment of habitat to lower reaches for YoY and juveniles, this habitat was much clearer in the sub-adults (e.g., SA4, SA5, SA6), which spent much less time in the middle reaches compared to the younger fish.

The assigned lifetime habitats of all fish using multi-elemental signatures were compared with a simplified lifetime habitat assignment approach using validated Sr and Ba sea chemical signature thresholds (Sr:Ca = 5.19 – 6.65 × 10^{-3}; Ba:Ca = 0.011 – 0.0154 × 10^{-3}), the lifetime habitat profiles of 24 individual *M. cephalus* individuals were assigned to two broad environments: marine and brackish environments (Figure 5.6). Similar to RF habitat assignment, all fish exhibited Sr and Ba values at the larval life that were consistent with a marine origin. Unlike the model, all capture locations could be assigned correctly using the validated Sr and Ba thresholds. The habitat assignment between the simplified method and the RF model matched for 63% of the fish. In some cases (e.g., J3), the estuary recruitment was clear as shown by Sr and

Ba, at the end of larval life; however, the model did not capture this, and instead, the individual was assigned at sea. Similarly, another individual (J7) had two peaks in Ba corresponding to Sr, which indicated brackish environment usage; however, this fish was also assigned sea throughout its lifetime, despite being captured in the estuary. Furthermore, the extremely high Ba during the lifetime of one subadult (SA3) and corresponding Sr showed that this fish lived its entire life in the estuary after recruitment at the end of larval life which was contradicting the assignment of sea by RF along the transect.

The *M. cephalus* growth annulus, which has been shown to occur during the winter season (Smith and Deguara 2003), coincided with high Sr indicating that fish might be in the lower reaches or sea (marine environment) during the winter period, except for two 4 year old sub-adults (SA2 and SA3) which were assigned middle (brackish environment) reaches during the deposition of their first growth annulus. In this study only two fish had reached sexual maturity; one made multiple movements between the three habitats (SA5) and the other (SA6) spent the majority of its lifetime at sea, entering the estuary just before its capture in the lower reaches.

Assigning lifetime habitat types to all individuals was challenging, primarily due to occasional discrepancies between the two habitat assignment methods; however, there were distinct patterns in broad habitat use. Approximately 20% of individuals showed predominantly marine environment signature (which indicated the sea and lower reaches), while 17% were dominated by brackish environment signature, and the remaining individuals utilised all habitat types more evenly throughout the lifetime.

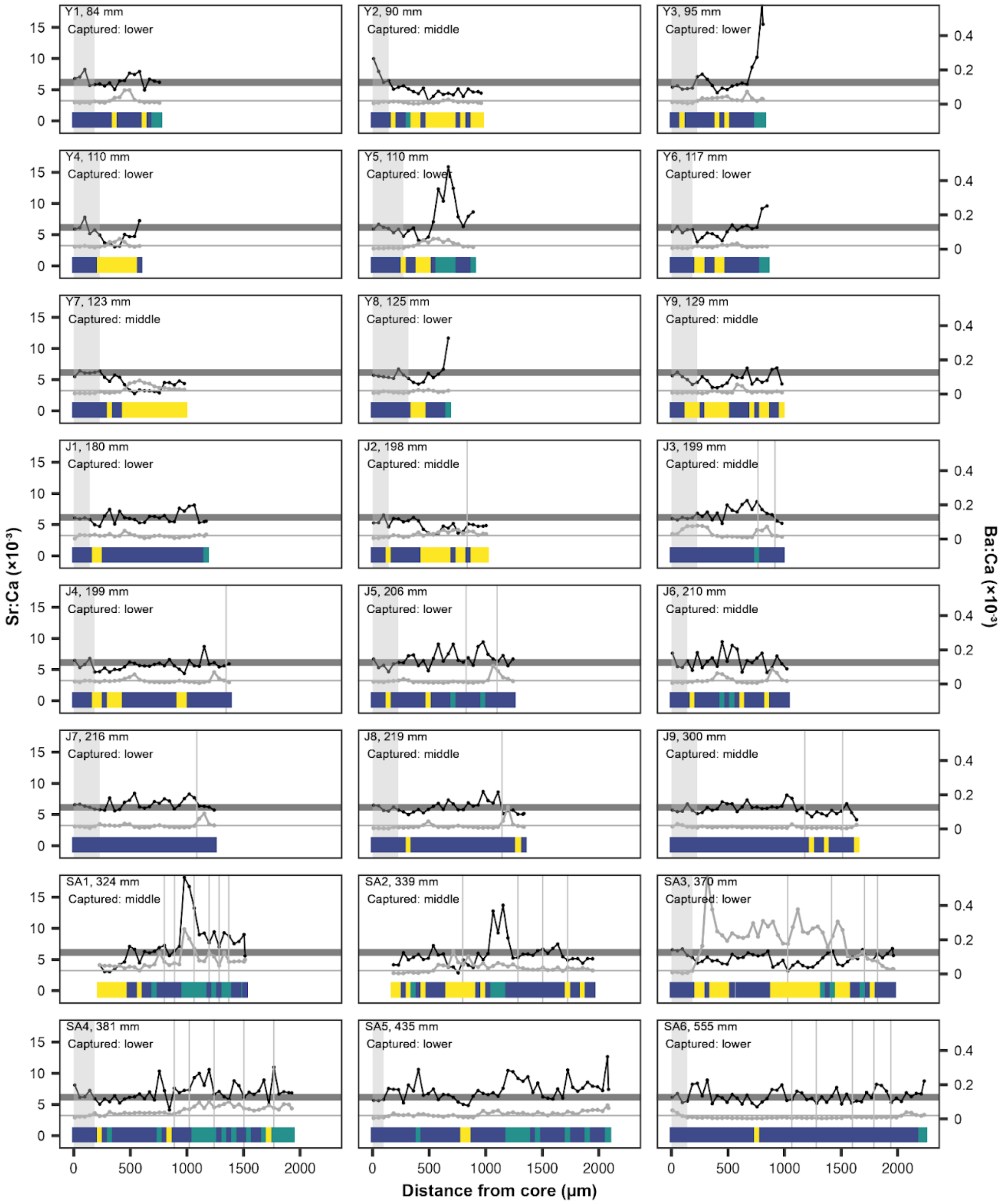

Figure 5.6. Sr:Ca (black) and Ba:Ca (grey) profiles of 24 *Mugil cephalus* all sampled in the Kowie Estuary, South Africa. The grey vertical panel = larval life and growth annulus, dark grey horizontal bands and the grey dotted line = threshold values indicative of a sea chemical signature for Sr:Ca and Ba:Ca, respectively. Fish are categorized by life stage: Y = young-of-year, J = juvenile, and SA = sub-adult. Otolith annuli for individuals J1, J6, and SA5 were unclear and thus excluded from analysis; larval signatures were not detected in SA1 and SA2. Length at 50% maturity is 440 mm FL (Wallace 1975).

5.4. Discussion

To our knowledge, this study is the first to examine the use of otolith microchemical signatures to characterise the diversity of lifetime habitat use of *M. cephalus* from a warm-temperate South African estuary. Using controlled laboratory trials, we validated the incorporation of sea chemical Sr and Ba signatures across ontogeny. Given that otolith morphology and elemental incorporation in *M. cephalus* can vary across habitat types (Fortunato et al. 2017), experimental validation was essential. Our validation experiment showed that the mean Sr:Ca concentration during the larval life at sea (6.11×10^{-3}) did not differ significantly from the signature incorporated in the laboratory (5.94×10^{-3}). However, Sr values from laboratory trials displayed broader variability, likely reflecting individual physiological differences in the rate of Sr incorporation, a process known to be influenced by temperature and metabolic activity and further affected by the ontogenetic development (Sturrock et al. 2012). Because the laboratory temperature was constant, it is plausible that variation in Sr uptake occurred from differences in physiological responses to two months of captivity.

Similar to Sr concentrations, although Ba concentrations displayed an inverse pattern, the mean Ba:Ca concentration at sea (0.012×10^{-3}) and in the laboratory (0.014×10^{-3}) were statistically similar, however, Ba values from the marine samples were highly variable, occasionally reaching extremely low and high concentrations. This variability is likely driven by localised upwelling along the South African coast, particularly near the Port Alfred study site where frequent wind-driven upwelling introduces cold, nutrient-rich water from depth (Lutjeharms et al. 2000; James et al. 2013). Since Ba incorporation into otoliths is influenced by both diet and environmental Ba availability (Elsdon and Gillanders 2005; Tian et al. 2019), the observed variability aligns with known upwelling dynamics in the area. Indeed, these upwelling events are corroborated by a decade-long temperature dataset from the region, which documents episodic drops in coastal sea temperature (see Chapter 2 for long term temperature changes at the Port Alfred coastline).

Multiple studies have shown that for fish occupying habitats with distinct environmental conditions during early life stages, their otolith chemical signatures can be used to discriminate against such habitats throughout their lifetime using RF algorithm (Mercier et al. 2012; Tournois et al. 2013; 2017; Gonzalez et al. 2023), and using Sr and Ba (Chang et al. 2004b; Kraus and Secor 2005; Wang 2014). In this study, we successfully discriminated the sea as the larval habitat for *M. cephalus* based on both methods. However, the distinction between sea and estuary lower reaches environments can be challenging, particularly in systems like the Kowie Estuary, where polyhaline conditions (salinity 30–35) produce marine-like signatures (Kruger 2010; Whitfield and Elliott 2011). However, it is well known that *M. cephalus* spawning occurs at sea, followed by ontogenetic habitat shifts as larvae recruit into estuaries (Whitfield et al. 2012). These shifts are often associated with changes in diet and morphology, and are reflected on the otolith structure thus allowing for reconstruction of this period (Hsu et al. 2009). In South Africa, estuarine entry occurs at highly variable sizes, with many individuals transitioning from the surf zone as post-flexion larvae (8–12 mm standard length [SL]), entering estuaries around 15–25 mm SL approximately 30 days post-hatch (Wallace 1975; Whitfield et al. 2023). The recruitment of *M. cephalus* into estuaries takes place over several months, and variation in size at recruitment is attributed to the extended spawning period of the species (Wallace 1975). Our findings reflect similar trends, with otolith size (a proxy for age, Gallardo-Cabello et al. 2012) positively correlated with fish size during recruitment and that some individuals showed early recruitment, while others had prolonged marine larval phases, overall indicating flexible recruitment strategies.

The exact location of *M. cephalus* spawning in South Africa remains uncertain. While most global evidence supports offshore marine spawning (Whitfield et al. 2012), some studies suggest spawning may occur closer to estuary mouths or even within surf zones (Ibáñez et al. 2012). However, spawning in the estuary is unlikely as evidenced by gonadal resorption in adults that failed to reach marine spawning grounds in St Lucia, South Africa as a result of mouth closure caused by extended drought conditions (Wallace 1975). In addition, *M. cephalus* in Australia also displayed skipped spawning as a result of suboptimal environmental conditions leading to failure to reach the sea (Fowler et al. 2016; Myers et al. 2020).

The application of multivariate statistical and machine learning techniques enabled the successful discrimination of *M. cephalus* habitat use across the sea, lower, and middle reaches of the Kowie Estuary, with an overall classification accuracy of 86% based on multi-elemental otolith signatures (Sr, Ba, Mg, Mn, Rb). Reassignment accuracy was highest for the sea and middle estuary, likely due to the high environmental variation such as salinity and temperature between these habitats. However, there was a high classification error for the lower reaches (more than 70%). This was likely due to strong tidal influence in the estuary mouth region, which leads to similar physical and chemical conditions, particularly salinity and temperature between the sea and the lower reaches. Sr was identified as the primary discriminant element with Ba identified as the second. However, the lack of significant Sr differences between the sea and lower estuary highlights their shared marine influence and salinity overlap. As reported by previous studies, the salinity values in the lower Kowie Estuary can reach up to 35 (Kruger 2010; Murray 2016), indicating near-marine conditions. This overlap suggests that Sr may be best used to distinguish between broadly defined marine (sea and lower reaches) and brackish (middle reaches) environments, compared to fine-scale estuarine gradients.

Unexpectedly, Ba concentrations in the lower reaches were significantly higher than those at sea despite both habitats having high Sr and closely resembled values from the middle estuary. Since Ba is expected to decrease with increasing salinity (Elsdon and Gillanders 2005) and is sensitive to both environmental and physiological factors (Sturrock et al. 2015; Nelson and Powers 2019), its elevated levels in the lower reaches may reflect species-specific osmoregulatory responses or environmental inputs such as coastal upwelled water and/or catchment runoff (Kültz 2015). Additional elements such as Mn and Rb were also elevated in the lower reaches of the estuary, possibly linked to anthropogenic influences (Tournois et al. 2017) including nutrient inputs from sewage effluent and catchment runoff which have been reported in Kowie Estuary (McKenzie and Hay 2000). Elevated Rb:Sr ratios have been associated with wastewater contamination (Smith et al. 2021), and may reflect cumulative effects of land use, freshwater discharge and tidal mixing (McKenzie and Hay 2000; Hicks et al. 2010; Fortunato et al. 2017). Furthermore, since *M. cephalus* prefers the muddy bottom habitats in estuaries (Gallardo-Cabello et al. 2012), its benthic foraging behaviour may contribute to the resuspension of bottom sediments, and therefore the elemental composition in the otolith may also partially reflect chemical signatures of these sediments.

Lifetime habitat assignment results suggest that early life stages of *M. cephalus* exhibit high degrees of habitat connectivity, with many young fish showing high use of all three habitats (sea, lower and middle reaches) across their lifetimes. However, this pattern does not necessarily imply regular migrations between the estuary and coastal marine environment during the early life stages, as previous studies have shown that both YOY and juvenile *M. cephalus* may be passively washed out from estuaries during high flow events (e.g. river flooding), thus complicating the interpretation of natural versus forced movement (e.g., Blaber 1977; Whitfield 2017). Despite this, the wide use of habitats by young fish may also reflect exploratory behaviour and the seeking of optimal foraging or refuge habitats (Whitfield et al. 2012). Furthermore, the results showed that most *M. cephalus* individuals used the middle reaches of the estuary, during their first year of life with increasing evidence of habitat fidelity with age. This pattern supports the idea that younger *M. cephalus* display higher mobility and behavioural plasticity, possibly as a strategy to locate suitable conditions for growth and survival. Wang et al. (2011) similarly observed that juvenile *M. cephalus* tend to exhibit greater phenotypic plasticity and more variable migratory trajectories compared to older individuals. In the Kowie Estuary, sub-adults were more frequently associated with the lower reaches, particularly polyhaline zones. This may reflect physiological tolerances, proximity to the marine environment and habitat availability areas in the lower estuary are characterised by high reed beds and anthropogenic effluents.

Findings from the present study align with results from acoustic telemetry research in Chapter 3. Larger (sub-adult and adult) *M. cephalus* used certain habitats in the lower reaches considerably, an area dominated by extensive seagrass beds (Mukhari, in prep). In the Western Mediterranean, Cardona (2000) reported similar ontogenetic patterns, with juveniles avoiding polyhaline and euhaline waters, while adults preferred these habitats and avoided freshwater reaches. Additionally, other studies also demonstrated that larger individuals are more abundant in the lower estuarine reaches due to the availability of preferred prey, such as Foraminifera (Blaber 1977; Górski et al. 2015).

Patterns of habitat partitioning have also been observed in systems with multiple sympatric mugilid species. For example, in Taiwan, largescale mullet *Planiliza macrolepis* dominates high-salinity habitats, while *M. cephalus* occupies lower-salinity zones (Chang and Iizuka 2012). A similar partitioning may occur in the Kowie Estuary, which supports several mugilid species (Whitfield et al. 1994; Ziko in prep), underscoring the need for species-specific monitoring and management strategies. Collectively, this spatial and temporal variability in habitat use across life stages suggests a high degree of ecological plasticity in *M. cephalus*, potentially reflecting adaptive responses to dynamic estuarine conditions (Górski et al. 2015).

Since *M. cephalus*, like many other teleosts, forms the opaque zone in its otoliths during winter corresponding to periods of reduced somatic growth driven by lower temperatures and physiological stress (Campana 1999), we were able to infer seasonal habitat use by aligning annulus deposition timing with habitat assignments. This temporal resolution revealed a clear seasonal spatial pattern. Most individuals were assigned to marine or lower estuarine habitats during winter, while transitions to the middle reaches occurred in summer. These seasonal patterns align with acoustic telemetry results (Chapter 3) which showed that most but not all fish of various sizes left the estuary in autumn and returned in spring driven by riverine temperatures. Notably, only two sub-adults (4+ years) occupied the middle reaches during winter of their first annulus deposition, indicating that the use of this area might be limited during the winter season. These seasonal movements likely reflect physiological responses to dynamic estuarine conditions, such as temperature and this partial migration pattern shown by *M. cephalus*, whereby some fish migrate and others remain resident can be explained by conditional strategy. In the Kowie Estuary, key environmental drivers such as river and sea temperature affect the movement patterns of *M. cephalus*. For example, during winter when cold river temperatures enters the estuary, individuals shift their movement downstream and the opposite pattern was observed in summer, when the cold upwelled sea waters penetrate the lower reaches of the estuary (Chapter 3).

This spatio-temporal plasticity supports the concept of intrapopulation behavioural structuring, wherein individuals within a single population adopt divergent strategies in response to environmental heterogeneity (Chapman et al. 2011). These differences often reflect individual differences in physiological tolerance (e.g., to temperature

(Mukhari et al. 2025) and salinity-likely affected by river flow, Chapter 3) and life history stage, which plays an important role in population resilience against changing environments. These findings are consistent with theories suggesting that behavioural diversification within populations can serve as an adaptive mechanism to buffer against environmental unpredictability, anthropogenic impacts and climate changes (Wen et al. 2010). In the context of *M. cephalus*, individual variation in habitat use across seasons may represent an evolutionary strategy that enhances persistence in estuarine ecosystems subject to pronounced seasonal and interannual variability.

Overall, three broad patterns of habitat use were observed in this study: 20% of individuals used mostly marine habitat, 17% brackish, and the remainder displayed migratory behaviour. This suggests the possible existence of contingency within this population, a strategy common in most animals, where access to multiple connected habitats can enhance population survival and resilience. Both telemetry (Chapter 3) and otolith microchemistry revealed high individual variability: some fish were recorded moving into the sea and neighbouring estuaries, while others showed high use of specific areas within the estuary (e.g. the dense seagrass bed approximately 3 to 4 km from the estuary mouth). The global diversity of life-history strategies in this species, from marine residency in Australia (Fowler et al. 2016) to estuarine residency in South Korea (Bae and Kim 2020), emphasises the importance of maintaining habitat connectivity and accounting for spatial population structure in management efforts.

Using both RF algorithms and the simplified Sr and Ba based approach, the two methods yielded consistent habitat assignments for 67% of individuals, including assigning sea as the larval life habitat for all fish by both methods. Furthermore, the Sr-Ba method was effective in distinguishing between brackish and marine habitats, including assigning capture location, however, lacked the fine-scale resolution to discriminate among habitats within the estuary (especially with simultaneous elevation of Ba and Sr in the lower reaches). In contrast, the RF model demonstrated greater sensitivity in resolving spatial variation within the estuary, particularly between the lower and middle reaches.

The high overlap in environmental conditions observed during this study is not uncommon; otolith microchemistry has been used to discriminate both large-scale habitats (inter-seascape connectivity) (Avigliano et al. 2016) and small-scale habitats (intra-seascape connectivity), such as a single estuary (Elsdon et al. 2008) with various outcomes. This indicates that geographic distance alone is a poor predictor of chemical distinctiveness. Rather, the effectiveness of otolith chemistry in resolving spatial structure depends on: (1) environmental heterogeneity – fish must occupy areas with sufficiently different water chemistry; (2) residence time – the duration fish remain in a particular environment prior to capture affects element uptake; and (3) element selection – some elements may better reflect spatial differences due to their chemical behaviour and biological incorporation rates on certain species (Sturrock et al. 2012). Although this study managed to capture lifetime habitats use of *M. cephalus* of various age (37.5% YoY, 37.5% juveniles and 25% sub-adults), the life history stages in this study are representative of most estuary-associated fish populations within estuaries. However, sampling only took place in one season, and since the chemical composition of elements in estuaries are subject to fluctuations, owing to the dynamic nature of estuaries, there is a need for multiple sampling representing seasonal and inter-annual trends in order to clearly see the variation in chemical signatures of the YoY cohorts.

In conclusion, the results of this chapter showed that lifetime habitat use patterns of *M. cephalus* are more diverse than previously described, with heterogeneity in brackish and marine use, highlighting the importance of connectivity throughout life cycle stages. Through the integration of RF machine learning with conventional elemental ratio analysis, we demonstrated a robust approach for identifying habitat use patterns, particularly when interpreted alongside complementary tools such as acoustic telemetry. This chapter represented the first application of LA-ICPMS and RF machine learning to infer lifetime habitat use in a South African estuary-associated species and provides a valuable proof of concept. The development of such integrative methods can enhance our capacity to inform targeted conservation and management strategies, particularly protecting key habitats essential to early development, recruitment and adult persistence in both commercially important and vulnerable species.

CHAPTER 6

GENERAL DISCUSSION

Understanding the risks and vulnerabilities faced by estuary-associated species under increasing anthropogenic pressures and climate variability requires an ecosystem-based approach (Hazen et al. 2012; Gillanders et al. 2022). This approach integrates individual spatial and temporal movement dynamics to uncover population-level responses, thus revealing the broader processes that shape species persistence (Hazen et al. 2012). Understanding how individuals interact with and adapt to changing environments is key to interpreting their ecology (Gillanders et al. 2022). This is particularly true for estuary-associated species such as *Mugil cephalus*, that rely on habitat connectivity, both intra- and inter-specific (across marine to freshwater continuum), to successfully complete their life cycle (Figure 6.1). By adopting a multi-method approach, this study was able to provide insights on the movement of *M. cephalus* from a temperate South African estuary. As indicated by previous studies (Honda et al. 2012; Crook et al. 2016; Miles et al. 2018), complementary techniques such as acoustic telemetry and otolith microchemistry can provide information of different spatial-temporal scales that can strengthen our understanding of fish movement. This multi-method study uncovered the spatio-temporal movement patterns of *M. cephalus* in relation to environmental variability, and (i) identified key hotspots habitats within the Kowie Estuary (acoustic telemetry, Chapter 3), (ii) demonstrated the critical role of intra- and inter- seascape connectivity throughout the species' life cycle (from larval recruitment into estuaries to seasonal movement between the estuary and marine environment) (otolith microchemistry, Chapter 5; acoustic telemetry, Chapter 3), and (iii) demonstrated the importance of linking movement ecology data with both environmental (acoustic telemetry, Chapter 3) and physiological drivers (ecophysiology, Chapter 4). This holistic approach has not only provided much needed insights on the ecology of this cosmopolitan species in its southern distribution, but has also provided valuable information which can guide responsive management efforts, including broader ecosystem-based conservation plans for this, and other estuary-associated species, and the estuarine ecosystems they inhabit.

Movement ecology paradigm

Movement is defined as a change in position of individuals over time (Joo et al. 2022), and is a fundamental process of life and changes at both spatial and temporal scales as driven by internal (physiology) and external (environmental) factors (Nathan et al. 2008). To comprehensively understand movement ecology, Nathan et al. (2008) introduced a conceptual framework to explain the processes driving animal movement, known as the movement ecology paradigm. Firstly, there is the need to understand how animals, taking into consideration the motion capacity of individuals and external factors. Secondly, it is important to understand why animals move, which includes their internal drivers. Thirdly, understanding the navigation capacity of movement will help researchers understand when (temporal scale) and where (spatial scale) animals move. And lastly, it is important to understand the ecological drivers and evolutionary consequences of these movements. The movement ecology paradigm links the theoretical aspects with empirical data of movement studies in order to understand the ecological drivers of observed spatiotemporal patterns (Joo et al. 2022).

The data collected on *M. cephalus* during this study align with almost all aspects of the movement ecology paradigm (Figure 6.1). This is also the first study on the African continent to assess the movements of *M. cephalus* across various spatial and temporal scales, linking this to environmental variables. The results of this study support both external and internal drivers of the movement ecology paradigm as a result of changes in life cycle stages. Therefore, through this unifying framework, this thesis answers questions related to the external and internal drivers of movement of the estuary-associated *M. cephalus* using a multi-method approach – information that is crucial for management of this species in the face of increasing anthropogenic pressures on estuaries and associated species, and impacts of climate change.

These results show that movement of *M. cephalus* throughout its life cycle is not random but is a response to their ever-changing environment. Following marine recruitment (Figure 6.1), early juvenile *M. cephalus* move into estuaries. These highly productive systems serve as critical developmental habitats through the provision of high quality food resources (Chuwen et al. 2009), and refuge from predation (Whitfield 1994; Ibáñez et al. 2012) until they reach adult life stages. From as early as one year of age, *M. cephalus* use various habitats within the estuary and the nearby coastal environment (Chapter 3 and 5), and their movements are driven by both external and internal factors as explained through the movement ecology paradigm.

External factors

Movement is driven by the interplay between internal state, motion and navigation capacity of an animal which interacts with external environmental factors in space and time (Nathan et al. 2008). Among these, external abiotic and biotic drivers, such as temperature, salinity, hydrodynamics, resource distribution and anthropogenic disturbance can act as both cues and constraints, mediating habitat use and triggering directional movements (Joo et al. 2022). For estuary-associated species environmental gradients within estuaries are especially dynamic and can act as strong selective pressures on physiological traits, behavioural strategies and ultimately movement patterns.

The results from acoustic telemetry (Chapter 3) highlighted that *M. cephalus* of various sizes spent a high proportion of time (83.5%) within the Kowie Estuary. During this period, individuals used the entire length of the system, thus highlighting the importance of diverse habitats offered by the Kowie Estuary and the critical role of intra-seascape connectivity in linking these habitats (Figure 6.1). Specific areas, such as Station 4 in the middle reaches, were identified as “hotspots,” with some individuals showing highly site fidelity (as high as 92%) in this habitat. Individuals also moved to the upper reaches including the estuary-river interface where they spent relatively lower but substantial proportions of time (up to 35%) in these habitats. In contrast, the least visited habitats were the marina and the estuarine mouth which accounted for a total of only 2% of the time. There was monthly and seasonal variation in habitat use within the estuary throughout the study, indicating temporal shifts in spatial distribution. This pattern of spatial and temporal habitat use was further shown by movements beyond the estuary — inter-seascape connectivity with more than half of the tagged individuals (58%) undertaking sea trips to the marine environment and/or adjacent estuaries for a period of one to 30 days mostly during autumn (Figure 6.1).

This intra- and inter-seascape connectivity was further demonstrated by the lifetime movement patterns reconstructed from otolith microchemistry (Chapter 5). In addition to ontogenetic transitions from marine to estuarine environments, these results showed a clear variation in lifetime salinity exposure among individuals of different sizes, such that from one year of age there was a clear seasonal shift in habitat use and transitions (Figure 6.1). For example, in the winter season (as shown by annulus deposition), most fish occupy the sea and/or lower reaches instead of the middle reaches compared to summer. Models showed that both river flow and water temperature (both river and sea temperature) were the key external drivers of daily fish movement in the Kowie Estuary. By addressing the how, where and when animal move aspects of the movement ecology paradigm, both these chapters revealed that movement of *M. cephalus* in a warm temperate South African estuary is in response to external factors such as environmental change particularly river flow and temperature (Figure 6.1).

River flow has long been recognized as one of the primary abiotic filters shaping estuarine fish distributions (Poff 1997; Whitfield 2020), through changes in salinity, turbidity and nutrient delivery, and can also act as an olfactory cue for many species guiding habitat transitions along the estuarine gradient (Barletta et al. 2008). High freshwater inflow, particularly during the rainy season, leads to salinity gradients in the middle and lower reaches of an estuary, which has been associated with increased fish abundance in this area compared to the upper reaches (Barletta et al. 2008). During this study, elevated river flow in October 2023 corresponded with downstream shifts in individual fish locations (Chapter 3). This likely reflects behaviour in response to changes in physicochemical conditions such as decreased salinity. These patterns of downstream displacement observed during periods of high river flow may be explained by the increased energetic cost to *M. cephalus* associated with maintaining internal homeostasis under dilute conditions (Marais 1978; Varsamos et al. 2005). Although, *M. cephalus* is described as a euryhaline species that can tolerate high salinities of up to 70 (Wallace 1975; Whitfield et al. 2012; Whitfield 2021), its high tolerance is most likely facilitated by robust osmoregulatory mechanisms; however, reduced salinity appears more physiologically costly for some species (Kültz 2015), with only few *M. cephalus* populations recorded penetrating the river systems for prolonged periods (Bok 1983; Fowler et al. 2016). In the laboratory, *M. cephalus* have been shown to consume on average ~18 $mg.h^{-1}$ more oxygen in freshwater than in seawater, suggesting elevated metabolic costs in hypo-osmotic environments (Marais 1978). This aligns with broader findings across other euryhaline species, where metabolic rates increase under low-salinity conditions due to the energetic cost of active ion regulation (Prosser 1991; Nordlie 2003). This is also consistent with personal observations during this study whereby adult *M. cephalus* in the Kowie River exhibited sluggish behaviour, body injuries and reduced responsiveness, such that they could not be tagged.

In addition to salinity, temperature is also a major drivers of species movement and distribution, because temperature affects the physiological processes of ectotherms (Brett 1971; Pörtner and Knust 2007), such as metabolic rates, growth, reproduction, foraging and performance (Pörtner and Farrell 2008). The seasonal movements of *M. cephalus* in the Kowie Estuary, downstream in winter and upstream in summer were strongly influenced by temperatures. In winter, the cold riverine water (around 11 °C) lowers the temperature in the upper reaches while in summer, the upwelled seawater, as cold as 9 °C can penetrate into lower reaches, these upwelling events are common in the Port Alfred region (James and Harrison 2010; Goschen et al. 2012). This suggests that temperature operates as both a constraint and a driver, shaping the extent and direction of habitat use across the length of the estuary. Notably, in this study, the temperature-driven movement varied across individuals, highlighting potential differences in thermal sensitivity, acclimation capacity and life stage-specific responses. Other studies have investigated this variability; for example, in gilt-head seabream *Sparus aurata*, vulnerability to thermal stress differs markedly based on ontogenetic stage, with larvae being most susceptible and juveniles exhibiting the highest tolerance due to their capacity to upregulate cytoprotective proteins (Fonseca et al. 2021). This developmental shift in thermal plasticity may also explain the heterogeneous responses observed in our study, where not all *M. cephalus* showed synchronous seasonal downstream movements. Consequently, life-stage-specific physiological constraints likely play a key role in shaping movement patterns, particularly in thermally variable habitats like estuaries. Temperature effects on survival have been described for salmonid species with a narrow thermal range, and survival is compromised due to thermal stress unless they can move and access cooler water (Elliott and Elliott 2010; Frechette et al. 2018).

Considerable individual variability in both residency and habitat connectivity was observed in this study (Chapter 3 and 5), with a subset of individuals displaying partial migration – some engaged in trips to sea and neighbouring estuaries, while others remained resident within the Kowie Estuary. Partial migration, whereby coexistence of resident ("stayers") and migratory ("movers") contingents exists in a single population, is a widespread strategy across diverse taxa (Fromentin and Powers 2005; Gahagen et al. 2015; Steffen et al. 2023). This strategy produces different types of migrants and residents that are a key factor underlying the species resilience, stability and success across a range of estuarine and coastal systems, since different contingents are exposed to different habitats that lead to independent outcomes (Kraus and Secor 2005; Gahagen et al. 2015; Steffen et al. 2023). The outcome of the current study is similar to the behaviour of other *M. cephalus* populations observed using otolith microchemistry (Chang et al. 2004a; Górski et al. 2015; Fowler et al. 2016) and acoustic telemetry (Myers et al. 2020).

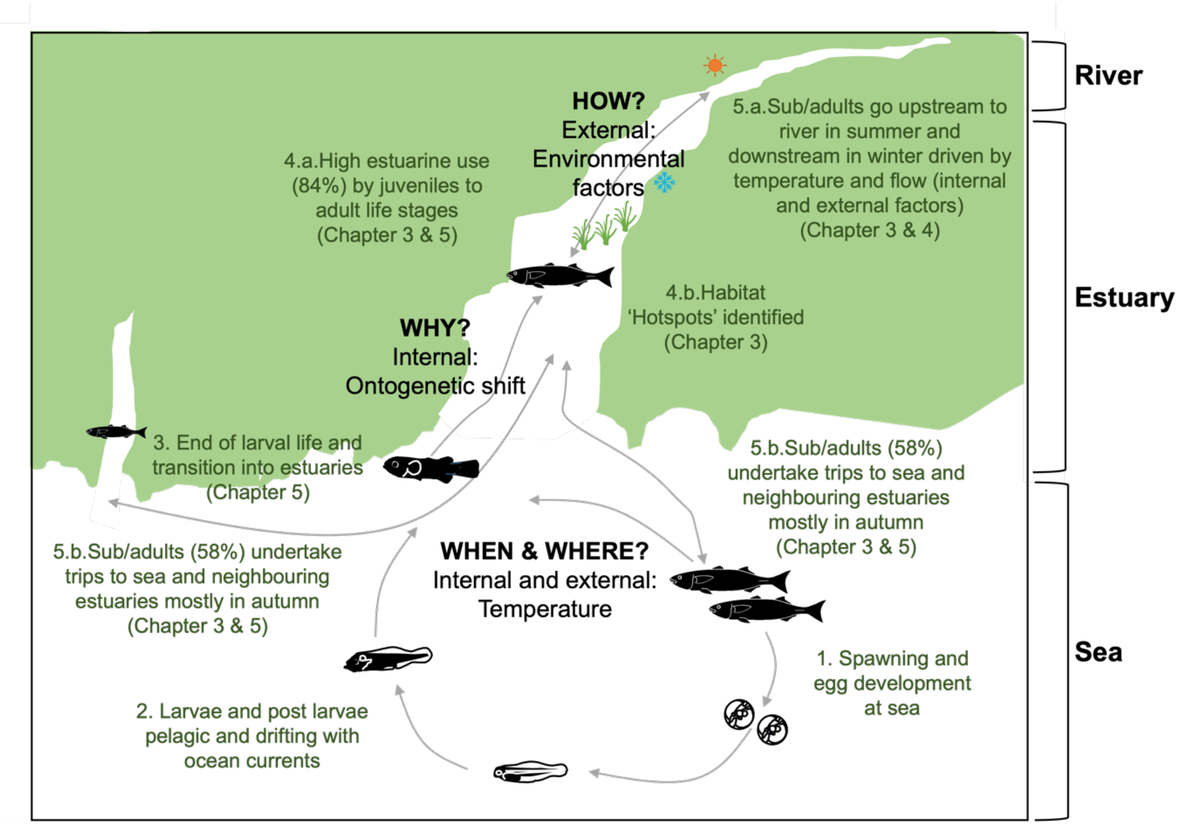

Figure 6. 1. A graphical representation of the general life cycle of *Mugil cephalus* across multiple habitats (adapted from Whitfield et al. 2012), highlighting the predominant movement patterns assessed during this study (from number 3 to 5). The numbers represent the order of events during the life cycle.

Internal state

To get a holistic understanding of movement ecology, it is important to determine the internal drivers of individual movement (Nathan et al. 2008). This includes motivation and readiness to move and can be affected by developmental stage (age and reproductive status), physiological condition, energetic demands, personality and morphology among other factors (Nathan et al. 2008; Joo et al. 2022; Cooke et al. 2022). A combination of acoustic telemetry (Chapter 3) and otolith microchemistry (Chapter 5) results demonstrated how, where and when *M. cephalus* move at a temporal and spatial scale (Figure 6.1); however, there is a need to understand why and the role of internal drivers in shaping such movement behaviour. Changes in water temperature were identified as one of the important drivers of movements within and out of the Kowie Estuary and to further explore this, the temperature tolerance of this species was explored through laboratory experiments. The experiment (Chapter 4) results indicated that *M. cephalus* collected from a temperate estuary has a broad thermal breath with an upper (CT_{max}) critical thermal limit of 37.7 °C and lower critical thermal limit (CT_{min}) of 3.2 °C. However, thermal stress of this species (breakpoints in ventilation rates) was identified at temperatures below (29.3 °C) and above critical limits (13.5 °C), which aligned with *in situ* winter river temperatures and summer upwelling temperatures therefore justifying the observed seasonal movements patterns. Prior to reaching the loss of equilibrium (LOE), there were noticeable behavioural changes in *M. cephalus* such as restless activity and some jumping (out of experimental tanks) to escape unfavourable conditions during a simulated heating event. Although all fish in this study experienced the same environmental variability, there was individual differences, for example some individuals had a broad thermal breadth while others had a narrow thermal breadth, identified as either more cold- or warm-tolerant.

In the wild (Chapter 3 and Chapter 4), individual variation was also shown during seasonal shifts in habitat use when some but not all fish moved downstream during the cooler winter months, most likely indicating seasonal thermal stress (as a result of cold riverine temperatures). As such, we can hypothesise that individuals with a wide thermal tolerance are likely to remain in the upper reaches while those with a narrower thermal breadth would be more susceptible to thermal stress during such temperature extremes, and are more likely to move to more suitable habitats. According to Kerr et al. (2009), conditional strategy, which is the interaction between individual physiological conditions and the environment, is the most widely accepted mechanism driving intrapopulation variability. Dodson et al. (2013) discussed that alternative migratory tactics can co-exist in all individuals within a population; however, individuals might adopt one or another tactic depending on both environmental conditions and individual genetic make-up. Therefore, conditions (e.g., temperature, flow, habitat quality) experienced during development may influence which tactic is adopted. Therefore, in this study, the individual movement as a result of temperature change can be considered environmental conditions. This combined with individual conditions (cold- versus warm-tolerant) are likely to influence an individual's decision to stay or migrate. The coexistence of both migratory and resident individuals within the population can be explained by the fact that not all individuals are able to participate in migration, and there are associated benefits and costs to both. The individual variation observed in this study, when considered alongside the integrated findings from the three data chapters, supports the presence of a conditional strategy within this population and highlights the role of internal state as a key driver within the movement ecology paradigm.

Climate change implications

The predicted global impacts of climate change include the increase in intensity and frequency of extreme events such as upwelling and marine heat waves, which can place strong selection pressures on biota with predicted severe ecological impacts (Potts et al. 2015; Grant et al. 2017; Smale et al. 2019; Stillman 2019). Coastal fish, in particular, have been shown to be at high risk of climate change impacts (Gattuso et al. 2018; Nagelkerken and Connell 2015; Potts et al. 2015), with predicted impacts including changes in distribution and abundance, altered migration patterns, reduced recruitment success and changes in trophic cascades (Nagelkerken and Connell 2015; Vinagre et al. 2019). Consequently, the physiological tolerance of species to environmental stressors, together with their phenotypic plasticity and capacity to adapt both physiologically and behaviourally (Webster et al. 2017; Lennox et al. 2024), will determine the winners and losers under climate change (Somero 2010). In Taiwan, the increasing sea surface temperatures over the last two decades as a result of global warming (maximum warming of 3.5 °C) has been identified as the major cause of decline in Mugilidae catches and the subsequent northward shift in distribution (Lan et al. 2014, 2017). This study, along with other previous studies, has shown that fish can experience physiological stress under rapid temperature fluctuations, and use movement as a behavioural response strategy to avoid unfavourable conditions; however, this can depend on the availability of such suitable habitat (Heupel and Simpfendorfer 2008; Vasconcelos et al. 2013; Murray et al. 2018; Allison et al. 2021; Lennox et al. 2024). In estuary-associated species such as *M. cephalus*, which are already absent from the upper and lower reaches of the estuary during specific times of the year, further cooling due to intensified coastal upwelling (generally during summer) and extreme cold riverine water (generally during winter) could limit the population into increasingly narrow thermal refuges. With the potential impacts of climate change estimated in the study site region (i.e. warm temperate biogeographic region; James et al. 2013; Potts et al. 2015), most estuary-associated species such as *M. cephalus* may encounter seasonal thermal bottlenecks (or otherwise known as ‘habitat squeeze’ (Coutant 2013; Kraus et al. 2015) (Figure 6.2) as a result of reduced riverine habitat availability in winter and thermally unsuitable coastal waters during summer upwelling events (Grant et al. 2017). This phenomenon has been observed in other estuarine and coastal systems, where both vertical and horizontal habitat compression reduces resilience to environmental change and anthropogenic stressors (Scavia et al. 2002; Gillanders et al. 2011b). Other impacts of a changing climate may include a decline in reproductive outputs of species such as *M. cephalus*, as previous studies have shown their ability to skip spawning and reabsorb gonads as a result of unfavourable environmental conditions (Wallace 1975; Fowler et al. 2016). Therefore, thermal thresholds and environmental variability can drive movements and habitat use patterns of *M. cephalus* as observed in this study and other estuary-associated species, and this highlights a broader concern in the face of global climate change.

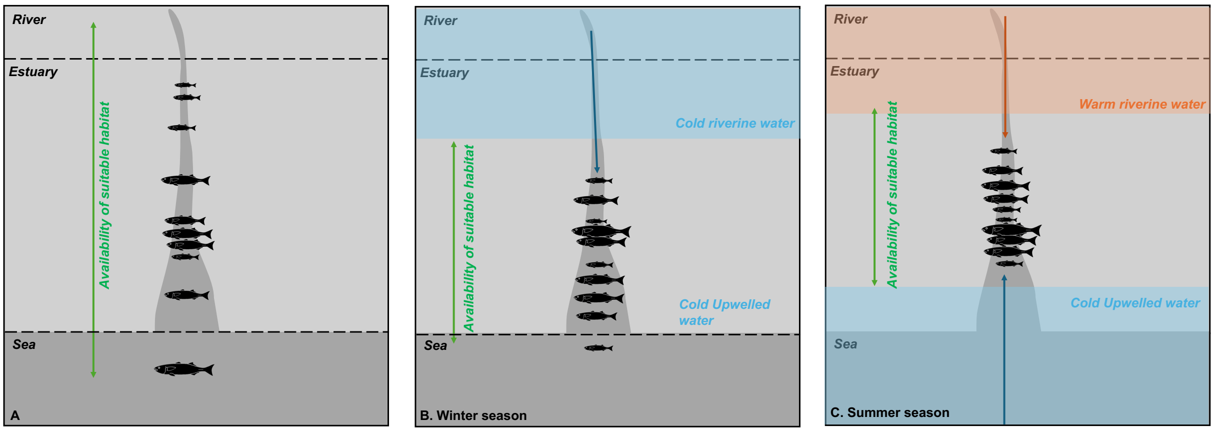

Figure 6. 2. Schematic representation of the (A) fish movement and habitat use in the Kowie Estuary under current conditions, and the effect of temperature change such as (B) decreased river water temperature in winter, and (C) decreased sea water temperature as a result of upwelling events combined with an increase in river water temperature in summer, both of which predicted to increase in frequency and intensity as a result of climate change (figure adapted from Grant et al. 2017).

Management implications

Estuaries in South Africa support significant economic activity through recreational, subsistence and small-scale fisheries, contributing billions of rands annually and sustaining secondary industries such as tourism and boat services (Lamberth and Turpie 2003; Turpie and Clark 2007). Effective estuarine management must, therefore, balance ecological conservation with the socio-economic needs of diverse user groups, including recreational, commercial, artisanal and subsistence fishers (Adams et al. 2020). Further, South African estuaries are threatened by coastal development and anthropogenic activities, which may lead to loss of estuarine habitats and their ecosystem services (Whitfield 1998; van Niekerk et al. 2019). Recently, a systematic approach to identify and rank global pressures on estuaries in order to inform prioritisation of management interventions was developed (van Niekerk et al. 2022). Building on earlier work (van Niekerk et al. 2013), six key pressure categories, including, flow modification, pollution, exploitation of living resources, land-use, development and manipulation of estuary mouths and introduction of invasive species, were rated and reviewed based on their relative influence on estuarine systems and the expected trajectories of change within the South African context. This assessment showed that overfishing remains the biggest threat, affecting approximately 78% of estuaries in South Africa, followed by land-use and development (40%), pollution (34%), flow modification (15%), and the emerging threats of invasive species (8%). Species that undertake spawning-related migrations are especially vulnerable to fishing pressure (Russell et al. 2014). Yet, only 35% worldwide have management plans in place such as marine protected areas or seasonal closures (Russell et al. 2014). Despite many reports on their global decline, effective management of these species is challenging because their migration pathways (such as estuarine mouths, Whitfield 2021) are heavily targeted by fishers during their most vulnerable period (i.e., spawning migrations) compounding the risk of population collapse without management interventions (Russell et al. 2014; Myers et al. 2020). Multiple estuary-associated species including mugilids exhibit similar migratory behaviour, however, remain unprotected due to lack of information regarding their movement patterns and the amount of fishing pressure they face during certain periods (Myers et al. 2020).

Mugilidae species are ecologically important, being at the bottom of the food web where they are prey and play an energy transfer link for higher trophic predators including piscivorous fish and birds (Whitfield 2021). Moreover, they have been recognised as potential ecological indicators of climate change (James et al. 2013; Whitfield 2016). Therefore, their ecological role is functionally similar to that of a traditional forage fish, defined as small-medium size fish with shoaling behaviour, intermediate trophic level and strongly responsive to climatic changes (Engelhard et al. 2014; Rountos 2016). In addition to their ecological importance, forage species such as mugilids in South Africa are valued by subsistence and recreational fishers. However, due to their dual role as both a key prey for higher trophic level predators and as exploitable fishery resources, they are challenging to sustainably manage and regulate even at global level (Engelhard et al. 2014). Effective management of forage species requires consideration of their ecological role as prey and the need for sustainable harvest practices that maintain spawning biomass and ecosystem integrity (e.g., through size and bag limits).

In South Africa, there are currently no size or bag limits for any Mugilidae species in commercial fisheries, and a bag limit of up to 50 fish per person daily for recreational (bait) and subsistence/small-scale fishing (Whitfield and Lamberth 2012; Inshore Fisheries Management 2023). Such harvest regulations are likely unsustainable, particularly in light of climate-induced habitat shifts, ongoing anthropogenic pressures and the challenge of illegal gillnetting in South African estuaries (Wildtrust 2022; Stephen Lamberth, DFFE *pers. comm.*). Gillnetting in South African estuaries has been identified as a major problem due to its destructive nature, including high bycatch of juveniles and associated mortality (Wildtrust 2022). In areas where gillnetting mugilids is permitted, such as South Africa's West Coast, there is limited law enforcement and often Total Allowable Effort (TAE) is exceeded, with gillnet length restrictions being largely ignored (Wildtrust 2022). Given their vulnerability, socio-economic and ecological importance (Crosetti 2016), the importance of movement ecology research to inform adaptive conservation and management strategies in an era of changing climate has never been more pressing (Fraser et al. 2018; Lennox et al. 2024).

Estuary management in South Africa is primarily addressed through estuary management plans, which aim to maintain a predefined standard of ecosystem health and ecological functioning that will ensure a desired level of estuary services of both economic and social value (Huppert et al. 2003), as well as biological attributes and ecological needs of species occupying these systems (Day 1981). However, the success of estuary management plans depend on availability of reliable scientific data, particularly interactions between humans and the living resources (Nsubunga 2004). This study demonstrated the importance of habitat connectivity in enabling individuals to move across spatial and temporal gradients to track favourable thermal and salinity regimes. However, in estuaries such as the Kowie Estuary, physical barriers (e.g., weirs, causeways, degraded mouth dynamics) may constrain access to upstream or downstream habitats, resulting in fish being unable to behaviourally compensate for rapid environmental change which may lead to reduced growth and impaired recruitment. Furthermore, the differential response of individuals, as seen in chapters 3,4 and 5 likely reflect variation in age, condition or thermal plasticity, indicates that conservation strategies must account for intraspecific variation and the potential vulnerability of specific life stages. For example, hotspot habitats (e.g., Station 4, see Chapter 3) may serve as refugia for various individuals and should be prioritized in spatial planning. Flow regulation upstream of estuaries also warrants careful consideration. River flow, controlled through dams, common in many South African catchments, can exacerbate hyper or hyposalinity, thus disrupt chemical cue pathways, and impair migration triggers, especially for species that depend on olfactory navigation or salinity pulses to guide estuarine re-entry and movement (Svensson et al. 2014; Whitfield 2017). Environmental flow allocations that maintain seasonal variability and mimic historical flow regimes may enhance both ecological function and fish movement opportunities. Finally, this study reinforces the need for integrated eco-physiological monitoring in estuarine management frameworks. By incorporating experimental data on thermal responses into predictive movement models, managers can more accurately anticipate how estuarine species may respond to projected climate shifts, habitat modification, or pollution.

Previous studies, along with the current findings, highlight the Kowie Estuary as a hotspot of fish species richness, attributed to its provision of abundant food resources, due to availability of macrophyte habitats which provide shelter for multiple species (Whitfield et al. 1994). However, South African estuaries exhibit substantial spatial and temporal variability and are embedded within broader riverine and marine ecosystems, where they are affected by other regulations (controlling water use, marine resources, coastal development, etc.) making one-size-fits-all management strategies ineffective due to the cascading impacts from these interconnected systems (Nsubunga 2004). As such, there is urgent need for targeted, regionally informed management responses, supported by robust monitoring and adaptive research frameworks to ensure the long-term resilience and functionality of estuarine ecosystems (van Niekerk et al. 2022).The observed patterns in this study support the view that movement decisions in estuary-associated fish reflect the outcome of interacting external cues and internal constraints. Temperature acts as an ecological filter (Poff 1997) that shapes habitat accessibility, while river flow modifies these gradients and introduces chemical cues that may influence spatial orientation. These environmental drivers, filtered through individual physiology and behavioural flexibility, collectively shape the emergent space-use patterns across time. The heterogeneity observed among individuals further highlights the importance of integrating intraspecific variation and developmental plasticity into movement models, especially under climate change scenarios. As warming temperatures, altered rainfall regimes, and increased estuarine fragmentation continue to transform environmental baselines, the success of *M. cephalus* populations may hinge on the plasticity and resilience of their most vulnerable life stages. Hence, understanding both external environmental drivers and internal physiology of movement ecology is critical, as emphasized by the movement ecology paradigm, for anticipating and mitigating the impacts of climate change, particularly through the long-term management of suitable thermal refuges.

Therefore, the findings of this research have several management implications. First, a comprehensive stock assessment in the estuarine systems, such as the Kowie Estuary, is recommended to estimate *M. cephalus* population biomass and identify fisheries that target this species. Based on these data, harvest regulations such as size and bag limits can be established to protect spawning individuals and sustain biomass for ecological functioning. Second, protection of critical habitats, particularly those identified as nursery habitats and spawning aggregation sites, should be prioritized for protection. For example, in the case of this study, the high residency to the estuary and identification of the hotspot identified in the middle reaches of the estuary (see Chapter 3) should be included in the Kowie estuarine management plan. However, such spatial conservation initiatives need to be considered alongside the socio-ecological implications thereof. Additionally, seasonal closures during winter spawning season to ensure reproductive success could also be included. Third, regular monitoring and enforcement capacity should be strengthened to ensure compliance with fisheries regulations. Fourth, engineering modifications to existing barriers, such as redesigning the Kowie weir into a bridge structure that allows continuous water flow would improve habitat connectivity and facilitate upstream movement. Finally, there is a need for community education and awareness especially regarding migratory species' biology and ecology.

Examples from New South Wales, Australia, illustrate a suite of stringent management tools applicable to estuarine migratory species, including *M. cephalus*. For example, for recreational and subsistence fisheries, a size limit of 30 cm TL and bag limit of 20 is enforced, and for live bait the maximum length is set at 15 cm TL and a total of 20 is the bag limit (Department of Primary Industries and Regional Development 2024). Furthermore, a routine stock assessment assist in regulating harvest by multiple fisheries including commercial fisheries i.e., though gear type and size limitations, seasonal efforts and mapping sensitive habitats for habitat conservation (Department of agriculture and fisheries 2018). Together these measures aim to preserve vulnerable life stages and sufficient biomass for the ecosystem functioning, objectives that are directly relevant to *M. cephalus* in the Kowie Estuary and other estuarine-dependent species. Therefore, adopting an ecosystem-based estuary management plan that integrates controlled harvest with habitat protection will not only support the sustainability of *M. cephalus* populations but also benefit other estuarine-dependent species exhibiting similar movement ecologies. Thus, the recommendations derived from this study have relevance beyond mullet, contributing to broader goals of maintaining biodiversity, ecological function and fisheries productivity in South African estuaries.

Future research directions

Future research should build on the integrative framework developed in this thesis by expanding both spatial and temporal scales of investigation. For example, long-term acoustic monitoring and coordinated multiple estuary studies including the neighbouring estuaries could help determine whether the movement patterns and habitat connectivity of *M. cephalus* observed in the Kowie Estuary are consistent across other systems with differing hydrological characteristics. For acoustic telemetry and tagging small size fish such as mugilids, future studies must adhere to the recommended 2% tag burden guidelines (Winter 1996) because the two post-tagging mortality events occurring in this study suggest that excessive tag load likely contributes to physiological stress and mortality. Therefore, efforts could be made to ensure that tag burden remains below this threshold and consider using smaller transmitters or size-selective tagging to improve post-release survival (Thiem et al. 2011). For experimental work, future studies on thermal tolerance could consider respirometry experiments and acclimating euryhaline fish such as *M. cephalus* to different temperatures and salinity to better predict resilience under projected warming scenarios. Collectively, these approaches would advance our understanding of how partial migration, habitat plasticity and thermal constraints interact to shape the persistence of *M. cephalus* in dynamic coastal environments.

REFERENCES

Able KW. 2005. A re-examination of fish estuarine dependence: evidence for connectivity between estuarine and ocean habitats. *Estuarine, Coastal and Shelf Science* 64(1): 5–17.

Able KW, Grothues TM, Turnure JT, Malone MA, Henkes GA. 2014. Dynamics of residency and egress in selected estuarine fishes: evidence from acoustic telemetry. *Environmental Biology of Fishes* 97(1): 91–102.

Able KW, Simenstad CA, Strydom NA, Bradley M, Sheaves M. 2022. Habitat use and connectivity. In: Whitfield AK, Able KW, Blaber SJM, Elliot M (eds.), *Fish and Fisheries in Estuaries: A Global Perspective*. pp 188–254.

Adams JB, Whitfield AK, Van Niekerk L. 2020. A socio–ecological systems approach towards future research for the restoration, conservation and management of southern African estuaries. *African Journal of Aquatic Science* 45(1–2):231–41.

Alfonso S, Gesto M, Sadoul B. 2021. Temperature increase and its effects on fish stress physiology in the context of global warming. *Journal of Fish Biology* 98: 1496–1508.

Allison C, Muller C, Childs AR, Froneman W, Bailey LA, Potts WM. 2021. When cooling is worse than warming: investigations into the thermal tolerance of an endemic reef fish, *Boopsoidea inornata*. *African Journal of Marine Science* 43: 239–249.

Allouche O, Tsoar A, Kadmon R. 2006. Assessing the accuracy of species distribution models: prevalence, kappa and the true skill statistic (TSS). *Journal of Applied Ecology* 43(6): 1223–1232.

Austin M. 2007. Species distribution models and ecological theory: a critical assessment and some possible new approaches. *Ecological Modelling* 200: 1–9.

Avigliano E, Carvalho B, Velasco G, Tripodi P, Vianna M, Volpedo AV. 2016. Nursery areas and connectivity of the adult anadromous catfish (*Genidens barbus*) revealed by otolith–core microchemistry in the south–western Atlantic Ocean. *Marine and Freshwater Research* 68(5): 931–40.

Avigliano E, Martínez G, Stoessel L, Méndez A, Bordel N, Pisonero J, Volpedo A. 2020. Otoliths as indicators for fish behaviour and procurement strategies of hunter-gatherers in North Patagonia. *Heliyon* 6(3).

Bae SE, Kim JK. 2020. Otolith microchemistry reveals the migration patterns of the flathead grey mullet *Mugil cephalus* (Pisces: Mugilidae) in Korean waters. *Journal of Ecology and Environment* 44: 1–11.

Baker R, Barnett A, Bradley M, Abrantes K, Sheaves M. 2019. Contrasting seascape use by a coastal fish assemblage: a multi-methods approach. *Estuaries and Coasts* 42(1): 292–307.

Barletta M, Amaral CS, Corrêa MF, Guebert F, Dantas DV, Lorenzi L, Saint-Paul U. 2008. Factors affecting seasonal variations in demersal fish assemblages at an ecocline in a tropical-subtropical estuary. *Journal of Fish Biology* 73(6): 1314–36.

Bartoń K. 2025. MuMIn: Multi-Model Inference. *R package version* 1.48.11, <https://CRAN.R-project.org/package=MuMIn>.

Bates AE, Morley SA. 2020. Interpreting empirical estimates of experimentally derived physiological and biological thermal limits in ectotherms. *Canadian Journal of Zoology* 98: 237–244.

Bates D, Maechler M, Bolker B, Walker S. 2015.Fitting Linear Mixed-Effects Models Using lme4. *Journal of Statistical Software* 67(1): 1-48.

Bath GE, Thorrold SR, Jones CM, Campana SE, McLaren JW, Lam JW. 2000. Strontium and barium uptake in aragonitic otoliths of marine fish. *Geochimica et cosmochimica acta* 64(10): 1705–1714.

Beck MW, Heck KL, Able KW, Childers DL, Eggleston DB, Gillanders BM, Halpern B, Hays,CG, Hoshino K, Minello TJ, Orth RJ, Sheridan PF, Weinstein MP. 2001. The identification, conservation and management of estuarine and marine nurseries for fish and invertebrates. *BioSience* 51: 633–641.

Beitinger TL, Wayne AB, Robert WM. 2000. Temperature tolerances of North American freshwater fishes exposed to dynamic changes in temperature. *Environmental Biology of Fishes* 58: 237–275.

Bennett AF, Lenski RE. 1993 Evolutionary adaptation to temperature II. Thermal niches of experimental lines of Escherichia coli. *Evolution* 4: 1–2.

Bice CM, Zampatti BP, Morrongiello JR. 2018. Connectivity, migration and recruitment in a catadromous fish. *Marine and Freshwater Research* 69(11): 1733–45.

Bichy JB. 2004. A life history assessment on the reproduction and growth of striped mullet, *Mugil cephalus*, in North Carolina. MSc thesis, North Carolina State University, United States of America.

Biolé FG, Thompson GA, Vargas CV, Leisen M, Barra F, Volpedo AV, Avigliano E. 2019. Fish stocks of *Urophycis brasiliensis* revealed by otolith fingerprint and shape in the Southwestern Atlantic Ocean. *Estuarine, Coastal and Shelf Science* 229: 106406.

Biro PA, Beckmann C, Stamps JA. 2010. Small within-day increases in temperature affects boldness and alters personality in coral reef fish. *Proceedings of the Royal Society B: Biological Sciences* 277: 71–77.

Blaber SJ. 1977. The feeding ecology and relative abundance of mullet (Mugilidae) in Natal and Pondoland estuaries. *Biological Journal of the Linnean Society* 9(3): 259–75.

Blaber SJ, Cyrus DP, Albaret JJ, Ching CV, Day JW, Elliott M, Fonseca MS, Hoss DE, Orensanz J, Potter IC, Silvert W. 2000. Effects of fishing on the structure and functioning of estuarine and nearshore ecosystems. *iCES Journal of marine Science* 57(3): 590–602.

Blaber SJ, Whitfield AK. 1977. The feeding ecology of juvenile mullet (Mugilidae) in south-east African estuaries. *Biological Journal of the Linnean Society* 9(3): 277–84.

Bok AH. 1983. The demography, breeding biology and management of two mullet species (Pisces: Mugilidae) in the Eastern Cape, South Africa. PhD thesis, Rhodes University, South Africa.

Bok AH. 1984. Extensive culture of two mullet species in freshwater impoundments in the eastern Cape. *African Zoology* 19(1):31–6.

Boyden CR, Aston SR, Thornton I. 1979. Tidal and seasonal variations of trace elements in two Cornish estuaries. *Estuarine and Coastal Marine Science* 9(3): 303–317.

Branch GM, Griffiths CL. 1988. The Benguela ecosystem. Part v. The coastal zone. *Oceanography and Marine Biology Annual Review* 26: 395–486.

Breiman L. 2001. Random forests. Machine Learning 45: 5–32.

Brett JR.1971 Energetic responses of salmon to temperature. A study of some thermal relations in the physiology and freshwater ecology of sockeye salmon (*Oncorhynchus nerka*). *American Zoologist* 11: 99–113.

Buckel JA, Sharack BL, Zdanowicz VS. 2004. Effect of diet on otolith composition in *Pomatomus saltatrix*, an estuarine piscivore. *Journal of Fish Biology* 64(6): 1469–84.

Burnham KP, Anderson DR. 2002. Model selection and multimodel inference: a practical information-theoretic approach. New York, NY: Springer New York.

Campana SE. 1999. Chemistry and composition of fish otoliths: pathways, mechanisms and applications. *Marine Ecology Progress Series* 188: 263–297.

Campana SE. 2005. Otolith elemental composition as a natural marker of fish stocks. In: Cadrin SX, Friedland KD, Waldman JR (eds.), *Stock identification methods*. Academic Press. pp 227–245.

Campana SE, Chouinard GA, Hanson JM, Frechet A, Brattey J. 2000. Otolith elemental fingerprints as biological tracers of fish stocks. *Fisheries Research* 46(1–3): 343–357.

Campana SE, Neilson JD. 1985. Microstructure of fish otoliths. *Canadian Journal of Fisheries and Aquatic Sciences* 42(5): 1014–1032.

Cardona L. 2016. Food and feeding of Mugilidae. In: Crosetti D, Blaber SJM (eds.), *Biology, ecology and culture of grey mullets (Mugilidae)*. CRC Press. pp 165–195.

Carr MH, Robinson SP, Wahle C, Davis G, Kroll S, Murray S, Schumacker EJ, Williams M. 2017. The central importance of ecological spatial connectivity to effective coastal marine protected areas and to meeting the challenges of climate change in the marine environment. Aquatic Conservation: *Marine and Freshwater Ecosystems* 27: 6–29.

Chang CW, Iizuka Y. 2012. Estuarine use and movement patterns of seven sympatric Mugilidae fishes: The Tatu Creek estuary, central western Taiwan. *Estuarine, Coastal and Shelf Science* 106: 121–126.

Chang CW, Iizuka Y, Tzeng WN. 2004a. Migratory environmental history of the grey mullet *Mugil cephalus* as revealed by otolith Sr:Ca ratios. *Marine Ecology Progress Series* 269: 277e288.

Chang CW, Lin SH, Iizuka Y, Tzeng WN. 2004b. Relationship between Sr:Ca ratios in otoliths of grey mullet Mugil cephalus and ambient salinity: validation, mechanisms, and applications. *Zoological Studies* 43: 74e85.

Chapman BB, Hulthén K, Brodersen J, Nilsson PA, Skov C, Hansson LA, Brönmark C. 2012. Partial migration in fishes: causes and consequences. *Journal of Fish Biology* 81(2): 456–78.

Chapman DD, Feldheim KA, Papastamatiou YP, Hueter RE. 2015. There and back again: a review of residency and return migrations in sharks, with implications for population structure and management. *Annual Review of Marine Science* 7: 547–70.

Chapman BB, Brönmark C, Nilsson JÅ, Hansson LA. 2011. The ecology and evolution of partial migration. *Oikos* 120(12): 1764–1775.

Childs AR. 2013. Estuarine-dependency and multiple habitat use by dusky kob *Argyrosomus japonicus* (Pisces: Sciaenidae). PhD thesis, Rhodes University, South Africa.

Childs AR, Cowley PD, Næsje TF, Booth AJ, Potts WM, Thorstad EB, Økland F. 2008. Do environmental factors influence the movement of estuarine fish? A case study using acoustic telemetry. *Estuarine, Coastal and Shelf Science* 78(1):227-36.

Childs AR, Cowley PD, Næsje TF, Bennett RH. 2015. Habitat connectivity and intra-population structure of an estuary-dependent fishery species. *Marine Ecology Progress Series* 537: 233–245.

Chuwen BM, Hoeksema SD, Potter IC. 2009. Factors influencing the characteristics of the fish faunas in offshore, deeper waters of permanently-open, seasonally-open and normally-closed estuaries. *Estuarine, Coastal and Shelf Science* 81(3): 279–95.

Clark J. 1968. Seasonal movements of striped bass contingents of Long Island Sound and the New York Bight. *Transactions of the American Fisheries Society* 97(4):320–43.

Clark S, Edwards AJ. 1999. An evaluation of artificial reef structures as tools for marine habitat rehabilitation in the Maldives. *Aquatic Conservation: Marine and Freshwater Ecosystems* 9(1): 5–21.

Clarke AD, Telmer KH, Shrimpton JM. 2015. Movement patterns of fish revealed by otolith microchemistry: a comparison of putative migratory and resident species. *Environmental Biology of Fishes* 98(6): 1583–1597.

Conover DO. 1990. The relation between capacity for growth and length of growing season: evidence for and implications of countergradient variation. *Transactions of the American Fisheries Society* 119(3): 416–30.

Cooke RS, Woodfine T, Petretto M, Ezard TH. 2016. Resource partitioning between ungulate populations in arid environments. *Ecology and Evolution* 6(17):6354–65.

Cooke SJ, Bergman JN, Twardek WM, Piczak ML, Casselberry GA, Lutek K, Dahlmo LS, Birnie-Gauvin K, Griffin LP, Brownscombe JW, Raby GD. 2022. The movement ecology of fishes. *Journal of Fish Biology* 101(4): 756–79.

Cooke SJ, Hinch SG, Farrell AP, Patterson DA, Miller-Saunders K, Welch DW, Donaldson MR, Hanson KC, Crossin GT, Mathes MT, Lotto AG. 2008. Developing a mechanistic understanding of fish migrations by linking telemetry with physiology, behavior, genomics and experimental biology: an interdisciplinary case study on adult Fraser River sockeye salmon. *Fisheries* 33(7):321–39.

Coutant CC. 2013. When is habitat limiting for striped bass? Three decades of testing the temperature–oxygen squeeze hypothesis. *American Fisheries Society Symposium* 80: 65–91.

Cowen RK, Gawarkiewicz G, Pineda J, Thorrold SR, Werner FE. 2007. Population connectivity in marine systems an overview. *Oceanography* 20(3): 14–21.

Cowles RB, Bogert CM. 1944. A preliminary study of thermal requirements in desert reptiles. Bulletin of the American Museum of Natural History 83: 265–296.

Cowley PD, Bennett RH, Childs AR, Murray TS. 2017. Reflection on the first five years of South Africa's Acoustic Tracking Array Platform (ATAP): status, challenges and opportunities. *African Journal of Marine Science* 39(4): 363–72.

Cox DK. 1974. Effects of three heating rates on the critical thermal maximum of bluegill. In: Gibbons JW, Sharitz RR (eds), *Thermal Ecology, AEC Symposium Series, National Technical Information Service*. Springfield, pp 158–163.

Crook DA, Buckle DJ, Allsop Q, Baldwin W, Saunders TM, Kyne PM, Woodhead JD, Maas R, Roberts B, Douglas MM. 2016. Use of otolith chemistry and acoustic telemetry to elucidate migratory contingents in barramundi *Lates calcarifer*. *Marine and Freshwater Research* 68(8):1554–66.

Crosetti D. 2016. Current state of grey mullet fisheries and culture. Biology, ecology and culture of grey mullet (Mugilidae). 388–450. CRC Press.

Crossin GT, Cooke SJ, Goldbogen JA, Phillips RA. 2014. Tracking fitness in marine vertebrates: current knowledge and opportunities for future research. *Marine Ecology Progress Series* 496: 1–7.

Crossin GT, Heupel MR, Holbrook CM, Hussey NE, Lowerre-Barbieri SK, Nguyen VM, Raby GD, Cooke SJ. 2017. Acoustic telemetry and fisheries management. *Ecological Applications* 27(4): 1031–49.

Currey LM, Heupel MR, Simpfendorfer CA, Williams AJ. 2015. Assessing environmental correlates of fish movement on a coral reef. *Coral Reefs* 34(4): 1267–77.

Currie RJ, Bennett, WA, Beitinger TL. 1998. Critical thermal minima and maxima of three freshwater game–fish species acclimated to constant temperatures. *Environmental Biology of Fishes* 51: 187–200.

Cushman SA, Gutzweiler K, Evans JS, McGarigal K. 2010. The gradient paradigm: a conceptual and analytical framework for landscape ecology. In: *Cushman SA, Heuttmann F (eds.), Spatial complexity, informatics, and wildlife conservation*. Tokyo: Springer Japan. pp 83–108.

Dalvi RS, Pal AK, Tiwari LR, Das T, Baruah K. 2009. Thermal tolerance and oxygen consumption rates of the catfish *Horabagrus brachysoma* (Günther) acclimated to different temperatures. *Aquaculture* 295(1–2): 116–119.

Darnaude AM, Arnaud-Haond S, Hunter E, Gaggiotti O, Sturrock A, Beger M, Volckaert F, Pérez-Ruzafa A, López-López L, Tanner SE, Turan C. 2022. Unifying approaches to Functional Marine Connectivity for improved marine resource management: the European SEA–UNICORN COST Action. *Research Ideas and Outcomes* 8: e80223.

Darwood MA, Koshio S, Ishikawa M, El–Sabagh M, Yokoyama S, Wang WL, Yukun Z, Olivier A. 2017. Physiological response, blood chemistry profile and mucus secretion of red sea bream (*Pagrus major*) fed diets supplemented with *Lactobacillus rhamnosus* under low salinity stress. *Fish Physiology and Biochemistry* 43(1): 179–92.

Das T, Pal AK, Chakraborty SK, Manush SM, Chatterjee N, Mukherjee SC. 2004. Thermal tolerance and oxygen consumption of Indian Major Carps acclimated to four temperatures. *Journal of Thermal Biology* 29: 157–163.

DAY JH. 1981. Sediments, turbidity and light penetration. In: Day JH (ed.), *Estuarine ecology with particular reference to Southern Africa*. Balkema, Cape Town. pp. 45 –56.

Day Jr JW, Yáñez-Arancibia A, Kemp WM, Crump BC. 2012. Introduction to estuarine ecology. *Estuarine Ecology* 12: 1–8.

Department of Agriculture and Fisheries. (2018). Stock assessment of the Australian east coast sea mullet (*Mugil cephalus*) fishery. State of Queensland. Available at: https://era.dpi.qld.gov.au/id/eprint/6757/1/Mullet_stock_assessment_report_2018.pdf?utm_source=chatgpt.com [Accessed: November 2025].

Department of Primary Industries and Regional Development. (2024). NSW Recreational Salwater Fishing guide. NWS Government. Available at: https://www.dpi.nsw.gov.au/__data/assets/pdf_file/0012/600222/NSWDPIRD-Saltwater-Fishing-Guide-2024.pdf?utm_source=chatgpt.com [Accessed: November 2025].

Desforges JE, Birnie-Gauvin K, Jutfelt F, Gilmour KM, Eliason EJ, Dressler TL, McKenzie DJ, Bates AE, Lawrence MJ, Fangue N, Cooke SJ. 2023. The ecological relevance of critical thermal maxima methodology for fishes. *Journal of Fish Biology* 102: 1000–1016.

Di Santo V. 2022. EcoPhysioMechanics: Integrating energetics and biomechanics to understand fish locomotion under climate change. *Integrative and Comparative Biology* 62(3): 711–20.

Dingle H, Drake VA. 2007. What is migration? *Bioscience* 57(2): 113–21.

Diouf K, Panfili J, Labonne M, Aliaume C, Tomás J, Do Chi T. 2006. Effects of salinity on strontium: calcium ratios in the otoliths of the West African black–chinned tilapia *Sarotherodon melanotheron* in a hypersaline estuary. *Environmental Biology of Fishes* 77(1): 9–20.

Donaldson MR, Cooke SJ, Patterson DA, Macdonald JS. 2008. Cold shock and fish. *Journal of Fish Biology* 73(7): 1491–1530.

Donaldson MR, Hinch SG, Suski CD, Fisk AT, Heupel MR, Cooke SJ. 2014. Making connections in aquatic ecosystems with acoustic telemetry monitoring. *Frontiers in Ecology and the Environment* 12(10): 565–73.

Doudoroff P. 1942. The resistance and acclimatization of marine fishes to temperature changes. I. Experiments with *Girella nigricans* (Ayres). *The Biological Bulletin* 83: 219–244.

Dowd WW, Felicia AK, Mark WD. 2015. Thermal variation, thermal extremes and the physiological performance of individuals. *The Journal of Experimental Biology* 12: 1956–1967.

Duncan MI, James NC, Bates AE, Goschen WS, Potts WM. 2019. Localised intermittent upwelling intensity has increased along South Africa's south coast due to El Niño–Southern Oscillation phase state. *African Journal of Marine Science* 41: 325–330.

Dunning JB, Danielson BJ, Pulliam HR. 1992. Ecological processes that affect populations in complex landscapes. *Oikos* 1: 169–75.

Edwards JE, Buijse AD, Winter HV, Bijleveld AI. 2025. Seasonal coastal residency and large-scale migration of two grey mullet species in temperate European waters. *Movement Ecology* 13(1):2.

Elliott M, McLusky DS. 2002. The need for definitions in understanding estuaries. *Estuarine, Coastal and Shelf Science* 55: 815–27.

Elliott M, Quintino V. 2007. The estuarine quality paradox, environmental homeostasis and the difficulty of detecting anthropogenic stress in naturally stressed areas. *Marine pollution bulletin* 54(6): 640–5.

Elsdon TS, Gillanders BM. 2003. Reconstructing migratory patterns of fish based on environmental influences on otolith chemistry. *Reviews in Fish Biology and Fisheries* 13: 217–235.

Elsdon TS, Gillanders BM. 2005. Alternative life-history patterns of estuarine fish: barium in otoliths elucidates freshwater residency. *Canadian Journal of Fish Aquatic Science* 62: 1143–1152.

Elsdon TS, Gillanders BM. 2006. Temporal variability in strontium , calcium , barium , and manganese in estuaries: Implications for reconstructing environmental histories of fish from chemicals in calcified structures. *Estuarine Coastal and Shelf Science* 66: 147–156.

Elsdon TS, Wells BK, Campana SE, Gillanders BM, Jones CM, Limburg KE, Secor DH, Thorrold SR, Walther BD. 2008. Otolith chemistry to describe movements and life−history parameters of fishes: hypotheses, assumptions, limitations and inferences. In: Gibson RN, Atkinson RJA , Gordon JDM (eds.), *Oceanography and marine biology*. CRC Press. pp 303−336.

Eme J, Bennett WA. 2009. Critical thermal tolerance polygons of tropical marine fishes from Sulawesi, Indonesia. *Journal of Thermal Biology* 34: 220–225.

Engelhard GH, Peck MA, Rindorf A, C. Smout S, Van Deurs M, Raab K, Andersen KH, Garthe S, Lauerburg RA, Scott F, Brunel T. 2014. Forage fish, their fisheries, and their predators: who drives whom?. *ICES Journal of Marine Science* 71(1):90–104.

Flávio H, Baktoft H. 2021. actel: Standardised analysis of acoustic telemetry data from animals moving through receiver arrays. *Methods in Ecology and Evolution* 12: 196–203.

Fortunato RC, Galán AR, Alonso IG, Volpedo A, Dura VB. 2017. Environmental migratory patterns and stock identification of Mugil cephalus in the Spanish Mediterranean Sea, by means of otolith microchemistry. *Estuarine, Coastal and Shelf Science* 188: 174–180.

Fowler AM, Smith SM, Booth DJ, Stewart J. 2016. Partial migration of grey mullet (*Mugil cephalus)* on Australia’s east coast revealed by otolith chemistry. *Marine Environmental Research* 119: 238–244.

Fraser KC, Davies KT, Davy CM, Ford AT, Flockhart DT, Martins EG. 2018. Tracking the conservation promise of movement ecology. *Frontiers in Ecology and Evolution* 6: 150.

Fox J, Weisberg S. 2019. An R Companion to Applied Regression, Third edition. Sage. Thousand Oaks CA. <https://www.john-fox.ca/Companion/>.

Frechette DM, Dugdale SJ, Dodson JJ, Bergeron NE. 2018. Understanding summertime thermal refuge use by adult Atlantic salmon using remote sensing, river temperature monitoring, and acoustic telemetry. *Canadian Journal of Fisheries and Aquatic Sciences* 75(11): 1999–2010.

Fromentin JM, Powers JE. 2005. Atlantic bluefin tuna: population dynamics, ecology, fisheries and management. *Fish and Fisheries* 6(4): 281–306.

Fry FEJ, Brett JR, Clawson GH. 1942. Lethal limits of temperature for young goldfish. *Revue Canadienne de Biologie* 1: 50–56.

Fry FEJ, Black VS, Black EC. 1947. Influence of temperature on the asphyxiation of young goldfish (*Carassius auratus* L.) under various tensions of oxygen and carbon dioxide. *The Biological Bulletin* 92(3): 217–224.

Gahagan BI, Fox DA, Secor DH. 2015. Partial migration of striped bass: revisiting the contingent hypothesis. *Marine Ecology Progress Series* 525: 185–97.

Gallardo-Cabello M, Espino-Barr E, Cabral-Solís EG, Puente-Gómez M, Garcia-Boa A. 2012. Study of the otoliths of striped mullet Mugil cephalus Linnaeus, 1758 in Mexican Central Pacific. *Journal of Fisheries and Aquatic Science* 7(6): 346.

Garcia AM, Raseira MB, Vieira JP, Winemiller KO, Grimm AM. 2003. Spatiotemporal variation in shallow-water freshwater fish distribution and abundance in a large subtropical coastal lagoon. *Environmental Biology of Fishes* 68(3): 215–28.

Gattuso JP, Magnan AK, Bopp L, Cheung WW, Duarte CM, Hinkel J, Mcleod E, Micheli F, Oschlies A, Williamson P, Billé R. 2018. Ocean solutions to address climate change and its effects on marine ecosystems. *Frontiers in Marine Science* 5: 337.

Gehrke PC, Harris JH. 2001. Regional-scale effects of flow regulation on lowland riverine fish communities in New South Wales, Australia. Regulated Rivers: Research and Management: *An International Journal Devoted to River Research and Management* 17(4-5): 369–91.

Gillanders BM, Elsdon TS, Halliday IA, Jenkins GP, Robins JB, Valesini FJ. 2011b. Potential effects of climate change on Australian estuaries and fish utilising estuaries: a review. *Marine and Freshwater Research* 62: 1115–1131.

Gillanders BM, Elsdon TS, Roughan M. 2011a. Connectivity of estuaries. *Treatise on Estuarine and Coastal Science* 7: 119–42.

Gillanders BM, Izzo C, Doubleday ZA, Ye Q. 2015. Partial migration: growth varies between resident and migratory fish. *Biology Letters* 11(3): 20140850.

Gillanders BM, McMillan MN, Reis-Santos P, Baumgartner LJ, Brown LR, Conallin J, Feyrer FV, Henriques S, James NC, Jaureguizar AJ, Pessanha AL. 2022. Climate change and fishes in estuaries. *Fish and Fisheries in Estuaries: A Global Perspective* 1: 380–457.

Gonzalez JG, Frédou T, Duarte-Neto PJ, Labonne M, Lira AS, Soares AP, Darnaude AM. 2023. Importance of estuaries for the horse–eye jack Caranx latus in northeastern Brazil: a case study of underestimated connectivity at the land–sea interface. Marine Ecology Progress *Series* 731: 27–49.

Górski K, De Gruijter C, Tana R. 2015. Variation in habitat use along the freshwater–marine continuum by grey mullet Mugil cephalus at the southern limits of its distribution. *Journal of Fish Biology* 87(4): 1059–1071.

Goschen WS, Schumann EH, Bernard KS, Bailey SE, Deyzel SH. 2012. Upwelling and ocean structures off Algoa Bay and the south-east coast of South Africa. *African Journal of Marine Science* 34(4): 525–36.

Grant GN, Cowley PD, Bennett RH, Childs AR, Whitfield AK. 2017. Influences of selected geophysical and environmental drivers on the movement patterns of *Rhabdosargus holubi* in a southern African estuary. *Environmental Biology of Fishes* 100(10): 1265–83.

Green DG. 1994. Connectivity and complexity in landscapes and ecosystems. *Pacific Conservation Biology* 1(3): 194–200.

Grober–Dunsmore R, Pittman SJ, Caldow C, Kendall MS, Frazer TK. 2009. A landscape ecology approach for the study of ecological connectivity across tropical marine seascapes. In: *Ecological connectivity among tropical coastal ecosystems*. Dordrecht: Springer Netherlands. pp 493–530.

Gvoždík L. 2018. Just what is the thermal niche? *Oikos* 1: 1701–1710.

Hampton SL, Moloney CL, van Der Lingen CD, Labonne M. 2018. Spatial and temporal variability in otolith elemental signatures of juvenile sardine off South Africa. *Journal of Marine Systems* 188: 109–116.

Harrell F. 2024. Hmisc: Harrell Miscellaneous. R package version 5.1-3, <https://CRAN.R-project.org/package=Hmisc>.

Harrison TD. 2001. Length-weight relationships of fishes from South African estuaries. *Journal of applied Ichthyology* 17(1): 46–48.

Harrison TD, Whitfield AK. 2006. Estuarine typology and the structuring of fish communities in South Africa. *Environmental Biology of Fishes* 75(3): 269–93.

Hartig F. 2024. DHARMa: Residual Diagnostics for Hierarchical (Multi-Level / Mixed) Regression Models. R package version 0.4.7, <https://CRAN.R-project.org/package=DHARMa>.

Hartill BW, Morrison MA, Smith MD, Boubée J, Parsons DM. 2003. Diurnal and tidal movements of snapper (*Pagrus auratus*, Sparidae) in an estuarine environment. *Marine and Freshwater Research* 54(8): 931–40.

Hays GC, Bailey H, Bograd SJ, Bowen WD, Campagna C, Carmichael RH, Casale P, Chiaradia A, Costa DP, Cuevas E, De Bruyn PN. 2019. Translating marine animal tracking data into conservation policy and management. *Trends in Ecology and Evolution* 34(5): 459–73.

Hazen EL, Maxwell SM, Bailey H, Bograd SJ, Hamann M, Gaspar P, Godley BJ, Shillinger GL. 2012. Ontogeny in marine tagging and tracking science: technologies and data gaps. *Marine Ecology Progress Series* 457: 221–40.

Heinecken TJE, Grindley JR. 1982. Report No. 10. Kowie (CSE 10). Estuaries of the Cape: Part II: synopses of available information on individual systems. *CSIR Research Report* 409: 1–58.

Heupel MR, Simpfendorfer CA. 2008. Movement and distribution of young bull sharks *Carcharhinus leucas* in a variable estuarine environment. *Aquatic Biology* 1(3): 277–89.

Heupel MR, Webber DM. 2012. Trends in acoustic tracking: where are the fish going and how will we follow them?. *American Fisheries Society Symposium* 76: 219–231.

Heupel MR, Semmens JM, Hobday AJ. 2006. Automated acoustic tracking of aquatic animals: scales, design and deployment of listening station arrays. *Marine and Freshwater Research* 57(1): 1–13.

Hicks A, Barbee NC, Swearer SE, Downes BJ. 2010. Estuarine geomorphology and low salinity requirement for fertilisation influence spawning site location in the diadromous fish, *Galaxias maculatus*. *Marine and Freshwater Research* 61(11): 1252–1258.

Hinz H, Anglada P, Gayá Vilar A, Reñones O, Catanese G, Castro–Fernández J, Gil MD, Grau A, Moranta J. 2023. Macrophyte complexity influences habitat choices of juvenile fish. *Marine Biology* 170(10): 125.

Hockersmith EE, Beeman JW. 2012. A history of telemetry in fishery research. In: Adams NS , Beeman JW, Eiler JH (eds.), *Telemetry Techniques: A User Guide for Fisheries Research*. American Fisheries Society, Bethesda, Maryland. pp. 7–20.

Hoegh-Guldberg O, Bruno JF. 2010. The impact of climate change on the world's marine ecosystems. *Science* 328 (5985): 1523–1528.

Hoese HD. 1985. Jumping mullet-the internal diving bell hypothesis. *Environmental Biology of Fishes* 13(4): 309–314.

Holbach A, Cowley PD, Kramar U, Neumann T. 2012. Otolith chemistry of fishes from Kosi Bay, South Africa: A preliminary multiple analytical methods approach to reconstruct fish migrations. *Estuarine, Coastal and Shelf Science* 109: 30–40.

Holbrook C, Hayden T, Binder T, Pye J. 2024. glatos: A package for the Great Lakes acoustic telemetry observation system. R package version 0.8.0, commit aa0d75ed063d114a11e6763f2ab4b4bd5ee189fd, <https://github.com/ocean-tracking-network/glatos>.

Honda K, Arai T, Kobayashi S, Tsuda Y, Miyashita K. 2012. Migratory patterns of exotic brown trout *Salmo trutta* in south-western Hokkaido, Japan, on the basis of otolith Sr: Ca ratios and acoustic telemetry. *Journal of Fish Biology* 80(2):408–26.

Houlihan DF, Innes AJ. 1984. The cost of walking in crabs: aerial and aquatic oxygen consumption during activity of two species of intertidal crab. *Comparative Biochemistry Physiology* 77: 325–334.

Hsu CC, Chang CW, Iizuka Y, Tzeng WN. 2009. A growth check deposited at estuarine arrival in otoliths of juvenile flathead mullet (*Mugil cephalus* L.). *Zoological Studies* 48(3): 315–324.

Huppert DD, Johnson RL, Leahy J, Bell K. 2003. Interactions between human communities and estuaries in the Pacific Northwest: Trends and Implications for Management. *Estuaries* 26(4): 994–1009.

Hussey NE, Kessel ST, Aarestrup K, Cooke SJ, Cowley PD, Fisk AT, Harcourt RG, Holland KN, Iverson SJ, Kocik JF, Mills Flemming JE. 2015. Aquatic animal telemetry: a panoramic window into the underwater world. *Science* 348(6240):1255642.

Ibáñez AL, Chang CW, Hsu CC, Wang CH, Iizuka Y, Tzeng WN. 2012. Diversity of migratory environmental history of the mullets *Mugil cephalus* and *M. curema* in Mexican coastal waters as indicated by otolith Sr: Ca ratios. *Ciencias Marinas* 38(1): 73–87.

Inshore Fisheries management (2023) Permit Conditions: Commercial Smallnets: Gillnet/Driftnet/Setnet Fishery Area A-F&H. Available at:

https://www.dffe.gov.za/sites/default/files/docs/licensesandpermits/permitcondition_netfisharea_afh2022.2023.pdf [Accessed: 20 July 2025].

Jackson SE, Sylvester P. 2008. Calibration strategies for elemental analysis by LA–ICP–MS. *Signal* 10(1,000): 100.

James NC, Harrison TD. 2010. A preliminary survey of the estuaries on the southeast coast of South Africa, Cape Padrone–Great Fish River, with particular reference to the fish fauna. *Transactions of the Royal Society of South Africa* 65(3): 149–64.

James NC, Van Niekerk L, Whitfield AK, Potts WM, Götz A, Paterson AW. 2013. Effects of climate change on South African estuaries and associated fish species. *Climate Research* 57: 233–248.

James NC, Whitfield AK, Harrison TD. 2016. Grey mullet (Mugilidae) as possible indicators of global warming in South African estuaries and coastal waters. *Marine Environmental Research* 122: 188–95.

Jonsson B, Jonsson N. 1993. Partial migration: niche shift versus sexual maturation in fishes. *Reviews in Fish Biology and Fisheries* 3(4):348-65.

Joo R, Picardi S, Boone ME, Clay TA, Patrick SC, Romero-Romero VS, Basille M. 2022. Recent trends in movement ecology of animals and human mobility. *Movement Ecology* 10(1): 26.

Jutfelt F. 2020. Metabolic adaptation to warm water in fish. *Functional Ecology* 34: 1138–1141.

Kellermann V, Sgrò CM. 2018. Evidence for lower plasticity in CT_{MAX} at warmer developmental temperatures. *Journal of Evolutionary Biology* 31(9): 1300–1312.

Kerr LA, Cadrin SX, Secor DH. 2010. The role of spatial dynamics in the stability, resilience, and productivity of an estuarine fish population. *Ecological Applications* 20(2): 497–507.

Kerr LA, Secor DH, Piccoli P. 2009. Partial migration of fishes as exemplified by the estuarine-dependent white perch. *Fisheries* 34: 114–123.

Kessel ST, Cooke SJ, Heupel MR, Hussey NE., Simpfendorfer CA, Vagle S, Fisk AT. 2014. A review of detection range testing in aquatic passive acoustic telemetry studies. *Reviews in Fish Biology and Fisheries* 24(1): 199–218.

Kraft S, Gandra M, Lennox RJ, Mourier J, Winkler AC, Abecasis D. 2023. Residency and space use estimation methods based on passive acoustic telemetry data. *Movement Ecology* 11(1): 12.

Kramer DL, Chapman MR. 1999. Implications of fish home range size and relocation for marine reserve function*. Environmental Biology of Fishes* 55: 65–79.

Kraus RT, Secor DH. 2005. Application of the nursery-role hypothesis to an estuarine fish. *Marine Ecology Progress Series* 291: 301–5.

Kraus RT, Secor DH, Wingate RL. 2015. Testing the thermal-niche oxygen-squeeze hypothesis for estuarine striped bass. Environmental Biology of Fishes. 98(10): 2083–92.

Kruger M, Strydom NA. 2011. Plankton dynamics associated with the convergence zone of a shear front in the permanently open Kowie Estuary, South Africa. *African Zoology* 46(1): 47–59.

Kruger M. 2010. Spatio-temporal dynamics of ichthyoplankton in the Kowie Estuary, South Africa. MSc thesis, Rhodes University, South Africa.

Labonne M, Morize E, Scolan P, Lae R, Dabas E, Bohn M. 2009. Impact of salinity on early life history traits of three estuarine fish species in Senegal. *Estuarine, Coastal and Shelf Science* 82(4): 673–81.

Lamberth SJ, Turpie JK. 2003. The role of estuaries in South African fisheries: economic importance and management implications. *African Journal of Marine Science* 25: 131–57.

Lan KW, Lee MA, Zhang CI, Wang PY, Wu LJ, Lee KT. 2014. Effects of climate variability and climate change on the fishing conditions for grey mullet (*Mugil cephalus* L.) in the Taiwan Strait. *Climatic Change* 126(1): 189–202.

Lan KW, Zhang CI, Kang HJ, Wu LJ, Lian LJ. 2017. Impact of fishing exploitation and climate change on the grey mullet Mugil cephalus stock in the Taiwan Strait. *Marine and Coastal Fisheries* 9(1): 271–80.

Lennox RJ, Afonso P, Birnie-Gauvin K, Dahlmo LS, Nilsen CI, Arlinghaus R, J Cooke S, Souza AT, Jarić I, Prchalová M, Říha M. 2024. Tracking aquatic animals to understand a world increasingly shaped by a changing climate and extreme weather events. *Canadian Journal of Fisheries and Aquatic Sciences* 81(3): 326–339.

Lenth R. 2025. emmeans: Estimated Marginal Means, aka Least–Squares Means. R package version 1.11.1, <https://CRAN.R-project.org/package=emmeans>.

Lin J, Liu Y, Yang Y, Hu Z. 2016. Calibration and correction of LA–ICP–MS and LA–MC–ICP–MS analyses for element contents and isotopic ratios. *Solid Earth Sciences* 1(1): 5–27.

Lowe Jr CH, Vance VJ. 1955. Acclimation of the critical thermal maximum of the reptile *Urosaurus ornatus*. *Science* 122(3158):73–4.

Lutjeharms JR, Cooper J, Roberts M. 2000. Upwelling at the inshore edge of the Agulhas Current. *Continental Shelf Research* 20(7): 737–61.

Marais JFK. 1978. Routine oxygen consumption of *Mugil cephalus*, *Liza dumerili* and *L. richardsoni* at different temperatures and salinities. *Marine Biology* 50: 9–16.

Martin GB, Wuenschel MJ. 2006. Effect of temperature and salinity on otolith element incorporation in juvenile gray snapper *Lutjanus griseus*. *Marine Ecology Progress Series* 324: 229–239.

Matley JK, Klinard NV, Martins AP, Aarestrup K, Aspillaga E, Cooke SJ, Cowley PD, Heupel MR, Lowe CG, Lowerre-Barbieri SK, Mitamura H. 2022. Global trends in aquatic animal tracking with acoustic telemetry. *Trends in Ecology and Evolution* 37(1): 79–94.

McKenzie M, Hay D. 2000. Eastern Cape Estuaries management Programme. Water Research Commission Report No. 1018/01. Scottsville.

Menasveta P. 1981. Lethal temperature of marine fishes of the Gulf of Thailand. *Journal of Fish Biology* 18(5): 603–7.

Mercier L, Mouillot D, Bruguier O, Vigliola L, Darnaude AM. 2012. Multi-element otolith fingerprints unravel sea− lagoon lifetime migrations of gilthead sea bream Sparus aurata. Marine Ecology Progress Series 444:175–94.

Mery F, Burns JG. 2010. Behavioural plasticity: an interaction between evolution and experience. *Evolutionary Ecology* 24(3): 571–83.

Meyer RP, Pachauri LA. 2014. Contribution of working groups I, II and III to the fifth assessment report of the Intergovernmental Panel on Climate Change. Synthesis Report.

Miles NG, Butler GL, Diamond SL, Bishop DP, van der Meulen DE, Reinfelds I, Walsh CT. 2018. Combining otolith chemistry and telemetry to assess diadromous migration in pinkeye mullet, *Trachystoma petardi* (Actinopterygii, Mugiliformes). *Hydrobiologia* 808(1): 265–81.

Millidine KJ, Metcalfe NB, Armstrong JD. 2008. The use of ventilation frequency as an accurate indicator of metabolic rate in juvenile Atlantic salmon (*Salmo salar*). *Canadian Journal of Fisheries and Aquatic Sciences* 65(10): 2081–2087.

Muggeo VMR 2008. segmented: an R Package to Fit Regression Models with Broken-Line Relationships. R News, 8/1, 20-25. URL https://cran.r-project.org/doc/Rnews/.

Mukhari DL, Childs AR, Ziko BA, Murray TS. 2025. Assessing the thermal tolerance of a cosmopolitan species, *Mugil cephalus. African Journal of Maine Science* (Accepted: 02 July 2025).

Murray TS, Cowley PD, Bennett RH, Childs AR. 2018 .Fish on the move: connectivity of an estuary-dependent fishery species evaluated using a large-scale acoustic telemetry array. *Canadian Journal of Fisheries and Aquatic Sciences* 75(11): 2038–2052.

Murray TS, Elston C, Parkinson MC, Filmalter JD, Cowley PD. 2022. A decade of South Africa’s acoustic tracking array platform: an example of a successful ocean stewardship programme. *Frontiers in Marine Science* 9: 886554.

Murray TS. 2016. Estuary-dependency and multiple habitat connectivity of juvenile leervis *Lichia amia* (Pisces: Carangidae) and the factors influencing their movements. PhD Thesis, Rhodes University, South Africa.

Myers OM, Reyier E, Ahr B, Cook GS. 2020. Striped mullet migration patterns in the Indian River Lagoon: A network analysis approach to spatial fisheries management. *Marine and Coastal Fisheries* 12(6):423-40.

Nagelkerken I, Connell SD. 2015. Global alteration of ocean ecosystem functioning due to increasing human CO_2 emissions. *Proceedings of the National Academy of Sciences* 112(43): 13272–7.

Nathan R, Getz WM, Revilla E, Holyoak M, Kadmon R, Saltz D, Smouse PE. 2008. A movement ecology paradigm for unifying organismal movement research. *Proceedings of the National Academy of Sciences* 105(49): 19052–9.

Nazir A, Khan MA. 2021. Using otoliths for fish stock discrimination: status and challenges. *Acta Ichthyologica et Piscatoria* 51: 199–218.

Ndour I, Diadhiou HD, Thiaw OT. 2013. Reproduction of yellow mullet *Mugil cephalus* on Northern Coast of Senegal, West Africa. *Aquaculture, Aquarium, Conservation and Legislation* 6(5): 439–45.

Neiffer DL, Stamper MA. 2009. Fish sedation, anesthesia, analgesia, and euthanasia: considerations, methods, and types of drugs. *ILAR journal* 50: 343–60.

Nelson TR, Powers SP. 2019. Validation of species specific otolith chemistry and salinity relationships. *Environmental Biology of Fishes* 102(5): 801–815.

Nordlie FG. 2003. Fish communities of estuarine salt marshes of eastern North America, and comparisons with temperate estuaries of other continents. *Reviews in Fish Biology and Fisheries* 13(3): 281–325.

Nsubuga YN. 2004. Towards sustainable utilisation of the fishery resources of the Kowie Estuary, South Africa. PhD thesis, Rhodes University, South Africa.

Olds AD, Connolly RM, Pitt KA, Maxwell PS. 2012. Habitat connectivity improves reserve performance. *Conservation Letters* 5(1): 56–63.

Olds AD, Connolly RM, Pitt KA, Pittman SJ, Maxwell PS, Huijbers CM, Moore BR, Albert S, Rissik D, Babcock RC, Schlacher TA. 2016. Quantifying the conservation value of seascape connectivity: a global synthesis. *Global Ecology and Biogeography* 25(1):3–15.

Ogle DH, Doll JC, Wheeler AP, Dinno A. 2025. FSA: Simple Fisheries Stock Assessment Methods. R package version 0.9.6, <https://CRAN.R-project.org/package=FSA>.

Palumbi SR. 2003. Population genetics, demographic connectivity, and the design of marine reserves. *Ecological Applications* 13(1): 146–58.

Panfili J, Darnaude AM, Lin YJ, Chevalley M, Iizuka Y, Tzeng WN, Crivelli AJ. 2012. Habitat residence during continental life of the European eel *Anguilla anguilla* investigated using linear discriminant analysis applied to otolith Sr: Ca ratios. *Aquatic Biology* 15(2): 175–85.

Patterson TA, Thomas L, Wilcox C, Ovaskainen O, Matthiopoulos J. 2008. State–space models of individual animal movement. *Trends in Ecology and Evolution* 23(2): 87–94.

Pease AA, Jacobs GR, Mendoza-Carranza M, Rodiles-Hernández R, Wenger SJ, Capps KA. 2023. Otolith microchemistry highlights the importance of extensive connectivity for conservation of an iconic migratory fish in a large tropical river basin. Aquatic Conservation: *Marine and Freshwater Ecosystems* 33(9): 969–980.

Peterson ML, Fuller AN, Demko D. 2017. Environmental factors associated with the upstream migration of fall-run chinook salmon in a regulated river. *North American Journal of Fisheries Management* 37(1): 78–93.

Pörtner H, Knust R. 2007. Climate change affects marine fishes through the oxygen limitation of thermal tolerance. *Science* 315: 95–97.

Pörtner HO, Farrell AP. 2008. Physiology and climate change. *Science* 322(5902): 690–2.

Pörtner HO. 2010. Oxygen- and capacity-limitation of thermal tolerance: a matrix for integrating climate-related stressor effects in marine ecosystems. *Journal of Experimental* Biology 213: 881–893.

Poff NL. 1997. Landscape filters and species traits: towards mechanistic understanding and prediction in stream ecology. *Journal of the North American Benthological Society* 16(2):391–409.

Potter IC, Warwick RM, Hall NG, Tweedley JR. 2015. The physico-chemical characteristics, biota and fisheries of estuaries. *Freshwater Fisheries Ecology* 7: 48–79.

Potts WM, Götz A, James N. 2015. Review of the projected impacts of climate change on coastal fishes in southern Africa. *Reviews in Fish Biology and Fisheries* 25(4):603-30.

Prakoso VA, Kim KT, Ryu JH, Min BH, Chang YJ. 2019. Oxygen consumption of *Mugil cephalus* on several temperatures under brackish water conditions. In: *IOP Conference Series: Earth and Environmental Science Volume* 278. Number: 1. pp 012060.

Prakoso VA, Subagja J, Chang YJ. 2015. Low water temperature and its effects on stress response of grey mullets *Mugil cephalus* acclimated in freshwater. *Indonesian Aquaculture Journal* 10(1):41–45.

Prichard CG, Jonas JL, Student JJ, Watson NM, Pangle KL. 2018. Same habitat, different species: otolith microchemistry relationships between migratory and resident species support interspecific natal source classification. *Environmental Biology of Fishes* 101: 1025–1038.

Prosser CL (ed.). 1991. Comparative animal physiology, environmental and metabolic animal physiology. Volume 1. John Wiley and Sons.

Prosser CL. 1973. Water: osmotic balance; hormonal regulation. *Comparative animal physiology* 1: 1–78.

Pulliam HR. 1988. Sources, sinks, and population regulation. *The American Naturalist* 132(5): 652–61.

R Core Team. 2024. R: A language and environment for statistical computing. R Foundation for Statistical Computing, Vienna, Austria.

Ray GC. 2005. Connectivities of estuarine fishes to the coastal realm. *Estuarine, Coastal and Shelf Science 64* (1): 18–32.

Reis-Santos P, Tanner SE, Elsdon TS, Cabral HN, Gillanders BM. 2013. Effects of temperature, salinity and water composition on otolith elemental incorporation of *Dicentrarchus labrax*. *Journal of Experimental Marine Biology and Ecology* 446: 245–252.

Rijnsdorp AD, Peck MA, Engelhard GH, Möllmann C, Pinnegar JK. 2009. Resolving the effect of climate change on fish populations. *Journal of Marine Science* 66: 1570–1583.

Rogers TA, Fowler AJ, Steer MA, Gillanders BM. 2019. Discriminating natal source populations of a temperate marine fish using larval otolith chemistry. *Frontiers in Marine Science* 6: 711.

Roloson SD, Landsman SJ, Tana R, Hicks BJ, Carr JW, Whoriskey F, van den Heuvel MR. 2020. Otolith microchemistry and acoustic telemetry reveal anadromy in non–native rainbow trout (*Oncorhynchus mykiss*) in Prince Edward Island, Canada. *Canadian Journal of Fisheries and Aquatic Sciences* 77(7): 1117–30.

Rountos KJ. 2016. Defining forage species to prevent a management dilemma. *Fisheries* 41(1):16–7.

Royal Alfred Marina. 2025. Available at https://royalalfredmarina.com/ [Accessed: 30 June 2025]

Russell A, Taylor MD, Barnes TC, Johnson DD, Gillanders BM. 2022. Habitat transitions by a large coastal sciaenid across life history stages, resolved using otolith chemistry. *Marine Environmental Research* 76: 105614.

Scavia D, Field JC, Boesch DF, Buddemeier RW, Burkett V, Cayan DR, Fogarty M, Harwell MA, Howarth RW, Mason C, Reed DJ. 2002. Climate change impacts on US coastal and marine ecosystems. *Estuaries* 25(2): 149–64.

Schumann EH, Gray RR, Shone RW. 2001. Tidal flow structures and sedimentation in the lower Kowie estuary, Port Alfred, South Africa. *Transactions of the Royal Society of South Africa* 56(1): 11–24.

Secor DH. 1999. Specifying divergent migrations in the concept of stock: the contingent hypothesis. *Fisheries Research* 43(1-3):13–34.

Secor DH, Henderson-Arzapalo A, Piccoli PM. 1995. Can otolith microchemistry chart patterns of migration and habitat utilization in anadromous fishes? *Journal of Experimental Marine Biology and Ecology* 192(1): 15–33.

Sheaves M. 2009. Consequences of ecological connectivity: the coastal ecosystem mosaic. *Marine Ecology Progress Series* 391: 107–15.

Sheaves M, Baker R, Nagelkerken I, Connolly RM. 2015. True value of estuarine and coastal nurseries for fish: incorporating complexity and dynamics. *Estuaries and Coasts* 38(2): 401–14.

Shen KN, Jamandre BW, Hsu CC, Tzeng WN, Durand JD. 2011. Plio-Pleistocene sea level and temperature fluctuations in the northwestern Pacific promoted speciation in the globally–distributed flathead mullet Mugil cephalus. *BMC Evolutionary Biology* 11(1): 83.

Sheppard JN, James NC, Whitfield AK, Cowley PD. 2011. What role do beds of submerged macrophytes play in structuring estuarine fish assemblages? Lessons from a warm-temperate South African estuary. *Estuarine, Coastal and Shelf Science* 95(1): 145–55.

Sirot C, Ferraton F, Panfili J, Childs AR, Guilhaumon F, Darnaude AM. 2017. ElementR: An R package for reducing elemental data from LA-ICPMS analysis of biological calcified structures. *Methods in Ecology and Evolution* 8(12): 1659–1667.

Skov C, Chapman BB, Baktoft H, Brodersen J, Brönmark C, Hansson LA, Hulthén K, Nilsson PA. 2013. Migration confers survival benefits against avian predators for partially migratory freshwater fish. *Biology Letters* 9(2): 20121178.

Smale DA, Wernberg T, Oliver EC, Thomsen M, Harvey BP, Straub SC, Burrows MT, Alexander LV, Benthuysen JA, Donat MG, Feng M. 2019. Marine heatwaves threaten global biodiversity and the provision of ecosystem services. *Nature Climate Change* 9(4): 306–12.

Smith JP, Boyd TJ, Cragan J, Ward MC. 2021. Dissolved rubidium to strontium ratio as a conservative tracer for wastewater effluent–sourced contaminant inputs near a major urban wastewater treatment plant. *Water Research* 205: 117691.

Smith KA, Deguara K. 2003. Formation and annual periodicity of opaque zones in sagittal otoliths of *Mugil cephalus* (Pisces: Mugilidae). *Marine and Freshwater Research* 54(1):57–67.

Soeth M, Spach HL, Daros FA, Adelir-Alves J, de Almeida AC, Correia AT. 2019. Stock structure of Atlantic spadefish *Chaetodipterus faber* from Southwest Atlantic Ocean inferred from otolith elemental and shape signatures. *Fisheries* Research 211: 81–90.

Somero GN. 2010. The physiology of climate change: how potentials for acclimatization and genetic adaptation will determine ‘winners’ and ‘losers’. *Journal of Experimental Biology* 213(6): 912–920.

South African Weather Service (SAWS). 2025. Available at: https://www.weathersa.co.za/ [Accessed: 30 June 2025]

Soyinka OO. 2008. The feeding ecology of Mugil cephalus (Linnaeus) from a high brackish tropical lagoon in South-west, Nigeria. *African Journal of Biotechnology* 7(22): 4192–4198.

Steffen C, Stephens S, Dance MA, Lippi DL, Jensen CC, Wells RD, Rooker JR. 2023. Estuarine–coastal connectivity and partial migration of southern flounder in the Gulf of Mexico. *Estuarine, Coastal and Shelf Science* 294: 108545.

Stillman JH. 2019. Heat waves, the new normal: summertime temperature extremes will impact animals, ecosystems, and human communities. *Physiology* 34(2): 86–100.

Sturrock AM, Hunter E, Milton JA, Johnson RC, Waring CP, Trueman CN, Johnson RC, Waring CP, Tryeman CN. 2015. Quantifying physiological influences on otolith microchemistry. *Methods in Ecology and Evolution* 6: 806–816.

Sturrock AM, Trueman CN, Darnaude AM, Hunter E. 2012. Can otolith elemental chemistry retrospectively track migrations in fully marine fishes? *Journal of Fish Biology* 81: 766–795.

Svensson GP, Strandh M, Löfstedt C. 2014. Movements in the olfactory landscape. In Hansson LA, Akesson S (eds.), *Animal movement across scales*. Oxford: Oxford University Press. Pp 195–218.

Sylvester JR. 1975. Critical thermal maxima of three species of Hawaiian estuarine fish: a comparative study. *Journal of Fish Biology* 7(2): 257–262.

Szekeres P, Eliason EJ, Lapointe D, Donaldson MR, Brownscombe JW, Cooke SJ. 2016. On the neglected cold side of climate change and what it means to fish. *Climate Research* 69: 239–45.

Taylor PD, Fahrig L, Henein K, Merriam G. 1993. Connectivity is a vital element of landscape structure. *Oikos* 1: 571–3.

Thiem JD, Taylor MK, McConnachie SH, Binder TR, Cooke SJ. 2011. Trends in the reporting of tagging procedures for fish telemetry studies that have used surgical implantation of transmitters: a call for more complete reporting. *Reviews in Fish Biology and Fisheries* 21(1):117–26.

Thomson JM. 1966. The grey mullets. *Oceanography and Marine Biology Annual Review* 4:301–35.

Tian H, Liu J, Cao L, Dou S. 2019. Interactive effects of strontium and barium water concentration on otolith incorporation in juvenile flounder *Paralichthys olivaceus*. *Plos one* 14(6): e0218446.

Tournois J, Ferraton F, Velez L, McKenzie DJ, Aliaume C, Mercier L, Darnaude AM. 2013. Temporal stability of otolith elemental fingerprints discriminates among lagoon nursery habitats. *Estuarine, Coastal and Shelf Science* 131: 182–93.

Tournois J, Darnaude AM, Ferraton F, Aliaume C, Mercier L, McKenzie DJ. 2017. Lagoon nurseries make a major contribution to adult populations of a highly prized coastal fish. *Limnology and Oceanography* 62(3): 1219–33.

Turpie J, Clark B. 2007. *Development of a conservation plan for temperate South African estuaries on the basis of biodiversity importance. Ecosystem Health and Economic Costs and Benefits-Final Report*. CAPE Regional Estuarine Management Programme.

Van der Walt KA, Porri F, Potts WM, Duncan MI, James NC. 2021. Thermal tolerance, safety margins and vulnerability of coastal species: Projected impact of climate change induced cold water variability in a temperate African region. *Marine Environmental Research* 169: 105346.

Van Niekerk L, Adams JB, James NC, Lamberth SJ, MacKay CF, Turpie JK, Rajkaran A, Weerts SP, Whitfield AK. 2020. An estuary ecosystem classification that encompasses biogeography and a high diversity of types in support of protection and management. *African Journal of Aquatic Science* 45(1–2): 199–216.

Van Niekerk L, Lamberth SJ, James NC, Taljaard S, Adams JB, Theron AK, Krug M. 2022. The vulnerability of South African estuaries to climate change: A review and synthesis. *Diversity* 14: 697.

Vander Vorste R, Obedzinski M, Nossaman Pierce S, Carlson SM, Grantham TE. 2020. Refuges and ecological traps: Extreme drought threatens persistence of an endangered fish in intermittent streams. *Global Change Biology* 26: 3834–3845.

Varsamos S, Nebel C, Charmantier G. 2005. Ontogeny of osmoregulation in postembryonic fish: a review. Comparative Biochemistry and Physiology Part A: Molecular and Integrative *Physiology* 141(4): 401–29.

Vasseur DA, DeLong JP, Gilbert B, Greig HS, Harley CD, McCann KS, Savage V, Tunney TD, O'Connor MI. 2014. Increased temperature variation poses a greater risk to species than climate warming. *Proceedings of the Royal Society B: Biological Sciences* 281(1779): 20132612.

Vélez–Espino LA, McLaughlin RL, Robillard M. 2013. Ecological advantages of partial migration as a conditional strategy. *Theoretical Population Biology* 85: 1–1.

Verhelst P, Brys R, Cooke SJ, Pauwels I, Rohtla M, Reubens J. 2023. Enhancing our understanding of fish movement ecology through interdisciplinary and cross-boundary research. *Reviews in Fish Biology and Fisheries* 33(1): 111–35.

Vinagre C, Costa MJ, Wood SA, Williams RJ, Dunne JA. 2019. Potential impacts of climate change and humans on the trophic network organization of estuarine food webs. *Marine Ecology Progress Series* 616:13-24.

Vinagre C, Leal I, Mendonça V, Flores AA. 2015. Effect of warming rate on the critical thermal maxima of crabs, shrimp and fish. *Journal of Thermal Biology* 47: 19–25.

Vinagre C, Salgado J, Cabral HN, Costa MJ. 2011. Food web structure and habitat connectivity in fish estuarine nurseries-impact of river flow. *Estuaries and Coasts* 34: 663–674.

Vivier L, Cyrus DP, Jerling HL. 2010. Fish community structure of the St Lucia estuarine system under prolonged drought conditions and its potential for recovery after mouth breaching. *Estuarine, Coastal and Shelf Science* 86(4): 568–79.

Wallace JH. 1975. Aspects of the biology and ecology of the estuarine fishes of the east coast of South Africa. PhD thesis. University of Natal. South Africa.

Wallace JH, van der Elst RP. 1975. The estuarine fishes of the east coast of South Africa. Part 3. Reproduction. Investigational Report of the Oceanographic Research Institute 40: 1 – 48 .

Walsh WA, Swanson C, Lee CS. 1991. Combined effects of temperature and salinity on embryonic development and hatching of striped mullet, *Mugil cephalus*. *Aquaculture* 97(2−3): 281−289.

Wang CH. 2014. Otolith elemental ratios of flathead mullet Mugil cephalus in Taiwanese waters reveal variable patterns of habitat use. *Estuarine, Coastal and Shelf Science* 151: 124–130.

Wang CH, Hsu CC, Chang CW, You CF, Tzeng WN. 2010. The migratory environmental history of freshwater resident flathead mullet *Mugil cephalus* L. in the Tanshui River, northern Taiwan. *Zoological Studies* 49(4): 504–514.

Wang CH, Hsu CC, Tzeng WN, You CF, Chang CW. 2011. Origin of the mass mortality of the flathead grey mullet (*Mugil cephalus*) in the Tanshui River, northern Taiwan, as indicated by otolith elemental signatures. *Marine Pollution Bulletin* 62(8): 1809–1813.

Webster MS, Colton MA, Darling ES, Armstrong J, Pinsky ML, Knowlton N, Schindler DE. 2017. Who should pick the winners of climate change?. *Trends in ecology and evolution* 32(3):167–173.

Welch RJ, Childs AR, Murray TS, Darnaude AM, James NC. 2025. The role of acoustic telemetry in assessing fish connectivity within marine seascapes: A global review. *Journal of Fish Biology* 106(5): 1285–304.

Wen CC, Pratchett MS, Shao KT, Kan KP, Chan BK. 2010. Effects of habitat modification on coastal fish assemblages. *Journal of Fish Biology* 77(7):1674-87.

Whitfield AK. 1990. Life–history styles of fishes in South African estuaries. *Environmental Biology of Fishes* 28(1): 295–308.

Whitfield AK. 2005. Fishes and freshwater in southern African estuaries–a review. *Aquatic Living Resources* 18(3): 275–89.

Whitfield AK. 2016. Ecological role of Mugilidae in the coastal zone. Biology, ecology and culture of grey mullets (Mugilidae). In: Crosetti D, Blaber SJ (eds.), *Biology and culture of grey mullets (Mugilidae)*. CRC Press. pp 324–348.

Whitfield AK. 2017. The role of seagrass meadows, mangrove forests, salt marshes and reed beds as nursery areas and food sources for fishes in estuaries. *Reviews in Fish Biology and Fisheries* 27(1): 75–110.

Whitfield AK. 2020. Littoral habitats as major nursery areas for fish species in estuaries: a reinforcement of the reduced predation paradigm. *Marine Ecology Progress Series* 649: 219–34.

Whitfield AK. 2021. When the flathead mullet left St Lucia. *African Journal of Marine Science* 43: 161–169.

Whitfield AK, Blaber SJM. 1978. Food and feeding ecology of piscivorous fishes at Lake St Lucia, Zululand. *Journal of Fish Biology* 13: 675–691.

Whitfield AK, Elliott M. 2011. Ecosystem and biotic classifications of estuaries and coasts. *Treatise on Estuarine and Coastal Science* 99–124.

Whitfield AK, Lamberth SJ. 2012. Mugilidae (Mugil cephalus), In: Mann BQ (ed.), *Southern African Marine Linefish Species Profiles*. Special Publication, Oceanographic Research Institute. Durban 9: 130–131.

Whitfield AK, Panfili J, Durand JD. 2012. A global review of the cosmopolitan flathead mullet *Mugil cephalus* Linnaeus 1758 (Teleostei: Mugilidae), with emphasis on the biology, genetics, ecology and fisheries aspects of this apparent species complex. *Reviews in Fish Biology and Fisheries* 22: 641–81.

Whitfield AK, Paterson AW, Bok AH, Kok HM. 1994. A comparison of the ichthyofaunas in two permanently open eastern Cape estuaries. *African Zoology* 29(2):175–85.

Whitfield AK, Houde ED, Neira FJ, Potter IC. 2023. Importance of marine-estuarine-riverine connectivity to larvae and early juveniles of estuary-associated fish taxa. *Environmental Biology of Fishes* 106(10): 1983–2009.

Wickham H. 2016. ggplot2: Elegant Graphics for Data Analysis. Springer-Verlag New York. https://ggplot2.tidyverse.org.

Wildtrust. 2022. Policy influencing South African sharks and rays. Management: legal and illegal gillnetting. WILDTRUST Policy Brief, number 1. Pp 7.

Wilson JG. 2002. Productivity, fisheries and aquaculture in temperate estuaries. *Estuarine, Coastal and Shelf Science* 55(6): 953–967.

Wilson DT, McCormick MI. 1997. Spatial and temporal validation of settlement–marks in the otoliths of tropical reef fishes. *Marine Ecology Progress Series* 153: 259–271.

Winter JD. 1996. Advances in underwater telemetry. In Murphy BR, Willis DW (eds.), *Fisheries techniques. 2nd ed*. American Fisheries Society, Bethesda, Md. pp. 555–590.

Yoshinaga J, Nakama A, Morita M, Edmonds JS. 2000. Fish otolith reference material for quality assurance of chemical analyses. *Marine Chemistry* 69(1–2): 91–97.

Young GC, Potter IC. 2002. Influence of exceptionally high salinities, marked variations in freshwater discharge and opening of estuary mouth on the characteristics of the ichthyofauna of a normally-closed estuary. *Estuarine, Coastal and Shelf Science* 55(2):223–46.

Ziko BA, Childs AR, Mukhari DL, Murray TS. In review. Will I survive? Assessing the thermal tolerance of an estuary-dependant mugilid *Chelon dumerili* in a changing climate*. African Journal of Marine Science*

APPENDICES

Chapter 3

Appendix 1. Top five outputs and ranking of the linear mixed effects models (LMM) to assess the influence of various environmental variables on average daily position of *Mugil cephalus* tagged in the Kowie Estuary, South Africa. The selected best-fit model (lowest AIC) is presented in boldface.

Model	AIC	LogLik	BIC
station ~ flow + river + sea + sqrt(rainfall) + (1 | fish_code)	**9687.1**	**-4836.5**	**9725.7**
station ~ flow + river + sqrt(rainfall) + (1 | fish_code)	9712.5	-4850.2	9745.9
station ~ flow + river + sea + (1 | fish_code)	9689.5	-4838.7	9722.6
station ~ flow + river + (1 | fish_code)	9716.3	-4853.1	9743.9
station ~ flow + sea + sqrt(rainfall) + (1 | fish_code)	9735.1	-4861.5	9768.2

Appendix 2. Detailed monthly movements of acoustically tagged *Mugil cephalus* in the Kowie Estuary, South Africa between March 2023 and April 2024.

MARCH 2023

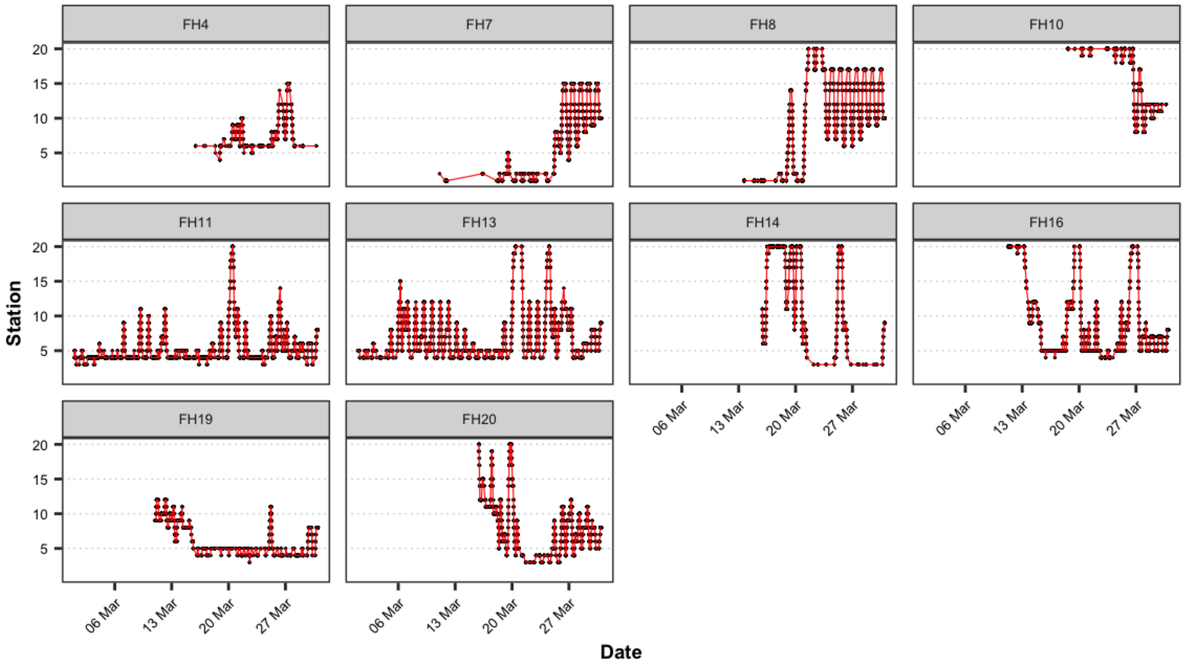

APRIL 2023

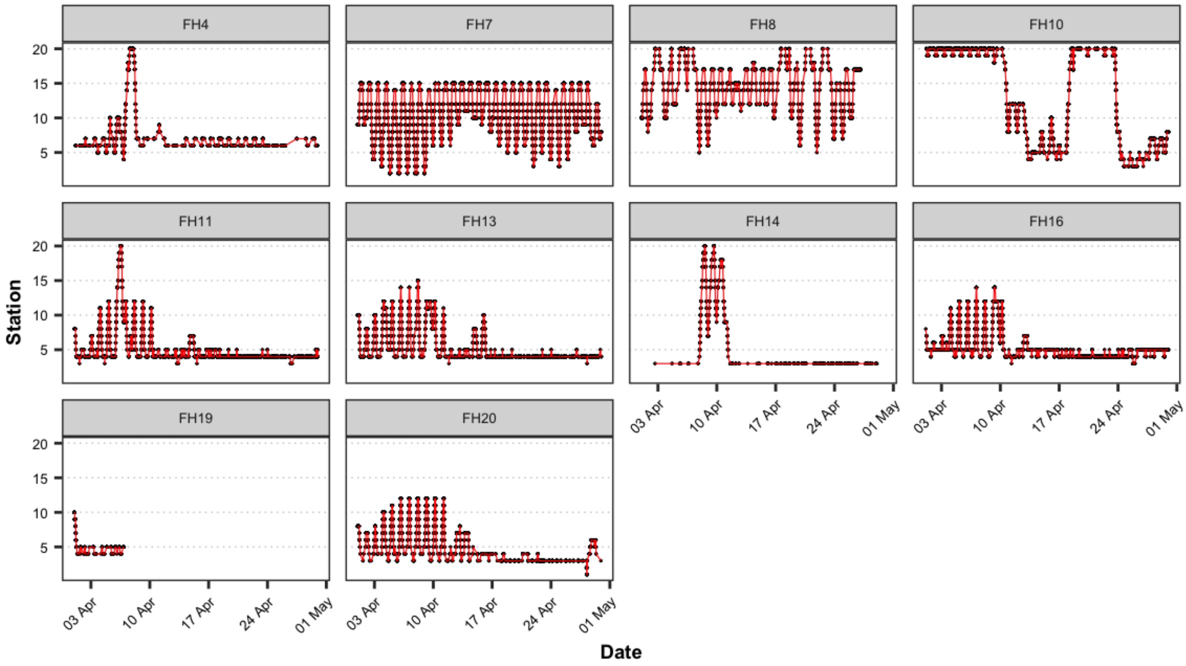

MAY 2023

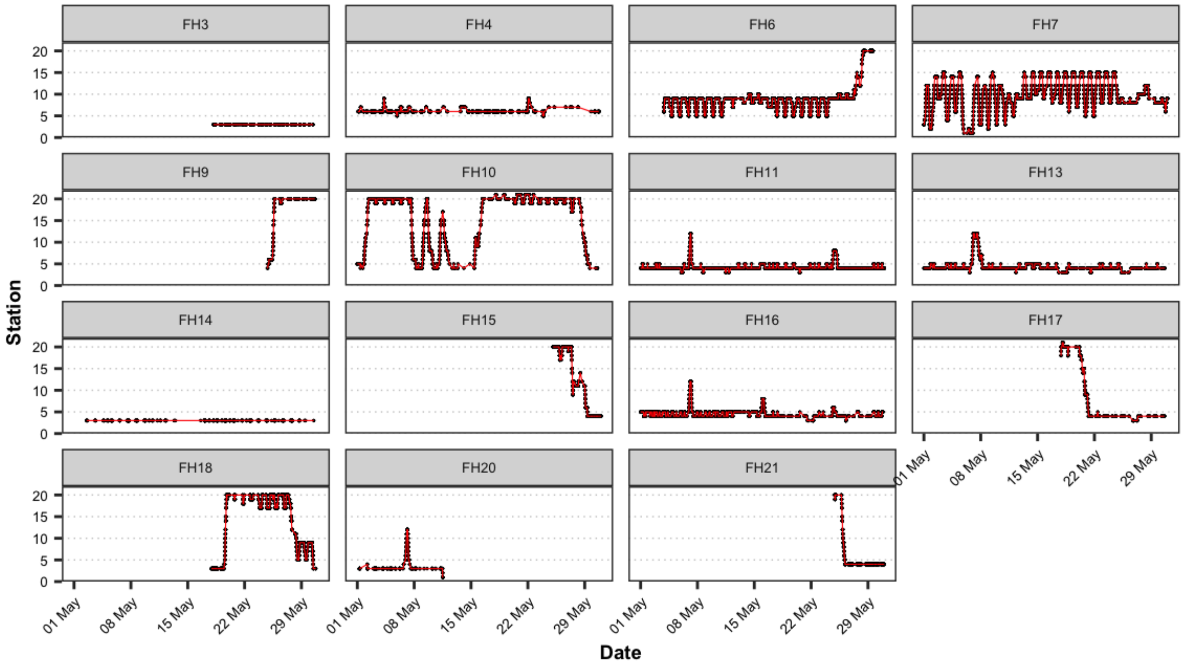

JUNE 2023

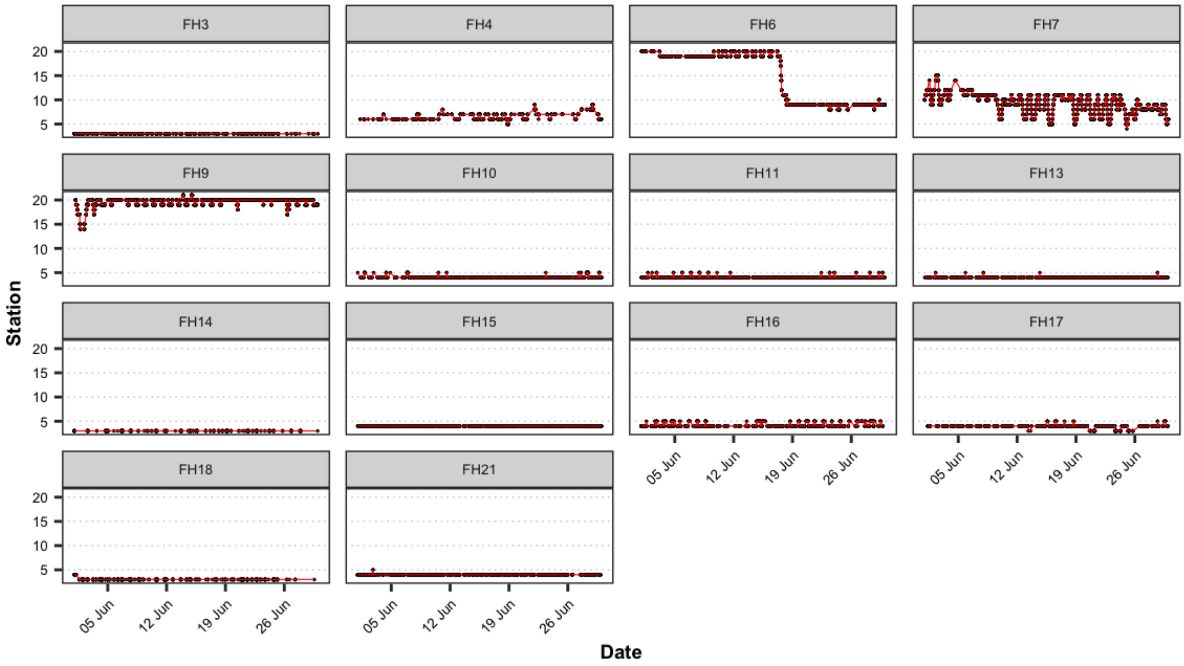

JULY 2023

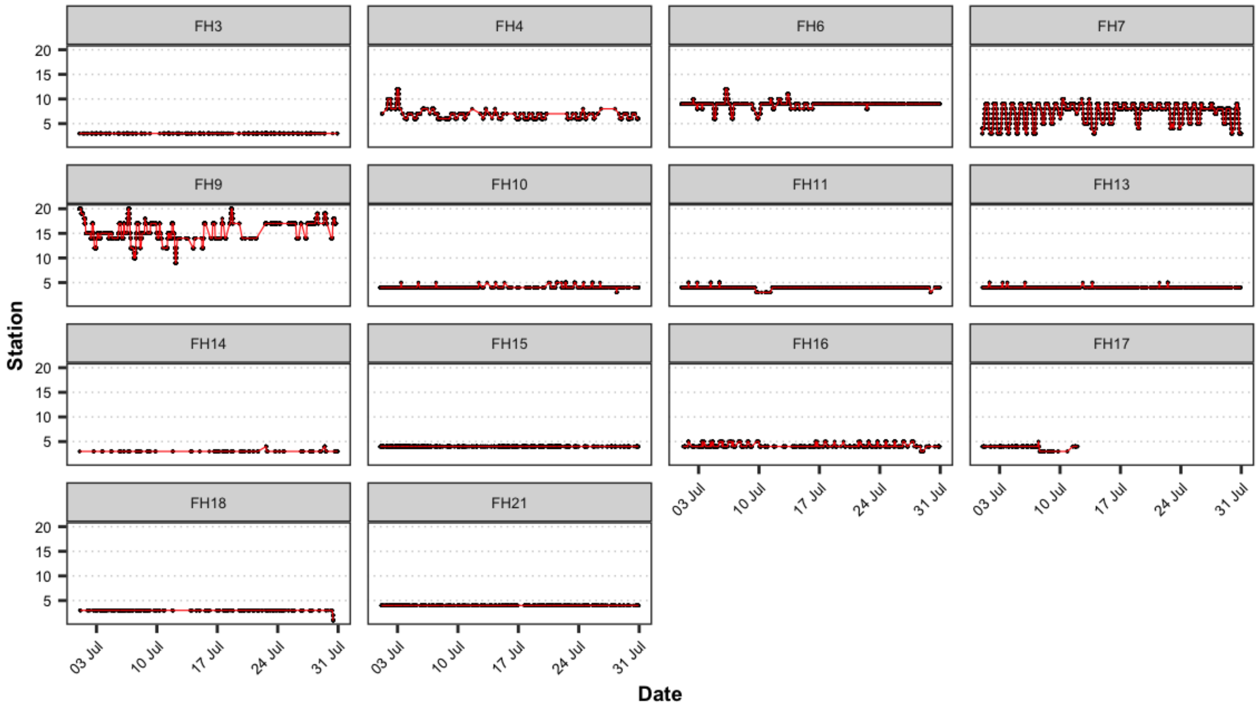

AUGUST 2023

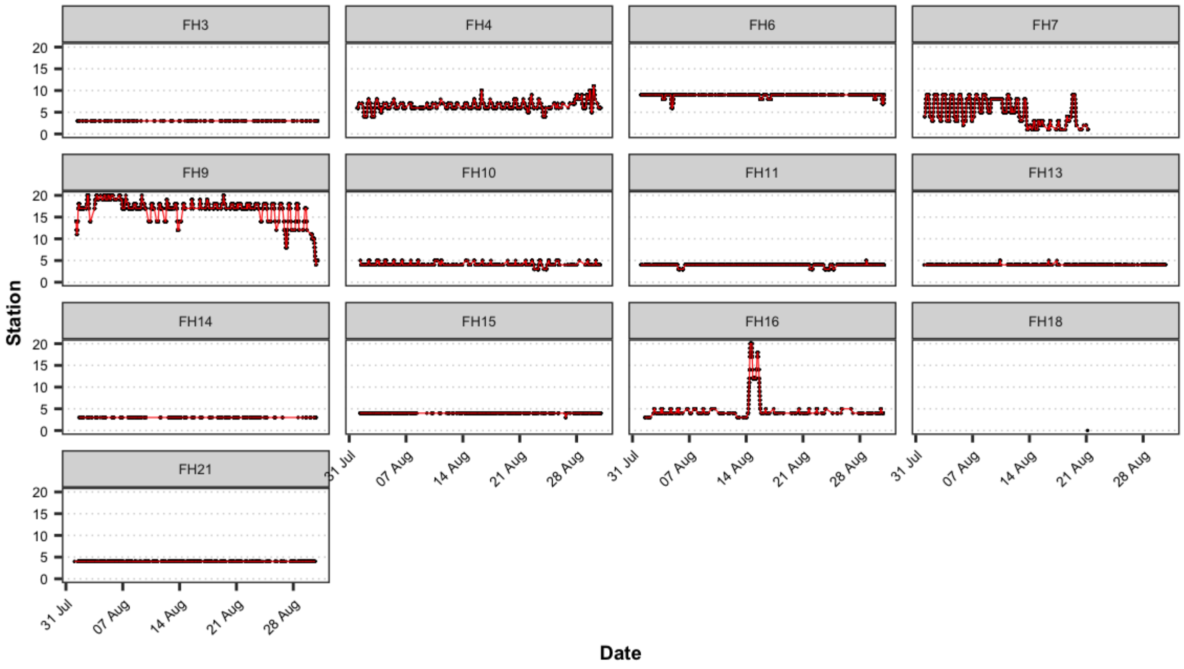

SEPTEMBER 2023

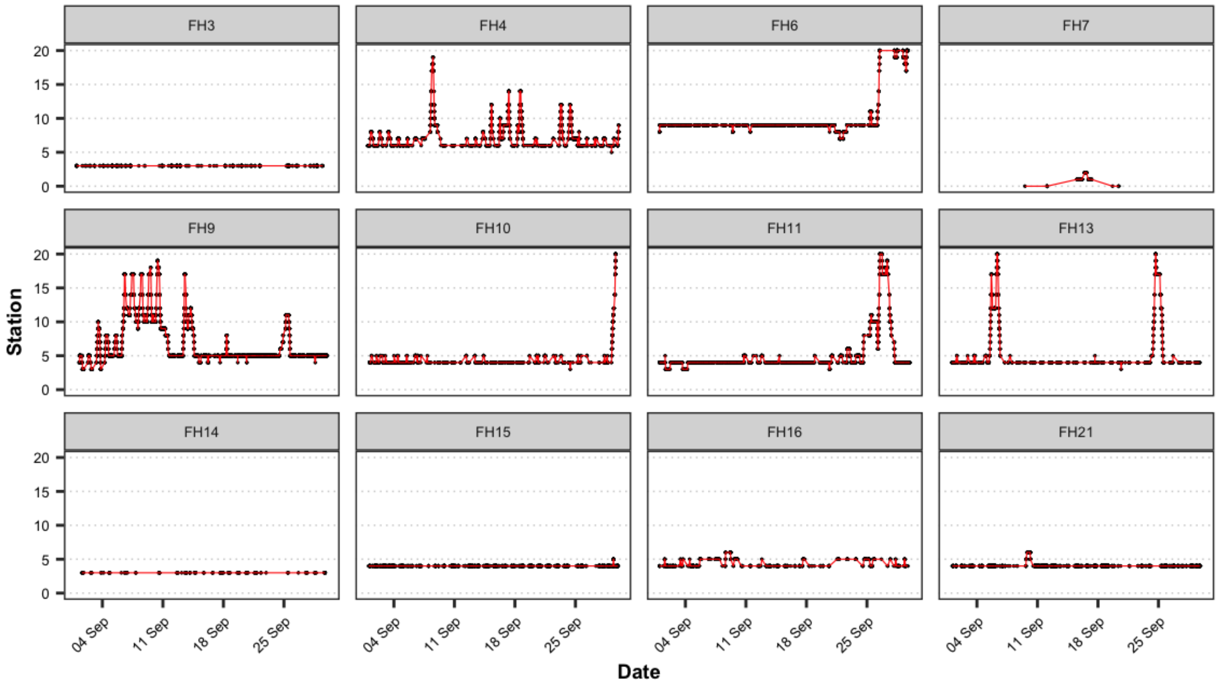

OCTOBER 2023

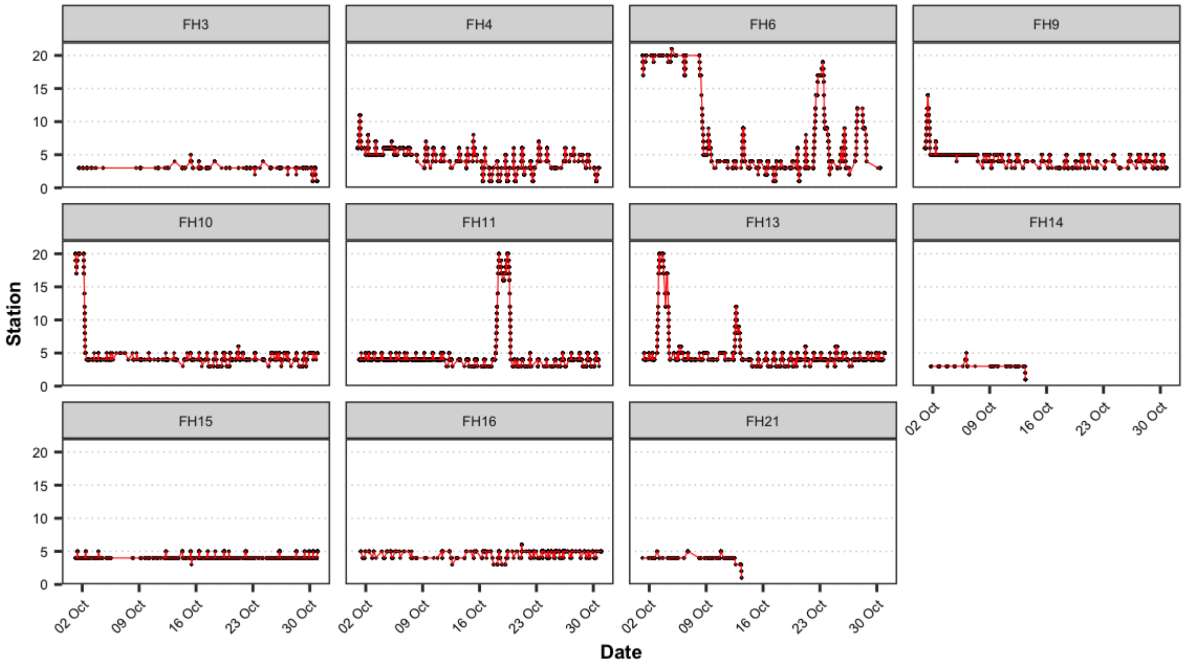

NOVEMBER 2023

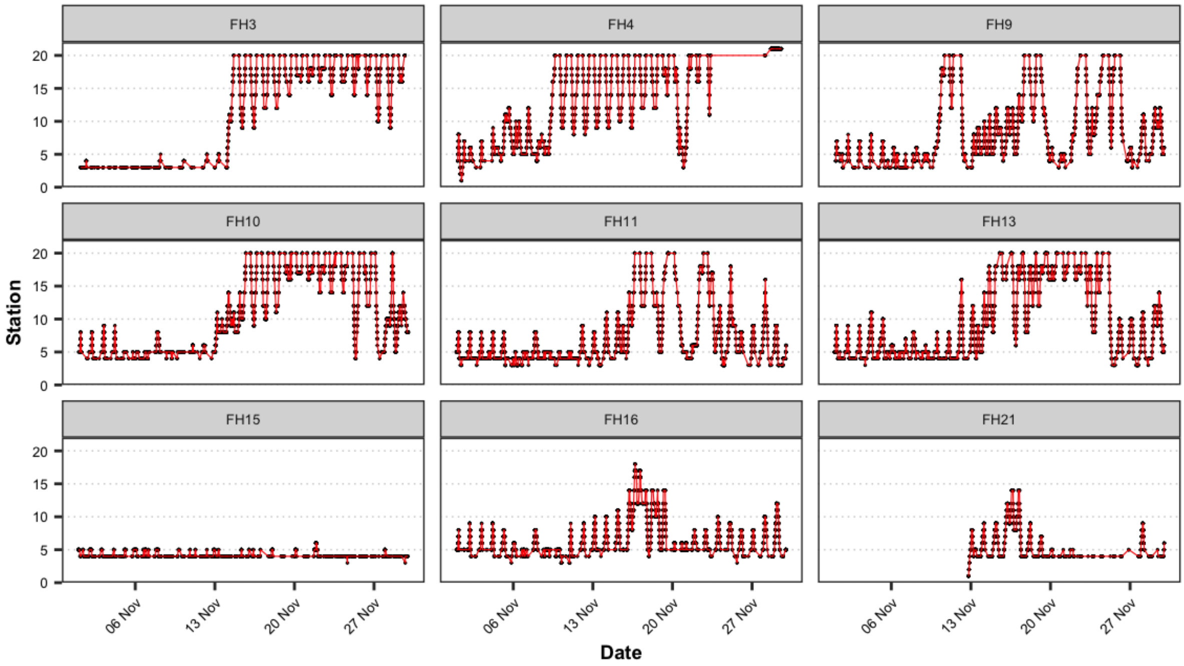

DECEMBER 2023

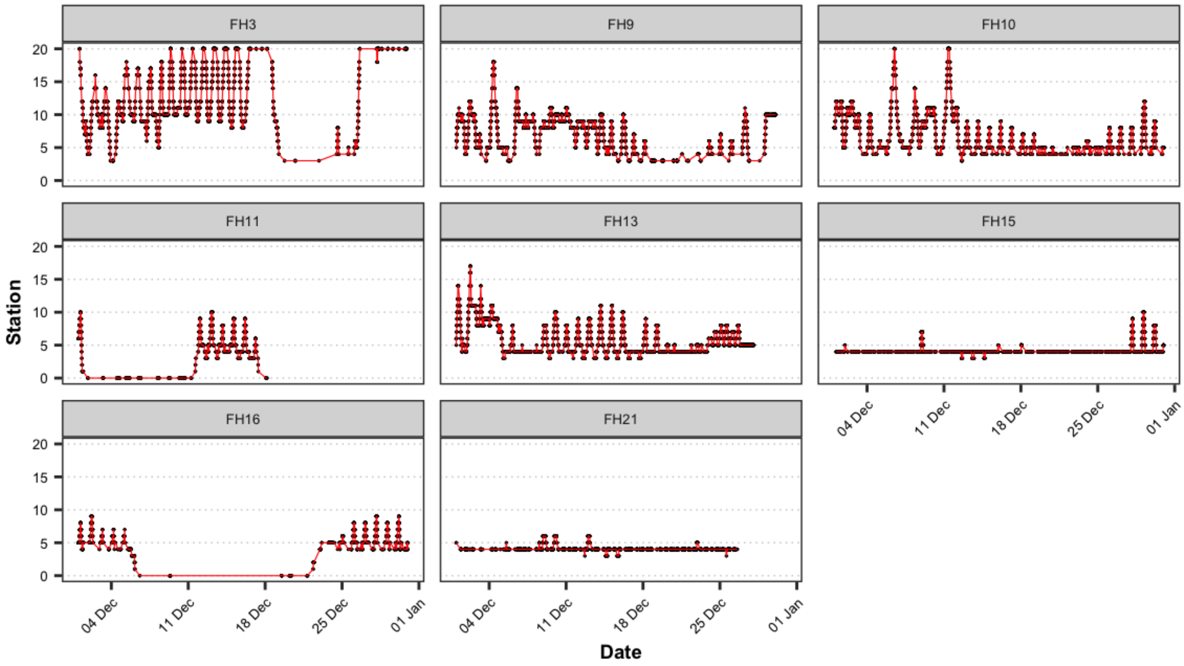

JANUARY 2024

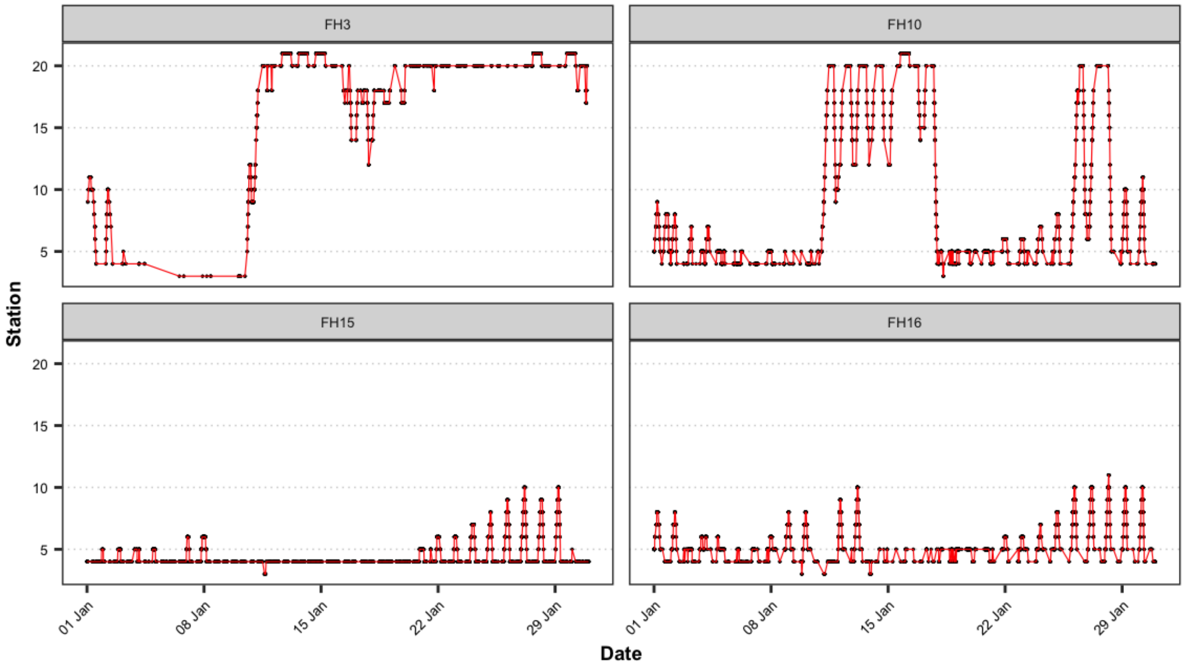

FEBRUARY 2024

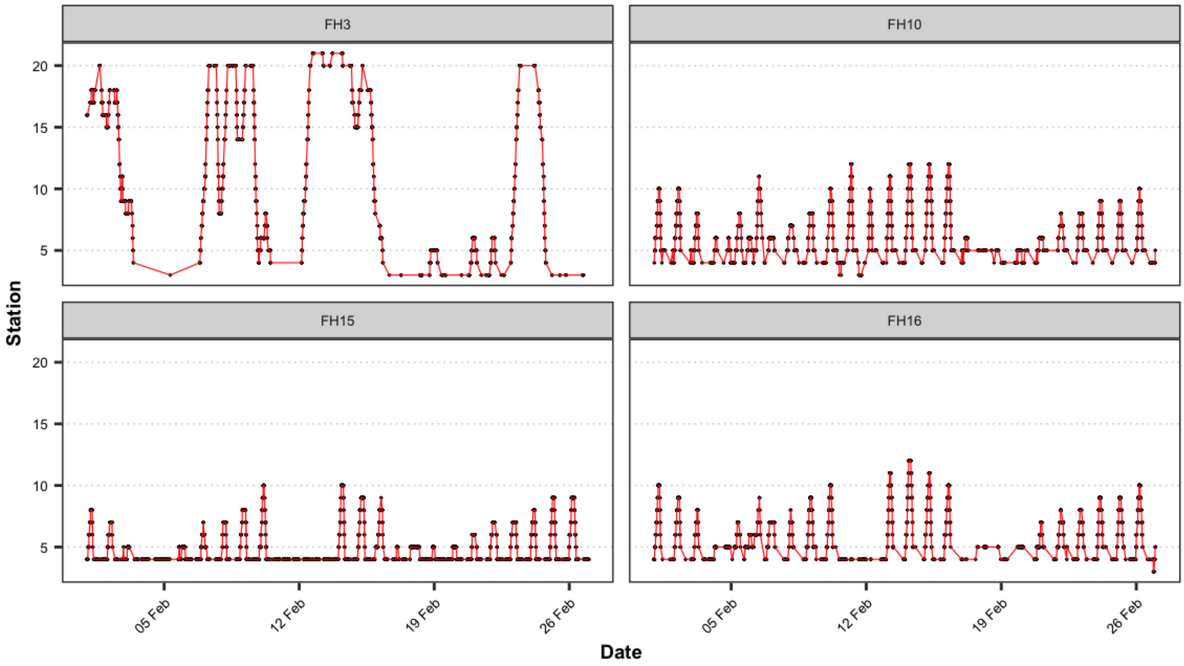

MARCH 2024

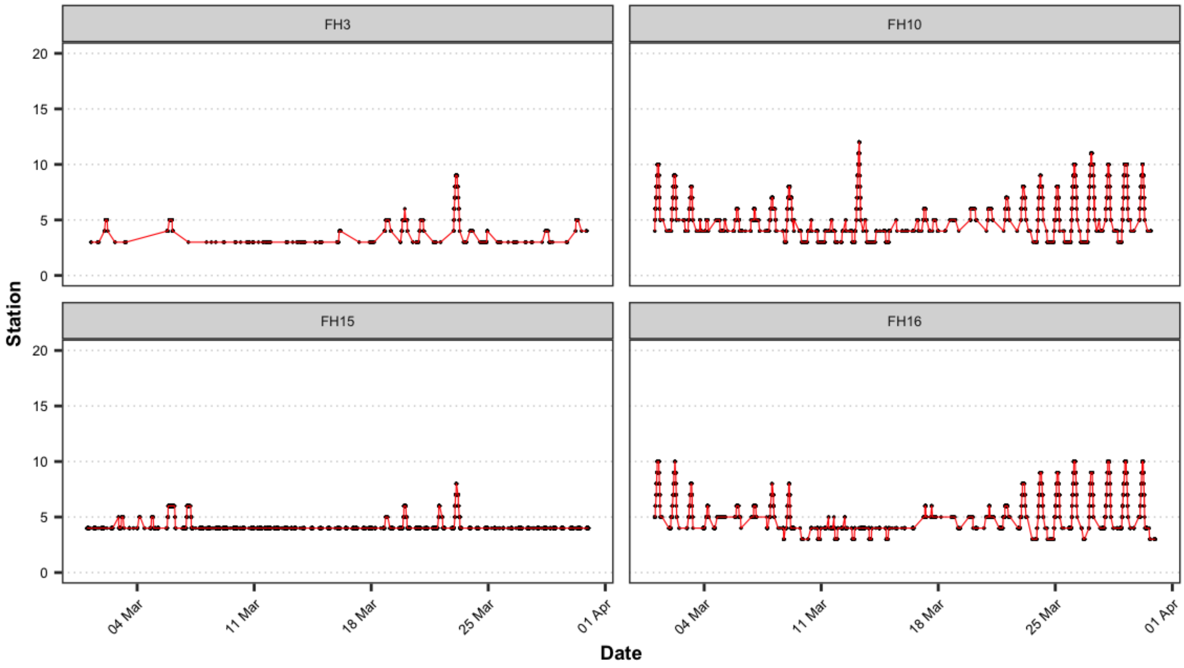

APRIL 2024

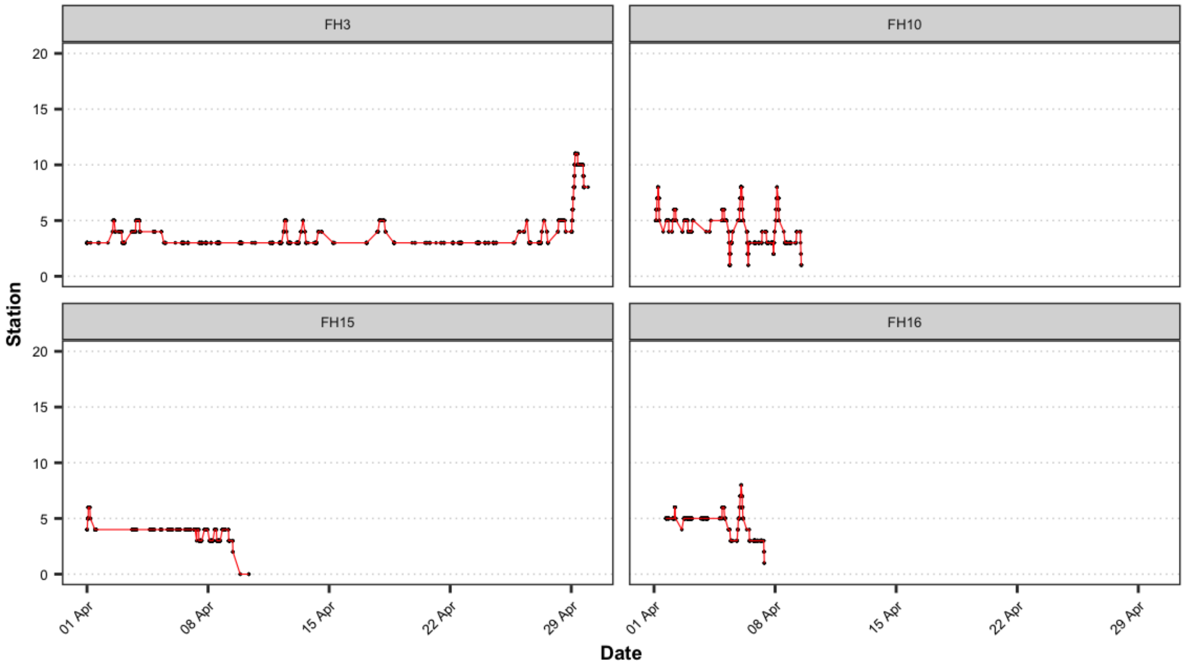

Chapter 4

Appendix 3. The rate of temperature change in the experimental tanks during the *Mugil cephalus* CT$_{max}$ and CT$_{min}$ trials.

	Rate of temperature change (average ± SD) (°C.min^{-1})	
	CT$_{max}$	**CT$_{min}$**
Tank 1	0.045 ± 0.02	0.02 ± 0.01
Tank 2	0.045 ± 0.02	0.02 ± 0.01
Tank 3	0.039 ± 0.01	0.02 ± 0.01
Tank 4	0.045 ± 0.01	0.02 ± 0.00
Tank 5	0.05 ± 0.04	0.02 ± 0.01